University of Ljubljana

Faculty of Electrical Engineering

Maria Scuderi

Identification and description of molecular transport mechanisms across cell membrane due to electroporation

Identifikacija in opis mehanizmov molekularnega transporta preko celične membrane pri elektroporaciji

DOCTORAL DISSERTATION

Ljubljana, 2024

University of Ljubljana

Faculty of Electrical Engineering

Maria Scuderi

Identification and description of molecular transport mechanisms across cell membrane due to electroporation

DOCTORAL DISSERTATION

Mentor: Lea Rems, Ph.D.

Co-mentor: Janja Dermol-Černe, Ph.D.

Ljubljana, 2024

Univerza v Ljubljani

Fakulteta za elektrotehniko

Maria Scuderi

Identifikacija in opis mehanizmov molekularnega transporta preko celične membrane pri elektroporaciji

DOKTORSKA DISERTACIJA

Mentorica: doc. dr. Lea Rems, univ. dipl. inž. el.

Somentorica: doc. dr. Janja Dermol-Černe, mag. inž. el.

Ljubljana, 2024

Univerza v Ljubljani
Fakulteta za elektrotehniko

Tržaška 25
p.p. 2999
1001 Ljubljana, Slovenija
telefon: 01 476 84 11
faks: 01 426 46 30
www.fe.uni-lj.si
e-mail: dekanat@fe.uni-lj.si

Senat Fakultete za elektrotehniko Univerze v Ljubljani je na seji dne, 10.06.2021 odobril kandidatki:

MARIA SCUDERI

temo za doktorsko disertacijo z naslovom:

Identifikacija in opis mehanizmov molekularnega transporta preko celične membrane pri elektroporaciji

Identification and description of molecular transport mechanisms across cell membrane due to electroporation

Komisija za doktorski študij Univerze v Ljubljani je po pooblastilu Senata Univerze v Ljubljani temo potrdila na seji dne: 28.09.2021.

Senat Fakultete za elektrotehniko Univerze v Ljubljani je kandidatu na seji dne, 01.02.2024 priznal naslednje izvirne prispevke k znanosti:

1 Primerjava različnih vrst pulzov v smislu njihove enakovrednosti za vnos cisplatina pri elektrokemoterapiji.

2 Določitev števila molekul cisplatina, potrebnih za doseganje citotoksičnega učinka.

3 Vrednotenje obstoječih modelov elektroporacije za napovedovanje molekularnega transporta in drugih povezanih pojavov na ravni posamezne celice.

Komisija za zagovor doktorske disertacije:

izr. prof. dr. David Nedeljković, predsednik
prof. dr. Damijan Miklavčič, član
prof. dr. Gregor Dolinar, član
prof. dr. Hao Lin, član
doc. dr. Lea Rems, mentorica
doc. dr. Janja Dermol-Černe, somentorica

UNIVERZA V LJUBLJANI Fakulteta za elektrotehniko 2 Ljubljana

Dekan:
prof. dr. Marko Topič

Univerza v Ljubljani
Fakulteta za elektrotehniko

Tržaška cesta 25, p.p. 2999
1000 LJUBLJANA, Slovenia
telefon: +386 1 476 84 11
faks: +386 1 426 46 30
www.fe.uni-lj.si
e-mail: dekanat@fe.uni-lj.si

I, the undersigned student, SCUDERI MARIA, registration number 64190425, the author of the written final work of studies, entitled: Identification and description of molecular transport mechanisms across cell membrane due to electroporation,

DECLARE,

1. [1] a) The written final work of studies is a result of my independent work.
   b) The written final work of studies is a result of own work of more candidates and fulfils the conditions determined by the Statute of UL for joint final works of studies and is a result of my independent work in the required share.
2. The printed form of the written final work of studies is identical to the electronic form of the written final work of studies.
3. I have acquired all the necessary permissions for the use of data and copyrighted works in the written final work of studies and have clearly marked them in the written final work of studies.
4. I have acted in accordance with ethical principles during the preparation of the written final work of studies and have, where necessary, obtained agreement of the ethics commission.
5. I give my consent to use of the electronic form of the written final work of studies for the detection of content similarity with other works, using similarity detection software that is connected with the study information system of the university member.
6. I transfer to the UL – free of charge, non-exclusively, geographically and time-wise unlimited – the right of saving the work in the electronic form, the right of reproduction, as well as the right of making the written final work of studies available to the public on the world wide web via the Repository of UL.
7. I give my consent to publication of my personal data that are included in the written final work of studies and in this declaration, together with the publication of the written final work of studies.
8. I give my consent to use of my birth date in COBISS record.

In: Ljubljana Date:
5. 2. 2024

Student's signature:
Maria Scuderi

[1] Choose a) or b).

Preface

The present doctoral dissertation is the result of experimental work and numerical modeling related to the electroporation of individual biological cells. The work was carried out within the doctoral degree programme of Electrical Engineering at the University of Ljubljana, Faculty of Electrical Engineering in the Laboratory of Biocybernetics. The dissertation includes four research papers published in peer-reviewed journals.

- **Paper 1: M. Scuderi**, M. Reberšek, D. Miklavčič, and J. Dermol-Černe, "The use of high-frequency short bipolar pulses in cisplatin electrochemotherapy in vitro," *Radiology and oncology*, vol. 53, no. 2, pp. 194–205, 2019.

- **Paper 2: M. Scuderi,** J. Dermol-Černe, J. Ščančar, S. Marković, L. Rems, and D. Miklavčič, "The equivalence of different types of electric pulses for electrochemotherapy with cisplatin - an in vitro study," *Radiology and Oncology*, vol. 58, no. 1, pp. 51–66, 2024.

- **Paper 3: M. Scuderi**, J. Dermol-Černe, C. A. da Silva, A. Muralidharan, P. E. Boukany, and L. Rems, "Models of electroporation and the associated transmembrane molecular transport should be revisited," *Bioelectrochemistry*, vol. 147, p. 108216, 2022.

- **Paper 4: M. Scuderi,** J. Dermol-Černe, T. Batista Napotnik, S. Chaigne, O. Bernus, D. Benoist, D. C. Sigg, L. Rems, and D. Miklavčič, "Characterization of Experimentally Observed Complex Interplay between Pulse Duration, Electrical Field Strength, and Cell Orientation on Electroporation Outcome Using a Time-Dependent Nonlinear Numerical Model," *Biomolecules*, vol. 13, no. 5, p. 727, 2023.

This work was supported by the Slovenian Research and Innovation Agency (ARIS) by research core funding no. P2-0249 and by Medtronic, Inc. Experiments were performed within the Network of the research infrastructural centres of the University of Ljubljana, which is financially supported by the Slovenian Research and Innovation Agency through infrastructural grant I0-0022. Other specific acknowledgments are indicated in the included papers. Unless otherwise indicated, all illustrations are the original work of the author.

Acknowledgements

I am deeply grateful to my mentors Dr. Lea Rems and Dr. Janja Dermol-Černe. Thank you for your guidance, encouragement, and constructive feedback which were essential in achieving the set goals of my thesis. Most of all thank you for always being there for me when I needed help and for your patience.

I would also like to thank Prof. Dr. Damijan Miklavčič for providing me the opportunity to join the LBK group and to work on many interesting projects. Thank you for introducing me to the scientific world, and for the suggestions, knowledge, and support during my Ph.D. study.

I would like to thank Dr. Aswin Muralidharan, Clarissa Amaral da Silva, and Prof. Dr. Pouyan E. Boukany of the Delft University of Technology, Department of Chemical Engineering, for the interesting discussions about electroporation models, Prof. Dr. Janez Ščančar and Dr. Stefan Marković of the Jožef Stefan Institute, Department of Environmental Sciences who measured the cisplatin samples with inductively coupled plasma-mass spectrometry, Dr. Sebastien Chaigne, Prof. Dr. Olivier Bernus, and Dr. David Benoist of IHU-Lyric University of Bordeaux for performing in vitro experiments on rat cardiomyocyte, and Dr. Daniel C. Sigg working at Medtronic for the interesting discussions on pulsed field ablation.

I would like to thank my colleagues and ex-colleagues of the Laboratory of Biocybernetics. Thank you for the stimulating discussions, for your comments, and for your help. Thank you for making the office a friendly and welcoming place to work.

Last but not least, I am extremely grateful to my family who always supported me and believed in me. Thank you to all my friends who always cheered me up and encouraged me to persevere during tough times.

Table of Contents

Abstract

Electroporation is a phenomenon which results in transient increase in cell membrane permeability for ions and molecules when exposing biological cells to short high-voltage electric pulses. If cells survive the exposure to electric pulses, electroporation is called reversible; otherwise, if cells die, electroporation is called irreversible. Electroporation is used in biomedicine for electrochemotherapy, gene electrotransfer, transdermal drug delivery, DNA vaccination, and as an ablation method to treat heart arrhythmia and tumors. It is also used for various purposes in biotechnology, food processing, and environmental applications, such as extraction of compounds from plant tissue, inactivation of bacteria, cell fusion, and genetic engineering of microorganisms.

Electrochemotherapy uses electroporation to enhance the delivery of chemotherapeutic drugs into tumor cells. It is successfully used in clinics to treat cutaneous and subcutaneous tumors with ongoing trials for the treatment of deep-seated tumors. However, the monopolar pulses with duration of 100 µs, used classically for electrochemotherapy, cause pain and muscle contractions. To overcome these drawbacks the use of bursts of high-frequency short bipolar pulses has been suggested. Furthermore, recent efforts have been focused on making electrochemotherapy a systemic treatment by combining it with gene electrotransfer for immunotherapy. Gene electrotransfer is also based on electroporation, where millisecond pulses are used for intracellular delivery of DNA molecules that code for proteins able to stimulate the immune response. Thus, using pulse types alternative to classical 100 µs pulses could be beneficial for improving the electrochemotherapy treatment. However, it is not well understood whether different types of pulses can be equally effective for electrochemotherapy. Therefore, the first aim of the dissertation was to investigate how different types of pulses affect cisplatin uptake and cytotoxicity. We performed *in vitro* experiments using cisplatin and three types of pulses: classical electrochemotherapy pulses, high-frequency bipolar pulses, and millisecond pulses. We demonstrated that all tested types of pulses can be considered equivalent in terms of cisplatin uptake and cytotoxicity and can potentially replace classical, i.e., monopolar 100 µs electrochemotherapy pulses.

For electrochemotherapy to be successful two main conditions need to be met: (i) the entire tumor must be exposed to a sufficiently high electric field that results in

electroporation of the tumor cells and (ii) a sufficient amount of a chemotherapeutic drug (typically bleomycin or cisplatin) must enter the cells to bind to DNA and kill the tumor cells. The pulse parameters needed to successfully treat cutaneous tumors are provided in the standard operating procedures, whereas the treatment of deep-seated tumors is guided by a computational model that predicts the distribution of the electric field inside a tissue depending on the electrode configuration. To further improve such computational treatment planning, it would be useful to upgrade the model with a description of electroporation and the associated uptake of chemotherapeutic drugs into tumor cells. To enable the development of such models, it is necessary to determine the number of cisplatin molecules needed inside the cell to achieve a cytotoxic effect. Therefore, the second aim of the dissertation was to quantify the number of cisplatin molecules, delivered into cells by different types of pulses, and determine the lethal number that results in eradication of almost all treated cells. We found that the number of cisplatin molecules needed to achieve a cytotoxic effect is in the range of 2-7 $\times 10^7$ molecules per cell, irrespective of the type of pulses used.

Mathematical models are also useful for understanding the phenomenon of electroporation. Many different models that describe electroporation and the associated transmembrane molecular transport are present in the literature. Whilst these models differ in their theoretical description, they typically show good agreement with a specific set of data. It is not clear if any of the models can be applied to describe the molecular transport for the broad range of pulse parameters and other experimental conditions used in electroporation research. Therefore, the third aim of the dissertation was to critically assess existing mechanistic models describing electroporation-mediated transmembrane transport of ions and molecules at the single-cell level. We confronted the models with a broad range of experimental measurements and observed that none of the models was reliable enough to predict molecular transport in all tested conditions. We underlined the limitations of the models and proposed further research to improve them. Nevertheless, the existing models can still help interpret certain experimental results, such as the influence of cardiomyocyte orientation on electroporation using pulses of different durations.

Keywords: electroporation, electrochemotherapy, cisplatin, numerical modeling, molecular transport.

Povzetek

Če biološko celico izpostavimo električnemu polju z dovolj visoko jakostjo, dosežemo začasno povečanje prevodnosti in prepustnosti celične membrane. Ta pojav se imenuje elektroporacija. Če celice preživijo izpostavljenost električnim pulzom, se elektroporacija imenuje reverzibilna; če celice umrejo, se elektroporacija imenuje ireverzibilna. Elektroporacija se v biomedicini uporablja pri elektrokemoterapiji, genski terapiji, vnosu zdravilnih učinkovin skozi kožo, cepljenju z DNK ter kot metoda ablacije za zdravljenje srčnih aritmij ali tumorjev. Uporablja se tudi za različne namene v biotehnologiji in predelavi hrane, na primer za ekstrakcijo snovi iz rastlinskega tkiva, uničevanje bakterij, zlivanje celic in genski inženiring mikroorganizmov.

Pri elektrokemoterapiji z elektroporacijo izboljšamo vnos kemoterapevtskih učinkovin v tumorske celice, kar se v klinikah uspešno uporablja za zdravljenje kožnih in podkožnih tumorjev, v teku pa so tudi študije za zdravljenje globlje ležečih tumorjev. Monopolarni pulzi s trajanjem 100 µs, ki jih običajno dovajamo pri elektrokemoterapiji, povzročajo bolečine in krčenje mišic. Z dovajanjem vlakov visokofrekvenčnih kratkih bipolarnih pulzov lahko omilimo bolečine in krčenje mišic. Nedavno so se pojavile študije, kjer elektrokemoterapijo kombiniramo z imunsko gensko terapijo in dosežemo sistemsko zdravljenje. Pri genski terapiji, ki temelji na elektroporaciji, se uporabljajo milisekundni pulzi za znotrajcelični prenos molekul DNK, ki kodirajo beljakovine, sposobne spodbuditi imunski odziv. Z dovajanjem različnih pulzov, ki so alternativni klasičnim 100 µs pulzom, bi lahko izboljšali zdravljenje z elektrokemoterapijo. Ker še ni povsem jasno, ali so lahko različne vrste pulzov enako učinkovite pri elektrokemoterapiji, je bil prvi cilj disertacije raziskati, kako različne vrste pulzov vplivajo na vnos cisplatina in na citotoksičnost. Izvedli smo poskuse in vitro z dovajanjem cisplatina in treh vrst pulzov: klasičnih elektrokemoterapevtskih pulzov, visokofrekvenčnih bipolarnih pulzov in milisekundnih pulzov. Dokazali smo, da lahko vse preizkušene vrste pulzov štejemo za enakovredne v smislu vnosa cisplatina in citotoksičnosti.

Za uspešno elektrokemoterapijo morata biti izpolnjena dva glavna pogoja: i) celoten tumor mora biti izpostavljen dovolj visokemu električnemu polju, ki povzroči elektroporacijo tumorskih celic, in ii) zadostna količina kemoterapevtika (običajno bleomicina ali cisplatina) mora vstopiti v celice, da se veže na DNK in uniči tumorske celice.

Parametri pulzov, ki so potrebni za uspešno zdravljenje kožnih tumorjev, so določeni v standardnih operativnih postopkih, medtem ko je zdravljenje globokih tumorjev načrtovano z računalniškim modelom, ki predvideva porazdelitev električnega polja v tkivu glede na postavitev elektrod. Za nadaljnje izboljšanje takšnega računalniškega načrtovanja zdravljenja bi bilo koristno model nadgraditi z opisom elektroporacije in z njo povezanega vnosa kemoterapevtskih učinkovin v tumorske celice. Za razvoj takih modelov je treba določiti število molekul cisplatina, potrebnih v celici za citotoksični učinek. Drugi cilj disertacije je bil torej izmeriti število molekul cisplatina, ki jih v celice vnesemo z različnimi vrstami pulzov, in določiti zadostno število, ki povzroči celično smrt. Ugotovili smo, da je število molekul cisplatina, potrebnih za doseganje citotoksičnega učinka, v razponu 2-7 $\times 10^7$ molekul na celico ne glede na vrsto dovedenih pulzov.

Za razumevanje pojava elektroporacije so koristni matematični modeli. V literaturi je veliko različnih modelov, ki opisujejo elektroporacijo in z njo povezan prenos molekul skozi celično membrano. Čeprav se ti modeli razlikujejo v svojem teoretičnem opisu, običajno kažejo dobro ujemanje z določenim nizom podatkov. Ni jasno, ali je mogoče katerega od modelov uporabiti za opis molekularnega transporta za širok razpon parametrov pulzov in drugih eksperimentalnih pogojev. Tretji cilj disertacije je bil kritično oceniti obstoječe mehanistične modele transporta ionov in molekul skozi elektroporirano celično membrano. Modele smo preverjali na širokem naboru eksperimentalnih meritev in ugotovili, da nobeden od modelov ni bil dovolj zanesljiv za napoved molekularnega transporta v vseh preizkušenih pogojih. Poudarili smo omejitve modelov in predlagali nadaljnje raziskave za izboljšanje in nadgradnjo obstoječih modelov. Kljub omejitvam lahko obstoječi modeli še vedno pomagajo pri razlagi nekaterih eksperimentalnih rezultatov, na primer vpliva orientacije kardiomiocitov v električnem polju in trajanja pulzov na učinkovitost elektroporacije.

Ključne besede: elektroporacija, elektrokemoterapija, cisplatin, numerično modeliranje, molekularni transport.

Razširjeni povzetek v slovenščini

I. Uvod

Če biološko celico izpostavimo električnemu polju z dovolj visoko jakostjo, dosežemo začasno povečanje prevodnosti in prepustnosti celične membrane. Ta pojav se imenuje elektroporacija. Elektroporacija omogoča povečan transport ionov in molekul, za katere je celična membrana v normalnih pogojih slabo prepustna ali celo neprepustna, skozi celično membrano [1], [2]. Elektroporacija je lahko reverzibilna ali ireverzibilna. Če si celice po izpostavitvi električnemu polju opomorejo in ponovno vzpostavijo homeostazo, pojav imenujemo reverzibilna elektroporacija. Če pa so poškodbe prevelike in celice odmrejo, pojav imenujemo ireverzibilna elektroporacija. Elektroporacijo uporabljamo v biomedicini: reverzibilno elektroporacijo pri elektrokemoterapiji, genski terapiji in vnosu zdravilnih učinkovin skozi kožo, ireverzibilno elektroporacijo pa kot metodo odstranjevanja tkiva za zdravljenje tumorjev ali srčnih aritmij [3]–[7], v biotehnologiji [8] in v živilski tehnologiji [9].

I.1 Elektrokemoterapija

Elektrokemoterapija (EKT) predstavlja varno in učinkovito lokalno zdravljenje kožnih in podkožnih tumorjev različnih histologij [10], [11]. Leta 2006 so bili objavljeni standardni operativni postopki za uspešno zdravljenje kožnih tumorjev s premerom manjšim od 3 cm [12], [13], pred kratkim pa so bili standardni operativni postopki prilagojeni tudi za zdravljenje večjih tumorjev [14]. Danes je EKT uveljavljeno zdravljenje po vsej Evropi, kar dokazuje vključenost v smernice Nacionalnega inštituta za zdravje in klinično odličnost v Združenem kraljestvu (*angl.* National Institute for Health and Care Excellence) [15], [16] in pred kratkim objavljeni Evropski interdisciplinarni dokumenti na podlagi soglasja (*angl.* European consensus-based interdisciplinary documents) za zdravljenje ploščatoceličnega karcinoma kože, bazalnoceličnega karcinomoma, melanoma in Kaposijevega sarkoma [17]–[22]. V teku so tudi raziskave za zdravljenje globlje ležečih tumorjev z EKT [23]–[28].

Pri EKT najprej v žilo ali v tumor vnesemo kemoterapevtik, nato na tumorsko tkivo dovedemo kratke visokonapetostne električne pulze, ki zagotovijo elektroporacijo celične membrane, glej sliko I.1. Kemoterapevtski zdravili, ki se najpogosteje uporabljata pri EKT, sta bleomicin in cisplatin [29]. Elektroporacija poveča vnos in posledično citotoksičnost bleomicina za več sto do tisočkrat, cisplatina pa za več desetkrat v primerjavi z

neelektroporirano kontrolo [30]–[32]. Posledično so pri EKT za doseganje citotoksičnega učinka potrebni manjši odmerki kemoterapevtskih zdravil kot pri standardni kemoterapiji.

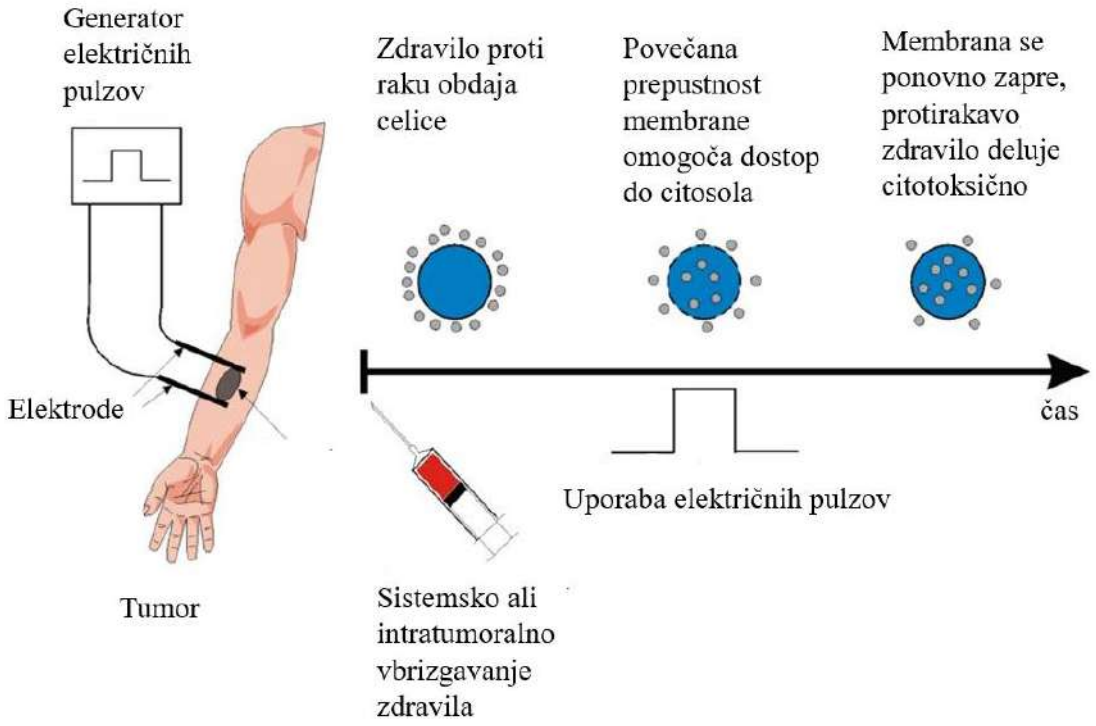

Slika I.1. Shema za zdravljenje z EKT. Najprej bolniku v žilo ali v tumor vbrizgamo kemoterapevtik. Nato dovedemo električne pulze, ki zagotovijo elektroporacijo tumorskih celic in omogočijo vnos kemoterapevtika v celice. Kemoterapevtik se veže na DNK tumorskih celic in prepreči njihovo delitev, kar povzroči smrt tumorskih celic. Slika je povzeta po [29].

Pri EKT običajno s ponavljalno frekvenco 1 Hz ali 5 kHz dovedemo osem 100 µs dolgih monopolarnih pulzov [14], glej sliko I.2a. Dovajanje tovrstnih pulzov na tumorsko tkivo lahko povzroči tudi neželeno stimulacijo okoliških vzdražnih celic, tj. mišičnih in živčnih celic (npr. motoričnih živcev in nociceptorjev), kar pri bolniku med dovajanjem pulzov povzroči nehoteno krčenje mišic in bolečino. Pri EKT moramo zato uporabiti lokalno ali splošno anestezijo in sredstva za sproščanje mišic, pri zdravljenju globlje ležečih tumorjev v bližini srca pa moramo dovajanje pulzov uskladiti s srčnim ritmom [33], [34]. Bolečine in krčenje mišic je mogoče nekoliko ublažiti z dovajanjem pulzov z višjo ponavljalno frekvenco [35], [36] in s prilagoditvijo oblike elektrod [37], [38], največ pa obeta uporaba posebne oblike pulzov, tj. vlakov visokofrekvenčnih kratkih bipolarnih pulzov [37], [39], glej sliko I.2b. Te vlake pulzov dovajamo s ponavljalno frekvenco približno 1 Hz. Vsak vlak pulzov je sestavljen iz zaporedja bipolarnih pulzov, pri čemer ima vsak pulz 0,5−10 µs dolg pozitiven in negativen del. Ponavljalna frekvenca posameznih

bipolarnih pulzov v vlaku znaša več 100 kHz. Številne študije na živalih [40]–[42] in ljudeh [39], [43] so pokazale, da z vlaki visokofrekvenčnih kratkih bipolarnih pulzov ublažimo bolečino in mišično krčenje v primerjavi z daljšimi monopolarnimi pulzi. Nadalje sta študiji *in vitro* [44] in na živalih [45] pokazali, da se lahko vlaki visokofrekvenčnih kratkih bipolarnih pulzov uporabimo tudi za vnos kemoterapevtskih učinkovin v tumorske celice pri EKT. Nedavni pregled študij na ljudeh je pokazal varnost in učinkovitost uporabe vlakov visokofrekvenčnih kratkih bipolarnih pulzov za zdravljenje kožnih tumorjev z EKT [46].

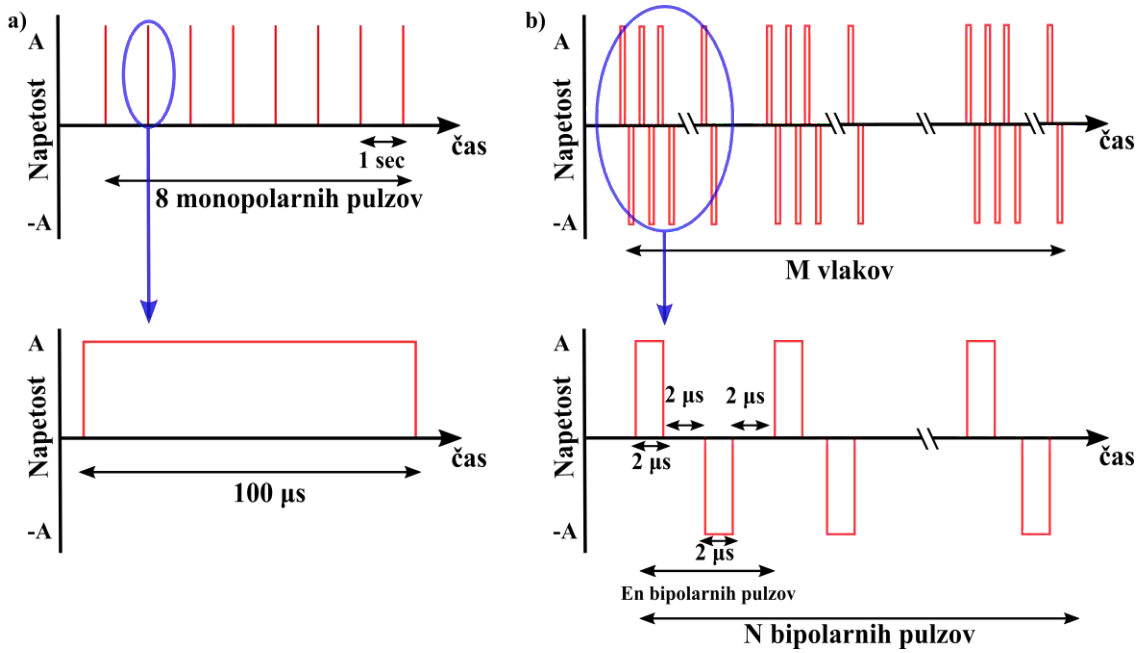

Slika I.2. Primerjava klasičnih pulzov, ki se uporabljajo za EKT, in vlaka visokofrekvenčnih kratkih bipolarnih pulzov. a) Klasični EKT pulzi: osem 100 µs dolgih monopolarnih pulzov, dovedenih s ponavljalno frekvenco 1 Hz (*zgoraj*) s trajanjem posameznega pulza 100 µs (*spodaj*). b) Vlaki visokofrekvenčnih kratkih bipolarnih pulzov: M vlakov s ponavljalno frekvenco 1 Hz (*zgoraj*). Vsak vlak je sestavljen iz N bipolarnih pulzov s kratkim trajanjem posameznega pulza približno 2 µs in visoko ponavljalno frekvenco 125 kHz (*spodaj*).

EKT poveča vnos in citotoksičnost kemoterapevtikov v tumorske celice, začasno zmanjša pretok krvi v tumorju in povzroči aktivacijo imunskega odziva. Vse to prispeva k uspešnemu uničenju tumorja. Začasno zmanjšanje pretoka krvi podaljša zadrževanje zdravila v tumorskem tkivu na več ur. Poleg tega lahko EKT povzroči tudi smrt endotelijskih celic in s tem uničenje žil, kar vodi v smrt tumorskih celic zaradi dolgotrajne hipoksije [47]–[49]. Tudi imunski odziv ima pomembno vlogo pri zdravljenju z EKT. Sproščanje molekul iz elektroporiranih celic, med katerimi so tudi s poškodbo povezani molekulski vzorci (vzorci DAMP, *angl.* damage-associated molecular patterns) in tumorski antigeni, lahko spodbudi imunski sistem in aktivira imunogeno celično smrt. V številnih študijah na pasjih in človeških bolnikih so preizkusili EKT v kombinaciji z gensko terapijo (GET) s plazmidno

DNK z zapisom za interlevkin-12 (IL-12), ki spodbuja imunski sistem [50], [51]. Kombinirano zdravljenje z EKT in GET je bilo doslej uporabljeno le pri nekaterih kožnih metastazah, vendar je uspešno izzvalo sistemski imunski odziv in v nekaterih primerih uspelo povzročiti delni ali popolni odziv oddaljenih, nezdravljenih zasevkov (abskopalni učinek).

Študije torej kažejo, da bi zamenjava klasičnih EKT pulzov (8 × 100 μs) s pulzi drugačnih oblik oz. z drugačno vrsto pulzov lahko imela določene prednosti. Vlaki visokofrekvenčnih kratkih bipolarnih pulzov bi bili manj boleči in bi povzročali manj neželenega krčenja mišic med izvajanjem EKT. Pri kombiniranju EKT in GET se trenutno za EKT uporabljajo klasični EKT pulzi, za GET pa daljši milisekundni pulzi, ki naj bi bili učinkovitejši za vnos plazmidne DNK v celice tkiva. Če bi za EKT lahko uporabili isto vrsto pulzov kot za GET, bi kombinacijo EKT in GET lahko izvajali s preprostejšimi in cenovno dostopnejšimi generatorji električnih pulzov. Vseeno pa je najprej potrebno določiti primerljivost različnih vrst pulzov za povečanje vnosa in kemoterapevtikov.

I.2 Elektroporacija in transport molekul skozi celično membrano

Celična membrana je sestavljena iz lipidnega dvosloja in v membrano vgrajenih beljakovin. Pri fizioloških pogojih celična membrana deluje kot selektivna pregrada, ki ločuje notranjost celice od zunanjosti in omogoča prehajanje skozi membrano le določenim ionom in molekulam. Zapleten sistem membranskih proteinov med drugim vključuje ionske kanale in črpalke. Ionski kanali in črpalke na membrani vzdržujejo mirovno transmembransko napetost (TMN), ki se glede na vrsto celice giblje med −40 mV in −90 mV [52], [53]. Lipidi in membranski proteini so evolucijsko dobro prilagojeni na delovanje pod takimi napetostmi.

Celico lahko z električnega vidika obravnavamo kot prevodno telo (citosol), obdano z dielektrično ovojnico (celična membrana) v prevodni zunajcelični raztopini. Ko celico izpostavimo električnemu polju, se na membrani ustvari dodatna, vsiljena TMN, ki se prišteje mirovni TMN. Če seštevek mirovne in vsiljene TMN doseže dovolj visoko vrednost, se v celični membrani pojavijo strukturne spremembe, ki povečajo njeno prepustnost za ione in molekule [54]–[56]. Simulacije molekularne dinamike [57], teoretično modeliranje [58] in poskusi na lipidnih dvoslojih [59] kažejo, da se z višanjem TMN poveča verjetnost nastanka por v lipidnem dvosloju [60]–[62]. Nastanek por v

lipidnem dvosloju je danes splošno sprejet mehanizem elektroporacije. Električni pulzi poleg nastanka por povzročajo še kemične spremembe lipidov zaradi lipidne peroksidacije [63], [64] in lahko poškodujejo ali vplivajo na delovanje nekaterih membranskih proteinov, kot so napetostno odvisni ionski kanali [65]–[67]. Tako peroksidacija lipidov kot poškodbe membranskih proteinov prispevajo k povečani prepustnosti celične membrane.

Na vsiljeno TMN vplivajo geometrija in orientacija celic v električnem polju ter prevodnost zunajcelične raztopine [68]–[70]. Vsiljena TMN se povečuje sorazmerno z jakostjo zunanjega električnega polja. Poleg tega se vsiljena TMN spreminja s položajem na celični membrani in doseže največjo absolutno vrednost na delih membrane, ki so najbližje elektrodama [71]–[73]. Povečanje prepustnosti celične membrane opazimo le na območju membrane, kjer TMN po absolutni vrednosti preseže določeno kritično vrednost [72], [74], [75]. Poleg same vrednosti TMN na povečanje prepustnosti vplivajo še drugi dejavniki, kot so parametri dovedenih električnih pulzov (število, oblika, trajanje in jakost) ter ionska sestava zunajcelične raztopine.

Povečanje prepustnosti membrane lahko zaznamo na več načinov, npr. i) s tehniko vpete krpice membrane (*angl.* patch clamp), s katero neposredno merimo spremembe ionskega toka skozi celično membrano ali napetosti na ravni celične membrane [76], [77], ii) z meritvami sprememb prevodnosti gostih celičnih suspenzij, iz katerih lahko določimo spremembe v prevodnosti celične membrane [78], [79], iii) s spremljanjem osmotskega nabrekanja celic po elektroporaciji [80], [81], najpogosteje pa z iv) opazovanjem transporta molekul, ki sicer slabo prehajajo membrano, skozi celično membrano. Primeri takih molekul so fluorescenčna barvila, nanodelci, kemoterapevtiki in nukleinske kisline [82].

Transport majhnih molekul (< 4 kDa) skozi elektroporirano membrano lahko poteka s pomočjo naslednjih mehanizmov: difuzija, elektroforeza, elektroosmoza in endocitoza [1], [83]–[85], glej sliko I.3. Med dovajanjem pulzov, ko je prisotno zunanje električno polje, je transport molekul pretežno posledica elektroforeze in deloma elektroosmoze. Po koncu dovajanja pulzov je transport pretežno posledica difuzije, deloma pa tudi elektroforeze zaradi neničelne TMN [86]. Po dovajanju pulzov je mogoče opaziti tudi vnos molekul v celico z endocitozo [83], [87]. Transport makromolekul, kot je DNK, skozi celično membrano je precej bolj zapleten proces v primerjavi s transportom majhnih molekul [83], [88], [89]. Pri transportu DNK ima pomembno vlogo elektroforeza, zato se za vnos DNK v

celico večinoma uporabljajo daljši milisekundni pulzi [90] ali kombinacija močnega kratkega pulza in enega ali več šibkih dolgih pulzov [91], [92].

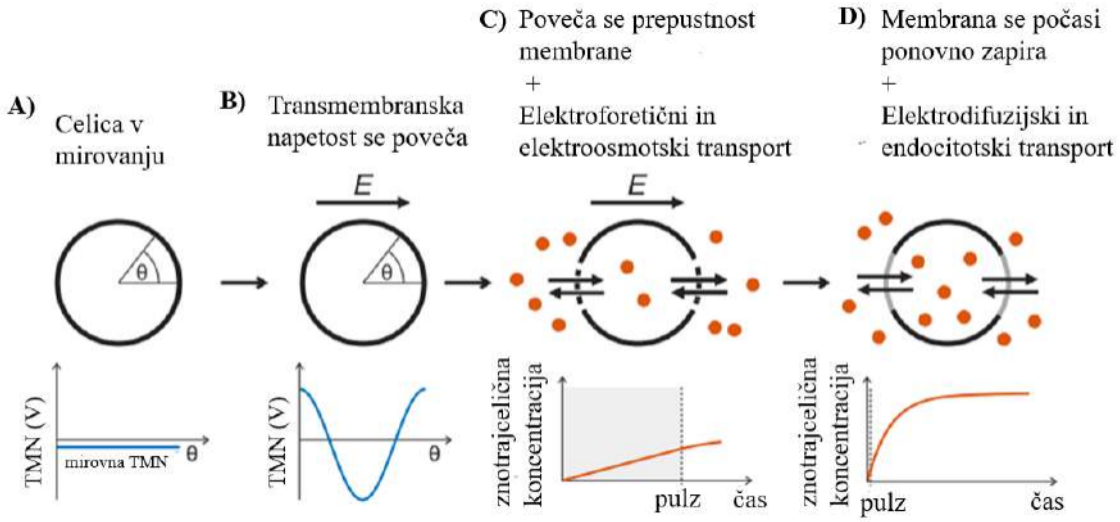

Slika I.3. Shematski prikaz elektroporacije in transporta molekul skozi celično membrano. A) Celica v mirovanju. B) Ob izpostavitvi celice električnemu polju se ustvari vsiljena TMN, ki se spreminja glede na položaj na membrani. C) Na območjih, kjer TMN preseže določen prag, se poveča transport ionov in molekul skozi celično membrano (vnos in iznos). Rdeče pike na sliki prikazujejo le vnos molekul v celico. Med pulzom je transport pretežno elektroforetski in deloma elektroosmotski. D) Po pulzu je transport elektrodifuzijski in v nekaterih primerih endocitotski. Po izpostavitvi električnemu polju se celična membrana ponovno zapre in prenos snovi skozi celično membrano se s časom zmanjšuje. Črtkana črta na spodnjem grafu (C, D) označuje konec trajanja pulza. Slika je povzeta po [93].

I.3 Modeli elektroporacije in transporta molekul skozi celično membrano

Matematični modeli pomagajo razumeti osnovne mehanizme biološkega sistema z uporabo fizikalnih in matematičnih zakonov. Hkrati je uporaba matematičnih modelov pogosto manj zamudna in cenejša od eksperimentalnega dela. Elektroporacija je proces, ki vključuje različne prostorsko-časovne ravni, od molekularne ravni (nekaj nanometrov) do ravni tkiva (nekaj centimetrov), in različne fizikalne pojave (električne, termične, kemične itd.). Zato so raziskovalci razvili matematične modele na več ravneh, da bi prostorsko in časovno opisali pojav elektroporacije in z njo povezan transport molekul skozi celično membrano. Te matematične modele lahko v grobem razdelimo na mehanistične in fenomenološke.

Mehanistični modeli temeljijo na fizikalnih in matematičnih zakonih. Parametri mehanističnih modelov imajo fizikalni pomen, kar olajša znanstveno razlago rezultatov. Mehanistični modeli v glavnem pripisujejo povečanje prepustnosti celične membrane nastanku por v lipidnem dvosloju zaradi vpliva TMN. Ena skupina modelov uporablja kinetično shemo, ki opisuje prehod med različnimi stanji por, nastalih v celični membrani

[94], [95]. Prehod med posameznimi stanji por je eksponentno odvisen od TMN. Druga skupina modelov opisuje pore v obliki funkcije porazdelitve por, opisane v prostoru polmera por. Ta funkcija porazdelitve por se dinamično spreminja s TMN [96], [97]. Transport molekul skozi pore lahko opišemo z Nernst-Planckovimi enačbami. Nekateri modeli upoštevajo tako elektroforetski kot difuzijski transport [96], [98], [99], medtem ko nekateri modeli zanemarjajo elektroforetsko komponento in upoštevajo dodatne transportne mehanizme, kot je endocitoza [95].

Fenomenološki modeli opisujejo eksperimentalne podatke brez uporabe fizikalnih ali matematičnih zakonov. Fenomenološki modeli elektroporacije, na katere naletimo v literaturi, so farmakokinetski [85], nadomestna električna vezja [100] ali empirične enačbe, ki opisujejo povečanje prepustnosti [101], [102] ali površinski delež v membrani nastalih por [103], [104].

Trenutno obstaja več modelov, ki opisujejo pojav elektroporacije in transporta molekul skozi celično membrano in so bili kvalitativno in/ali kvantitativno vrednoteni z eksperimentalnimi meritvami. Zanimivo je, da so modeli, ki so bili razviti z upoštevanjem različnih teoretičnih opisov membranske prepustnosti in transporta molekul, pokazali dobro ujemanje z eksperimentalnimi rezultati. Še vedno pa ni jasno, kateri model je najustreznejši za opis pojava elektroporacije in transporta molekul skozi celično membrano ter ali je ta model veljaven v širokem razponu parametrov pulzov in eksperimentalnih pogojev, ki se uporabljajo pri elektroporaciji.

II. Namen

Glavni namen disertacije je bil bolje razumeti pojav reverzibilne elektroporacije in predvsem molekularnega transporta skozi celično membrano pri EKT z izvajanjem poskusov *in vitro* in z uporabo numeričnih modelov na ravni posameznih bioloških celic.

Za uspešno zdravljenje kožnih tumorjev z EKT zdravniki upoštevajo priporočila, zapisana v standardnih operativnih postopkih [13], [14]. Ti postopki določajo vrsto anestezije, vrsto kemoterapevtske učinkovine, način injiciranja učinkovine ter vrste elektrod, generatorjev in parametrov pulzov, ki jih je treba uporabiti za zdravljenje. Po standardnih operativnih postopkih se pri EKT dovede osem monopolarnih pulzov dolžine 100 µs, dovedenih s ponavljalno frekvenco 1 Hz ali 5 kHz. Različne študije kažejo, da bi pulzi z alternativnimi parametri lahko imeli določene prednosti pri zdravljenju z EKT. Pokazano je bilo, da uporaba vlakov visokofrekvenčnih kratkih bipolarnih pulzov omili bolečino in zmanjša krčenje mišic v primerjavi s klasičnimi EKT pulzi [39].

Predklinične in klinične študije so pokazale smiselnost kombinirane terapije EKT in GET. Z GET vnesemo DNK z zapisom za beljakovine, ki spodbujajo imunski odziv, s čimer dosežemo sistemsko zdravljenje tumorjev. GET običajno izvajamo z milisekundnimi pulzi. Pred uporabo alternativnih vrst pulzov za EKT je najprej potrebno ugotoviti, ali so različne vrste pulzov enako učinkovite pri povečanju vnosa in citotoksičnosti kemoterapevtikov kot klasični EKT pulzi. Zato smo v tej disertaciji raziskali učinke različnih vrst pulzov na vnos in citotoksičnost cisplatina v celice *in vitro*.

Za uspeh EKT ne zadostuje le dovajanje dovolj visokega električnega polja, ki poviša prepustnost celičnih membran tumorskega tkiva, temveč moramo obenem v tumorske celice vnesti zadostno količino kemoterapevtske učinkovine. Zato smo v disertaciji eksperimentalno določili število molekul cisplatina, potrebnih za citotoksični učinek pri uporabi različnih vrst pulzov.

Transport molekul skozi elektroporirano celično membrano je ključnega pomena za različna zdravljenja, ki temeljijo na elektroporaciji, med drugim EKT, GET in vnos zdravil skozi kožo. Matematični modeli lahko služijo kot pomembno orodje za preučevanje vpliva parametrov pulzov na transport različnih vrst molekul. Trenutno je v literaturi na voljo veliko različnih modelov, ki opisujejo pojav elektroporacije in transporta skozi celično membrano. Vendar ni jasno, kateri od modelov je najustreznejši ter ali je kateri od modelov veljaven v širokem razponu parametrov pulzov in eksperimentalnih pogojev, ki se

uporabljajo za elektroporacijo. Zato v disertaciji podamo tudi pregled obstoječih matematičnih modelov in jih kritično ocenimo.

III. Rezultati in razprava

Raziskovalno delo, opravljeno v času doktorskega študija, je predstavljeno v štirih člankih, objavljenih v mednarodnih recenziranih revijah s faktorjem vpliva. V tem poglavju so na kratko povzeti in predstavljeni rezultati vsakega izmed njih.

III.1 Bi za elektrokemoterapijo lahko uporabljali različne vrste pulzov?

S poskusi *in vitro* smo želeli ugotoviti, ali je mogoče z vlaki visokofrekvenčnih kratkih bipolarnih pulzov doseči reverzibilno elektroporacijo, ki bi omogočila učinkovit vnos kemoterapevtika cisplatina v celice za namene EKT (članek 1, [44]).

Poskuse *in vitro* smo izvedli na celični liniji mišjega melanoma (B16-F1). Primerjali smo dve različni vrsti pulzov: i) osem monopolarnih pulzov s trajanjem 100 µs in ponavljalno frekvenco 1 Hz ter ii) osem vlakov visokofrekvenčnih kratkih bipolarnih pulzov s ponavljalno frekvenco vlakov 1 Hz. Pri obeh vrstah pulzov je čas, ko se dovedena napetost razlikuje od nič, enak 800 µs. Rezultati naše raziskave kažejo, da je mogoče z uporabo 100 µM cisplatina doseči podoben citotoksični učinek z obema vrstama pulzov ob ustrezno prilagojeni jakosti električnega polja. Le-ta je za klasične EKT pulze znašala 1,2 kV/cm, za vlake visokofrekvenčnih kratkih bipolarnih pulzov pa 3 kV/cm (sliki III.1 in III.2). Ustrezna jakost električnega polja, pri kateri obenem pride do največjega deleža preživelih in največjega deleža celic s povišano prepustnostjo celične membrane, je bila določena na sliki 2 v članku [44]. Poleg tega rezultati, prikazani na slikah III.1 in III.2, kažejo, da se citotoksični učinek cisplatina okrepi, če uporabimo kombinacijo električnih pulzov in cisplatina (polna zelena črta), v primerjavi z uporabo samo cisplatina (prekinjena rdeča črta).

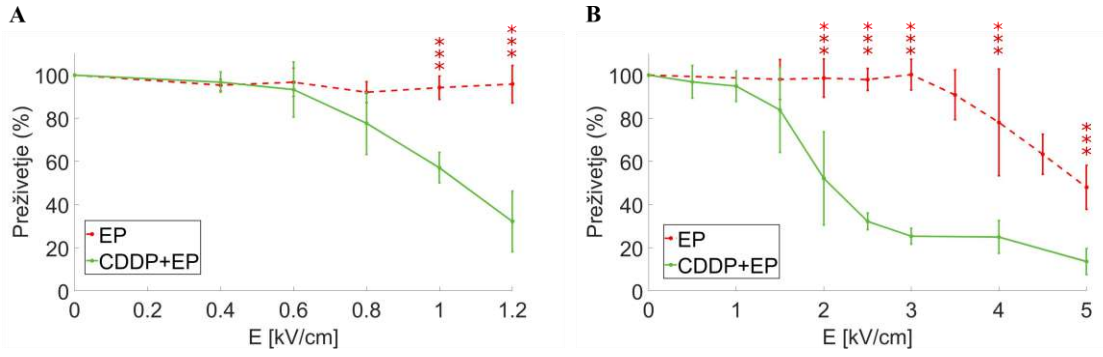

Slika III.1. Citotoksičnost pri koncentraciji cisplatina (CDDP) 100 µM in različnih jakostih električnega polja: (A) osem 100 µs dolgih monopolarnih pulzov, dovedenih s ponavljalno frekvenco 1 Hz; (B) 8 vlakov visokofrekvenčnih kratkih bipolarnih pulzov 1-1-1-1 µs, dovedenih s ponavljalno frekvenco vlakov 1 Hz. Vsaka točka predstavlja povprečje ± standardni odklon 3□6 poskusov. *- Izvedli smo (A) dvofaktorsko analizo variance (ANOVA) ali (B) dvofaktorsko ANOVA na rangih. (A) Pri 0,8 kV/cm (P = 0,036), 1 kV/cm in 1,2 kV/cm (P < 0,001) so se elektroporirani (EP) vzorci statistično razlikovali od CDDP+EP vzorcev. (B) Pri električnih poljih > 2 kV/cm, so se EP vzorci statistično razlikovali od CDDP+EP vzorcev (P < 0,001). Slika je povzeta po [44].

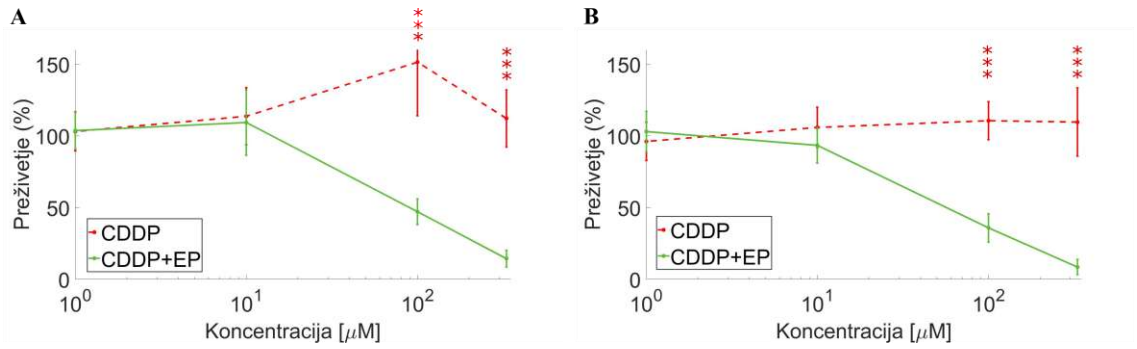

Slika III.2. Citotoksičnost pri različnih koncentracijah cisplatina (CDDP) in stalnem električnem polju: (A) 1,2 kV/cm, osem 100 µs dolgih monopolarnih pulzov s ponavljalno frekvenco 1 Hz; (B) 3 kV/cm, 8 vlakov visokofrekvenčnih kratkih bipolarnih pulzov 1-1-1-1 µs, dovedenih s ponavljalno frekvenco vlakov 1 Hz. Vsaka točka predstavlja povprečje ± standardni odklon 3□7 poskusov. *- CDDP vzorci so se statistično razlikovali od CDDP+EP vzorcev (EP = elektroporacija) (P < 0,001). Slika je povzeta po [44].

V naslednji študiji smo poleg vlakov visokofrekvenčnih kratkih bipolarnih pulzov preučevali tudi vpliv milisekundnih pulzov na vnos in citotoksičnost cisplatina (članek 2). Milisekundni pulzi se običajno uporabljajo za vnos plazmidne DNK, ki kodira beljakovine za stimulacijo imunskega odziva pri kombiniranju EKT in GET. Izvedli smo poskuse EKT *in vitro* z uporabo treh različnih vrst pulzov: i) osem monopolarnih 100 µs dolgih pulzov, ki se običajno uporabljajo pri EKT, ii) osem vlakov visokofrekvenčnih kratkih bipolarnih pulzov in iii) osem 5 ms pulzov. Pri vseh treh različnih vrstah pulzov smo opazili podoben vnos in citotoksični učinek cisplatina (slika III.3), pri čemer je bila jakost posamezne vrste pulzov ustrezno prilagojena.

S kombinacijo rezultatov na slikah III.3A in B smo določili število molekul cisplatina, ki je potrebno za doseganje citotoksičnega učinka. To število je v razponu 2–7×10^7 molekul cisplatina na celico, ne glede na vrsto pulzov, kar prikazuje slika III.3C. Razpon števila molekul cisplatina za doseganje citotoksičnega učinka se ujema s predhodno študijo, ki so jo objavili Vižintin in sod. [105]. V omenjeni študiji so uporabili enake eksperimentalne protokole kot v naši študiji, pri čemer so primerjali klasične EKT pulze z nanosekundnimi pulzi.

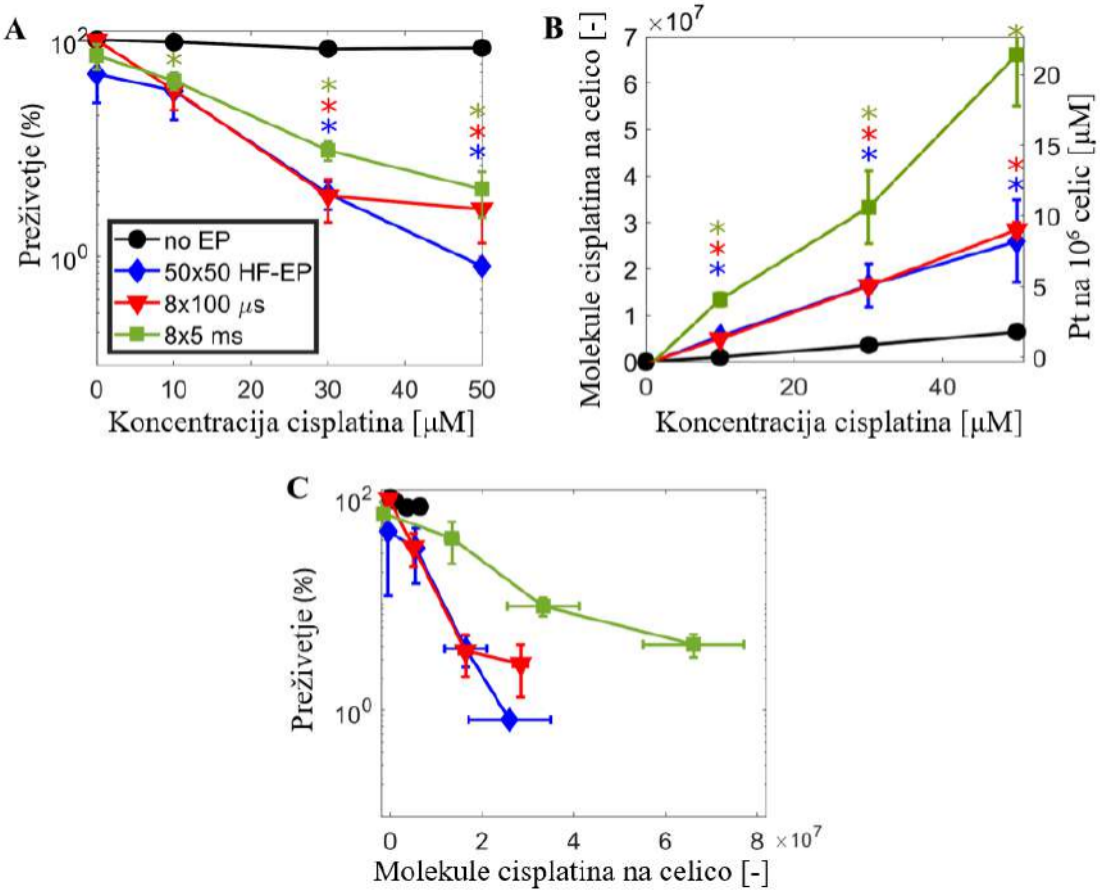

Slika III.3. Citotoksičnost cisplatina (A) in število molekul cisplatina na celico (B) pri različnih koncentracijah cisplatina in fiksni jakosti električnega polja: 1,4 kV/cm za vlake visokofrekvenčnih bipolarnih pulzov, 1,2 kV/cm za 8 × 100 µs pulze in 0,6 kV/cm za 8 × 5 ms pulze. Vsaka točka predstavlja povprečje ± standardni odklon 3–4 poskusov. *- Statistično značilne razlike v primerjavi s kontrolo ($p < 0,05$) z dvofaktorskim testom ANOVA. Barva zvezdice ustreza barvi črte za določeno vrsto testirano pulzov. C) Preživetje celic kot funkcija števila molekul cisplatina na celico v kombinaciji z elektroporacijo. Slika je povzeta po [106].

V študiji smo uporabili fenomenološki model, ki opisuje pojav elektroporacije in transport molekul skozi celično membrano. Ugotovili smo, da model dobro napove velikostni razred števila molekul cisplatina znotraj posamezne celice za vse testirane vrste pulzov (klasični EKT pulzi, nanosekundnih pulzi, milisekundni pulzi in vlaki visokofrekvenčnih kratkih bipolarnih pulzov), vendar je potrebna nadaljnja optimizacija modela za točnejše rezultate.

III.2 Vrednotenje mehanističnih modelov elektroporacije

Matematični modeli so ključno orodje za preučevanje odziva celic na izpostavitev električnim pulzom. Primerjava rezultatov modeliranja z eksperimentalnimi podatki lahko znanstvenikom pomaga bolje razumeti pojav elektroporacije. Zato smo se odločili proučiti

obstoječe mehanistične modele, ki opisujejo pojav elektroporacije in molekularnega transporta skozi celično membrano na ravni posamezne celice. Študijo smo pričeli s pregledom obstoječe literature, nato pa smo izbrali tri reprezentativne modele za nadaljnjo analizo: Miklavčič in Towhidi [95], Li in sod. [98], [99], in Smith [96]. Te modele v nadaljevanju označujemo kot MT2010 [95], LL2011 [98], [99], in S2011 [96]. Veljavnost modelov smo ovrednotili tako, da smo napovedi modelov primerjali z različnimi nabori eksperimentalnih meritev transporta majhnih molekul skozi celično membrano.

Napovedi modela MT2010 sta avtorja v svojem članku primerjala s kvalitativnimi meritvami znotrajcelične koncentracije barvila lucifer rumeno, izmerjenimi po izpostavitvi celic 1 ms dolgim pulzom različnih oblik, kar so v okviru predhodne študije opravili Kotnik in sod. [107]. V naši študiji smo model MT2010 nadalje primerjali s kvantitativnimi meritvami znotrajcelične koncentracije barvila lucifer rumeno, izmerjenimi po izpostavitvi celic pulzu dolžine bodisi 1 ms bodisi 100 µs [85]. Ugotovili smo, da model MT2010 precenjuje eksperimentalne vrednosti znotrajcelične koncentracije za en velikostni razred (slika III.4). S tem smo pokazali, da kvalitativno primerjanje napovedi modela z eksperimentalnimi meritvami ne zadostuje za validacijo modela.

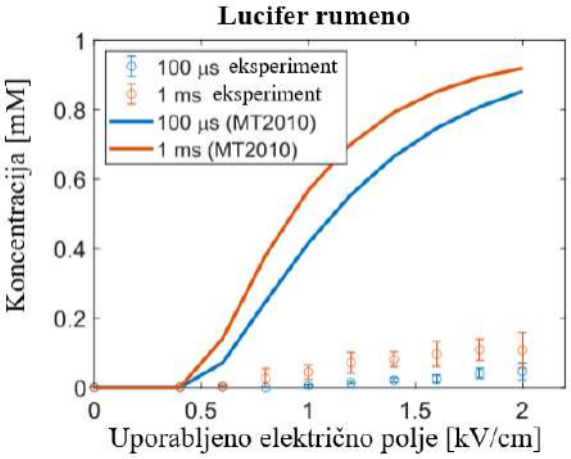

Slika III.4. Znotrajcelična koncentracija barvila lucifer rumeno kot funkcija jakosti električnega polja po dovajanju enega pulza dolžine bodisi 100 µs bodisi 1 ms. Krogi prikazujejo eksperimentalne meritve znotrajcelične koncentracije iz Puc et al. [85], polne črte pa napovedi modela MT2010. Slika je povzeta po [93].

Model S2011 je bil prvotno primerjan s kvantitativnimi eksperimentalnimi meritvami končnega vnosa barvila lucifer rumeno (Puc in sod. [85]) ter končnega vnosa kalceina (Canatella in sod. [108]) in se je z eksperimentalnimi rezultati odlično ujemal. V naši študiji smo model S2011 dodatno primerjali s kvantitativnimi meritvami časovnih

sprememb znotrajcelične koncentracije kalceina in propidija, ki so jih izmerili Sözer in sod. [109] pri izpostavitvi celic enemu 220 μs dolgemu pulzu jakosti 2,5 kV/cm, (glej sliko 4 članka 3 [93]) ali desetih 6 ns dolgih pulzov jakosti 200 kV/cm (slika III.5). Naši izračuni so pokazali, da model ni ustrezno opisal meritev Sözer in sod. S tem smo ugotovili, da za validacijo modela niso dovolj kvantitativne meritve končnega vnosa molekul, ampak so potrebne tudi meritve kinetike.

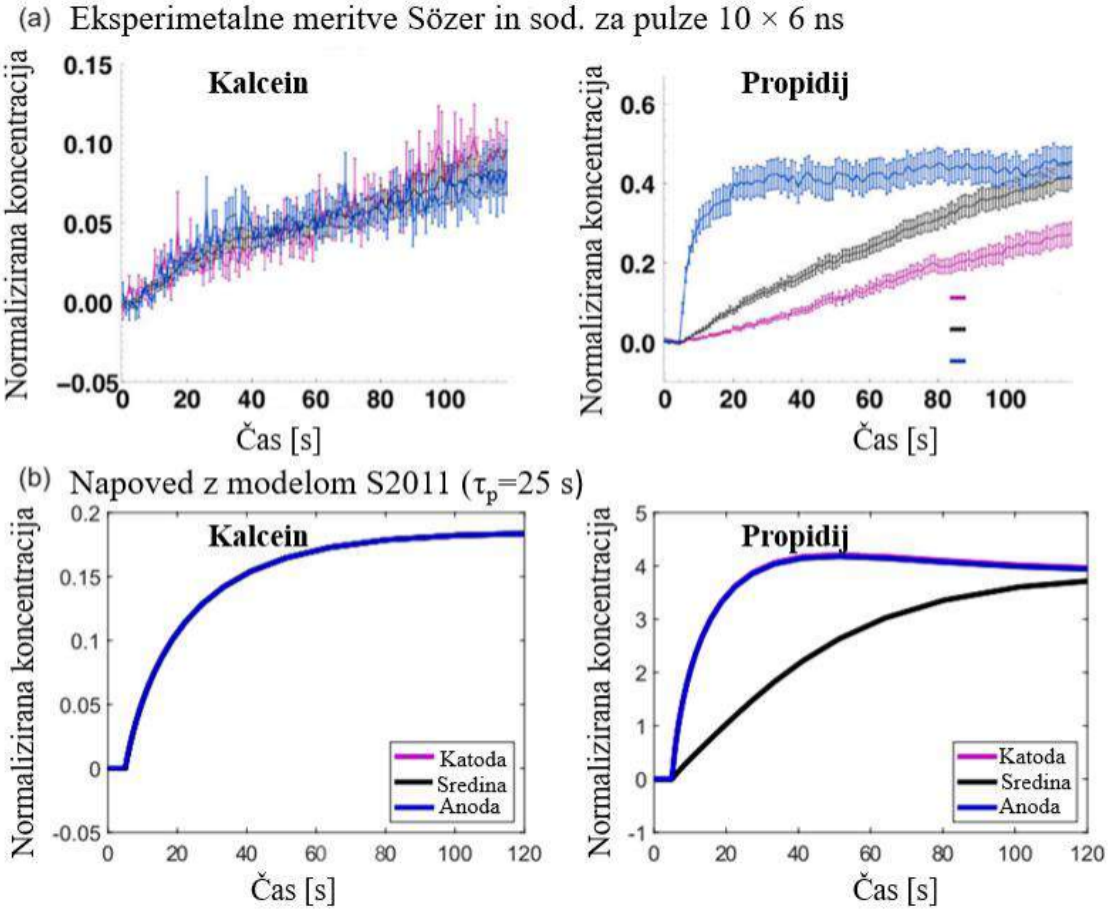

Slika III.5. Znotrajcelična koncentracija kalceina in propidija po dovajanju desetih pulzov dolžine 6 ns in jakosti 200 kV/cm. Znotrajcelična koncentracija je normalizirana glede na začetno zunajcelično koncentracijo. (a) Eksperimentalne meritve Sözer in sod. [109]. (b) Rezultati modeliranja z uporabo privzetih parametrov modela S2011. Pri tem bi bralca radi opozorili na različne y-osi v (a) in (b). Opazimo lahko, da normalizirana koncentracija propidija presega vrednost 1, kar je mogoče zato, ker se večina molekul propidija veže na nukleinske kisline in s tem omogoča stalen pretok prostega propidija v celico, dokler niso zasedena vsa vezavna mesta na nukleinskih kislinah. Slika je povzeta po [93].

Avtorja modela LL2011 sta v svojem članku pokazala, da se napovedi modela kvalitativno ujemajo z meritvami vnosa kalcija v celice, ki sta jih opravila Gabriel in Teissié [110]. V naši študiji smo model LL2011 dodatno primerjali z kvantitativnimi meritvami vnosa barvila lucifer rumeno [85], ki pa jih model ni ustrezno napovedal. Tako smo ugotovili, da noben od preizkušenih modelov ni dovolj zanesljiv za napovedovanje

transporta molekul skozi celično membrano pri širokem razponu parametrov pulzov ter da nobenega od modelov ni mogoče razumeti kot povsem potrjenega. Na koncu smo podali še priporočila za nadaljnji razvoj mehanističnih modelov elektroporacije in načrtovanje poskusov za njihovo validacijo.

Kljub temu, da imajo obstoječi mehanistični modeli elektroporacije precejšnje omejitve pri napovedovanju transporta molekul skozi celično membrano, jih lahko še vedno uporabimo kot pomoč pri interpretaciji določenih eksperimentalnih rezultatov. To smo pokazali v naslednji študiji, v kateri smo model elektroporacije uporabili za boljše razumevanje vpliva orientacije posameznega kardiomiocita na povišanje prepustnosti celične membrane in preživetje celic pri izpostavitvi pulzom različnih dolžin (članek 4 [111]). Izračune smo naredili za model kardiomiocita, ki ima daljšo os orientirano bodisi vzporedno bodisi pravokotno glede na smer zunanjega električnega polja, ter za pulze dolžine od 100 ns do 10 ms. Rezultati modeliranja so pokazali, da je pri pulzih, daljših od 10 μs in pri nižjih jakostih električnega polja vpliv elektroporacije najprej opazen pri vzporedni orientaciji, z višanjem jakosti električnega polja pa postane vpliv elektroporacije večji pri pravokotni orientaciji. Pri pulzih dolžine okoli 1 μs in nižjih jakostih polja je vpliv elektroporacije razmeroma neodvisen od orientacije, pri višjih jakostih električnega polja pa je vpliv elektroporacije višji pri pravokotno orientiranih celicah. Pri pulzih, krajših od 1 μs, pri vseh jakostih električnega polja velja, da je vpliv elektroporacije višji pri pravokotno orientiranih celicah (glej sliko 3 v članku [111]).

Rezultati modela se ujemajo z eksperimentalnimi rezultati Dermol-Černe in sod. [112] in Chaigne in sod. [113]. Chaigne in sod. so pokazali, da po izpostavitvi enemu 10 ms pulzu, kardiomiociti, orientirani vzporedno, odmrejo pri nižji električni poljski jakosti (240 V/cm) kot kardiomiociti, orientirani pravokotno na smer električnega polja (328 V/cm). To pomeni, da so vzporedno orientirani kardiomiociti bolj občutljivi na električno polje. Nasprotno pa pri uporabi enega pulza dolžine 100 μs pravokotno orientirani kardiomiociti odmrejo pri nižji jakosti električnega polja (595 V/cm) kot vzporedno orientirani kardiomiociti (1072 V/cm). Z modelom smo tudi pokazali, da pri 10 ms dolgih električnih pulzih z električnimi poljskimi jakostmi v območju ireverzibilne elektroporacije nastane več por pri vzporedno orientiranih kardiomiocitih kot pri pravokotno orientiranih (slika III.6A). Pri 100 μs dolgih električnih pulzih je bilo opažanje ravno obratno - pri električnih poljskih

jakostih v območju ireverzibilne elektroporacije je nastalo več por pri pravokotno orientiranih kardiomiocitih kot pri vzporedno orientiranih (slika III.6B).

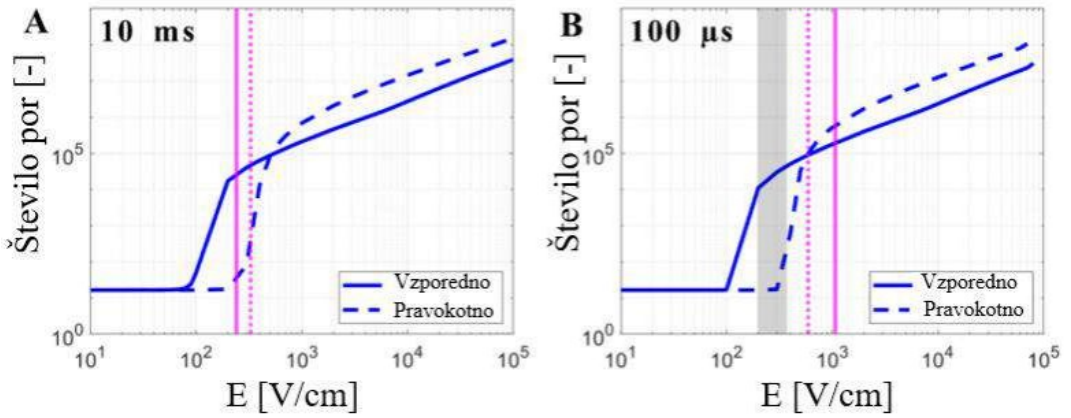

C

Prag električne poljske jakosti za ireverzibilno elektroporacijo (V/cm)		
Trajanje impulza	**Vzporedno**	**Pravokotno**
10 ms	240	328
100 µs	1072	595

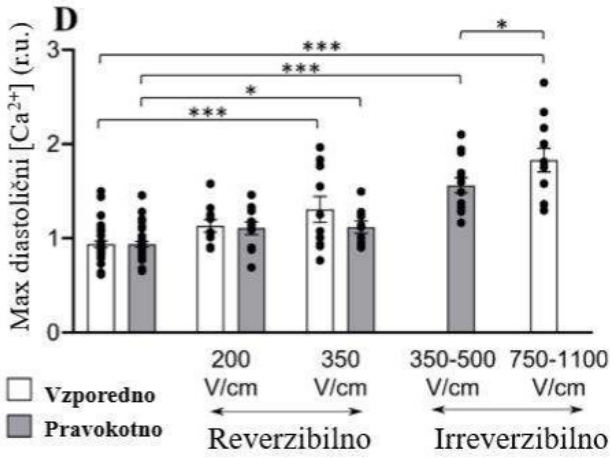

Slika III.6. Primerjava rezultatov modela in eksperimentov na primarnih kardiomiocitih. (A, B) Z modelom napovedano število por v membrani kardiomiocita v odvisnosti od električne poljske jakosti pri dovedenem enempulzu dolžine A) 10 ms ali B) 100 µs. Električno polje je usmerjeno vzporedno (polna modra črta) ali pravokotno (črtkana modra črta) glede na daljšo os celice. Navpični črti označujeta prag električne poljske jakosti za ireverzibilno elektroporacijo pri vzporedni oz. pravokotni orientaciji, ki sta navedeni v [113]. (C) Tabelarno prikazan prag električne poljske jakosti za ireverzibilno elektroporacijo, ki je bil eksperimentalno določen v [113], za vzporedno in pravokotno orientacijo. Električna poljska jakost je ocenjena kot količnik dovedene napetosti in razdalje med elektrodama (4 mm). (D) Primerjava največje znotrajcelične diastolične koncentracije Ca^{2+} za vzporedno in pravokotno orientacijo po izpostavitvi 100 µs pulzom z naraščajočo električno poljsko jakostjo [113]. Električne poljske jakosti, ki so po eksperimentalnih rezultatih nižje od praga za ireverzibilno elektroporacijo, so osenčene sivo v (B). V (D) je poleg posameznih vrednosti za vsako izmerjeno celico prikazano še povprečje ± standardni odklon za vsako skupino meritev. *: $p < 0,05$, ***: $p < 0,001$. Slika je povzeta po [111].

IV. Zaključek

V doktorski disertaciji smo pokazali, da za EKT lahko uporabljamo različne vrste pulzov in s tem potencialno izboljšamo zdravljenje. V disertaciji smo tudi pokazali, da imajo obstoječi matematični modeli elektroporacije precejšnje omejitve pri napovedovanju transporta molekul skozi celično membrano v širokem razponu parametrov električnih pulzov. Rezultati študij so podrobno opisani v člankih, zato je to poglavje namenjeno predvsem pregledu zaključkov posameznih študij in predlogih za nadaljnje delo.

V EKT študijah *in vitro* (članka 1 in 2) smo primerjali učinek različnih vrst pulzov, tj. klasičnih EKT pulzov, vlakov visokofrekvenčnih kratkih bipolarnih pulzov in milisekundnih pulzov na vnos in citotoksičnost cisplatina. Po optimizaciji jakosti pulzov smo z vsemi tremi vrstami pulzov dosegli podoben vnos cisplatina v celice in podobno stopnjo citotoksičnosti, kar pomeni, da so te vrste pulzov enakovredne glede povečanja citotoksičnosti cisplatina pri EKT. V nadaljevanju bo potrebno oceniti učinkovitost teh vrst pulzov še *in vivo*, saj k uspešnosti EKT prispevata tudi vpliv elektroporacije na ožilje tumorja in imunski odziv. V študijah, ki združujejo EKT in GET, običajno najprej dovedejo klasične EKT pulze za vnos kemoterapevtika v celice, nato pa dovedejo še milisekundne pulze za vnos plazmidne DNK. Za GET običajno uporabljajo milisekundne pulze, saj zagotavljajo močnejšo elektroforetsko silo, ki omogoči interakcijo DNK molekul s celično membrano in vnos DNK v celico. Koristno bi bilo, če bi za EKT in GET lahko uporabili enako vrsto pulzov, saj bi to poenostavilo terapijo in omogočilo uporabo preprostejših pulznih generatorjev. V nadaljevanju bi bilo zanimivo preveriti učinkovitost zdravljenja z enakimi pulzi tako za EKT kot GET in vivo.

Tounekti in sod. [114] so določili, da za celično smrt zadostuje nekaj tisoč molekul bleomicina na celico. V *in vitro* študiji, v kateri smo izvajali EKT poskuse z uporabo cisplatina, smo eksperimentalno določili še število molekul cisplatina, potrebnih za celično smrt (članek 2). Območje potrebnih molekul cisplatina je 2-7x10^7 molekul na celico ne glede na vrsto pulzov, kar se ujema s študijo, ki so jo objavili Vižintin in sod. [105]. Iz tega lahko sklepamo, da je število molekul cisplatina, potrebnih za celično smrt, neodvisno od vrste dovedenih pulzov. Kljub temu je potrebno upoštevati, da se pogoji *in vitro* razlikujejo od pogojev *in vivo*. V naših *in vitro* poskusih je zunajcelična koncentracija 50 μM cisplatina

zadoščala za vnos dovolj velikega števila molekul cisplatina za celično smrt, vendar bi *in vivo* lahko bila potrebna drugačna zunajcelična koncentracija cisplatina. Pri poskusih s celicami v suspenziji cisplatin enakomerno obdaja celice in količina cisplatina v zunajceličnem prostoru je velika. Zato se vnos cisplatina skozi elektroporirano membrano ustavi šele, ko se celična membrana zaceli. Pri poskusih *in vivo* pa je količina cisplatina v zunajceličnem prostoru omejena, saj so celice v tkivu tesno skupaj, zunajcelični prostor pa je manjši od znotrajceličnega. Vnos zdravil *in vivo* je lahko omejen tudi zaradi zmanjšanja žilnega pretoka [47], [49], nanj pa lahko vplivajo povečan intersticijski tlak, neenakomerna porazdelitev kemoterapevtika in limfni obtok, vezava zdravila na netarčne molekule ter metabolizem [114]–[117].

Pri načrtovanju zdravljenja globlje ležečih tumorjev z EKT trenutno upoštevamo le pokritost tumorja z dovolj visoko jakostjo električnega polja, ki zadostuje za povišanje prepustnosti celičnih membran tumorskih celic [118], [119]. Zgolj povišanje prepustnosti celične membrane pa ne zagotavlja vnosa zadostnega števila molekul kemoterapevtika in s tem uspešnosti zdravljenja z EKT. V prihodnje bi bilo smiselno nadgraditi načrtovanje zdravljenja z modelom, ki opisuje transport kemoterapevtika po tumorskem tkivu in vnos kemoterapevtika v tumorske celice. Za dosego tega cilja najprej potrebujemo zanesljiv model, ki opisuje transport molekul skozi elektroporirano celično membrano. V disertaciji smo zato primerjali obstoječe mehanistične modele, ki opisujejo pojav elektroporacije in molekularnega transporta skozi celično membrano posameznih celic (članek 3). Ugotovili smo, da i) kvalitativno primerjanje napovedi modela z eksperimentalnimi meritvami ne zadostuje za validacijo modela, ii) za validacijo modela niso dovolj kvantitativne meritve končnega vnosa molekul, ampak so potrebne tudi meritve kinetike vnosa molekul in iii) poskusi, namenjeni validaciji modela, morajo biti načrtovani tako, da so dovolj specifični in lahko potrdijo ali ovržejo različne napovedi modela. Nadalje smo ugotovili, da noben od obstoječih mehanističnih modelov ni dovolj zanesljiv za opis transporta molekul skozi celično membrano v širokem razponu parametrov pulzov, ki se uporabljajo za elektroporacijo. Potrebno je torej nadaljnje delo in izboljšanje obstoječih modelov. Možna izboljšava je vključitev peroksidacije lipidov in poškodb membranskih beljakovih kot mehanizma povečanja prepustnosti membrane. Dodatne raziskave so potrebne, da bi bolje razumeli, kako in zakaj pride do oksidacije lipidov in poškodb membranskih beljakovin, ter

kako kinetika teh procesov vpliva na transport skozi celično membrano. Kljub temu lahko obstoječi mehanistični modeli še vedno pomagajo pri interpretaciji nekaterih eksperimentalnih rezultatov, na primer vpliva orientacije kardiomiocitov na elektroporacijo z različno dolgimi pulzi, kot smo pokazali v članku 4. Obenem pa lahko že preprostejši fenomenološki modeli že zadoščajo za dani praktični namen, kot je opis velikostnega razreda vnosa cisplatina, doseženega z različnimi vrstami pulzov, kot smo prikazali v članku 2.

V. Izvirni prispevki k znanosti

Primerjava različnih vrst pulzov v smislu njihove enakovrednosti za vnos cisplatina v celice pri elektrokemoterapiji

S poskusi *in vitro* smo primerjali učinek klasičnih 100 µs monopolarnih EKT pulzov, vlakov visokofrekvenčnih kratkih bipolarnih pulzov in monopolarnih milisekundnih pulzov na vnos in citotoksičnost cisplatina. Ker lahko vlaki visokofrekvenčnih kratkih bipolarnih pulzov ublažijo bolečine in krčenje mišic med zdravljenjem z elektroporacijo, smo primerjali učinek kratkih bipolarnih pulzov in klasičnih EKT pulzov (članek 1). Predklinične in klinične študije so pokazale, da uporaba EKT v kombinaciji z gensko terapijo s plazmidno DNK, ki kodira beljakovine za stimulacijo imunskega odziva, lahko nadgradi EKT iz lokalnega v sistemsko zdravljenje. Ker pri genski terapiji običajno dovajamo milisekundne pulze, smo v naših raziskavah s cisplatinom preizkusili tudi milisekundne pulze. Ugotovili smo, da sta vnos in citotoksičnost cisplatina neodvisna od izbrane vrste pulzov, če ustrezno prilagodimo dovedeno električno poljsko jakost. Sklepamo torej, da bi za EKT lahko uporabljali različne vrste pulzov. Potrebne so nadaljnje študije *in vivo*, da bi raziskali, kako te različne vrste pulzov vplivajo na imunski odziv in krvni pretok v tumorskem žilju, ki sta pomembna mehanizma, ki prispevata k uspešnemu zdravljenju EKT.

Določitev števila molekul cisplatina, ki je potrebno za citotoksični učinek

Načrtovanje zdravljenja z numeričnimi izračuni porazdelitve električnega polja v tumorju in okoliškem tkivu pomaga določiti optimalne parametre za zdravljenje globlje ležečih tumorjev. Za uspešnost zdravljenja z EKT ne zadostuje zgolj pokritost tumorskega tkiva z dovolj visokim električnim poljem, ki poviša prepustnost celičnih membran tumorskih celic. Enako pomembno je tudi, da v tumorske celice vnesemo zadostno količino kemoterapevtika, zato smo eksperimentalno določili število molekul cisplatina v celici, ki jih potrebujemo za doseganje citotoksičnega učinka (članek 2). S poskusi *in vitro* smo določili vnos in citotoksičnost cisplatina, pri čemer smo celice izpostavili različnim vrstam pulzov. Z združitvijo rezultatov vnosa cisplatina in citotoksičnosti cisplatina smo določili število molekul cisplatina, potrebnih v posamezni celici za doseganje citotoksičnega učinka. Število potrebnih molekul znaša od 2 do 7×10^7 molekul cisplatina na celico. Naši rezultati nadalje kažejo, da lahko enakovredno uporabimo različne vrste pulzov: klasične EKT pulze,

vlake visokofrekvenčnih kratkih bipolarnih pulzov, milisekundne pulze in nanosekundne pulze, saj vsi omogočajo vnos zadostnega števila molekul cisplatina na celico ob ustrezni prilagoditvi električnega polja. Tako bi za EKT lahko uporabljali različne vrste pulzov, kar potrjuje ugotovitve prvega izvirnega znanstvenega prispevka.

Vrednotenje obstoječih modelov elektroporacije za napovedovanje molekularnega transporta in/ali drugih povezanih pojavov na ravni posamezne celice

Primerjali smo obstoječe matematične modele, ki opisujejo elektroporacijo in transport molekul skozi celično membrano na ravni posameznih celic. Najprej smo na podlagi pregleda literature naredili pregled različnih mehanističnih in fenomenoloških modelov. Nato smo kritično ovrednotili tri izbrane mehanistične modele, ki so bili podlaga za vse druge objavljene modele, tako da smo njihove napovedi primerjali z različnimi kvantitativnimi meritvami transporta molekul skozi celično membrano po elektroporaciji. Dva od preizkušenih modelov opisujeta elektroporacijo kot nastanek lipidnih por, opisanih s porazdelitveno funkcijo por, in upoštevata transport molekul skozi pore zaradi elektroforetskega in difuzijskega transporta. Tretji model opisuje povišanje prepustnosti celične membrane z uporabo kinetične sheme in upošteva transport molekul skozi pore zaradi difuzije in endocitoze. Ugotovili smo, da noben od preizkušenih modelov ni dovolj zanesljiv za napovedovanje transporta molekul v celotnem razponu parametrov pulzov in za različne majhne molekule, ki se uporabljajo pri raziskavah elektroporacije (članek 3). Kljub temu so lahko obstoječi mehanistični modeli še vedno koristni pri interpretaciji nekaterih rezultatov poskusov, na primer vpliva orientacije kardiomiocitov na elektroporacijo z uporabo različno dolgih pulzov (članek 4). Poleg tega lahko tudi fenomenološki modeli zadoščajo za praktične namene, kot je opis velikostnega reda vnosa cisplatina, doseženega z različnimi vrstami pulzov (članek 2).

1. Introduction

When pulsed electric field of sufficient strength is applied to a biological cell, a transient increase of cell membrane permeability and conductivity can be observed, and this phenomenon is called electroporation. Electroporation allows the transport of ions and molecules that otherwise cannot permeate or poorly permeate across the intact membrane [1], [2]. Electroporation can be reversible or irreversible. If the cells recover and re-establish their homeostasis after pulse application, electroporation is called reversible. Otherwise, if the damage is too extensive and the cells die, electroporation is called irreversible. Electroporation is used in biomedicine (e.g., reversible electroporation is used for electrochemotherapy, gene therapy, and transdermal drug delivery, whereas irreversible electroporation is used as an ablation technique to treat tumors or heart arrhythmias) [3]–[7], in biotechnology [8], and food processing [9].

1.1. Electrochemotherapy

Electrochemotherapy (ECT) is a safe, highly efficient, local treatment used in clinics to treat cutaneous and subcutaneous tumors of different histologies [10], [11]. In 2006, the standard operating procedures were published to successfully treat cutaneous tumors smaller than 3 cm in diameter [12], [13] and were recently updated considering the treatment of larger tumors [14]. Nowadays, ECT is a well-recognized treatment across Europe, as evidenced by the UK's National Institute for Health and Care Excellence guidance [15], [16] and recent European consensus-based interdisciplinary documents for squamous cell carcinoma of the skin, basal cell carcinoma, melanoma, and Kaposi's sarcoma [17]–[22]. Currently, there are ongoing trials for the treatment of deep-seated tumors using ECT [23]–[28].

In ECT, first, the chemotherapeutic drug is administered intravenously or intratumorally, and then short high-intensity electric pulses are applied to the tumor tissue resulting in cell membrane electroporation. The two most used chemotherapeutic drugs in ECT are bleomycin and cisplatin [29]. Electroporation potentiates the influx of the drugs into the tumor cells, and consequently the cytotoxicity of bleomycin by several hundred to thousands folds and of cisplatin by several tens fold compared to non-electroporated controls [30]–[32]. Thus, in ECT lower doses of chemotherapeutic drugs are needed to achieve a cytotoxic effect than in standard chemotherapy.

Conventionally, eight monopolar pulses of 100 µs duration are applied with a 1 Hz or 5 kHz pulse repetition rate [14], see Figure 1 a. However, the delivery of these pulses to the tumor tissue unintendedly stimulates also surrounding excitable cells, i.e., muscle and nerve cells (e.g., motor nerves and nociceptors) provoking muscle contractions and pain in the patient during the treatment. When treating cutaneous tumors, muscle contractions can potentially cause the displacement of the electrodes if insufficient pressure is exerted on them by the operator during pulse delivery. Such displacement might result in low electropermeabilization and failure of ECT due to the reduced/loss of electrical contact [120]. On the other hand, when too high pressure is exerted on the electrodes by the operator a larger contact area is considered which requires a higher electric current. If the current exceeds a given level (e.g. 12 A) some electroporators for safety reasons will discontinue pulse delivery resulting in reduced ECT efficiency [120]. Furthermore, when treating deep-seated tumors, long needle electrodes are invasively inserted around the target volume. The displacement of electrodes could potentially increase the tissue trauma caused by needles which might result in harmful effects on the nearby vital structures and affect the electric field distribution which might lead to suboptimal treatment [121]. Thus, there is a need to use local or general anesthesia and muscle relaxants. When performing ECT of deep-seated tumors in proximity to the heart, the pulses need to be synchronized with the heart rhythm [33], [34].

Pain and muscle contractions can be reduced by applying pulses at a higher repetition rate [35], [36], by optimizing the design of the electrodes such that the muscle volume crossed by the current is reduced as much as possible [37], [38], or by delivering bursts of high-frequency short bipolar pulses [37], [39]. These bursts contain a series of short (0.5−10 µs) bipolar pulses that are applied at a repetition rate of approximately 1 Hz, see Figure 1 b. *In vivo* [40]–[42], and human studies [43] have shown that the use of bursts of high-frequency short bipolar pulses to achieve irreversible electroporation mitigates pain and muscle contraction compared to longer monopolar pulses. Recently, *in vitro* [44] and *in vivo* [45] studies have demonstrated that bursts of high-frequency short bipolar pulses can be used for the uptake of chemotherapeutic drugs and thus have the potential to be applied for ECT. Recent reports on humans indeed demonstrated the safety, tolerability, and efficacy of using bursts of high-frequency short bipolar pulses for the treatment of cutaneous tumors with ECT [46].

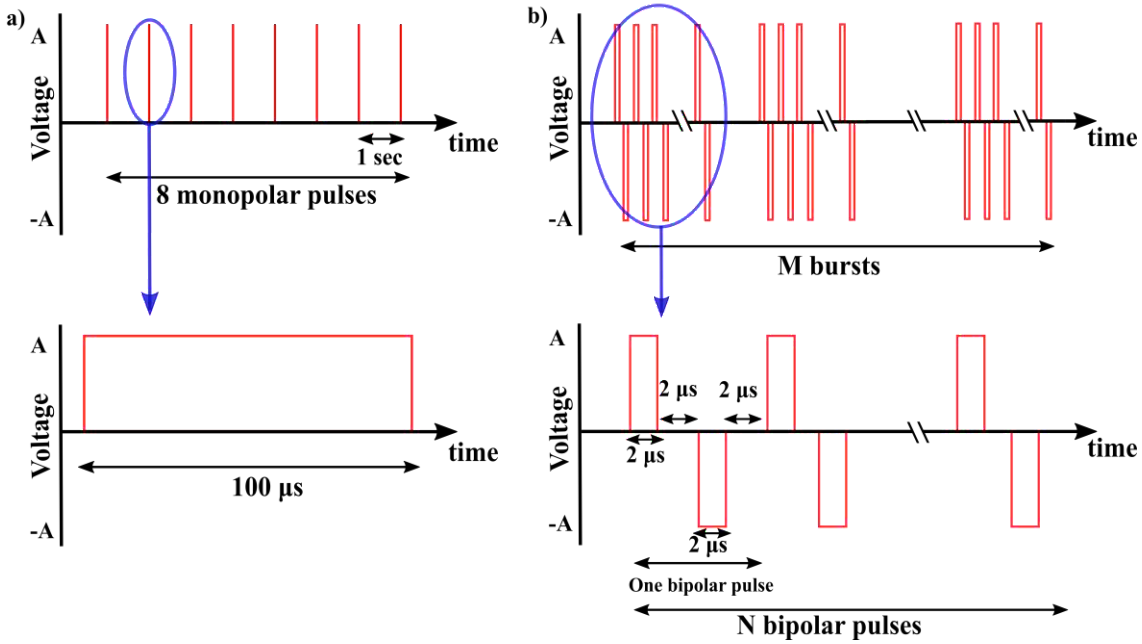

Figure 1. Pulses parameters as a function of the time with high enough amplitude represented in the figure with the letter A. Figure 1a top shows the classical pulses used in ECT: 8 monopolar pulses at 1 Hz repetition frequency having 100 µs pulse duration (Figure 1 a bottom). Figure 1 b top shows the bursts of high-frequency short bipolar pulses: M bursts at 1 Hz repetition frequency. Each bust contains N bipolar pulses with a short pulse duration of ~2 µs for the positive phase and ~2 µs for the negative phase (Figure 1 b bottom) at high repetition frequency of few kHz.

In ECT the mechanisms that contribute to tumor eradication are the potentiated uptake and cytotoxicity of the chemotherapeutic drugs, the reduction of the blood flow, and the involvement of immune response. Electroporation transiently and reversibly reduces the vascular flow of the tumor tissue, the so-called vascular lock, prolonging the drug entrapment in the tumor tissue for several hours. Additionally, a vascular-disrupting effect is also observed due to endothelial cell death which leads to tumor cell death due to long-lasting hypoxia in the affected vessels [47]–[49]. The immune response plays an important role in eradicating tumor tissue during ECT. The release of molecules such as damage-associated molecular patterns (DAMP) and tumor antigens after electroporation can stimulate the immune system inducing immunogenic cell death. Multiple studies in canine and human patients have thus tested ECT in combination with gene electrotransfer (GET) of plasmid DNA encoding for interleukin-12 (IL-12), which stimulates the immune system [50], [51]. Usually in GET millisecond pulses are used to electrophoretically drive the molecules of DNA towards the cell membrane. The combined ECT and GET treatment applied to 19 patients with metastatic melanoma successfully evoked a systemic immune

response and succeeded in producing a partial response in 8 patients (42%) or a complete response in 2 patients (10 %) of distant, non-treated nodules (abscopal effect) [50].

Changing the conventional 8 × 100 μs pulses with an alternative type of pulse could be advantageous in ECT. For example, using bursts of high-frequency short bipolar pulses, which mitigate pain and muscle contraction, or millisecond pulses, which in combination with protein-encoding DNA, stimulate the immune response. However, it remains unclear how these pulse parameters affect drug uptake and its cytotoxicity.

1.2. Cell membrane permeability and molecular transport

Under physiological conditions, a biological cell maintains through a complex system of ion channels and pumps a resting transmembrane voltage (TMV) which, depending on the cell type, ranges between -40 mV and -90 mV [52], [53]. The plasma membrane acts as a selective barrier separating the cell interior from the external environment allowing the inflow and the outflow of specific molecules through the membrane. The transport of solutes occurs by several mechanisms: i) by simple diffusion through the lipid bilayer of uncharged small polar molecules such as O_2 and CO_2; ii) by electrodiffusion through membrane proteins (transporters and channels) of small organic ions or inorganic ions; iii) osmosis; iv) endocytosis; and v) by the use of ion pumps [122].

A biological cell can be considered, from the electrical point of view, as a conductive body (cytosol) surrounded by a dielectric shell (cell membrane) embedded by a conductive extracellular solution. Thus, when an external electric field is applied to a biological cell, an additional TMV is induced across the cell membrane which superimposes onto the resting TMV. If the summed TMV is sufficiently high by absolute value, structural changes occur in the cell membrane which increases the membrane permeability to different ions and molecules disrupting membrane barrier function [54]–[56]. According to molecular dynamics simulations [57], theoretical predictions [58], and experimental investigations on lipid systems [59] the induced TMV increases the probability of formation of pores in the lipid bilayer [60]–[62]. Nowadays, such pore formation is widely recognized as a mechanism of membrane electroporation. Additionally to the pore formation, electric pulses also cause chemical changes to the lipids through lipid peroxidation [63], [64] and can damage or modulate the function of certain membrane proteins like voltage-gated ion channels [65]–[67]. Both lipid peroxidation and membrane protein damage can contribute

to the increased cell membrane permeability. The induced TMV is affected by cell geometry, cell orientation, and composition of the extracellular medium [68]–[70]. The induced TMV increases linearly with the strength of the applied electric field. Furthermore, the induced TMV varies with position on the membrane and reaches the maximal absolute value at the regions of the cell membrane that are facing the electrodes [71]–[73]. As electroporation increases the membrane conductivity, the membrane starts discharging through the permeabilized membrane, which saturates or even decreases the induced TMV, and limits further increase in membrane permeability. Thus, electroporation is a highly dynamic process that depends considerably on the parameters of the applied electric pulses.

Electroporation can be determined indirectly by measuring the transmembrane transport (i.e., inflow and outflow) of molecules that otherwise poorly permeate the membrane, by monitoring cell swelling [80], [81], by impedance measurements of the cell membrane from which we can extract the conductivity and resistivity of the sample during electroporation [78], [79], and by voltage clamp techniques which measure the transmembrane ion current in a single cell [76], [77]. The transport of molecules across an electroporated membrane occurs in the regions of the membrane where a sufficiently high TMV is induced [72], [74], [75] and is detected by using fluorescent dyes, functional molecules such as cisplatin and bleomycin, magnetic nanoparticles, and nucleic acids [82]. The uptake of molecules is affected by pulse parameters (number of pulses, pulse shape, pulse duration, and pulse amplitude), solute characteristics (size, charge), and extracellular conditions (conductivity of the extracellular medium [98], [123], [124]).

The mechanisms of transmembrane molecular transport of small molecules (<4 kDa) are diffusion, electrophoresis, electroosmosis, and endocytosis [1], [83]–[85]. During pulse application, the transport of molecules is mainly due to electrophoresis and possibly due to electroosmosis. After pulse application, the transport is mainly diffusive, but can also have an electrophoretic component due to nonzero transmembrane voltage [86]. Endocytic uptake of molecules can also be observed after the pulse application [83], [87]. The transport of macromolecules such as DNA is a multistep and more complex process compared to a small molecule uptake [83], [88], [89]. Usually, long millisecond pulses are used for the uptake of macromolecules [90] or a combination of a strong short pulse with one or several weak long pulses increases the DNA transfection efficiency suggesting that the former type

of pulses is mainly responsible for creating the pores, whereas the latter one assists DNA translocation electrophoretically [91], [92].

1.3. Model of electroporation and transmembrane molecular transport

Mathematical models help scientists understand the underlying mechanisms of a biological system by using physical and mathematical laws. Employing mathematical models is often less time-consuming and less expensive than experimental work and can be calculated at any time on a computer. Electroporation is a process that involves different spatiotemporal scales, ranging from the molecular level (i.e., nanometres) to the tissue level (i.e., few centimeters), and different physical phenomena (i.e., electric, thermal, chemical, etc.). Thus, multiphysics and multiscale mathematical models have been developed by researchers to describe spatially and temporally the phenomenon of electroporation and the related transmembrane molecular transport. These mathematical models can be broadly divided into mechanistic and phenomenological.

The mechanistic models aim to describe empiric/experimental results by using physical laws. Therefore, the model parameters have a physical meaning, which facilitates the scientific interpretation of the results. Existing mechanistic models of electroporation mainly attribute the increase of cell membrane permeability to the formation of pores in the lipid bilayer due to the increase in TMV. Mechanistic models can be divided into two larger groups. The first group of models uses a kinetic scheme that describes the transition between distinct states of pores created in the cell membrane. The forward transition between each porous state depends exponentially on the TMV [94]. The molecular transport through pores in these models has been described assuming diffusive transport only [94] or considering additional endocytotic-like transport [95]. The second group of models describes pores in terms of a pore distribution function described in the pore radius space. This pore distribution function changes dynamically with the TMV [96], [97]. The molecular transport through pores in these models has been described using the Nernst-Planck equations considering both electrophoretic and diffusional transport [96], [98], [99].

The phenomenological models describe the experimental results without using any physical laws and are based on empirical correlations. Therefore, it is not possible to explain why the variables of the model interact the way they do. The phenomenological models of electroporation present in the literature can be compartmental [85], based on equivalent

circuit [100], based on arbitrary mathematical functions which describe the increase in membrane permeability [101], [102] or the fraction of pores formed in the membrane [103], [104].

Currently, several models that describe the phenomenon of electroporation and transmembrane transport of molecules exist and have been qualitatively and/or quantitatively compared with experimental measurements. Interestingly, different models developed using different theoretical descriptions of membrane permeability and molecular transport, showed good agreement with experimental data. However, it is still not clear and well understood which model can be considered the best to describe the phenomenon of electroporation and transmembrane transport of molecules and if the model is valid when using a broad range of experimental data and conditions.

1.4. Aims of the dissertation

The overarching aim of this dissertation was to better understand the phenomenon of reversible electroporation and transmembrane molecular transport in ECT by performing *in vitro* experiments and by using numerical models in individual biological cells.

Clinicians follow the recommendations written in the standard operating procedure to successfully treat cutaneous tumors with ECT [13], [14]. Such protocols specify the type of anesthesia, the type of drug, the route of drug administration, and the types of electrodes, generators, and pulse parameters to be used during the treatment. However, the use of the classical ECT pulses causes pain and muscle contraction in the patients. It has been observed that the use of bursts of high-frequency short bipolar pulses reduces pain and muscle contraction in the patient which are otherwise present when using the classical ECT pulses. Furthermore, many efforts are focused on making ECT a systemic treatment combining it with immunotherapy. Preclinical and clinical studies have shown that the use of classical ECT pulses in combination with gene electrotransfer (use of millisecond pulses and protein-encoding DNA) which stimulates the immune system contributes to systemic tumor eradication. Thus, different types of pulses might improve ECT treatments, but it is not clear and well-understood how different types of pulses will affect ECT. Therefore, in this dissertation, the effect of different types of pulses on cisplatin uptake and its cytotoxicity as one of the two dominant drugs used clinically are investigated.

For the success of ECT not only the application of a high-enough electric field to permeabilize the tumor tissue is needed but also the transport of a sufficient number of the chemotherapeutic drug into a cell is needed to achieve its cytotoxic effect. Therefore, in this dissertation, the number of cisplatin molecules needed inside a cell to achieve a cytotoxic effect has been quantified when using different types of pulses.

The transport of molecules through electropermeabilized cell membranes is crucial for the success of electroporation-based treatments such as ECT, GET, and transdermal drug delivery. However, investigating the phenomenon of electroporation and the transport of molecules with *in vitro* experiments can be demanding and time-consuming because many parameters can affect the outcome such as cell and solute characteristics, pulse parameters, and experimental conditions. Thus, mathematical models can be a useful tool to study the response of cells to different pulse parameters. Currently, many different models that describe the phenomenon of electroporation and transmembrane transport are described in the literature and are considered validated when compared to a specific set of experimental data. However, it is not clear if any model is good enough to describe the phenomenon of electroporation for a broad range of pulse parameters. Therefore, in this dissertation, we critically assess the existing mathematical models with respect to how well they describe transmembrane transport in different experimental conditions.

2. Research papers

The research work carried out during the doctoral studies is presented in four papers published in international peer-reviewed scientific journals with impact factors. This chapter first gives a brief overview of the papers and their connections, followed by all papers in their original format.

The electric pulses conventionally used for ECT in the clinic cause pain and muscle contraction in the patient, thus there is the need to use anesthesia and muscle relaxants during the treatment. The use of bursts of high-frequency short bipolar pulses has been suggested by many *in vivo* animal and human studies as a solution to reduce/mitigate pain and muscle contraction. Bursts of high-frequency bipolar pulses have been mainly used to perform irreversible electroporation; however, an *in vitro* study [125] has shown that bursts of high-frequency short bipolar pulses can also be used for the uptake of small molecules. Therefore, the main objective of the first paper *The use of high-frequency short bipolar pulses in cisplatin electrochemotherapy in vitro (Scuderi et al. 2019)* was to verify if bursts of high-frequency short bipolar pulses, which mitigate pain and muscle contractions, unlike the conventional ECT pulses, can potentially be used for reversible electroporation in ECT. For this purpose, we performed *in vitro* experiments using a mouse skin melanoma cell line and applied either 8 monopolar pulses of 100 μs duration (conventional ECT pulses) or bursts of high-frequency short bipolar pulses. We compared the cytotoxicity of cisplatin between the two different types of pulses with the same on-time of 800 μs. A similar cytotoxic effect was observed using the two different types of pulses. However, when using bursts of high-frequency short bipolar pulses, a higher electric field was needed to achieve a similar cytotoxic effect than using conventional ECT pulses.

Preclinical and clinical studies have shown that the use of ECT in combination with gene electrotransfer (i.e., use of millisecond pulses with protein-encoding DNA) stimulates the immune response which contributes to tumor eradication in ECT treatment. Furthermore, in the first paper, we showed that bursts of high-frequency short bipolar pulses can be used to achieve reversible electroporation in ECT. Thus, replacing the conventional 8× 100 μs monopolar pulses with alternative types of pulses might be beneficial for the ECT treatment. Furthermore, the success of ECT not only depends on the application of a

sufficiently high electric field to the tumor tissue but also the transport of a sufficient number of cisplatin molecules inside a cell. In the second paper *The equivalence of different types of electric pulses for electrochemotherapy with cisplatin - an in vitro study (Scuderi et al. 2024)* we investigated how different types of pulses affect cisplatin uptake and cisplatin cytotoxicity and determined the number of internalized cisplatin molecules needed to achieve a cytotoxic effect. We performed *in vitro* experiments applying three different types of pulses: i) 8 monopolar pulses of 100 μs duration conventionally used in ECT, ii) bursts of high-frequency short bipolar pulses which reduce pain and muscle contractions, and iii) 8 monopolar pulses of 5 ms duration which stimulate an immune response. We observed a similar uptake and cytotoxic effect of cisplatin using all three tested types of pulses when the electric field for each type of pulses was properly adjusted. The number of cisplatin molecules needed to achieve a cytotoxic effect was in the range of $2\text{-}7\times10^7$ cisplatin molecules per cell for all three types of pulses. Furthermore, we tested a phenomenological model describing electroporation and the associated transmembrane transport and demonstrated that the model predicts quantitatively the number of cisplatin molecules in a single cell relatively well but requires further improvement.

Mathematical models are an essential tool to investigate the response of cells to an external applied electric field. Many different models have been developed to better understand the phenomenon of electroporation and transmembrane molecular transport by comparing the modeling results with experimental data. These models, despite their different theoretical descriptions of membrane permeability and molecular transport, generally showed good agreement with experimental data. However, it was not clear if the models can be universally applied to a full range of experimental data. Therefore, the main objective of the third paper *Models of electroporation and the associated transmembrane molecular transport should be revisited (Scuderi et al. 2022)* was to critically assess the existing mechanistic models that describe the phenomenon of electroporation and transmembrane molecular transport of small molecules (< 4 kDa). We focused on three mechanistic models, which formed the basis for all other published models, and compared their predictions to a broad range of quantitative measurements of molecular transport. We observed that none of the tested models can be universally applied to the full range of experimental measurements. Even more importantly, we showed that none of the models

has been compared to a sufficient amount of experimental data to confirm the model's validity. Finally, we provided recommendations on how to improve the development of mechanistic models of electroporation and how to design experiments for thorough models.

While the existing mechanistic models of electroporation have strong limitations for predicting the transmembrane transport of different molecules, they can still aid in the interpretation of certain experimental results. We demonstrate this in the fourth paper *Characterization of the experimentally observed complex interplay between pulse duration, electrical field strength, and cell orientation on electroporation outcome using a time-dependent nonlinear numerical model (Scuderi et al. 2023).* This paper used numerical modelling to investigate how cell orientation, pulse duration, and pulse amplitude affect TMV and pore formation in an isolated cardiomyocyte. The modeling results helped explain how cell orientation with respect to the electric field direction can influence calcium uptake and cell death in a complex way, depending on the duration and amplitude of the applied electric pulses.

2.1. Paper 1

Title: **The use of high-frequency short bipolar pulses in cisplatin electrochemotherapy in vitro**

Authors: **Maria Scuderi**, Matej Reberšek, Damijan Miklavčič, and Janja Dermol-Černe

Publication: Radiology and Oncology vol. 53, no. 2, pp. 194–205, June 2019

Impact Factor on the date of publication: 1.7 (2017)

Quartile:

- Q3 (Radiology, Nuclear Medicine & Medical Imaging)
- Q4 (Oncology)

Rank:

- 78/129 (Radiology, Nuclear Medicine & Medical Imaging)
- 190/223 (Oncology)

DOI: 10.2478/raon-2019-0025

sciendo Radiology and Oncology | Ljubljana | Slovenia | www.radioloncol.com RADIOLOGY AND ONCOLOGY

research article

The use of high-frequency short bipolar pulses in cisplatin electrochemotherapy in vitro

Maria Scuderi[1], Matej Rebersek[2], Damijan Miklavcic[2], Janja Dermol-Cerne[2]

[1] University of Padua, Department of Information Engineering, Padua, Italy
[2] University of Ljubljana, Faculty of Electrical Engineering, Ljubljana, Slovenia

Radiol Oncol 2019; 53(2): 194-205.

Received 4 February 2019
Accepted 23 April 2019

Correspondence to: Janja Dermol-Černe, Ph.D., University of Ljubljana, Faculty of Electrical Engineering, Tržaška cesta 25, SI-1000 Ljubljana, Slovenia. E-mail: Janja.dermol-cerne@fe.uni-lj.si

Disclosure: No potential conflicts of interest were disclosed.

Background. In electrochemotherapy (ECT), chemotherapeutics are first administered, followed by short 100 µs monopolar pulses. However, these pulses cause pain and muscle contractions. It is thus necessary to administer muscle relaxants, general anesthesia and synchronize pulses with the heart rhythm of the patient, which makes the treatment more complex. It was suggested in ablation with irreversible electroporation, that bursts of short high-frequency bipolar pulses could alleviate these problems. Therefore, we designed our study to verify if it is possible to use high-frequency bipolar pulses (HF-EP pulses) in electrochemotherapy.

Materials and methods. We performed *in vitro* experiments on mouse skin melanoma (B16-F1) cells by adding 1–330 µM cisplatin and delivering either (a) eight 100 µs long monopolar pulses, 0.4–1.2 kV/cm, 1 Hz (ECT pulses) or (b) eight bursts at 1 Hz, consisting of 50 bipolar pulses. One bipolar pulse consisted of a series of 1 µs long positive and 1 µs long negative pulse (0.5–5 kV/cm) with a 1 µs delay in-between.

Results. With both types of pulses, the combination of electric pulses and cisplatin was more efficient in killing cells than cisplatin or electric pulses only. However, we needed to apply a higher electric field in HF-EP (3 kV/cm) than in ECT (1.2 kV/cm) to obtain comparable cytotoxicity.

Conclusions. It is possible to use HF-EP in electrochemotherapy; however, at the expense of applying higher electric fields than in classical ECT. The results obtained, nevertheless, offer an evidence that HF-EP could be used in electrochemotherapy with potentially alleviated muscle contractions and pain.

Key words: electroporation; electrochemotherapy; high-frequency bipolar pulses; cisplatin; cell survival; drug uptake

Introduction

When a cell is exposed to a sufficiently high electric field, the permeability of the cell membrane rapidly increases due to membrane electroporation. This transiently increased membrane permeability allows for the exchange of ions and molecules between inside and outside of the cells.[1-4] If cells recover and survive, electroporation is called reversible. If the damage is too extensive, resealing too slow, cells cannot restore the homeostasis, and they die, electroporation is called irreversible. Electroporation depends on the characteristics of the cells (shape, size, cytoskeleton structure, membrane composition) and the electrical parameters (amplitude, duration, number of electrical pulses and repetition frequency). Electroporation is used in medicine[5-10] (electrochemotherapy, gene therapy, irreversible electroporation as an ablation technique and transdermal drug delivery), in biotechnology[11,12], (inactivation of microorganisms, extraction of biomolecules from microorganisms and plants, genetic transformation of microorganisms) and food processing.[13,14]

Electrochemotherapy (ECT) is used in clinics to treat patients with various types of cancer (*e.g.*, melanoma, head-neck tumors, breast, liver, intestinal tract, brain cancer).[15] The standard operating procedures for electrochemotherapy include intratumoral or intravenous delivery of the chemother-

apeutic drug, followed by the application of high-voltage 100 µs long monopolar pulses to the tumor area.[16–19] Two chemotherapeutics are currently used in clinics - bleomycin[20,21] and cisplatin (cis-diaminodichloroplatin (II), CDDP).[22,23] The cytotoxicity of the chemotherapeutic drugs is increased as the delivered pulses increase cell membrane permeability, and facilitate the influx of drugs into the tumor cells.[24,25] Drawbacks of the application of 100 µs long monopolar, high-voltage electric pulses at repetition frequency 1 Hz are pain, muscle contractions[26-28], the need to use muscle relaxants and general anesthesia[29] and to synchronize pulses with the heart rhythm.[30,31] These problems can be alleviated for example by applying pulses at higher frequency[26], by using special designs of electrodes[32,33], or, as it was recently demonstrated, by delivering bursts of short high-frequency bipolar pulses, *i.e.*, the so-called high-frequency irreversible electroporation (H-FIRE) pulses.[33-37] Treatment with H-FIRE pulses, however, comes at the expense of delivering pulses of considerably higher amplitudes.[38]

Mostly, H-FIRE pulses have been used to achieve irreversible electroporation. However, they can also be used to increase the uptake of molecules into cells[38] which could be applied in achieving reversible electroporation to treat tumors with electrochemotherapy. Thus, this study aimed to determine whether H-FIRE pulses could also be used in electrochemotherapy which we call high-frequency electroporation (HF-EP).

We delivered 8 bursts of 50 bipolar pulses, each consisting of 1 µs long positive and negative pulse, with a 1 µs delay between them with electric field from 0.5–5 kV/cm. We compared HF-EP to classic eight monopolar 100 µs long pulses, delivered at frequency 1 Hz, with electric field from 0.4–1.2 kV/cm. Cisplatin concentration was from 1 µM to 330 µM. We showed that HF-EP pulses indeed cause higher cytotoxicity of cisplatin *in vitro*; however, in comparison to the standard 100 µs long monopolar pulses, higher voltage pulses must be delivered to obtain comparable effect.

Materials and methods

Cell preparation

Mouse skin melanoma cell line B16-F1, obtained from the European Collection of Authenticated Cell Cultures (ECACC, cat. no. 92101203, Sigma Aldrich, Germany, mycoplasma free), was grown 2–4 days in 75 cm^2 cell culture flasks (TPP, Austria) until 80% confluency in Dulbecco's Modified Eagle's Medium (DMEM, cat. no. D5671, Sigma Aldrich, Germany) in an incubator (Kambič, Slovenia) at 37°C and humidified 5% CO_2. DMEM, used in this composition for all *in vitro* experiments, was supplemented with 10% fetal bovine serum (cat. no. F7524, Sigma Aldrich, Germany), 2 mM L-glutamine (cat. no. G7513, Sigma Aldrich, Germany) and antibiotics, 50 µg/ml gentamycin (cat. no. G1397, Sigma Aldrich, Germany), 1 U/ml penicillin-streptomycin (cat. no. P11-010, PAA, Austria).

Cell suspension was prepared by detaching the cells in the exponential phase of growth with 10x trypsin-EDTA (cat. no T4174, Sigma Aldrich, Germany), diluted 1:9 in Hank's basal salt solution (cat. no. H4641, Sigma Aldrich, Germany). After no more than 3 minutes, trypsin was inactivated by adding DMEM, and cells were transferred to a 50 ml centrifuge tube. Then, the cells were centrifuged (5 min, 180 g, 21°C) and re-suspended in DMEM at concentration 5x10^6 cells/ml (experiments to measure the optimal parameters of electroporation and resealing rate of cells), 5x10^4 cells/ml (experiments to measure the cytotoxicity of cisplatin without electroporation) or 2.2x10^{7}cells/ml (experiments to measure the cytotoxicity of cisplatin with electroporation). We performed experiments with different cell densities due to different requirements for cell number and sensitivities of the chosen assays. Even at the highest concentration (2.2x10^7 cells/ml) we were still well below the concentration where shielding of the electric field and decreased uptake were observed.[39]

Electroporation setup

Two types of pulses were applied – 100 µs long monopolar pulses (*i.e.* classical electrochemotherapy) and bursts of short bipolar pulses (HF-EP pulses). They were applied between plate stainless-steel electrodes with 2 mm distance.[40] Between pulses, electrodes were cleaned in potassium-phosphate buffer (KPB, 10 mM KH_2PO_4/K_2HPO_4 in ratio 40.5:9.5, 1 mM $MgCl_2$, 250 mM sucrose) and dried with sterile gauze. 100 µs long monopolar pulses (8 pulses, delivered at repetition frequency 1 Hz, Figure 1A) of different voltages (80, 120, 160, 200, 240 V) were delivered by the commercially available BetaTech pulse generator (Electro cell B10, BetaTech, France) or BTX Gemini X2 pulse generator (Harvard Apparatus, USA). Short bipolar pulses of different voltages (HF-EP protocol, 100 V to 1000 V with a step of 100 V, Figure 1B) were delivered by a laboratory prototype pulse generator (University of Ljubljana) based on H-bridge digital

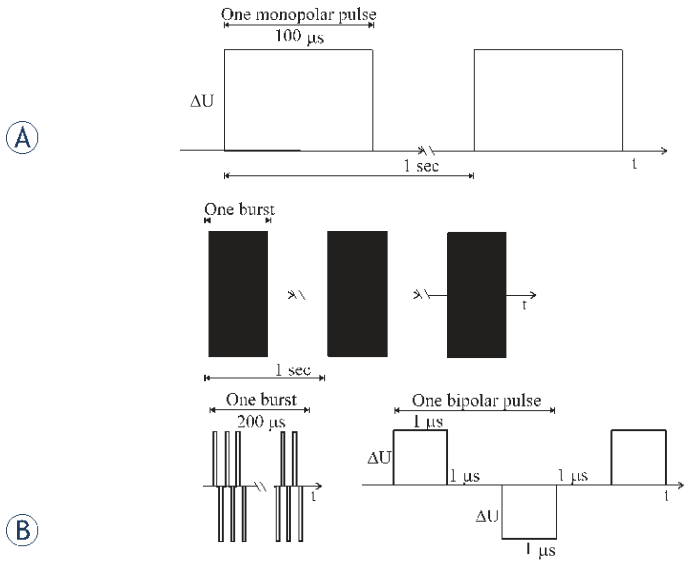

FIGURE 1. Scheme of the applied pulses. **(A)** 100 µs long monopolar pulses of amplitude ΔU (80 V – 240 V in a step of 40 V) were applied with a repetition frequency of 1 Hz. **(B)** Short bipolar pulses (HF-EP). Above: 8 bursts were applied with a repetition frequency of 1 Hz. Down left: One burst was 200 µs long and consisted of 50 bipolar pulses. Below right: One bipolar pulse of amplitude ΔU (100 V – 1000 V in a step of 100 V) consisted of 1 µs long positive pulse, 1 µs long negative pulse (both of voltage ΔU) with a 1 µs long delay between pulses.

amplifier with 1 kV MOSFETs (DE275-102N06A, IXYS, USA).[38,41] Short bipolar pulses were delivered in 8 bursts at repetition frequency 1 Hz, each containing 50 short bipolar pulses of 1 µs positive and 1 µs negative pulse. The delay between short bipolar pulses and between positive and negative pulse was 1 µs. The on-time (the time when the voltage was different from zero) of the HF-EP pulses was 800 µs, equivalent to the duration of the eight 100 µs long monopolar pulses. The duration of one short bipolar pulse was chosen as it successfully permeabilized cell membranes as previously demonstrated by an increased uptake of a fluorescent dye.[38] The voltage and the current were monitored in all experiments with an oscilloscope Wavesurfer 422, 200 MHz, a differential voltage probe ADP305 and a current probe CP030 or AP015, all from LeCroy, USA to ensure that delivered voltage and current were consistent at the same settings even if delivered with different generators.

Determination of permeability and resealing

In permeability experiments, just before pulse application, 60 µl of cell suspension was mixed with 6 µl of 1.5 mM propidium iodide (PI) (136 µM final concentration). In resealing experiments, PI was not added before pulse application but after electroporation. 60 µl of the cell suspension was electroporated, and 50 µl of the treated sample was transferred to a 1.5 ml centrifuge tube. In resealing experiments, 5 µl of PI (136 µM final concentration) was added to 50 µl of the treated sample 2 min, 5 min, 10 min or 20 min after pulse delivery. Two minutes after electroporation (permeability experiments) or PI addition (resealing experiments), the samples were diluted in 100 µl of KPB, and vortexed. The uptake of propidium was measured on the flow cytometer (Attune NxT; Life Technologies, Carlsbad, CA, USA). Cells were excited with a blue laser at 488 nm, and the emitted fluorescence was detected through a 574/26 nm band-pass filter. The measurement was finished when 10,000 events were acquired. Single cells were separated from all events by gating. Obtained data were analyzed using the Attune NxT software. The percentage of permeabilized cells was determined from the histogram of PI fluorescence.

Cell survival following electroporation only

60 µl of the cell suspension was electroporated, 50 µl was transferred to a 15 ml centrifuge tube, and two minutes after pulses delivery, the samples were diluted in 450 µl of DMEM and mixed with a pipette. When all the samples were finished, $5x10^4$ cells were transferred in each well on a 96-well plate in three technical repetitions. After 24 h of incubation at 37°C and humidified 5% CO_2, the survival assay was performed. 20 µl of MTS (CellTiter 96® AQueous One Solution Cell Proliferation Assay (MTS), Promega, USA) was added per well according to manufacturer's instructions and left in an incubator for 2h. MTS assay was used to quantify the number of viable cells evaluating their metabolic activity by measuring the formazan absorbance at 490 nm. After 2 h, the absorbance was measured on a spectrofluorometer (Tecan Infinite 200; Tecan, Grödig, Austria). Cell survival was calculated by first subtracting the background (only DMEM and MTS) from all measurements and then normalizing the absorbance of the treated samples to the absorbance of the control samples.

Cytotoxicity of cisplatin without electroporation

On the first day, $5x10^3$ B16-F1 cells were seeded per well on a 96-well plate and left for one day in an in-

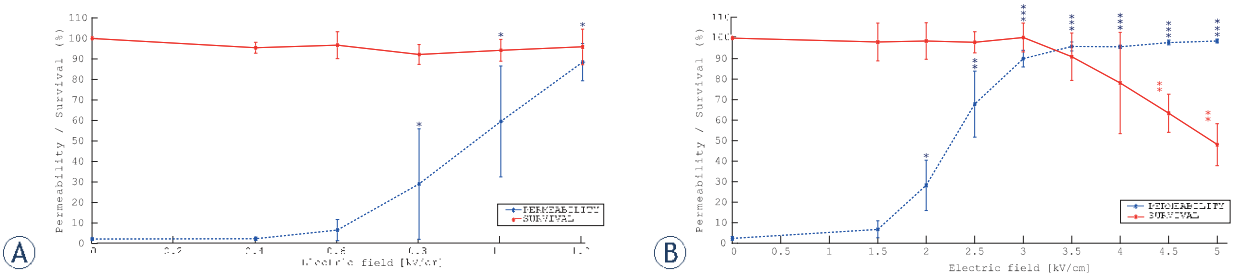

FIGURE 2. Cell membrane permeability and cell survival as a function of electric field for **(A)** 8 x 100 µs long monopolar pulses, delivered at repetition frequency 1 Hz; **(B)** 8 bursts of short bipolar pulses (HF-EP) of 1-1-1-1 µs, delivered at repetition frequency 1 Hz. Each data point was repeated 3–4 times (mean ± standard deviation). In the control sample, no pulses were applied. Note different scales on the x-axes. On **(A)**, the threshold of electroporation was at 0.8 kV/cm (P = 0.029, t-test) and survival did not decrease in comparison with control (one-sample t-test). On **(B)** the threshold of electroporation was at 2 kV/cm (P = 0.022, t-test), while the survival decreased at 4.5 kV/cm (P = 0.004, one-sample t-test). In Figure **2B**, blue asterisks refer to permeability curve and red asterisks to the survival curve.

cubator (Kambič, Slovenia) at 37°C and humidified 5% CO_2. On the second day (24 h after cell seeding), the 3.3 mM stock cisplatin (Accord HealthCare, Poland) was diluted in 0.9% NaCl (physiological solution) to obtain the 10x higher concentration of cisplatin than desired with the cells (1, 10, 100, 330 µM). Diluted cisplatin was then mixed with the DMEM in ratio 1:9 and cells were incubated in DMEM with cisplatin for 10 min, 1 h, 24 h or 48 h. After the indicated time, DMEM with cisplatin was substituted with DMEM only. On the fourth day (72 h after cell seeding), the MTS survival assay was performed as described in the subsection *Cell survival following electroporation only*.

Electroporation with cisplatin

We performed two types of experiments. We applied: 1) different electric fields at fixed cisplatin concentration (100 µM) to evaluate the effect of electric field on cell death; 2) fixed electric field (optimal value – long monopolar pulses E = 1.2 kV/cm and short bipolar (HF-EP) pulses E = 3 kV/cm) with different cisplatin concentrations to evaluate the effect of cisplatin concentration on cell survival. Optimal parameters of electroporation were determined with experiments described in the subsections *Determination of permeability and resealing*, and *Cell survival following electroporation only* and were chosen as those where the highest uptake of propidium iodide (*i.e.*, highest cell membrane permeability) and the highest cell survival were obtained.

The 3.3 mM stock cisplatin was diluted in 0.9% NaCl to obtain the desired concentrations of cisplatin with the cells (1, 10, 100, 330 µM) in both experiments. The drug was prepared fresh for each experiment. Right before experiments, 120 µl of cell suspension was mixed with 13.3 µl of cisplatin. 60 µl of the cell suspension with added cisplatin was transferred between the electrodes, and long monopolar or short bipolar (HF-EP) pulses were delivered (electroporation+cisplatin). The remaining 60 µl was used as a control and was transferred between the electrodes, but no pulses were delivered (only cisplatin). 50 µl of the treated and control sample were transferred in a 15 ml centrifuge tube. 10 minutes after pulse delivery, the samples were diluted 40x in full DMEM and vortexed. $5.5x10^3$ cells were transferred in each well on a 96-well plate in triplicates. The survival assay was performed as described in the subsection *Cell Survival* after 72 hours as previously suggested.[42]

Statistical analysis

Statistical analysis was performed using the software SigmaPlot v11 (Systat Software, San Jose, CA). We performed the t-test or one sample t-test when comparing two groups or one group towards normalized control. We performed the 1-way or 2-way ANOVA if the normality test was passed or the ANOVA on ranks if the normality test failed with the post-hoc Tukey test. The details on the performed test and the obtained P-value are written in respective figure captions in the Results section. On figures, one asterisk (*) signifies $P < 0.05$, two (**) $P < 0.01$ and three (***) $P < 0.001$.

Results

Electroporation with propidium iodide

First, we performed experiments to determine the optimal parameters of electroporation to be later

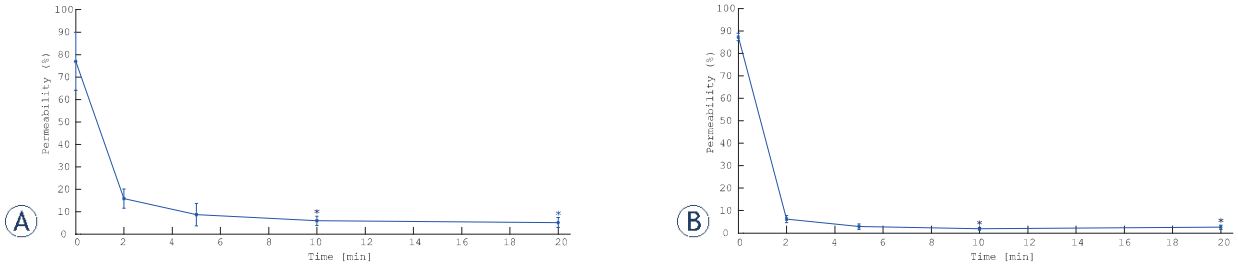

FIGURE 3. Cell membrane permeability as a function of different time of propidium iodide administration after electroporation for **(A)** 8 x 100 µs long monopolar pulses, delivered at a repetition frequency 1 Hz; **(B)** 8 bursts of short bipolar pulses (HF-EP) of 1-1-1-1 µs, delivered at repetition frequency 1 Hz. Each data point was repeated 4 times (mean ± standard deviation). We performed a 1-way ANOVA on ranks. For both types of pulses, there was a significant difference between 0 min vs 10 min and 20 min ($P < 0.05$), other pairwise comparisons were not significant.

used in the experiments with cisplatin. As optimal parameters of electroporation were considered those where the highest cell membrane permeability and the highest cell survival were achieved. In Figure 2 we can observe the permeability curves (blue dashed line) and the survival curves (red solid line) as a function of electric field amplitude for (A) 100 µs long monopolar pulses and (B) bursts of short bipolar (HF-EP) pulses. In Figure 2A we can see that the threshold of electroporation was at 0.8 kV/cm and highest uptake and survival were achieved at 1.2 kV/cm which was considered as the optimal point of electroporation. In Figure 2B we can see that the threshold of electroporation was at 2 kV/cm, the threshold for irreversible electroporation at 4.5 kV/cm and the highest uptake and survival for HF-EP pulses were obtained at 3 kV/cm which was chosen as the optimal point of electroporation with short bipolar pulses. Electric pulses of 1.2 kV/cm with 100 µs monopolar pulses and 3 kV/cm in HF-EP protocol were thus considered to be equivalent and were used in further experiments.

With the optimal parameters of electroporation, we measured the resealing of cell membranes after electroporation. Figure 3 shows the permeability curves obtained as a function of different time of exposure to propidium iodide after electroporation delivering (A) long monopolar pulses at E = 1.2 kV/cm and (B) HF-EP pulses at E = 3 kV/cm. Figure 3A and Figure 3B show a peak of permeability at 0 min, *i.e.*, right after the pulses are applied. Then, we can see a decrease in permeability that reaches a plateau after 10 min. We chose 10 min as the time after which cell membranes resealed. Accordingly, in the subsequent experiments, electroporated samples with cisplatin were diluted after 10 minutes.

Cytotoxicity of cisplatin without electroporation

We measured the cytotoxicity of cisplatin without electroporation at different cisplatin concentrations and incubation times on attached confluent cell monolayers (Figure 4). Cells were more affected if they were exposed to cisplatin for a longer time (24 h and 48 h incubation caused significantly higher cell death than 10 min and 1 h incubation). There was no difference if cells were incubated for 10 min vs 1 h and 24 h vs 48 h. There was no difference between 1 µM and 10 µM, but in general, cytotoxicity increased with higher cisplatin concentrations. After 10 min and 1 h of incubation (red solid and green dashed curve, respectively) there was a decrease in cell survival with increasing cisplatin concentration and at the highest tested concentration

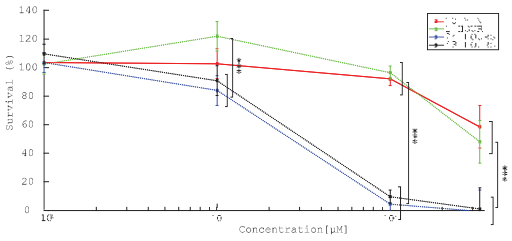

FIGURE 4. Cytotoxicity of cisplatin without electroporation at different concentrations and time of incubation. Each data point was repeated 4 times (mean ± standard deviation) and is normalized to the control sample in which cisplatin was substituted by 0.9% NaCl. A 2-way ANOVA was performed. 10 min or 1 h of incubation was different from 24 h or 48 h ($P < 0.001$) while there was no difference between 10 min vs 1 h and 24 h vs 48 h. 330 µM cisplatin was more cytotoxic than other tested concentrations ($P < 0.001$). There was no significant difference between 1 µM and 10 µM cisplatin; all other comparisons were significantly different ($P < 0.001$).

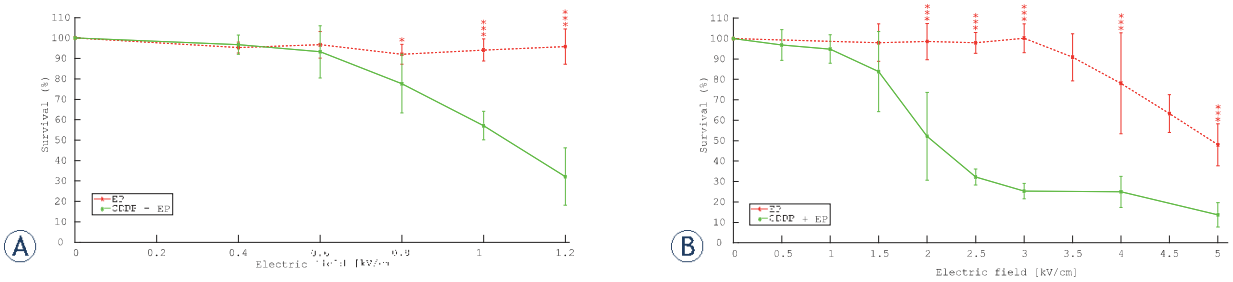

FIGURE 5. Cytotoxicity of cisplatin in combination with electroporation (EP) at fixed value of cisplatin (CDDP) 100 μM as a function of electric field: **(A)** 8 x 100 μs long monopolar pulses (ECT) were delivered at repetition frequency 1 Hz; **(B)** 8 bursts of short bipolar pulses (HF-EP) of 1-1-1-1 μs were delivered at repetition frequency 1 Hz. Each data point was repeated 3–6 times (mean ± standard deviation). Results are normalized to the control sample without an electric field and with 100 μM cisplatin. We performed a **(A)** 2-way ANOVA or **(B)** 2-way ANOVA on ranks. (A) At 0.8 kV/cm ($P = 0.036$) and 1 kV/cm and 1.2 kV/cm ($P < 0.001$) EP samples were significantly different from CDDP+EP samples. **(B)** At electric fields equal to or higher than 2 kV/cm EP samples were significantly different from CDDP+EP samples ($P < 0.001$).

(330 μM) we obtained 58.55% ± 14.90% and 48.12% ± 14.01% survival for 10 min and 1 h, respectively. After 24 h and 48 h (blue dotted and black dash-dot curve, respectively) of incubation, cell survival decreased rapidly to less than 10% already with 100 μM of cisplatin.

Cytotoxicity of cisplatin with electroporation - electrochemotherapy

First, we measured the cytotoxicity of cisplatin with electroporation at different electric fields and selected cisplatin (CDDP) concentration of 100 μM. In Figure 5, we can observe cell survival as a function of applied electric field, on Figure 5A for long monopolar pulses and Figure 5B for HF-EP pulses. The solid green line shows cell survival after electroporation with cisplatin and red dashed line survival after only electroporation without cisplatin. The red dashed curves of Figure 5A and B are already shown in Figure 2A and B. We can see in both Figure 5A and B that the combination of electric pulses and cisplatin is more efficient in achieving cell death than applying only electric pulses or only cisplatin (100% survival at 100 μM cisplatin and 10 min incubation time, Figure 4) and that cytotoxicity of cisplatin increases with increasing electric field, starting at 0.8 kV/cm for 100 μs long monopolar pulses and 2 kV/cm for short bipolar pulses, which coincides with the thresholds for reversible electroporation (Figure 2). In Figure 5A we can see that at $E = 1.2$ kV/cm with cisplatin 32.16% ± 14.08% of cells survive while when we apply only electric pulses, all cell survive. Similarly, in Figure 5B at E = 3 kV/cm 25.33% ± 3.73% of cells survive electroporation with cisplatin opposed to 100% when only electric pulses are applied.

Then, we measured cytotoxicity of cisplatin with electroporation at a fixed electric field (optimal point of electroporation with the highest cell membrane permeability and lowest survival - long monopolar pulses at E = 1.2 kV/cm and HF-EP pulses at E = 3 kV/cm) and different cisplatin concentrations. In Figure 6 we can see two cell survival curves obtained by applying 1) only cisplatin (red dashed curve) and 2) cisplatin in combination with electroporation (solid green curve). From the red dashed curve in Figure 6A and B we can see that cell survival does not decrease with increasing cisplatin concentration due to short incubation time (see also Figure 4). From the solid green curve in Figure 6 A and B we can see that the cytotoxicity of cisplatin increases when electric pulses are applied with increasing cisplatin concentration. A similar trend in survival is observed for both types of pulses.

Discussion

We aimed to determine whether it is possible to use bursts of short bipolar pulses (HF-EP) in *in vitro* electrochemotherapy (ECT) treatments instead of standard long monopolar pulses (classical ECT). We thus performed *in vitro* experiments on mouse skin melanoma cells, as melanoma is one of the cancers successfully treated with electrochemotherapy.[43]

Optimal treatment parameters

First, we determined the cytotoxic effects of cisplatin on a confluent monolayer of cells, because survival after longer exposure time was not possi-

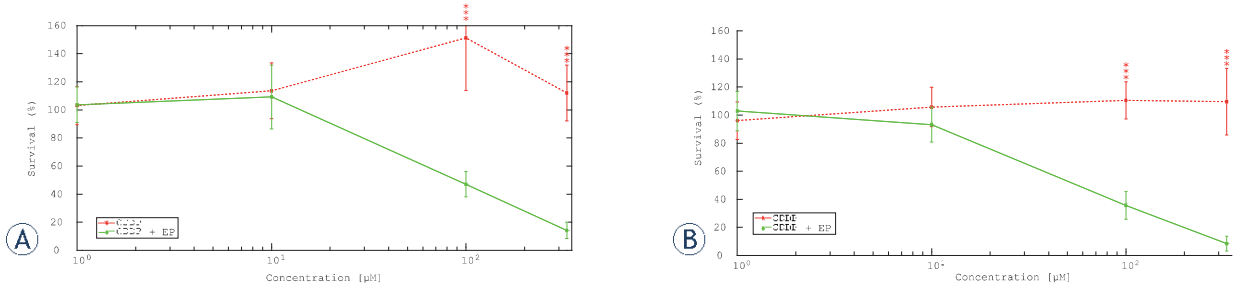

FIGURE 6. Cytotoxicity of cisplatin at different concentration of cisplatin (CDDP) and electroporation (EP) at a fixed value of electric field **(A)** 1.2 kV/cm, 8x100 μs long monopolar pulses, delivered at repetition frequency 1 Hz; **(B)** 3 kV/cm, 8 bursts of short bipolar pulses (HF-EP) of 1-1-1-1 μs, delivered at repetition frequency 1 Hz. Each data point was repeated 3-7 times (mean ± standard deviation). Each data was normalized to the control sample electroporated and with 0.9% NaCl instead of cisplatin. We performed a 2-way ANOVA. For both types of pulses, at 100 μM and 330 μM the CDDP samples were significantly different from the CDDP+EP samples ($P < 0.001$).

ble to evaluate on cell suspension (Figure 4). At 100 μM, short exposure (1 hour or less) did not affect survival. We decided to perform experiments with electroporation at 100 μM cisplatin in order to see possible potentiation of the cytotoxic effect of cisplatin after electroporation. Namely, using higher concentration could already decrease survival without applying electric pulses and we could not asses, if electroporation increases cytotoxicity. In the experiments assessing survival after incubation with cisplatin as determined by the MTS assay, 24 h and 48 h time points were not different one from another and we assumed that also 72 h exposure (which was used in the electroporation experiments) would yield similar results. However, we did not make experiments also at 72 h exposure time.

We determined the optimal parameters for experiments with cisplatin and electric pulses, *i.e.*, the optimal voltage of electric pulses, incubation time with cisplatin after pulse application and cisplatin concentration with a) 100 μs long monopolar pulses (ECT) and b) short bipolar pulses (HF-EP). In experiments with 8x100 μs monopolar pulses, the optimal electric field (highest uptake of propidium and the highest cell survival) was 1.2 kV/cm (Figure 2A) which is in agreement with other studies [44] and corroborates our existing data where cell permeabilization was detected via intracellular platinum measurements.[45] Unfortunately, we could not apply voltages higher than 240 V (1.2 kV/cm) due to the current limitations of the pulse generator. We determined that the optimal electric field with HF-EP pulses was 3 kV/cm (Figure 2B). With bipolar pulses, we had to apply 2.5-times higher electric field than with monopolar pulses to obtain comparable effect, which is in agreement with the results reported by Sweeney *et al.* for propidium uptake[38] and with the *in vitro* data on irreversible electroporation, where irreversible electroporation threshold increased 2.1-times, when 1 μs long pulses were applied in bursts instead as 100 μs long pulses.[46]

With the selected parameters of electroporation, we measured the resealing rate of cells after electroporation. We determined that after 10 min cell membrane is mostly resealed (Figure 3) and did all subsequent cisplatin experiments with 10 min incubation. Dilution of cells with permeable membranes would namely reduce or stop the influx too early or even cause efflux of cisplatin due to dilution and potential reversal of the direction of the concentration gradient.[47] This time range is in agreement with the existing *in vitro* studies, where the incubation time ranges from 5 minutes[23] to 60 minutes[48] as well as with the *in vivo* standard operating procedures where the pulses are applied between 8 and 28 minutes after intravenous drug injection.[19] With propidium iodide (PI) we could use shorter incubation times (2 minutes) as PI binds soon after entering the cell[49], but with cisplatin, we do not know how fast it binds, and we have to wait until cell membranes are completely resealed before the dilution is made. PI was used as a model for cisplatin as its molecular weight is in the same range as of cisplatin (668 g/mol and 300 g/mol for PI and cisplatin, respectively). The similarity in the shape of the permeabilization curve (Figure 2) and cell death due to cisplatin uptake (Figure 5) is another indicator that PI is an appropriate molecule to assess the uptake of cisplatin. Also, experiments with PI and flow cytometry are fast and easy to perform, enable screening of a wide range of parameters quicker than assessing cell survival or plati-

num uptake via mass spectrometry and are thus usually used to determine optimal parameters of electric pulses for electrochemotherapy *in vitro*.[50-52]

100 μM cisplatin concentration was chosen as we could (1) test several pulse parameters without reaching the limitations of the survival assay, (2) it is in a similar range as used in other *in vitro* studies.[23,45,48,53,54] Other tested concentrations (1, 10, 100, 330 μM) were chosen as they were already used in previous *in vitro* experiments.[23,45] (3) The IC50 value of cisplatin pooled together from several studies in[53] was determined to be between 0.83 μM and 1000 μM without electroporation and 0.083 μM and 106 μM with electroporation. As we determined graphically from Figure 6, the IC50 value was in our study 85 μM for monopolar, and 45 μM for bipolar pulses, which is in agreement with the literature and close to the 100 μM.

In our study, different cell densities were used due to different requirements for cell number and sensitivities of the chosen assays. However, even at the highest concentration ($2.2x10^7$ cells/ml) we were still well below the concentration where shielding of the electric field and decreased uptake were observed.[39] 72 h growth time after electrochemotherapy was chosen as it was shown that results of metabolic assays are highly dependent on evaluation time point and they correspond to the results of clonogenic assay better at later time points.[42]

Cytotoxicity of cisplatin with electroporation

We measured the cytotoxicity of cisplatin with electroporation at fixed cisplatin concentration of 100 μM and different electric fields (Figure 5). We were interested in the effect of electric field intensity on cisplatin cytotoxicity, as usually when treating tumors *in vivo*, the electric field distribution is inhomogeneous due to different dielectric properties of different tissues and various electrode configurations.[55,56] A similar tendency of cell survival as a function of the electric field was observed with monopolar as well as HF-EP pulses - we achieved greater cell death by applying cisplatin in combination with electric pulses than by only applying electric pulses. Survival decreased with increasing electric field. In Figure 5A, comparing the red curve with the green one, we can see that at $E = 1.2$ kV/cm cells die because of the cisplatin uptake and not due to irreversible electroporation. The survival after applying 1.2 kV/cm was still 100%, the survival with electric pulses and cisplatin dropped to 32.16% ± 14.08%. Similarly as with monopolar pulses, when applying bipolar pulses of E = 3 kV/cm, cells die due to the cisplatin uptake and not due to irreversible electroporation (Figure 5B). At E > 3 kV/cm cell death is due to the cytotoxic effect of cisplatin as well as irreversible electroporation. As expected and in accordance with previously published results for propidium iodide, we needed to deliver 2.5-times higher electric field with the HF-EP pulses to achieve a comparable effect.[38]

Interestingly, the shape of the permeabilization curve to propidium (Figure 2) corresponds perfectly to the shape of the survival curve after electrochemotherapy (Figure 5). The onset of membrane permeabilization is at 0.8 kV/cm for long monopolar pulses (Figure 2A) and at 2 kV/cm for HF-EP pulses (Figure 2B), which corresponds to the onset of the decrease in survival after electrochemotherapy (Figure 5). The plateau of membrane permeabilization for HF-EP pulses is reached at 3–3.5 kV/cm (Figure 2B) which corresponds to the reached plateau of survival (Figure 5B). Thus at our specific conditions, membrane permeability to propidium is a good indicator of cytotoxicity of cisplatin.

In Figure 6, we measured cytotoxicity of cisplatin with electroporation at a fixed electric field (monopolar pulses E = 1.2 kV/cm and short bipolar pulses E = 3 kV/cm) and different cisplatin concentrations. Namely, in tissues, inhomogeneous cisplatin concentration is expected, also initial cisplatin concentration is usually inhomogeneous after intratumoral injection.[45] Both (A) monopolar pulses at E = 1.2 kV/cm and (B) HF-EP pulses at E = 3 kV/cm show a similar behavior. In both Figures 6 A and B, the cytotoxicity of cisplatin increases more with cisplatin in combination with electric pulses than using only cisplatin.[23,25] Indeed, without electric pulses application, a high dose of cisplatin and/or longer incubation times need to be used to achieve a decrease in cell survival (Figure 4). However, applying 330 μM cisplatin with long monopolar pulses only 14.28% ± 5.84% of cell survived and with short bipolar pulses (HF-EP) only 8.45% ± 5.22% of cell survived. We must keep in mind, that with short bipolar pulses, 2.5-times higher electric field was applied to achieve a similar effect. From the red dashed curve in Figure 6A and B we can see that cell survival did not decrease with increasing cisplatin concentration. This result should be the same as in Figure 4 considering only the 10 min curve, but in Figure 4 cell survival slightly decreases with increasing cisplatin concentration. The reasons for this discrepancy could be the differences in the protocols: attached cell monolayers to measure the cytotoxicity of cisplatin without

electroporation and cells in suspension to measure the cytotoxicity of cisplatin in combination with electroporation. Also, the attached cells were diluted much less with fresh DMEM after exposure to cisplatin than cells in suspension. Besides, cell survival was measured after 48h for the attached cell and after 72 h for the cell in suspension.

Outlooks for using high-frequency electroporation in the clinics

HF-IRE pulses were reported to reduce muscle contractions in comparison with classic 100 µs pulses which was observed in several studies *in vivo*. For example, muscle contractions with HF-IRE pulses were much less noticeable than with 100 µs long monopolar pulses in experiments on rabbit liver.[33,37,38] Even in the absence of cardiac synchronization and paralytics, only minor muscle twitch was recorded in one out of 24 cases[39,60] when treating porcine liver. Sano *et al.* observed that HF-IRE waveforms reduced the intensity of muscle contractions in comparison with traditional IRE pulses on *ex-vivo* porcine model[34] and in *in vivo* murine tumor.[46] Arena *et al.* observed that HF-IRE pulses eliminated muscle contractions when electric pulses were applied to the brain of rats[37] and achieved blood-brain-barrier disruption without inducing local or distal muscle contractions.[61] Latouche *et al.* observed no evidence of muscle or nerve excitation or cardiac arrhythmia during any pulse delivery when treating intracranial meningioma in dogs.[35] In a first human study on high-frequency irreversible electroporation of prostate cancer, only a small amount of muscle relaxant was needed, and there were no visible muscle contractions during the pulse delivery process.[36] Additionally, the histological analysis in *in vivo* porcine experiments indicates that with HF-IRE rapid and reproducible ablation in the liver can be achieved, while preserving gross vascular/biliary architecture.[60] The mechanism for decreased muscle contractions is still unknown. However, different possible explanations were offered. It was suggested that (1) stimulation threshold raises faster than the threshold for irreversible electroporation with decreasing pulse length[62] which is a consequence of geometrical differences between nerve fibers and tumor cells.[63] (2) At around 1 µs there is an overlap of the depolarization threshold and electroporation threshold on the strength-intensity curve.[41] (3) The short negative pulse delivered after a positive pulse accelerated the passive repolarization and swamped the regenerative response, thus abolishing the action potential.[64] The pain was not yet evaluated, but promising results regarding muscle contractions indicate that we can expect less pain with HF-EP than with classical 100 µs pulses.

Before transfer to the clinical setting, more experiments *in vitro* as well *in vivo* need to be performed. In the scope of the current study, experiments with bleomycin are not feasible due to organizational reasons. However, we are planning to perform, in the future, experiments using bleomycin with HF-EP, as bleomycin is frequently used for ECT in the clinics. So, cytotoxicity of bleomycin and HF-EP needs to be assessed, and experiments determining intratumoral cisplatin/bleomycin concentration should be performed. The electric field needed to achieve cell death is with HF-EP higher than in classical EP, and thus the effect of high voltage on important structures in the vicinity of the tumors should be investigated, similarly as in[60] for hepatic veins. Also, temperature increase due to Joule heating has to be minimized for example by introducing a delay between bursts[36,59], limiting electric current or number of bursts[36,46,61] and avoiding increased temperature by optimizing treatment parameters.[35,37,58,61] The influence of HF-EP on muscle contractions, pain and heart rhythm should also be studied, as is being done for high-frequency irreversible electroporation. Currently, pulses in the published studies are being applied with laboratory prototypes - a clinical generator of bipolar pulses needs to be designed and certified before clinical use. However, electrode geometry could be the same as those used with the longer monopolar pulses, but electrical isolation of the wiring and stray capacitance should be re-evaluated.

Applying HF-EP pulses comes at the expense of delivering considerably higher pulse amplitude. However, we need to take into account that in our study, we focused on eight bursts in total on-time of 800 µs to enable comparison with the standard ECT protocol and be consistent with previous studies.[38] To obtain a good effect while keeping the applied voltage low, we could apply more bursts, longer pulses than 1 µs or asymmetrical bipolar pulses[34,65], although it was indicated that muscle contractions are increased with the asymmetrical waveforms. Also of importance is that with pulses in the range of a few microseconds, we are already in the range of the so-called cancellation effect which could be partially responsible for decreased effect of shorter pulses in comparison to longer pulses.[38,66] We can nevertheless conclude that HF-EP pulses can be successfully used in electrochemotherapy treat-

ments *in vitro*, however, at the expense of delivering electric pulses of higher amplitudes.[38]

Although still at the *in vitro* testing stage, we believe that the use of HF-EP pulses for electrochemotherapy in the clinics could potentially decrease the discomfort connected with muscle contractions and pain, simplifying the treatment procedure by lowering dose of muscle relaxants and anesthesia, and avoid synchronization with the electrocardiogram, while potentially achieving more homogeneous electric field distribution[67] and reducing the electrolytic contamination.[68]

Conclusions

In conclusion, with long monopolar and short bipolar pulses (HF-EP), we achieved similar efficiency of electrochemotherapy with cisplatin *in vitro*, however, with short bipolar pulses, we had to apply a much higher electric field for the same effect. Nevertheless, we believe that HF-EP pulses could eventually be translated into the clinical setting to be used in electrochemotherapy treatments to alleviate pain, reduce muscle contractions, decrease the needed dose of anesthetics and muscle relaxants while maintaining high treatment efficacy. Further studies of the HF-EP pulses for electrochemotherapy with bleomycin *in vitro* and *in vivo* are needed.

Acknowledgments

This work was supported by the Slovenian Research Agency (ARRS) [research core funding No. P2-0249 and IP-0510]. The research was conducted within the scope of the electroporation in Biology and Medicine (EBAM) European Associated Laboratory (LEA). Authors would like to thank L. Vukanović and D. Hodžić for their help in the cell culture laboratory and dr. T. Jarm for his help with the statistical analysis and M. Bernik for the linguistic revision of Slovenian abstract. M.S. would like to thank dr. E. Sieni for her help and acknowledge the Erasmus+ grant.

References

1. Kotnik T, Kramar P, Pucihar G, Miklavcic D, Tarek M. Cell membrane electroporation-part 1: the phenomenon. *IEEE Electr Insul Mag* 2012; **28:** 14-23. doi: 10.1109/MEI.2012.6268438
2. Weaver JC. Electroporation: a general phenomenon for manipulating cells and tissues. *J Cell Biochem* 1993; **51:** 426-35. doi: 10.1002/jcb.2400510407
3. Tsong TY. Electroporation of cell membranes. *Biophys J* 1991; **60:** 297-306. doi: 10.1016/S0006-3495(91)82054-9
4. Kotnik T, Rems L, Tarek M, Miklavčič D. Membrane electroporation and electropermeabilization: mechanisms and models. *Annu Rev Biophys* 2019; **48**. doi: 10.1146/annurev-biophys-052118-115451
5. Yarmush ML, Golberg A, Serša G, Kotnik T, Miklavčič D. Electroporation-based technologies for medicine: principles, applications, and challenges. *Annu Rev Biomed Eng* 2014; **16:** 295-320. doi: 10.1146/annurev-bioeng-071813-104622
6. Jiang C, Davalos RV, Bischof JC. A review of basic to clinical studies of irreversible electroporation therapy. *IEEE Trans Biomed Eng* 2015; **62:** 4-20. doi: 10.1109/TBME.2014.2367543
7. Scheffer HJ, Nielsen K, de Jong MC, van Tilborg AA, Vieveen JM, Bouwman AR, et al. Irreversible electroporation for nonthermal tumor Ablation in the clinical setting: a systematic review of safety and efficacy. *J Vasc Interv Radiol* 2014; **25:** 997-1011. doi: 10.1016/j.jvir.2014.01.028
8. Mali B, Jarm T, Snoj M, Serša G, Miklavčič D. Antitumor effectiveness of electrochemotherapy: a systematic review and meta-analysis. *Eur J Surg Oncol* 2013; **39:** 4-16. doi: 10.1016/j.ejso.2012.08.016
9. Haberl S, Miklavčič D, Serša G, Frey W, Rubinsky B. Cell membrane electroporation – part 2: the applications. *Electr Insul Mag IEEE* 2013; **29:** 29-37. doi: 10.1109/MEI.2013.6410537
10. Cadossi R, Ronchetti M, Cadossi M. Locally enhanced chemotherapy by electroporation: clinical experiences and perspective of use of electrochemotherapy. *Future Oncol* 2014; **10:** 877-90. doi: 10.2217/fon.13.235
11. Kotnik T, Frey W, Sack M, Meglič SH, Peterka M, Miklavčič D. Electroporation-based applications in biotechnology. *Trends Biotechnol* 2015; **33:** 480-8. doi: 10.1016/j.tibtech.2015.06.002
12. Golberg A, Sack M, Teissie J, Pataro G, Pliquett U, Saulis G, et al. Energy-efficient biomass processing with pulsed electric fields for bioeconomy and sustainable development. *Biotechnol Biofuels* 2016; **9:** 94. doi: 10.1186/s13068-016-0508-z
13. Toepfl S, Siemer C, Saldaña-Navarro G, Heinz V. Overview of pulsed electric fields processing for food. In: Sun DW, editor. *Emerging technologies for food processing*. Second edition. Amsterdam: Academic press; Elsevier; 2014. p. 93-114. doi: 10.1016/B978-0-12-411479-1.00006-1
14. Mahnič-Kalamiza S, Vorobiev E, Miklavčič D. Electroporation in food processing and biorefinery. *J Membr Biol* 2014; **247:** 1279-304. doi: 10.1007/s00232-014-9737-x
15. Campana LG, Edhemović I, Soden D, Perrone AM, Scarpa M, Campanacci L, et al. Electrochemotherapy - emerging applications technical advances, new indications, combined approaches, and multi-institutional collaboration. *Eur J Surg Oncol* 2019; **45:** 92-102. doi: 10.1016/j.ejso.2018.11.023
16. Miklavčič D, Mali B, Kos B, Heller R, Serša G. Electrochemotherapy: from the drawing board into medical practice. *Biomed Eng OnLine* 2014; **13:** 29. doi: 10.1186/1475-925X-13-29
17. Mir LM, Gehl J, Serša G, Collins CG, Garbay J-R, Billard V, et al. Standard operating procedures of the electrochemotherapy: Instructions for the use of bleomycin or cisplatin administered either systemically or locally and electric pulses delivered by the CliniporatorTM by means of invasive or non-invasive electrodes. *Eur J Cancer Suppl* 2006; **4:** 14-25. doi: 10.1016/j.ejcsup.2006.08.003
18. Gehl J, Serša G, Matthiessen LW, Muir T, Soden D, Occhini A, et al. Updated standard operating procedures for electrochemotherapy of cutaneous tumours and skin metastases. *Acta Oncol Stockh Swed* 2018; **57:** 874-82. doi: 10.1080/0284186X.2018.1454602
19. Marty M, Serša G, Garbay JR, Gehl J, Collins CG, Snoj M, et al. Electrochemotherapy – An easy, highly effective and safe treatment of cutaneous and subcutaneous metastases: results of ESOPE (European Standard Operating Procedures of Electrochemotherapy) study. *Eur J Cancer Suppl* 2006; **4:** 3-13. doi: 10.1016/j.ejcsup.2006.08.002
20. Mir LM, Tounekti O, Orlowski S. Bleomycin: revival of an old drug. *Gen Pharmacol* 1996; **27:** 745-8. doi: 10.1016/0306-3623(95)02101-9
21. Tounekti O, Pron G, Belehradek J, Mir LM. Bleomycin, an apoptosis-mimetic drug that induces two types of cell death depending on the number of molecules internalized. *Cancer Res* 1993; **53:** 5462-9. PMID: 7693342

22. Spreckelmeyer S, Orvig C, Casini A. Cellular transport mechanisms of cytotoxic metallodrugs: an overview beyond cisplatin. *Molecules* 2014; **19:** 15584-610. doi: 10.3390/molecules191015584

23. Serša G, Čemažar M, Miklavčič D. Antitumor effectiveness of electrochemotherapy with cis-diamminedichloroplatinum(II) in mice. *Cancer Res* 1995; **55:** 3450-5. PMID: 7614485

24. Tozon N, Serša G, Čemažar M. Electrochemotherapy: potentiation of local antitumour effectiveness of cisplatin in dogs and cats. *Anticancer Res* 2001; **21:** 2483-8. PMID: 11724311

25. Jaroszeski MJ, Dang V, Pottinger C, Hickey J, Gilbert R, Heller R. Toxicity of anticancer agents mediated by electroporation in vitro. *Anticancer Drugs* 2000; **11:** 201-8. PMID: 10831279

26. Županič A, Ribarič S, Miklavčič D. Increasing the repetition frequency of electric pulse delivery reduces unpleasant sensations that occur in electrochemotherapy. *Neoplasma* 2007; **54:** 246-50. PMID: 17447858

27. Miklavčič D, Pucihar G, Pavlovec M, Ribarič S, Mali M, Maček-Lebar A, et al. The effect of high frequency electric pulses on muscle contractions and antitumor efficiency in vivo for a potential use in clinical electrochemotherapy. *Bioelectrochemistry* 2005; **65:** 121-8. doi: 10.1016/j.bioelechem.2004.07.004

28. Arena CB, Davalos RV. Advances in therapeutic electroporation to mitigate muscle contractions. *J Membr Sci Technol* 2012; **2:** 1-3. doi: 10.4172/2155-9589.1000e102

29. Ball C, Thomson KR, Kavnoudias H. Irreversible electroporation: a new challenge in "Out of Operating Theater" anesthesia. *Anesth Analg* 2010; **110:** 1305-9. doi: 10.1213/ANE.0b013e3181d27b30

30. Mali B, Jarm T, Čorović S, Paulin-Kosir MS, Čemažar M, Serša G, et al. The effect of electroporation pulses on functioning of the heart. *Med Biol Eng Comput* 2008; **46:** 745-57. doi: 10.1007/s11517-008-0346-7

31. Deodhar A, Dickfeld T, Single GW, Hamilton WC, Thornton RH, Sofocleous CT, et al. Irreversible electroporation near the heart: ventricular arrhythmias can be prevented with ECG synchronization. *AJR Am J Roentgenol* 2011; **196:** W330-5. doi: 10.2214/AJR.10.4490

32. Golberg A, Rubinsky B. Towards electroporation based treatment planning considering electric field induced muscle contractions. *Technol Cancer Res Treat* 2012; **11:** 189-201. doi: 10.7785/tcrt.2012.500249

33. Yao C, Dong S, Zhao Y, Lv Y, Liu H, Gong L, et al. Bipolar microsecond pulses and insulated needle electrodes for reducing muscle contractions during irreversible electroporation. *IEEE Trans Biomed Eng* 2017; **64:** 2924-37. doi: 10.1109/TBME.2017.2690624

34. Sano MB, Fan RE, Cheng K, Saenz Y, Sonn GA, Hwang GL, et al. Reduction of muscle contractions during irreversible electroporation therapy using high-frequency bursts of alternating polarity pulses: a laboratory investigation in an ex vivo swine model. *J Vasc Interv Radiol JVIR* 2018; **29:** 893-8.e4. doi: 10.1016/j.jvir.2017.12.019

35. Latouche EL, Arena CB, Ivey JW, Garcia PA, Pancotto TE, Pavlisko N, et al. High-frequency irreversible electroporation for intracranial meningioma: A feasibility study in a spontaneous canine tumor model. *Technol Cancer Res Treat* 2018; **17:** 1-10. doi: 10.1177/1533033818785285

36. Dong S, Wang H, Zhao Y, Sun Y, Yao C. First human trial of high-frequency irreversible electroporation therapy for prostate cancer. *Technol Cancer Res Treat* 2018; **17:** 1-9. doi: 10.1177/1533033818789692

37. Arena CB, Sano MB, Rossmeisl JH, Caldwell JL, Garcia PA, Rylander M, et al. High-frequency irreversible electroporation (H-FIRE) for non-thermal ablation without muscle contraction. *Biomed Eng OnLine* 2011; **10:** 102. doi: 10.1186/1475-925X-10-102

38. Sweeney DC, Reberšek M, Dermol J, Rems L, Miklavčič D, Davalos RV. Quantification of cell membrane permeability induced by monopolar and high-frequency bipolar bursts of electrical pulses. *Biochim Biophys Acta BBA - Biomembr* 2016; **1858:** 2689-98. doi: 10.1016/j.bbamem.2016.06.024

39. Pucihar G, Kotnik T, Teissié J, Miklavčič D. Electropermeabilization of dense cell suspensions. *Eur Biophys J* 2007; **36:** 173-85. doi: 10.1007/s00249-006-0115-1

40. Dermol J, Miklavčič D. Mathematical models describing chinese hamster ovary cell death due to electroporation in vitro. *J Membr Biol* 2015; **248:** 865-81. doi: 10.1007/s00232-015-9825-6

41. Dermol-Černe J, Miklavčič D, Reberšek M, Mekuč P, Bardet SM, Burke R, et al. Plasma membrane depolarization and permeabilization due to electric pulses in cell lines of different excitability. *Bioelectrochemistry* 2018; **122**:103-14. doi: 10.1016/j.bioelechem.2018.03.011

42. Jakštys B, Ruzgys P, Tamošiūnas M, Šatkauskas S. Different cell viability assays reveal inconsistent results after bleomycin electrotransfer in vitro. *J Membr Biol* 2015; **248:** 857-63. doi: 10.1007/s00232-015-9813-x

43. Serša G, Štabuc B, Čemažar M, Miklavčič D, Rudolf Z. Electrochemotherapy with cisplatin: clinical experience in malignant melanoma patients. *Clin Cancer Res* 2000; **6:** 863-7. PMID: 10741708

44. Čemažar M, Jarm T, Miklavčič D, Maček Lebar A, Ihan A, Kopitar NA, et al. Effect of electric-field intensity on electropermeabilization and electrosensitivity of various tumor-cell lines in vitro. *Electro-Magnetobiology* 1998; **17:** 263-72. doi.org/10.3109/15368379809022571

45. Dermol-Černe J, Vidmar J, Ščančar J, Uršič K, Serša G, Miklavčič D. Connecting the in vitro and in vivo experiments in electrochemotherapy - a feasibility study modeling cisplatin transport in mouse melanoma using the dual-porosity model. *J Control Release* 2018; **286:** 33-45. doi: 10.1016/j.jconrel.2018.07.021

46. Sano MB, Arena CB, Bittleman KR, DeWitt MR, Cho HJ, Szot CS, et al. Bursts of Bipolar Microsecond Pulses Inhibit Tumor Growth. *Sci Rep* 2015; **5:** 14999. doi: 10.1038/srep14999

47. Puc M, Kotnik T, Mir LM, Miklavčič D. Quantitative model of small molecules uptake after in vitro cell electropermeabilization. *Bioelectrochemistry Amst Neth* 2003; **60:** 1-10. doi: 10.1016/S1567-5394(03)00021-5

48. Gehl J, Skovsgaard T, Mir LM. Enhancement of cytotoxicity by electropermeabilization: an improved method for screening drugs. *Anticancer Drugs* 1998; **9:** 319-25. PMID: 9635922

49. Pucihar G, Kotnik T, Miklavčič D, Teissié J. Kinetics of transmembrane transport of small molecules into electropermeabilized cells. *Biophys J* 2008; **95:** 2837-48. doi: 10.1529/biophysj.108.135541

50. Čemažar M, Serša G, Miklavčič D. Electrochemotherapy with cisplatin in the treatment of tumor cells resistant to cisplatin. *Anticancer Res* 1998; **18:** 463-6. PMID: 9891510

51. Saczko J, Kamińska I, Kotulska M, Bar J, Choromańska A, Rembiałkowska N, et al. Combination of therapy with 5-fluorouracil and cisplatin with electroporation in human ovarian carcinoma model in vitro. *Biomed Pharmacother* 2014; **68:** 573-80. doi: 10.1016/j.biopha.2014.05.005

52. Žakelj M, Prevc A, Kranjc S, Čemažar M, Todorovič V, Savarin M, et al. Electrochemotherapy of radioresistant head and neck squamous cell carcinoma cells and tumor xenografts. *Oncol Rep* 2019; **41:** 1658-68. doi: 10.3892/or.2019.6960

53. Todorovič V, Serša G, Flisar K, Čemažar M. Enhanced cytotoxicity of bleomycin and cisplatin after electroporation in murine colorectal carcinoma cells. *Radiol Oncol* 2009; **43:** 264-73. doi: 10.2478/v10019-009-0037-5

54. Vásquez JL, Ibsen P, Lindberg H, Gehl J. In vitro and in vivo experiments on electrochemotherapy for bladder cancer. *J Urol* 2015; **193:** 1009-15. doi: 10.1016/j.juro.2014.09.039

55. Kranjc M, Markelc B, Bajd F, Čemažar M, Serša I, Blagus T, et al. In situ monitoring of electric field distribution in mouse tumor during electroporation. *Radiology* 2015; **274:** 115-23. doi: 10.1148/radiol.14140311

56. Čorović S, Pavlin M, Miklavčič D. Analytical and numerical quantification and comparison of the local electric field in the tissue for different electrode configurations. *Biomed Eng OnLine* 2007; **6:** 37. doi: 10.1186/1475-925X-6-37

57. Dong S, Yao C, Zhao Y, Lv Y, Liu H. Parameters optimization of bipolar high frequency pulses on tissue ablation and inhibiting muscle contraction. *IEEE Trans Dielectr Electr Insul* 2018; **25:** 207-16. doi: 10.1109/TDEI.2018.006303

58. Zhao Y, Bhonsle S, Dong S, Lv Y, Liu H, Safaai-Jazi A, et al. Characterization of conductivity changes during high-frequency irreversible electroporation for treatment planning. *IEEE Trans Biomed Eng* 2018; **65:** 1810-9. doi: 10.1109/TBME.2017.2778101

59. Siddiqui IA, Latouche EL, DeWitt MR, Swet JH, Kirks RC, Baker EH, et al. Induction of rapid, reproducible hepatic ablations using next-generation, high frequency irreversible electroporation (H-FIRE) in vivo. *HPB* 2016; **18:** 726-34. doi: 10.1016/j.hpb.2016.06.015

60. Siddiqui IA, Kirks RC, Latouche EL, DeWitt MR, Swet JH, Baker EH, et al. High-frequency irreversible electroporation: Safety and efficacy of next-generation irreversible electroporation adjacent to critical hepatic structures. *Surg Innov* 2017; **24:** 276-83. doi: 10.1177/1553350617692202

61. Arena CB, Garcia PA, Sano MB, Olson JD, Rogers-Cotrone T, Rossmeisl JH, et al. Focal blood-brain-barrier disruption with high-frequency pulsed electric fields. *Technology* 2014; **2:** 206-13. doi: 10.1142/S2339547814500186

62. Rogers WR, Merritt JH, Comeaux JA, Kuhnel CT, Moreland DF, Teltschik DG, et al. Strength-duration curve for an electrically excitable tissue extended down to near 1 nanosecond. *IEEE Trans Plasma Sci* 2004; **32:** 1587-99. doi: 10.1109/TPS.2004.831758

63. Mercadal B, Arena CB, Davalos RV, Ivorra A. Avoiding nerve stimulation in irreversible electroporation: a numerical modeling study. *Phys Med Biol* 2017; **62:** 8060-79. doi: 10.1088/1361-6560/aa8c53

64. van den Honert C, Mortimer JT. The response of the myelinated nerve fiber to short duration biphasic stimulating currents. *Ann Biomed Eng* 1979; **7:** 117-25. doi: 10.1007/BF02363130.

65. Sano MB, Fan RE, Xing L. Asymmetric waveforms decrease lethal thresholds in high frequency irreversible electroporation therapies. *Sci Rep* 2017; **7:** 40747. doi: 10.1038/srep40747

66. Valdez CM, Barnes R, Roth CC, Moen E, Ibey B. The interphase interval within a bipolar nanosecond electric pulse modulates bipolar cancellation. *Bioelectromagnetics* 2018; **39:** 441-50. doi: 10.1002/bem.22134

67. Bhonsle SP, Arena CB, Sweeney DC, Davalos RV. Mitigation of impedance changes due to electroporation therapy using bursts of high-frequency bipolar pulses. *Biomed Eng Online* 2015; **14(Suppl 3):** S3. doi: 10.1186/1475-925X-14-S3-S3

68. Kotnik T, Miklavčič D, Mir LM. Cell membrane electropermeabilization by symmetrical bipolar rectangular pulses. Part II. Reduced electrolytic contamination. *Bioelectrochemistry* 2001; **54:** 91-5. doi: 10.1016/S1567-5394(01)00115-3

2.2. Paper 2

Title: **The equivalence of different types of electric pulses for electrochemotherapy with cisplatin -an in vitro study**

Authors: **Maria Scuderi,** Janja Dermol-Černe, Janez Ščančar, Stefan Marković, Lea Rems, and Damijan Miklavčič

Publication: Radiology and Oncology vol. 58, no. 1, pp. 51–66, February 2024.

Impact Factor on the date of publication: 2.4 (2022)

Quartile:

- Q3 (Radiology, Nuclear Medicine & Medical Imaging)
- Q4 (Oncology)

Rank:

- 98/203 (Radiology, Nuclear Medicine & Medical Imaging)
- 166/318 (Oncology)

DOI: doi: 10.2478/raon-2024-0005

The study was presented at MEDICON and CMBEBIH Conference and awarded with the 3rd prize in the IFMBE Young Investigator Competition

sciendo Radiology and Oncology | Ljubljana | Slovenia | www.radioloncol.com RADIOLOGY AND ONCOLOGY 51

research article

The equivalence of different types of electric pulses for electrochemotherapy with cisplatin – an *in vitro* study

Maria Scuderi[1], Janja Dermol-Cerne[1], Janez Scancar[2,3], Stefan Markovic[2,3], Lea Rems[1], Damijan Miklavcic[1]

[1] Faculty of Electrical Engineering, University of Ljubljana, Ljubljana, Slovenia
[2] Department of Environmental Sciences, Jožef Stefan Institute, Ljubljana, Slovenia
[3] Jožef Stefan International Postgraduate School, Ljubljana, Slovenia

Radiol Oncol 2024; 58(1): 51-66.

Received 20 November 2023
Accepted 5 December 2023

Correspondence to: Prof. Damijan Miklavčič, Ph.D., Faculty of Electrical Engineering, University of Ljubljana, Tržaška cesta 25, SI-1000 Ljubljana, Slovenia. E-mail: damijan.miklavcic@fe.uni-lj.si

Disclosure: No potential conflicts of interest were disclosed.

Background. Electrochemotherapy (ECT) is a treatment involving the administration of chemotherapeutics drugs followed by the application of 8 square monopolar pulses of 100 µs duration at a repetition frequency of 1 Hz or 5000 Hz. However, there is increasing interest in using alternative types of pulses for ECT. The use of high-frequency short bipolar pulses has been shown to mitigate pain and muscle contractions. Conversely, the use of millisecond pulses is interesting when combining ECT with gene electrotransfer for the uptake of DNA-encoding proteins that stimulate the immune response with the aim of converting ECT from a local to systemic treatment. Therefore, the aim of this study was to investigate how alternative types of pulses affect the efficiency of the ECT.

Materials and methods. We performed *in vitro* experiments, exposing Chinese hamster ovary (CHO) cells to conventional ECT pulses, high-frequency bipolar pulses, and millisecond pulses in the presence of different concentrations of cisplatin. We determined cisplatin uptake by inductively coupled plasma mass spectrometry and cisplatin cytotoxicity by the clonogenic assay.

Results. We observed that the three tested types of pulses potentiate the uptake and cytotoxicity of cisplatin in an equivalent manner, provided that the electric field is properly adjusted for each pulse type. Furthermore, we quantified that the number of cisplatin molecules, resulting in the eradication of most cells, was 2–7 × 10^7 per cell.

Conclusions. High-frequency bipolar pulses and millisecond pulses can potentially be used in ECT to reduce pain and muscle contraction and increase the effect of the immune response in combination with gene electrotransfer, respectively.

Key words: electrochemotherapy; electroporation; cisplatin uptake; phenomenological model; equivalent pulse parameters

Introduction

Electrochemotherapy (ECT) is a highly effective local treatment used in clinics to treat superficial tumors, specifically various types of skin tumors when standard treatments such as surgery, chemotherapy, and radiotherapy are not sufficient or applicable.[1,2] Over the past decade, ECT has also been successfully used for the treatment of deep-seated tumors, including tumors in the liver, bone, and pancreas.[3-9]

ECT essentially consists of two main steps.[10,11] First, a chemotherapeutic drug is injected intratumorally or intravenously. Second, short high-

intensity electric pulses that result in cell membrane electroporation are delivered to the tumor. Electroporation transiently increases the cell membrane permeability through the formation of pores/defects in the membrane and enhances the intracellular uptake of the chemotherapeutic drug. The drugs most often used in ECT are bleomycin and cisplatin, which kill cancerous cells by acting on DNA but poorly permeate the cell membrane.[1,12] Electroporation potentiates the uptake, and consequently the cytotoxicity, of bleomycin by several hundred to thousand folds and of cisplatin by several ten folds compared to nonelectroporated controls.[13-15] In addition to increased intracellular drug delivery, drug entrapment due to the blood flow modifying effect of electric pulses[16], the vascular disrupting effect[17,18] and immune system response[19,20] were identified to critically contribute to the success of ECT.[21]

Electroporation can be achieved with a wide range of pulse parameters (pulse shape, polarity, duration, amplitude, number, repetition rate, etc.). In ECT, conventionally 8 square monopolar pulses of 100 μs duration at a repetition frequency of 1 Hz or 5000 Hz are applied.[10,11,22] However, the use of 100 μs long pulses causes pain and muscle contractions[23,24] in the patient during the treatment. Furthermore, muscle contraction might lead to the displacement of the electrodes resulting in undertreatment[25] and in potential harm for the vital structures when treating deep-seated tumors.[26] Thus, there is a need to use local or general anesthesia and muscle relaxants and, when performing ECT of deep-seated tumors in proximity to the heart, the pulses need to be synchronized with the heart rhythm.[27-31] To overcome these drawbacks, recent studies suggest the use of bursts of short high-frequency bipolar pulses (1–10 μs pulse duration), which minimize pain and muscle contractions.[23,32,33] Such pulses are already used for the ablation of tumors[34] and cardiac tissue[35-37] by irreversible electroporation. Furthermore, *in vitro* and *in vivo* studies show that high-frequency bipolar pulses can potentially be used in ECT.[38,39] Recent reports demonstrated the safety, tolerability, and efficacy of using high-frequency bipolar pulses for the treatment of cutaneous tumors with ECT.[40-42]

In ECT preclinical and clinical studies have shown that immune response critically contributes to tumor eradication.[19,43,44] Thus, ECT has been tested in combination with gene electrotransfer (GET) which delivers protein-encoding DNA into tumor cell/tissue to induce immune stimulation.[45-47] Even if the combined ECT+GET treatment was applied only to some of the cutaneous metastases, this combination successfully evoked a systemic immune response and in some cases succeeded in producing a partial response or complete response of distant, non-treated nodules (i.e., abscopal effect).[48] GET, which is also based on electroporation, is traditionally achieved by the application of millisecond-duration electric pulses as it is believed that different transmembrane pathways/mechanisms are involved in chemotherapeutic vs. pDNA transport.[49] When ECT is used in combination with GET traditionally two different types of pulses would be necessary (conventional 8 × 100 μs pulses for ECT and millisecond duration pulses for GET).

Changing the conventional 8 × 100 μs pulses to an alternative type of pulse such as high-frequency bipolar pulses or millisecond pulses could thus be advantageous in ECT. However, it is not well understood whether the use of alternative types of pulses would compromise the efficiency of the ECT treatment. Recently, *in vitro* study by Radzevičiūtė *et al.*[50] and *in vivo* study by Novickij *et al.*[51] demonstrated that pulses of sub-microsecond duration can be as effective as the conventional pulses for ECT with bleomycin. Moreover, *in vitro* study by Vižintin *et al.*[52] demonstrated that sub-microsecond pulses can be as effective as the conventional 8 × 100 μs pulses for ECT with cisplatin. The study[52] also quantified the number of internalized cisplatin molecules needed for decreasing cell survival.

In this study, we expanded upon Vižintin *et al.*[52] and investigated how high-frequency bipolar pulses and millisecond duration pulses affect the uptake and cytotoxicity of cisplatin compared with conventional 8 × 100 μs pulses. We performed *in vitro* ECT experiments, quantified the number of internalized cisplatin molecules and determined cisplatin cytotoxicity for the selected types of pulses. Our results demonstrated that the tested types of pulses resulted in equivalent drug uptake and cytotoxicity, provided that the electric field strength was adjusted for each pulse type separately. The quantified number of internalized cisplatin molecules producing a cytotoxic effect was in agreement with the Vižintin *et al.*[52] study. We also tested a simple phenomenological model to describe the uptake of cisplatin molecules following cell exposure to different types of pulses. We discussed how the development of such models describing electroporative cisplatin uptake could provide a tool for treatment planning, using arbitrary types of pulses.

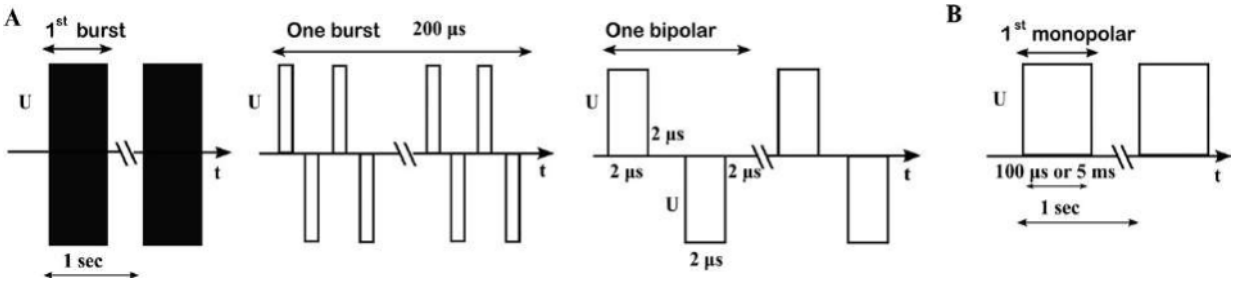

FIGURE 1. **(A)** 50 × 50 HF pulses. From left to right: 50 bursts were applied with a repetition frequency of 1 Hz; one burst with 200 µs total pulse on time and consisted of 50 bipolar pulses; one bipolar pulse of amplitude U consisted of a 2 µs long positive pulse, and a 2 µs long negative pulse (both of voltage U) with a 2 µs long interpulse delay. **(B)** 8 × 100 µs or 8 × 5 ms monopolar pulse of amplitude U and pulse duration of 100 µs or 5 ms were applied with a repetition frequency of 1 Hz

Materials and methods

Cell preparation

We used Chinese hamster ovary cell line (CHO-K1; cat. no. 85051005, European Collection of Authenticated Cell Cultures, United Kingdom). Cells were grown in 25 cm^2 culture flasks (no. 90026, TPP, Switzerland) for 2–4 days in an incubator at 37°C, in a humidified atmosphere with 5% CO_2. CHO cells were cultured in Ham-F12 growth medium (cat.no. N6658, Sigma Aldrich, Germany) supplemented with 10% fetal bovine serum (cat. No. F9665, Sigma Aldrich, Germany), L-glutamine (cat. No. G7513, Sigma Aldrich, Germany), antibiotics penicillin/streptomycin (cat.no. P0781, Sigma Aldrich, Germany), and gentamycin (cat.no. G1397, Sigma Aldrich, Germany). The cell suspension was prepared by detaching the cells in the exponential growth phase with 10x trypsin-EDTA (cat. no. T4174, Sigma Aldrich, Germany), diluted 1:9 in Hank's basal salt solution (cat. no. H4641, Sigma Aldrich, Germany). After no more than 2 minutes, trypsin was inactivated by adding Ham-F12, and cells were transferred to a 50 ml centrifuge tube. Then, the cells were centrifuged (5 min, 180 g, 21°C) and re-suspended in Dulbecco's Modified Eagle Medium (DMEM, cat. no. D5671, Sigma-Aldrich, Missouri, United States) supplemented with 10% FBS (cat. no. F9665, Sigma-Aldrich), 2.0 mM L-glutamine, 1 U/ml penicillin-streptomycin and 50 µg/ml gentamycin. The CHO cells were re-suspended at concentrations of 4 x 10^6 cells/ml (permeability and survival experiments for determination of the optimal electric field) and 4.2 x 10^6 cells/ml (for the clonogenic assay experiments and intracellular platinum concentration experiments).

Pulse parameters and pulse application

Three different types of pulses were used to perform experiments. For brevity, we refer to the three types of pulses used as 50 × 50 HF pulses, 8 × 100 µs pulses, and 8 × 5 ms pulses, and they are described in detail as follows. (i) The first type consisted of high-frequency bipolar pulses, specifically 50 bursts with a repetition frequency of 1 Hz. Each burst contained 50 short bipolar pulses having a pulse duration of 2 µs for the positive as well as for the negative pulse. The interpulse delay between consecutive bipolar pulses was 2 µs (Figure 1A). These high-frequency bipolar pulses were delivered by the pulse generator L-POR V0.1 (mPOR, Slovenia) at various voltages ranging from 80 V to 320 V with a step of 40 V. (ii) The second type of pulses consists of eight 100 µs monopolar pulses delivered at a repetition frequency of 1 Hz. These pulses were delivered by a prototype pulse generator based on H-bridge digital amplifier with 1 kV MOSFETs developed in our lab and described previously.[39] The voltage of these pulses varied from 80 V to 320 V with a step of 40 V, Figure 1B. (iii) The third type consists of eight 5 ms long monopolar pulses, delivered at a repetition frequency of 1 Hz. These pulses were delivered by BTX Gemini X2 pulse generator (Harvard Apparatus, USA). Note that the pulse on time (the time when the voltage was different than zero) was 20 ms for 50 × 50 HF pulses, 800 µs for 8 × 100 µs, and 40 ms for 8 × 5 ms pulses. The voltage of these pulses varied from 80 V to 160 V with a step of 20 V (Figure 1B). The electric pulses were applied to cells in suspension placed in 2 mm aluminium cuvette. To ensure the quality of the delivered pulses the voltage and the current were monitored in all

experiments with an oscilloscope Wavesurfer 422, 200 MHz, a differential voltage probe ADP305, and a current probe CP030 (from LeCroy, USA), according to the recommendations.[53]

Permeability and survival curves for determination of the optimal electric field strength

To select the optimal electric field strength, i.e., where the highest cell membrane permeability and highest survival are achieved, we determined the so-called permeability and survival curves for each of the tested types of pulses. The selected optimal electric field strength was later used in the experiments with cisplatin.

To determine the permeability curve, the cell suspension was mixed with YO-PRO-1 iodide (cat. no Y3603, Thermo Fisher Scientific, Massachusetts, USA) to a final concentration of 1 μM. 150 μl of cells-YO-PRO-1 mixture was transferred in a 2 mm aluminum cuvette and then pulses were applied. 20 μl of the treated sample was transferred to a 1.5 ml centrifuge tube. Three minutes after pulse delivery the treated sample was diluted in 150 μl of DMEM and vortexed. The uptake of YO-PRO-1 was measured on the flow cytometer (Attune NxT; Life Technologies, Carlsbad, CA, USA). Cells were excited with a blue laser at 488 nm, and the emitted fluorescence was detected through a 530/30 nm band-pass filter. For each measurement, we acquired 10,000 events. Single cells were separated from all events by gating. Obtained data were analyzed using the Attune NxT software. The percentage of permeabilized cells was determined from the histogram of YO-PRO-1 fluorescence (see Supplementary Info S1).

To determine the survival curve, 150 μl of cell suspension was transferred to a 2 mm aluminum cuvette and then pulses were applied. 20 μl of the treated sample was transferred to a 1.5 ml centrifuge tube, and 25 minutes after pulse delivery, the samples were diluted in 380 μl Ham-F12. The cell suspension was gently mixed and 100 μl were transferred per well of a 96-well plate in triplicates. After 24 h of incubation in a humidified atmosphere at 37°C and 5% CO_2, the MTS assay (CellTiter 96® AQueous One Solution Cell Proliferation Assay (MTS), Promega, USA[54]) was performed. The MTS assay was used to quantify the number of viable cells by evaluating their metabolic activity by measuring the formazan absorbance at 490 nm on a microplate reader (Tecan Infinite 200 pro; Tecan, Grödig, Austria). Cell survival was determined by first subtracting the background (signal from blank wells containing medium without cells) from all measurements and then normalizing the absorbance of the treated samples to the absorbance of the control sample.

Clonogenic assay

We determined cisplatin cytotoxicity in combination with electroporation pulses using the clonogenic assay which is based on the ability of a single cell to divide and grow into colonies.[55] On the day of the experiment, saline solution was used to dilute cisplatin (Cisplatin Kabi, 1 mg/ml, Fresenius Kabi, Germany or Cisplatin Accord, 1 mg/ml, Accord, UK) and prepare working solutions. The final concentrations of cisplatin during electroporation were 0 μM, 10 μM, 30 μM, and 50 μM. First, 150 μl of cell suspension with added specific cisplatin concentration was transferred to a 2 mm aluminium cuvette and then the suspension was exposed to the selected type of pulses of the optimal electric field as described in the subsection *Permeability and survival curves for determination of the optimal electric field strength*. Control samples received no pulses and no cisplatin. 25 minutes after pulse delivery, 5 μl of each sample (treated and control) was diluted in 495 μl Ham-F12 and mixed. Then, the number of cells in suspension was counted using Countess 3 Automated Cell Counter (Thermo Fisher Scientific). For each sample, specific dilutions were prepared to transfer ~100 live cells in each well of a 6-well plate in triplicates. Note that a higher number of cells was plated for the treated samples compared to the control sample[55] to compensate for the cells which died immediately after the treatment. After 7 days of incubation at 37 °C and humidified atmosphere with 5% CO_2, the growth medium was removed. The attached cells/colonies were fixed with methanol and stained with crystal violet for 10 minutes and washed. The colonies in each well were manually counted. First, we determined the average plating efficiency by dividing the number of counted colonies with the number of plated cells (specific for each experimental group). Then we determined cell survival by normalizing the average plating efficiency to the plating efficiency of the control sample.

Determination of intracellular platinum concentration

Cells were prepared and treated with electric pulses in the presence of different concentra-

tions of cisplatin, as described in previous section 25 minutes after pulse delivery, each sample was diluted in Ham-F12, centrifuged, and washed twice. The cell pellet was separated from the supernatant and the intracellular concentration of platinum was analyzed using inductively coupled plasma mass spectrometry (ICP-MS). To aid sample digestion, 0.1 ml of H_2O_2 and 0.1 ml of HNO_3 (both from Merck, Darmstadt, Germany), were added to the cell pellets. The tubes were then sealed with caps and Teflon tape and left overnight at 80°C. Following digestion, 1.8 ml of Milli-Q water (Direct-Q 5 Ultrapure water system; Merck Millipore, Massachusetts, USA) was added. The platinum content in the samples was then measured using ICP-MS (7900 ICP-MS; Agilent Technologies, California, USA) with ^{193}Ir (Merck, Darmstadt, Germany) used as an internal standard during the measurement.

To determine the amount of Pt per cell, the number of cells in the pellet was divided with the measured Pt in the cell pellet of each sample. To assess the number of cisplatin molecules per cell, it was assumed that 1 mol of Pt is equivalent to 1 mol of cisplatin. Control samples (not electroporated cells that were not incubated with cisplatin) were used for blank subtraction for all cisplatin-treated samples. To reduce cross-contamination of the instrument during the measurement, a mixture containing 1% HNO_3 and 1% HCl (Merck, Darmstadt, Germany) was used as a rinse between the sample runs.

Statistical analysis

Statistical analysis was performed using Prism 9.4.1 (GraphPad Software, USA). For permeability and survival experiments we performed one-way ANOVA if the normality test passed, or the ANOVA on ranks if the normality test failed with the Shapiro-Wilk test. For cisplatin cytotoxicity and cisplatin uptake experiments, we performed two-way ANOVA (independent variables: cisplatin concentration and pulse type). The normality test passed with the D'Agostino-Pearson test. Statistically significant difference was analyzed with respect to the control group (no cisplatin, no pulses) for all experiments. In the figures, the asterisk (*) indicates $p < 0.05$.

Modeling

To model the intracellular uptake of cisplatin molecules, we used the phenomenological model developed by Sweeney *et al.*[56], which is based on an equivalent circuit (Figure 2). The model considers a spherical cell exposed to electric pulses between parallel plate electrodes (homogenous electric field distribution), describes pores/defects formation as a two-state process, and considers diffusion as the only mechanism of transmembrane molecular transport. The model does not describe the cell spatially thus, the parameters used in the model are representative of the whole cell.

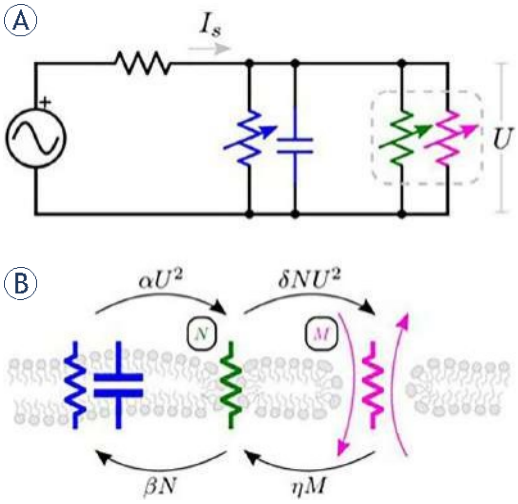

FIGURE 2. Schematic of the model that describes electroporation and molecular transport. (A) The equivalent circuit, which considers electroporation (membrane pore/defect formation) to be a two-step process, as depicted in (B). The blue capacitance and resistance represent the intact cell membrane. When the electric field is applied, the cell membrane becomes permeable first to small ions, indicating the first porous state (N) of the membrane represented by green resistance. Then the membrane becomes permeable to small molecules, indicating the second porous state (M) of the membrane represented by magenta resistance. Reproduced from Sweeney *et al.*[56] with permission.

The source current I_s describes how the electric field induces a voltage on the cell membrane. This induced transmembrane voltage (U) and I_s are described by:

$$\frac{dU}{d\tau} = I_s - U(1 + \gamma(N + M)) \quad [1]$$

$$I_s = \frac{\tau_{RC}\sigma_{EXT}hE_0}{U_0\varepsilon_m} \quad [2]$$

The term σ_{EXT} is the conductivity of the electroporation medium, h is the membrane thickness, E_0 is the applied electric field, U_0 is the electropo-

TABLE 1. Model parameters

Parameter	Symbol	Value	Reference
Electroporation threshold voltage	U_u	258 mV	56
Membrane thickness	h	5 nm	56
Cell radius	r	7.5 μm	56
Membrane time constant	τ_{RC}	1 μs	56
Membrane permittivity	ε_m	12 × 8.85 × 10^{-12} F/m	56
Solute radius	ρ_s	0.58 nm	58
Defect radius	ρ_a	0.8 nm	56
Solute radius/Defect radius	$\lambda_m = \rho_s / \rho_a$	0.7250	56
Solute diffusivity	D	1.670 × 10^{-9} m²/s	58,59
Parameter in N formation rate	α	2 × 10^{-6}	56
N relaxation rate	β	4 × 10^{-8}	56
Relative permeabilzed conductance	γ	1 × 10^{6}	56
Parameter in M formation rate	δ	1 × 10^{-3}	56
M relaxation rate	η	4 × 10^{-9}	56
Permeability coefficient	ξ	8.45 × 10^{-4}	56
Electroporation medium conductivity	σ	1.4 S/m	*

*Measured conductivity of DMEM using a conductometer (Mettler Toledo, S230)

ration threshold voltage and ε_m is the membrane dielectric permittivity.

The increase of the transmembrane voltage results in the formation of small pores/defects (first porous state N) allowing the transmembrane transport of ions only. The presence of ionic currents decreases the value of the transmembrane voltage. The formed pores/defects can expand radially to allow transmembrane uptake of small molecules (second porous state M). The transport of small molecules into the cell is assumed to be governed by diffusion only, i.e., due to a concentration gradient between the extracellular and intracellular environment. The first porous state N, where only small ions can pass through the cell membrane, and the second porous state M, where also small molecules can pass through the cell membrane, are described by equations [3] and [4], respectively. The normalized intracellular concentration (X) of a selected molecule (here cisplatin) that crosses the membrane in the M state is described by equation [5]. All the differential equations are expressed as a function of the normalized time (τ), which is defined as $\tau = t/\tau_{RC}$, where t is the real-time and τ_{RC} is the membrane charging time constant.

$$\frac{dN}{d\tau} = \alpha U^2 - \delta U^2 N - \beta N + \eta M \quad [3]$$

$$\frac{dM}{d\tau} = \delta U^2 N - \eta M \quad [4]$$

$$\frac{dX}{d\tau} = \xi M(1 - X) \quad [5]$$

We implemented the model using a custom script in Matlab 2019b (MathWorks, Natick, MA, USA) and verified that the model in its original form reproduces the published results.[56] The model was developed using the same cell line as in this study (CHO-K1) but based on quantitative measurements of propidium iodide uptake. Therefore, we modified the parameters related to the transported molecule, in our case cisplatin. Specifically, we changed the value of the solute radius (ρ_s), solute diffusivity (D), the permeability coefficient (ξ). The latter was determined by:

$$\xi = \frac{3\,H(\lambda_m) D\,\tau_{RC}}{rh} \quad [6]$$

The term $H(\lambda_m)$ is the hindrance factor evaluated using the Renkin equation[57], D is the diffusion constant of cisplatin, and r is the cell radius. We also adapted the conductivity of the electroporation medium (σ) to correspond to DMEM used in our experiments. The final model parameters are shown in Table 1. We performed calculations for

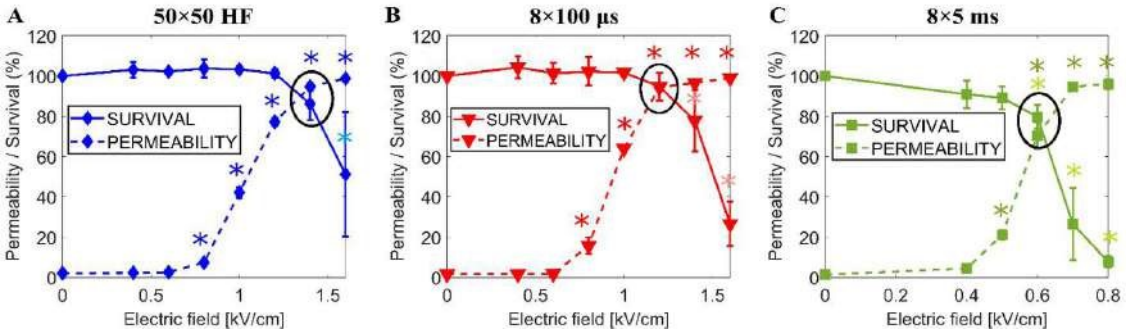

FIGURE 3. Cell survival (solid) and cell membrane permeability (dashed) as a function of the electric field when (A) 50 × 50 HF pulses; (B) 8 × 100 µs pulses; (C) 8 × 5 ms pulses are used. The chosen optimal electric fields are encircled. Each data point presents the mean ± standard deviation from 3–4 experiments. * = statistically significant differences from control ($p < 0.05$) performing one-way ANOVA if the normality test passed or otherwise ANOVA on ranks. The light blue, red, and green asterisks are related to survival experiments.

pulse parameters used in our present and preceding[52] studies: 50 × 50 HF pulses, 8 × 100 µs pulses, 8 × 5 ms pulses, and 1 × 200 ns pulse of 12.6 kV/cm and 25 × 400 ns pulses of 3.9 kV/cm applied at 10 Hz repetition frequency.

The output of the model is the time course of the intracellular concentration of cisplatin ($X_i = X \times X_e$, where X_e is the extracellular concentration of cisplatin) following the application of the electric pulses. We calculated the number of intracellular cisplatin molecules at time 25 minutes using:

$$N = X_i \frac{4}{3} \pi r^3 N_A \quad [7]$$

where $4/3\ \pi r^3$ is the average volume of a cell and N_A is the Avogadro number. The number of cisplatin molecules obtained with the model was then compared with the corresponding experimental measurements.

Results

The optimal electric field strength for each type of pulse

First, we performed experiments to determine the optimal electric field strength for each of the three tested types of pulses, to be later used in the experiments with cisplatin. As the optimal electric field strength, we consider the one in which the highest permeability and highest cell survival are achieved.

Figure 3 shows the experimentally determined permeability (dashed) and survival (solid) curves as a function of the applied electric field for A) 50 × 50 HF pulses, B) 8 × 100 µs pulses, and C) 8×5 ms pulses. Permeability curves show how the percentage of permeabilized cells increases with increasing electric field strength, whereas the survival curves show how the percentage of viable cells decreases with increasing electric field strength. The chosen optimal electric fields (i.e., highest permeability and highest survival) are 1.4 kV/cm for 50 × 50 HF pulses, 1.2 kV/cm for 8 × 100 µs pulses, and 0.6 kV/cm for 8 × 5 ms pulses.

Cytotoxicity vs. the number of intracellular cisplatin molecules

We next used the clonogenic assay to determine the cytotoxicity of cisplatin when exposing cells to the three types of pulses at their optimal electric field strength. Figure 4A shows how cell survival decreases as the extracellular concentration of cisplatin increases. In the absence of applied pulses, the tested cisplatin concentrations (0 µM, 10 µM, 30 µM, and 50 µM) do not affect cell viability (black curve). However, cytotoxicity is strongly potentiated with all three types of pulses, decreasing the cell survival to ~0.8% for 50 × 50 HF pulses, ~2.7% for 8 × 100 µs pulses, and ~4% for 8 × 5 ms pulses at the highest cisplatin concentration (50 µM) – note the logarithmic scale. Results for all three types of pulses are similar and are not statistically significantly different. Qualitatively similar results were obtained when measuring cell viability with the metabolic MTS assay (see Supplementary Info S2). However, as well known, the MTS assay reported better cell viability than the clonogenic assay for the same experimental conditions.[52,60]

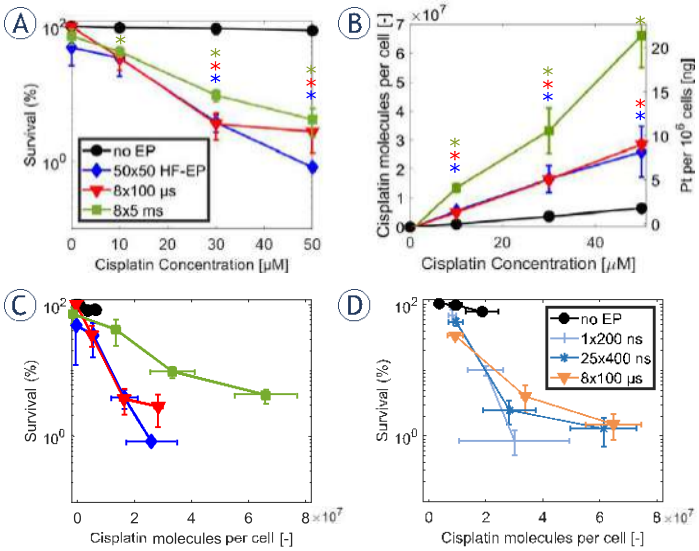

FIGURE 4. Cytotoxicity of cisplatin (A) and cisplatin molecules per cell (B) at different concentrations of cisplatin at a fixed electric field: 1.4 kV/cm for 50 × 50 HF pulses, 1.2 kV/cm for 8 × 100 μs pulses and 0.6 kV/cm for 8 × 5 ms pulses. Each data point presents the mean ± standard deviation from 3–4 experiments. *= statistically significant differences from control ($p < 0.05$) performing two-way ANOVA test. The color of the asterisk corresponds to the line color for a specific type of tested pulse. Cell survival as a function of cisplatin molecules per cell in combination with electroporation (C) our experimental data and (D) experimental data replotted from Vižintin *et al.*[52] with permission.

We also measured the mass of intracellular Pt for each tested condition using ICP-MS and determined the average number of intracellular cisplatin molecules per cell, assuming that 1 mol of Pt is equivalent to 1 mol of cisplatin (Figure 4B). When no electric pulses are applied (black line), the number of cisplatin molecules increases slightly with increasing cisplatin concentration due to passive (i.e., diffusion), and active (i.e., membrane transporters[61-63], endocytosis, pinocytosis, macrocytosis[64,65]) transport of cisplatin. However, when electric pulses are applied, the number of cisplatin molecules increases considerably. The greatest increase is observed for 8 × 5 ms pulses (up to 6.7 × 10^7 at 50 μM). Roughly 2 times lower increase is observed for both 50 × 50 HF pulses and 8 × 100 μs pulses. There is a statistically significant difference between 8 × 5 ms pulses and the other two types of tested pulses when extracellular cisplatin concentration is 50 μM.

To determine the number of intracellular cisplatin molecules needed to achieve a cytotoxic effect, we combined the data from Figures 4A and 4B and plotted cell survival as a function of the number of cisplatin molecules in Figure 4C. Consistent with previous observations[13,52], electroporation potentiates the cytotoxicity of cisplatin, as much lower survival is obtained with any of the three types of pulses compared with control for the same number of cisplatin molecules. The curves for 50 × 50 HF pulses and 8 × 100 μs pulses are almost overlapping, demonstrating that practically the same number of cisplatin molecules results in the same cytotoxic effect. Interestingly, in spite of two times higher Pt continent for 8 × 5 ms pulses the cytotoxicity is lower than when using 50 × 50 HF pulses or 8 × 100 μs pulses.

A previous study by Vižintin *et al.*[52] used the same experimental protocols and analysis as here, but compared two other types of pulses with conventional 8 × 100 μs pulses, namely, 1 × 200 ns pulse of 12.6 kV/cm and 25 × 400 ns pulses applied at 10 Hz repetition frequency of 3.9 kV/cm. Their results are replotted in Figure 4D. This comparison demonstrates that the number of intracellular cisplatin molecules required to achieve a certain cytotoxic effect can be achieved with different types of pulses, if the electric field is properly adjusted.

Modeling cisplatin uptake

Experimental data in previous section suggests that any type of pulses can be used for ECT, if it results in the same average number of internalized cisplatin molecules. Therefore, it would be useful to have a mathematical model for predicting the uptake of cisplatin molecules as a function of the pulse parameters. Figure 5 compares the measured uptake of cisplatin with prediction from a phenomenological model developed by Sweeney *et al.*[56] for all types of pulses used in this and previous study.[52] Note that the experimental data plotted in Figure 5 refer to the number of cisplatin molecules due to electroporation (i.e., we subtracted the uptake of cisplatin when no pulses were applied, black line Figure 4B). The model correctly predicts a proportional increase in the number of internalized molecules with increasing cisplatin concentration. The model also very well quantitatively predicts the number of cisplatin molecules experimentally obtained for 8 × 5 ms pulses, 1 × 200 ns pulses, and 25 × 400 ns pulses, but overestimates by ~2.5 and ~2 times the number of cisplatin molecules obtained for 50 × 50 HF pulses and 8 × 100 μs pulses, respectively. Nevertheless, for all pulse types, the model correctly captures the order of magnitude of the internalized cisplatin molecules.

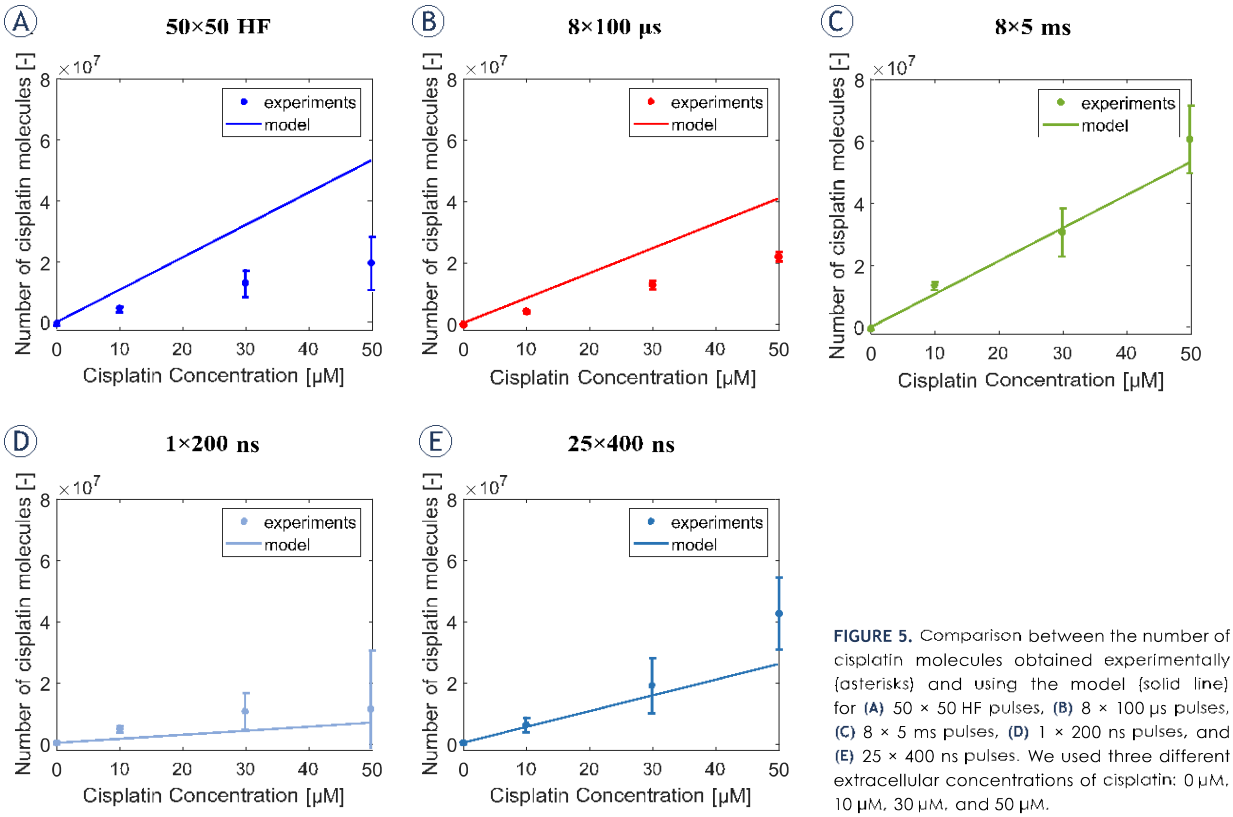

FIGURE 5. Comparison between the number of cisplatin molecules obtained experimentally (asterisks) and using the model (solid line) for **(A)** 50 × 50 HF pulses, **(B)** 8 × 100 µs pulses, **(C)** 8 × 5 ms pulses, **(D)** 1 × 200 ns pulses, and **(E)** 25 × 400 ns pulses. We used three different extracellular concentrations of cisplatin: 0 µM, 10 µM, 30 µM, and 50 µM.

Discussion

In this study, we investigated how different types of pulses affect ECT *in vitro*. Specifically, we determined cisplatin uptake and cytotoxicity using CHO cells. We also tested a model that describes electroporation and the associated transmembrane molecular transport to predict the number of cisplatin molecules in an individual cell.

Electroporation potentiates cisplatin uptake and cytotoxicity in a similar way for all tested types of pulses

Different types of pulses can be considered equivalent for electroporation when the electric field strength is adjusted for each type of pulses separately.[66] We thus first determined, for each selected type of pulses, how the electric field strength affects the percentage of cells that become permeable to YO-PRO-1 and the percentage of cells that survive the exposure to electric pulses in the absence of cisplatin. YO-PRO-1 is a nucleic acid stain that allows rapid screening of permeabilized cells using flow cytometry. The size of YO-PRO-1 (630 Da) is somewhat larger, but nevertheless comparable to cisplatin (300 Da). Therefore, cells that become permeable to YO-PRO-1 are expected to also become permeable to cisplatin. Cell survival was measured 24 hours after electroporation with the metabolic MTS assay. An *in vitro* study by Peng *et al.*[67] showed that 24 h is the adequate incubation time to measure cell survival following electroporation. The electric field strength, with the highest percentage of permeable cells and the highest percentage of viable cells, was 1.4 kV/cm for 50 × 50 HF pulses, 1.2 kV/cm for 8 × 100 µs pulses, and 0.6 kV/cm for 8 × 5 ms pulses. Consistent with Pucihar *et al.*[66], longer pulses (8 × 5 ms) require lower electric fields to obtain a similar fraction of permeabilized cells than shorter pulses (8 × 100 µs). *In vitro* studies [38,39] have observed that a higher electric field is needed for high-frequency bipolar pulses than for monopolar pulses of 100 µs duration, with equivalent treatment time, to achieve a similar fraction of permeabilized cells. However, in this study, a similar elec-

tric field of 1.2 kV/cm and 1.4 kV/cm is required for 8 × 100 µs and 50 × 50 HF pulses, respectively, to achieve a similar fraction of permeabilized cells. This is due to the use of a higher number of bursts and bipolar pulses that reduce the required pulse amplitude. The average cell survival at the optimal electric field was for all pulse types above 80% and was not statistically significantly different from control except for 8 × 5 ms pulses. Overall, in terms of electroporation, all the three tested types of pulses of the optimal electric field strength can be considered equivalent.

We then performed *in vitro* ECT experiments. We measured the cytotoxicity and the uptake of cisplatin when exposing cells to all three types of pulses with the optimal electric field strength in the presence of different extracellular concentrations of cisplatin (0 µM, 10 µM, 30 µM, 50 µM). For all three types of pulses, we observed that an increase in cisplatin concentration increased cell cytotoxicity and intracellular uptake of cisplatin, which is in agreement with previous studies using mouse skin melanoma cells.[13,38,52,68] Furthermore, the results for both cisplatin uptake and cytotoxicity were very similar for all three types of pulses, demonstrating that these pulse types can be considered, not only equivalent in terms of electroporation and transmembrane molecular transport, but also in terms of potentiation of cisplatin cytotoxicity and ECT. We also observed in Figures 4A and 4B that ~2 times higher amount of cisplatin molecules is needed for 8 × 5 ms pulses to achieve a similar cytotoxic effect as when using 50 × 50 HF pulses and for 8 × 100 µs pulses. Vižintin *et al.*[52] reported that the structure of cisplatin is not affected when nanosecond and 8×100 µs pulses are used. However we cannot completely exclude that the structure of cisplatin might be affected by the higher amount of electrochemical reaction caused by ms pulses (we saw bubble formation during experiments) which might lead to a lower cytotoxic effect of cisplatin.[62,69,70] Furthermore an *in vitro* study by Rols *et al.*[71] showed that electroporation, using millisecond pulses, can induce long term micropinocytosis, thus cisplatin molecules might be entrapped in vesicles and not express their cytotoxic effect.

By combining the results on cisplatin cytotoxicity and cisplatin uptake, we were able to determine the number of internalized cisplatin molecules needed to achieve a cytotoxic effect. For all tested types of pulses, this number was in the range of 2–7 $\times 10^7$ cisplatin molecules per cell. Same range was obtained by Vižintin *et al.*[52], who studied cisplatin cytotoxicity following exposure of cells to 1 × 200 ns and 25 × 400 ns pulses. Altogether the results suggest that, as long as the electric field is appropriately adjusted, different types of pulses can be used for potentiating cisplatin cytotoxicity, and consequently different types of pulses can be used for ECT. Thus, the 50 × 50 HF pulses, 8 × 100 µs, 8 × 5 ms pulses, 1 × 200 ns pulses, and 25 × 400 ns pulses of properly adjusted electric field strength can be considered for ECT.

Clinical relevance

ECT has been demonstrated as a locally effective treatment of tumors of various histotypes.[72] The consistent clinical success of ECT has been achieved through the meticulous development of pulse protocols, electrodes, and the publication of Standard Operating Procedures for cutaneous and subcutaneous tumors.[11] It has been later demonstrated that also deep-seated tumors can be successfully treated by ECT provided the tumor is covered by sufficiently high electric fields either as intraoperative[5] or percutaneous procedure.[31,73–75] Accordingly, Standard Operating Procedures have been updated.[10] With good success and acceptance by patients, larger tumors and patients with more extensive diseases were treated. Pain and muscle contraction-related high voltage pulse delivery became the most often reported side effects and alternative pulse waveforms that would maintain ECT efficacy but reduce pain and muscle contraction.[24] In this respect, high-frequency bipolar short pulses [33,34] and also nanosecond pulses [76,77] were suggested. Furthermore, recent studies investigate how high-frequency bipolar pulses and nanosecond pulses affect ECT. Our previous *in vitro* study[38] showed that similar cisplatin cytotoxicity is obtained by comparing high-frequency bipolar pulses and conventionally ECT pulses as soon as the electric field is properly adjusted. Lyons *et al.*[40] have recently demonstrated the safety and efficiency of using high-frequency bipolar pulses in ECT using bleomycin for the treatments of 97 lesions of different histological subtypes of cutaneous malignancies in 25 patients. The authors observed an overall response rate of 86% (complete response rate 63.6%) three months after the treatment which is in agreement with the overall response rate of 85% (complete response rate 73.7%) determined in the ESOPE study of 2006[22] and in a follow-on study using InspECT database in which the overall response is 85% (complete response rate 70%, partial response rate 15%).[72] Thus, the data published

by Lyons *et al.*[40] showed that the use of high frequency bipolar pulses is equivalent regarding the overall response rate to the use of classical ECT pulses. Furthermore, the patients that were treated with local anesthesia showed excellent tolerability to the treatment. Thus, the use of high frequency bipolar pulses might possibly reduce the need to use general anesthesia during ECT shortening the overall hospital stay, reducing the time needed to recover and the costs and increasing the safety of the treatment.[78]

A study by Vižintin *et al.*[52] compared the effects of conventional 8 × 100 µs pulses with nanosecond pulses on cisplatin uptake and cytotoxicity in cell lines *in vitro*. The authors showed that nanosecond pulses can be equally effective for ECT as conventional 8 × 100 µs pulses.[52,79] These results are in agreement with *in vitro* studies on a tumor model, murine Lewis lung carcinoma (LLC1) cell line, by Radzevičiūte *et al.*[50] and *in vivo* study by Novickij *et al.*[51] which show that nanosecond pulses can be as effective as when using the conventional ECT pulses in ECT when using bleomycin as chemotherapeutic drug.

Considerable efforts are also focused on making ECT a systemic treatment by combining it with immunotherapy.[20,48,80,81] Electrochemotherapy can induce immunogenic cell death through the release of damage-associated molecular patterns (DAMP) which serve as a signal to stimulate the immune system.[82-84] Massive liberation of tumor antigens together with DAMPs can activate the antigen-presenting dendritic cells.[85,86] Multiple studies in canine[87-89], in mice[47] and human patients[90] have thus been testing ECT in combination with gene electrotransfer (GET) of plasmid DNA encoding for interleukin-12 (IL-12), which stimulates the immune system.[45-47] Traditionally in GET millisecond duration pulses are used to deliver DNA into the cells.[91-93] Thus, when ECT is used in combination with GET two different types of pulses 8 × 100 µs pulses and millisecond pulses are used, respectively. However, it might be beneficial to use the same type of pulses when ECT is combined with GET as this would allow the use of simpler pulse generators.

In order to capitalize on a significant body of clinical evidence we tested equivalence of such pulses by *in vitro* test, specifically determining the amount of chemotherapeutic drug delivery by electroporation pulses. In this way equivalent pulses are determined by delivering the same drug amount into cells, thus producing the same cytotoxicity. Therefore, the replacement of classical ECT pulses with nanosecond and high frequency bipolar pulses would be beneficial to reduce muscle contractions and pain, potentially avoiding the need for anesthetics and muscle relaxants during the treatment. Furthermore, using the same pulses (either long or short, or bipolar) for delivering cytotoxic drugs into the cells, as well as pDNA to achieve simultaneous gene electrotransfer, is an attractive idea that may be within reach.[94]

Further development of mathematical models that can predict cisplatin uptake can help with electrochemotherapy treatment planning

For the success of ECT, all the tumor needs to be covered by an electric field of sufficient amplitude to permeabilize the cells/tissue, and a sufficient amount of chemotherapeutic drug is needed in the tumor.

In the Standard Operating Procedures all information related to the types of electrodes i.e., of fixed geometry, pulse parameters, and pulse generators[10,11,22] which guarantee a complete coverage of the tumor are provided. However, to treat deep-seated tumors long needles with variable configuration electrodes are used.[95] Thus, there is a need to determine the optimal position of the electrodes and the optimal pulse parameters for complete coverage of the tumor tissue. It is not trivial to determine how the electric field is distributed in biological tissues due to tissue-specific properties, the use of different types of electrode geometries, and pulse parameters. Treatment planning using numerical models helps clinicians to determine the optimal parameters to treat a specific tumor. Currently, in treatment planning a fixed threshold electric field is used to deem tissue permeabilized or not.[3,96] However, just a high-enough electric field does not guarantee cell death as simultaneously a high-enough extracellular cisplatin concentration is needed to obtain enough internalized cisplatin molecules for cell death. Our model presents a missing link in the complete model for treatment planning, connecting the external electric field, the number of internalized cisplatin molecules, and cell death. The first building block for the multiscale model of tissue electroporation was published in Dermol-Černe *et al.* 2018[68] where a model connecting extracellular and intracellular cisplatin concentration as a function of electric pulses was developed. Now, we went one step further and connected the intracellular cisplatin concentration with cell death.

A mathematical model that can also predict the uptake of molecules such as chemotherapeutics drugs (e.g., cisplatin and bleomycin) is needed to be determined for treatment planning for different pulse types is useful. Now we only need the final piece, and this is a model of cisplatin transport across the cell membrane as a function of electric pulses. Our previous study demonstrated that existing mechanistic models of electroporation have limited reliability for predicting the transmembrane transport of small molecules across a wide range of pulse parameters.[97] We observed that the contribution of electrophoretic transport during pulse delivery is often overestimated. Therefore, we decided to test a phenomenological model developed by Sweeney *et al.*[56] that neglects electrophoresis and takes into account only diffusion during and after pulse delivery. Furthermore, we selected this model since it is the simplest model that allows computation of the transmembrane transport of small molecules for arbitrary types of pulses. Indeed, the model is based on quantitative measurements of transmembrane transport of propidium iodide uptake (not cisplatin) induced by a single pulse of different pulse lengths (1, 10, 100, 1000 µs) and electric field strengths (1.7, 2.5, 3.2, 4 kV/cm) that are different from the ones used in our study. Despite its simplicity, and without any considerable model modifications (see the Modeling section), the model was able to predict the order of magnitude of cisplatin uptake for all tested pulse parameters. However, a basic parametric analysis (see Supplementary Info S3) showed that the results for different types of pulses depend in a different way on the model parameters. Therefore, a comprehensive parametric analysis and additional model development would be required, which is out of the scope of the present study (see the Clinical Relevance section). Based on the results obtained, we nevertheless expect that relatively simple models could be developed in the future as a tool for predicting cisplatin uptake.

Limitation of the study

The drawback of our study is the use of only one cell line i.e., the Chinese hamster ovary cells (CHO-K1) non-cancerous cells to perform *in vitro* ECT experiments. It was observed *in vitro* that cancer cells behave differently than normal cells.[98] However, an *in vitro* study published by Vižintin *et al.*[52] showed a similar platinum uptake when using CHO-K1 cells or mouse skin melanoma B16-F1 cells and applying 8 × 100 µs pulses. Thus, we expect that the observed equivalence of different pulse types observed in CHO-K1 cells would also be observed in different cancer cells.

It has been shown that the immune system plays an important role in the efficiency of ECT. Electroporation can potentiate the cytotoxicity and uptake of cisplatin but can also stimulate the immune response by releasing damage-associated molecular patterns (DAMP). In our *in vitro* study we demonstrated the equivalence of different types of pulses on cisplatin uptake and cytotoxicity. Similarly, a recent *in vitro* study by Polajžer *et al.*[99] showed the release of DAMP molecules (e.g. ATP, HMGB1, Calreticulin) albeit with some differences observed with different types of pulses.

We have focused on equivalent drug delivery to cells *in vitro* but this may be different *in vivo*. Thus, further studies in animals are needed to investigate the equivalence of different pulse types for drug entrapment by tumor blood flow modification, for the vascular disrupting action, and for the immune response in ECT.

Conclusions

Our study focused on the effect of different types of electric pulses in ECT, particularly in terms of cisplatin uptake and cisplatin cytotoxicity, using CHO cells *in vitro*. We demonstrate that different types of pulses such as classical ECT pulses, high frequency bipolar pulses and millisecond pulses potentiate cisplatin uptake and cisplatin cytotoxicity. Moreover, we observed similar cisplatin uptake and cisplatin cytotoxicity when using different types of pulses i.e., considered equivalent provided that the electric field is properly adjusted. Thus, equivalent electric pulses such as high frequency bipolar pulses and nanosecond can potentially be used in ECT to reduce pain and muscle contraction while maintaining the same efficacy in cisplatin uptake and cisplatin cytotoxicity as when using the classical ECT pulses. Moreover, our results show that using one type of pulse when combining ECT with EGT is a concept that might be readily achievable considering the equivalent pulse parameters.

In addition, we experimentally determine the number of cisplatin molecules needed to achieve a cytotoxic effect which is in the range of 2–7 × 10^7 cisplatin molecules per cell in agreement with previous study.[52] We also used a mathematical model describing electroporation and transmembrane molecular transport, as a tool to predict the number of cisplatin molecules into individual cells

when different types of pulses need to be tested. The future goal is to improve treatment planning by including a model that predicts the uptake of molecules such as cisplatin or bleomycin.

Acknowledgments

This research was funded by Slovenian Research and Innovation Agency (ARIS) research core funding No. P2-0249 and P1-0143. The work was performed within the network of the research and infrastructural center of the University of Ljubljana, which is financially supported by the Slovenian Research Agency through infrastructural grant I0-0022. The authors would like to thank Duša Hodžić for her help with cell culture, Angelika Vižintin for her help with the protocols for the experiments, and Daniel C. Sweeney for help with his published model.

References

1. Campana LG, Miklavčič D, Bertino G, Marconato R, Valpione S, Imarisio I, et al. Electrochemotherapy of superficial tumors – current status: basic principles, operating procedures, shared indications, and emerging applications. *Sem Oncol* 2019; **46:** 173-91. doi: 10.1053/j.seminoncol.2019.04.002

2. Campana LG, Edhemović I, Soden D, Perrone AM, Scarpa M, Campanacci L, et al. Electrochemotherapy – emerging applications technical advances, new indications, combined approaches, and multi-institutional collaboration. *Eur J Surg Oncol* 2019; **45:** 92-102. doi: 10.1016/j.ejso.2018.11.023

3. Miklavcic D, Snoj M, Zupanic A, Kos B, Cemazar M, Kropivnik M, et al. Towards treatment planning and treatment of deep-seated solid tumors by electrochemotherapy. *Biomed Eng Online* 2010; **9:** 1-12. doi: 10.1186/1475-925X-9-10

4. Cindrič H, Miklavčič D, Cornelis FH, Kos B. Optimization of transpedicular electrode insertion for electroporation-based treatments of vertebral tumors. *Cancers* 2022; **14:** 5412. doi: 10.3390/cancers14215412

5. Edhemovic I, Brecelj E, Gasljevic G, Marolt Music M, Gorjup V, Mali B, et al. Intraoperative electrochemotherapy of colorectal liver metastases. *J Surg Oncol* 2014; **110:** 320-7. doi: 10.1002/jso.23625

6. Bianchi G, Campanacci L, Ronchetti M, Donati D. Electrochemotherapy in the treatment of bone metastases: a phase II trial. *World J Surg* 2016; **40:** 3088-94. doi: 10.1007/s00268-016-3627-6

7. Granata V, Fusco R, Piccirillo M, Palaia R, Petrillo A, Lastoria S, et al. Electrochemotherapy in locally advanced pancreatic cancer: preliminary results. *Int J Surg* 2015; **18:** 230-6. doi: 10.1016/j.ijsu.2015.04.055.

8. Simioni A, Valpione S, Granziera E, Rossi CR, Cavallin F, Spina R, et al. Ablation of soft tissue tumours by long needle variable electrode-geometry electrochemotherapy: final report from a single-arm, single-centre phase-2 study. *Sci Rep* 2020; **10:** 2291. doi: 10.1038/s41598-020-59230-w

9. Tarantino L, Busto G, Nasto A, Nasto RA, Tarantino P, Fristachi R, et al. Electrochemotherapy of cholangiocellular carcinoma at hepatic hilum: a feasibility study. *Eur J Surg Oncol* 2018; **44:** 1603-9. doi: 10.1016/j.ejso.2018.06.025

10. Gehl J, Sersa G, Matthiessen LW, Muir T, Soden D, Occhini A, et al. Updated standard operating procedures for electrochemotherapy of cutaneous tumours and skin metastases. *Acta Oncol* 2018; **57:** 874-82. doi: 10.1080/0284186X.2018.1454602

11. Mir LM, Gehl J, Sersa G, Collins CG, Garbay JR, Billard V, et al. Standard operating procedures of the electrochemotherapy: instructions for the use of bleomycin or cisplatin administered either systemically or locally and electric pulses delivered by the CliniporatorTM by means of invasive or non-invasive electrodes. *Eur J Cancer Suppl* 2006; **4:** 14-25. doi: 10.1016/j.ejcsup.2006.08.003

12. Sersa G, Miklavcic D, Cemazar M, Rudolf Z, Pucihar G, Snoj M. Electrochemotherapy in treatment of tumours. *Eur J Surg Oncol EJSO* 2008; **34:** 232-40. doi: 10.1016/j.ejso.2007.05.016

13. Sersa G, Cemazar M, Miklavcic D. Antitumor effectiveness of electrochemotherapy with cis-diamminedichloroplatinum (II) in mice. *Cancer Res* 1995; **55:** 3450-5. PMID: 7614485

14. Orlowski S, Belehradek Jr J, Paoletti C, Mir LM. Transient electropermeabilization of cells in culture: increase of the cytotoxicity of anticancer drugs. *Biochem Pharmacol* 1988; **37:** 4727-33. doi: 10.1016/0006-2952(88)90344-9

15. Mir LM. Bases and rationale of the electrochemotherapy. *Eur J Cancer Suppl* 2006; **4:** 38-44. doi: 10.1016/j.ejcsup.2006.08.005

16. Jarm T, Cemazar M, Miklavcic D, Sersa G. Antivascular effects of electrochemotherapy: implications in treatment of bleeding metastases. *Expert Rev Anticancer Ther* 2010; **10:** 729-46. doi: 10.1586/era.10.43

17. Sersa G, Jarm T, Kotnik T, Coer A, Podkrajsek M, Sentjurc M, et al. Vascular disrupting action of electroporation and electrochemotherapy with bleomycin in murine sarcoma. *Br J Cancer* 2008; **98:** 388-98. doi: 10.1038/sj.bjc.6604168

18. Markelc B, Sersa G, Cemazar M. Differential mechanisms associated with vascular disrupting action of electrochemotherapy: intravital microscopy on the level of single normal and tumor blood vessels. *PloS One* 2013; **8:** e59557. doi: 10.1371/journal.pone.0059557

19. Serša G, Miklavčič D, Čemažar M, Belehradek Jr J, Jarm T, Mir LM. Electrochemotherapy with CDDP on LPB sarcoma: comparison of the anti-tumor effectiveness in immunocompotent and immunodeficient mice. *Bioelectrochem Bioenerg* 1997; **43:** 279-83. doi: 10.1016/S0302-4598(96)05194-X

20. Calvet CY, Mir LM. The promising alliance of anti-cancer electrochemotherapy with immunotherapy. *Cancer Metastasis Rev* 2016; **35:** 165-77. doi: 10.1007/s10555-016-9615-3

21. Miklavčič D, Mali B, Kos B, Heller R, Serša G. Electrochemotherapy: from the drawing board into medical practice. *Biomed Eng Online* 2014; **13:** 1-20. doi: 10.1186/1475-925X-13-29

22. Marty M, Sersa G, Garbay JR, Gehl J, Collins CG, Snoj M, et al. Electrochemotherapy – an easy, highly effective and safe treatment of cutaneous and subcutaneous metastases: results of ESOPE (European Standard Operating Procedures of Electrochemotherapy) study. *Eur J Cancer Suppl* 2006; **4:** 3-13. doi: 10.1016/j.ejcsup.2006.08.002

23. Sano MB, Fan RE, Cheng K, Saenz Y, Sonn GA, Hwang GL, et al. Reduction of muscle contractions during irreversible electroporation therapy using high-frequency bursts of alternating polarity pulses: a laboratory investigation in an ex vivo swine model. *J Vasc Interv Radiol* 2018; **29:** 893-8.e4. doi: 10.1016/j.jvir.2017.12.019

24. Fusco R, Di Bernardo E, D'Alessio V, Salati S, Cadossi M. Reduction of muscle contraction and pain in electroporation-based treatments: an overview. *World J Clin Oncol* 2021; **12:** 367. doi: 10.5306/wjco.v12.i5.367

25. Miklavcic D, Corovic S, Pucihar G, Pavselj N. Importance of tumour coverage by sufficiently high local electric field for effective electrochemotherapy. *Eur J Cancer Suppl* 2006; **4:** 45-51. doi: 10.1016/j.ejcsup.2006.08.006

26. Martin RC, Schwartz E, Adams J, Farah I, Derhake BM. Intra-operative anesthesia management in patients undergoing surgical irreversible electroporation of the pancreas, liver, kidney, and retroperitoneal tumors. *Anesthesiol Pain Med* 2015; **5:** e22786. doi: 10.5812/aapm.22786

27. Deodhar A, Dickfeld T, Single GW, Hamilton Jr WC, Thornton RH, Sofocleous CT, et al. Irreversible electroporation near the heart: ventricular arrhythmias can be prevented with ECG synchronization. *Am J Roentgenol* 2011; **196:** W330-5. doi: 10.2214/AJR.10.4490

28. Mali B, Jarm T, Corovic S, Paulin-Kosir MS, Cemazar M, Sersa G, et al. The effect of electroporation pulses on functioning of the heart. *Med Biol Eng Comput* 2008; **46:** 745-57. doi: 10.1007/s11517-008-0346-7

29. Ball C, Thomson KR, Kavnoudias H. Irreversible electroporation: a new challenge in "out of operating theater" anesthesia. *Anesth Analg* 2010; **110:** 1305-9. doi: 10.1213/ane.0b013e3181d27b30

30. Cannon R, Ellis S, Hayes D, Narayanan G, Martin RC. Safety and early efficacy of irreversible electroporation for hepatic tumors in proximity to vital structures. *J Surg Oncol* 2013; **107:** 544-9. doi: 10.1002/jso.23280

31. Spallek H, Bischoff P, Zhou W, de Terlizzi F, Jakob F, Kovàcs A. Percutaneous electrochemotherapy in primary and secondary liver malignancies–local tumor control and impact on overall survival. *Radiol Oncol* 2022; **56:** 102-10. doi: 10.2478/raon-2022-0003

32. Cvetkoska A, Maček-Lebar A, Trdina P, Miklavčič D, Reberšek M. Muscle contractions and pain sensation accompanying high-frequency electroporation pulses. *Sci Rep* 2022; **12:** 1-15. doi: 10.1038/s41598-022-12112-9

33. Arena CB, Sano MB, Rossmeisl JH, Caldwell JL, Garcia PA, Rylander MN, et al. High-frequency irreversible electroporation (H-FIRE) for non-thermal ablation without muscle contraction. *Biomed Eng Online* 2011; **10:** 1-21. doi: 10.1186/1475-925X-10-102

34. Dong S, Wang H, Zhao Y, Sun Y, Yao C. First human trial of high-frequency irreversible electroporation therapy for prostate cancer. *Technol Cancer Res Treat* 2018; **17:** 1533033818789692. doi: 10.1177/1533033818789692

35. van Es R, Konings MK, Du Pré BC, Neven K, van Wessel H, van Driel VJ, et al. High-frequency irreversible electroporation for cardiac ablation using an asymmetrical waveform. *Biomed Eng OnLine* 2019; **18:** 1-13. doi: 10.1186/s12938-019-0693-7

36. Ye X, Liu S, Yin H, He Q, Xue Z, Lu C, et al. Study on optimal parameter and target for pulsed-field ablation of atrial fibrillation. *Front Cardiovasc Med* 2021; **8:** 690092. doi: 10.3389/fcvm.2021.690092

37. Hartl S, Reinsch N, Füting A, Neven K. Pearls and pitfalls of pulsed field ablation. *Korean Circ J* 2022; **53:** 273-93. doi: 10.4070/kcj.2023.0023

38. Scuderi M, Rebersek M, Miklavcic D, Dermol-Cerne J. The use of high-frequency short bipolar pulses in cisplatin electrochemotherapy in vitro. *Radiol Oncol* 2019; **53:** 194-205. doi: 10.2478/raon-2019-0025

39. Sweeney DC, Reberšek M, Dermol J, Rems L, Miklavčič D, Davalos RV. Quantification of cell membrane permeability induced by monopolar and high-frequency bipolar bursts of electrical pulses. *Biochim Biophys Acta BBA-Biomembr* 2016; **1858:** 2689-98. doi: 10.1016/j.bbamem.2016.06.024

40. Lyons P, Polini D, Russell-Ryan K, Clover AJP. High-frequency electroporation and chemotherapy for the treatment of cutaneous malignancies: evaluation of early clinical response. *Cancers* 2023; **15:** 3212. doi: 10.3390/cancers15123212

41. Pfefferle V, Häfner HM, Saur A, Kofler K, Kofler L. Electrochemotherapy in analgosedation for patients with reduced ability to receive general anesthesia. *JDDG J Dtsch Dermatol Ges* 2022; **20:** 1384-6. doi: 10.1111/ddg.14855.

42. Pfefferle V, Leiter U, Grünke T, Kofler K, Häfner HM, Kofler L. Electrochemotherapy under analgosedation – case report of a patient with Kaposi's sarcoma. *J Eur Acad Dermatol Venereol* 2023; **37:** e209-11. doi: 10.1111/jdv.18518

43. Mir LM, Orlowski S, Belehradek Jr J, Paoletti C. Electrochemotherapy potentiation of antitumour effect of bleomycin by local electric pulses. *Eur J Cancer Clin Oncol* 1991; **27:** 68-72. doi: 10.1016/0277-5379(91)90064-k

44. Trotovšek B, Djokić M, Čemažar M, Serša G. New era of electrochemotherapy in treatment of liver tumors in conjunction with immunotherapies. *World J Gastroenterol* 2021; **27:** 8216. doi: 10.3748/wjg.v27.i48.8216

45. Heller R, Gilbert R, Jaroszeski MJ. Electrochemotherapy of murine melanoma using intratumor drug administration. *Methods Mol Med* 2000; **37:** 253-7. doi: 10.1385/1-59259-080-2:253.

46. Sedlar A, Jesenko T, Markelc B, Prosen L. Potentiation of electrochemotherapy by intramuscular IL-12 gene electrotransfer in murine sarcoma and carcinoma with different immunogenicity. *Radiol Oncol* 2012; **46:** 302-11. doi: 10.2478/v10019-012-0044-9

47. Ursic K, Kos S, Kamensek U, Cemažar M, Miceska S, Markelc B, et al. Potentiation of electrochemotherapy effectiveness by immunostimulation with IL-12 gene electrotransfer in mice is dependent on tumor immune status. *J Controlled Release* 2021; **332:** 623-35. doi: 10.1016/j.jconrel.2021.03.009

48. Sersa G, Teissie J, Cemazar M, Signori E, Kamensek U, Marshall G, et al. Electrochemotherapy of tumors as in situ vaccination boosted by immunogene electrotransfer. *Cancer Immunol Immunother* 2015; **64:** 1315-27. doi: 10.1007/s00262-015-1724-2

49. Rosazza C, Haberl Meglic S, Zumbusch A, Rols MP, Miklavcic D. Gene electrotransfer: a mechanistic perspective. *Curr Gene Ther* 2016; **16:** 98-129. doi: 10.2174/1566523216666160331130040

50. Radzevičiūtė E, Malyško-Ptašinskė V, Kulbacka J, Rembiałkowska N, Novickij J, Girkontaitė I, et al. Nanosecond electrochemotherapy using bleomycin or doxorubicin: influence of pulse amplitude, duration and burst frequency. *Bioelectrochemistry* 2022; **148:** 108251. doi: 10.1016/j.bioelechem.2022.108251

51. Novickij V, Balevičiūtė A, Malyško V, Želvys A, Radzevičiūtė E, Kos B, et al. Effects of time delay between unipolar pulses in high frequency nano-electrochemotherapy. *IEEE Trans Biomed Eng* 2021; **69:** 1726-32. doi: 10.1109/TBME.2021.3129176

52. Vizintin A, Markovic S, Scancar J, Kladnik J, Turel I, Miklavcic D. Nanosecond electric pulses are equally effective in electrochemotherapy with cisplatin as microsecond pulses. *Radiol Oncol* 2022; **56:** 326-35. doi: 10.2478/raon-2022-0028

53. Cemazar M, Sersa G, Frey W, Miklavcic D, Teissié J. Recommendations and requirements for reporting on applications of electric pulse delivery for electroporation of biological samples. *Bioelectrochemistry* 2018; **122:** 69-76. doi: 10.1016/j.bioelechem.2018.03.005

54. Protocol AG. CellTiter 96® AQueous One Solution Cell Proliferation Assay. Promega USA. [Internet]. [cited 2023 Oct 15]. Available at: https://www.promega.com/-/media/files/resources/protocols/technical-bulletins/0/celltiter-96-aqueous-one-solution-cell-proliferation-assay-system-protocol.pdf

55. Franken NA, Rodermond HM, Stap J, Haveman J, Van Bree C. Clonogenic assay of cells in vitro. *Nat Protoc* 2006; **1:** 2315-19. doi: 10.1038/nprot.2006.339

56. Sweeney DC, Douglas TA, Davalos RV. Characterization of cell membrane permeability in vitro part II: computational model of electroporation-mediated membrane transport. *Technol Cancer Res Treat* 2018; **17:** 1533033818792490. doi: 10.1177/1533033818792490

57. Mahnič-Kalamiza S, Miklavčič D, Vorobiev E. Dual-porosity model of solute diffusion in biological tissue modified by electroporation. *Biochim Biophys Acta BBA-Biomembr* 2014; **1838:** 1950-66. doi: 10.1016/j.bbamem.2014.03.004

58. Nejad MA, Urbassek HM. Diffusion of cisplatin molecules in silica nanopores: molecular dynamics study of a targeted drug delivery system. *J Mol Graph Model* 2019; **86:** 228-34. doi: 10.1016/j.jmgm.2018.10.021

59. Panczyk T, Jagusiak A, Pastorin G, Ang WH, Narkiewicz-Michalek J. Molecular dynamics study of cisplatin release from carbon nanotubes capped by magnetic nanoparticles. *J Phys Chem C* 2013; **117:** 17327-36. doi: 10.1021/jp405593u

60. Jakštys B, Ruzgys P, Tamošiūnas M, Šatkauskas S. Different cell viability assays reveal inconsistent results after bleomycin electrotransfer in vitro. *J Membr Biol* 2015; **248:** 857-63. doi: 10.1007/s00232-015-9813-x

61. Hucke A, Ciarimboli G. The role of transporters in the toxicity of chemotherapeutic drugs: focus on transporters for organic cations. *J Clin Pharmacol* 2016; **56:** S157-72. doi: 10.1002/jcph.706

62. Makovec T. Cisplatin and beyond: molecular mechanisms of action and drug resistance development in cancer chemotherapy. *Radiol Oncol* 2019; **53:** 148-58. doi: 10.2478/raon-2019-0018

63. Howell SB, Safaei R, Larson CA, Sailor MJ. Copper transporters and the cellular pharmacology of the platinum-containing cancer drugs. *Mol Pharmacol* 2010; **77:** 887-94. doi: 10.1124/mol.109.063172

64. Spreckelmeyer S, Orvig C, Casini A. Cellular transport mechanisms of cytotoxic metallodrugs: an overview beyond cisplatin. *Molecules* 2014; **19:** 15584-610. doi: 10.3390/molecules191015584

65. Shen DW, Pouliot LM, Hall MD, Gottesman MM. Cisplatin resistance: a cellular self-defense mechanism resulting from multiple epigenetic and genetic changes. *Pharmacol Rev* 2012; **64:** 706-21. doi: 10.1124/pr.111.005637

66. Pucihar G, Krmelj J, Reberšek M, Napotnik TB, Miklavčič D. Equivalent pulse parameters for electroporation. *IEEE Trans Biomed Eng* 2011; **58:** 3279-88. doi: 10.1109/TBME.2011.2167232

67. Peng W, Polajžer T, Yao C, Miklavčič D. Dynamics of cell death due to electroporation using different pulse parameters as revealed by different viability assays. *Ann Biomed Eng* 2023. [Internet]. doi: 10.1007/s10439-023-03309-8. Available at: https://www.researchgate.net/publication/373911137_Dynamics_of_Cell_Death_Due_to_Electroporation_Using_Different_Pulse_Parameters_as_Revealed_by_Different_Viability_Assays

68. Dermol-Černe J, Vidmar J, Ščančar J, Uršič K, Serša G, Miklavčič D. Connecting the in vitro and *in vivo* experiments in electrochemotherapy-a feasibility study modeling cisplatin transport in mouse melanoma using the dual-porosity model. *J Controlled Release* 2018; **286:** 33-45. doi: 10.1016/j.jconrel.2018.07.021

69. Daley-Yates PT, McBrien DC. Cisplatin metabolites in plasma, a study of their pharmacokinetics and importance in the nephrotoxic and antitumour activity of cisplatin. *Biochem Pharmacol* 1984; **33:** 3063-70. doi: 10.1016/0006-2952(84)90610-5

70. Gately DP, Howell SB. Cellular accumulation of the anticancer agent cisplatin: a review. *Br J Cancer* 1993; **67:** 1171-6. doi: 10.1038/bjc.1993.221

71. Rols MP, Femenia P, Teissie J. Long-lived macropinocytosis takes place in electropermeabilized mammalian cells. *Biochem Biophys Res Commun* 1995; **208:** 26-35. doi: 10.1006/bbrc.1995.1300

72. Clover AJP, de Terlizzi F, Bertino G, Curatolo P, Odili J, Campana LG, et al. Electrochemotherapy in the treatment of cutaneous malignancy: outcomes and subgroup analysis from the cumulative results from the pan-European International Network for Sharing Practice in Electrochemotherapy database for 2482 lesions in 987 patients (2008–2019). *Eur J Cancer* 2020; **138:** 30-40. doi: 10.1016/j.ejca.2020.06.020

73. Cornelis FH, Ben Ammar M, Nouri-Neuville M, Matton L, Benderra MA, Gligorov J, et al. Percutaneous image-guided electrochemotherapy of spine metastases: initial experience. *Cardiovasc Intervent Radiol* 2019; **42:** 1806-9. doi: 10.1007/s00270-019-02316-4

74. Tarantino L, Busto G, Nasto A, Fristachi R, Cacace L, Talamo M, et al. Percutaneous electrochemotherapy in the treatment of portal vein tumor thrombosis at hepatic hilum in patients with hepatocellular carcinoma in cirrhosis: a feasibility study. *World J Gastroenterol* 2017; **23:** 906. doi: 10.3748/wjg.v23.i5.906

75. Djokic M, Cemazar M, Stabuc M, Petric M, Smid LM, Jansa R, et al. Percutaneous image guided electrochemotherapy of hepatocellular carcinoma: technological advancement. *Radiol Oncol* 2020; **54:** 347-52. doi: 10.2478/raon-2020-0038

76. Gudvangen E, Kim V, Novickij V, Battista F, Pakhomov AG. Electroporation and cell killing by milli-to nanosecond pulses and avoiding neuromuscular stimulation in cancer ablation. *Sci Rep* 2022; **12:** 1-15. doi: 10.1038/s41598-022-04868-x

77. Kim V, Gudvangen E, Kondratiev O, Redondo L, Xiao S, Pakhomov AG. Peculiarities of neurostimulation by intense nanosecond pulsed electric fields: how to avoid firing in peripheral nerve fibers. *Int J Mol Sci* 2021; **22:** 7051. doi: 10.3390/ijms22137051

78. Jung J, Kim DH, Son J, Lee SK, Son BS. Comparative study between local anesthesia and general anesthesia in the treatment of primary spontaneous pneumothorax. *Ann Transl Med* 2019; **7:** 553. doi: 10.21037/atm.2019.09.89

79. Vižintin A, Marković S, Ščančar J, Miklavčič D. Electroporation with nanosecond pulses and bleomycin or cisplatin results in efficient cell kill and low metal release from electrodes. *Bioelectrochemistry* 2021; **140:** 107798. doi: 10.1016/j.bioelechem.2021.107798

80. Bendix MB, Houston A, Forde PF, Brint E. Electrochemotherapy and immune interactions; a boost to the system? *Eur J Surg Oncol* 2022; **48:** 1895-900. doi: 10.1016/j.ejso.2022.05.023

81. Groselj A, Bosnjak M, Jesenko T, Cemazar M, Markelc B, Strojan P, et al. Treatment of skin tumors with intratumoral interleukin 12 gene electrotransfer in the head and neck region: a first-in-human clinical trial protocol. *Radiol Oncol* 2022; **56:** 398-408. doi: 10.2478/raon-2022-0021

82. Napotnik TB, Polajžer T, Miklavčič D. Cell death due to electroporation–a review. *Bioelectrochemistry* 2021; **141:** 107871. doi: 10.1016/j.bioelechem.2021.107871

83. Kesar U, Markelc B, Jesenko T, Ursic Valentinuzzi K, Cemazar M, Strojan P, et al. Effects of electrochemotherapy on immunologically important modifications in tumor cells. *Vaccines* 2023; **11:** 925. doi: 10.3390/vaccines11050925

84. Calvet CY, Famin D, André FM, Mir LM. Electrochemotherapy with bleomycin induces hallmarks of immunogenic cell death in murine colon cancer cells. *Oncoimmunology* 2014; **3:** e28131. doi: 10.4161/onci.28131

85. Gerlini G, Di Gennaro P, Borgognoni L. Enhancing anti-melanoma immunity by electrochemotherapy and *in vivo* dendritic-cell activation. *Oncoimmunology* 2012; **1:** 1655-7. doi: 10.4161/onci.21991

86. Gerlini G, Sestini S, Di Gennaro P, Urso C, Pimpinelli N, Borgognoni L. Dendritic cells recruitment in melanoma metastasis treated by electrochemotherapy. *Clin Exp Metastasis* 2013; **30:** 37-45. doi: 10.1007/s10585-012-9505-1

87. Cemazar M, Ambrozic Avguslin J, Pavlin D, Sersa G, Poli A, Krhac Levacic A, et al. Efficacy and safety of electrochemotherapy combined with peritumoral IL-12 gene electrotransfer of canine mast cell tumours. *Vet Comp Oncol* 2017; **15:** 641-54. doi: 10.1111/vco.12208

88. Reed SD, Fulmer A, Buckholz J, Zhang B, Cutrera J, Shiomitsu K, et al. Bleomycin/interleukin-12 electrochemogene therapy for treating naturally occurring spontaneous neoplasms in dogs. *Cancer Gene Ther* 2010; **17:** 457-64. doi: 10.1038/cgt.2010.6

89. Tratar UL, Milevoj N, Cemazar M, Znidar K, Valentinuzzi KU, Brozic A, et al. Treatment of spontaneous canine mast cell tumors by electrochemotherapy combined with IL-12 gene electrotransfer: comparison of intratumoral and peritumoral application of IL-12. *Int Immunopharmacol* 2023; **120:** 110274. doi: 10.1016/j.intimp.2023.110274

90. Daud AI, DeConti RC, Andrews S, Urbas P, Riker AI, Sondak VK, et al. Phase I trial of interleukin-12 plasmid electroporation in patients with metastatic melanoma. *J Clin Oncol* 2008; **26:** 5896. doi: 10.1200/JCO.2007.15.6794

91. Sachdev S, Potočnik T, Rems L, Miklavčič D. Revisiting the role of pulsed electric fields in overcoming the barriers to *in vivo* gene electrotransfer. *Bioelectrochemistry* 2022; **144:** 107994. doi: 10.1016/j.bioelechem.2021.107994

92. Bulysheva A, Heller L, Francis M, Varghese I, Boye C, Heller R. Monopolar gene electrotransfer enhances plasmid DNA delivery to skin. *Bioelectrochemistry* 2021; **140:** 107814. doi: 10.1016/j.bioelechem.2021.107814

93. Smith TR, Patel A, Ramos S, Elwood D, Zhu X, Yan J, et al. Immunogenicity of a DNA vaccine candidate for COVID-19. *Nat Commun* 2020; **11:** 2601. doi: 10.1038/s41467-020-16505-0

94. Potočnik T, Maček Lebar A, Kos Š, Reberšek M, Pirc E, Serša G, et al. Effect of Experimental electrical and biological parameters on gene transfer by electroporation: a systematic review and meta-analysis. *Pharmaceutics* 2022; **14:** 2700. doi: 10.3390/pharmaceutics14122700

95. Geboers B, Scheffer HJ, Graybill PM, Ruarus AH, Nieuwenhuizen S, Puijk RS, et al. High-voltage electrical pulses in oncology: irreversible electroporation, electrochemotherapy, gene electrotransfer, electrofusion, and electroimmunotherapy. *Radiology* 2020; **295:** 254-72. doi: 10.1148/radiol.2020192190

96. Cindric H, Mariappan P, Beyer L, Wiggermann P, Moche M, Miklavcic D, et al. Retrospective study for validation and improvement of numerical treatment planning of irreversible electroporation ablation for treatment of liver tumors. *IEEE Trans Biomed Eng* 2021; **68:** 3513-24. doi: 10.1109/TBME.2021.3075772

97. Scuderi M, Dermol-Černe J, da Silva CA, Muralidharan A, Boukany PE, Rems L. Models of electroporation and the associated transmembrane molecular transport should be revisited. *Bioelectrochemistry* 2022; **147:** 108216. doi: 10.1016/j.bioelechem.2022.108216

98. Frandsen SK, Gehl J. A review on differences in effects on normal and malignant cells and tissues to electroporation-based therapies: a focus on calcium electroporation. *Technol Cancer Res Treat* 2018; **17:** 1533033818788077. doi: 10.1177/1533033818788077

99. Polajžer T, Miklavčič D. Immunogenic cell death in electroporation-based therapies depends on pulse waveform characteristics. *Vaccines* 2023; **11:** 1036. doi: 10.3390/vaccines11061036

2.3. Paper 3

Title: **Models of electroporation and the associated transmembrane molecular transport should be revised**

Authors: **Maria Scuderi**, Janja Dermol-Černe, Clarissa Amaral da Silva, Aswin Muralidharan, Pouyan E. Boukany, and Lea Rems

Publication: Bioelectrochemistry, vol. 147, p. 108216, October 2022

Impact Factor on the date of publication: 5.4 (2020)

Quartile:

- Q1 (Biophysics)
- Q1 (Biology)
- Q2 (Biochemistry & Molecular Biology)
- Q2 (Electrochemistry)

Rank:

- 9/71 (Biophysics)
- 12/93 (Biology)
- 77/295 (Biochemistry & Molecular Biology)
- 10/29 (Electrochemistry)

DOI: https://doi.org/10.1016/j.bioelechem.2022.108216

Bioelectrochemistry 147 (2022) 108216

Contents lists available at ScienceDirect

Bioelectrochemistry

journal homepage: www.journals.elsevier.com/bioelectrochemistry

Models of electroporation and the associated transmembrane molecular transport should be revisited

Maria Scuderi [a], Janja Dermol-Černe [a], Clarissa Amaral da Silva [b], Aswin Muralidharan [b], Pouyan E. Boukany [b], Lea Rems [a,*]

[a] University of Ljubljana, Faculty of Electrical Engineering, Tržaška cesta 25, SI-1000 Ljubljana, Slovenia
[b] Delft University of Technology, Department of Chemical Engineering, Van der Maasweg 9, 2629 HZ Delft, The Netherlands

ARTICLE INFO

Keywords:
Electropermeabilization
Mathematical modeling
Electrodiffusion
Molecular transport
Multiphysics
Multiscale

ABSTRACT

Electroporation has become a powerful tool for nonviral delivery of various biomolecules such as nucleic acids, proteins, and chemotherapeutic drugs to virtually any living cell by exposing the cell membrane to an intense pulsed electric field. Different multiphysics and multiscale models have been developed to describe the phenomenon of electroporation and predict molecular transport through the electroporated membrane. In this paper, we critically examine the existing mechanistic, single-cell models which allow spatially and temporally resolved numerical simulations of electroporation-induced transmembrane transport of small molecules by confronting them with different experimental measurements. Furthermore, we assess whether any of the proposed models is universal enough to describe the associated transmembrane transport in general for all the different pulse parameters and small molecules used in electroporation applications. We show that none of the tested models can be universally applied to the full range of experimental measurements. Even more importantly, we show that none of the models has been compared to sufficient amount of experimental data to confirm the model validity. Finally, we provide guidelines and recommendations on how to design and report experiments that can be used to validate an electroporation model and how to improve the development of mechanistic models.

1. Introduction

The theoretical basis for phenomena observed when biological cells are exposed to external electric fields has made important contributions in biomedicine, ranging from electric-field-based cell manipulation and cell sorting [1,2] to non-viral gene and drug delivery [3,4]. Early studies from the beginning of the 20th century found that from an electrical point of view, a cell can be viewed as a conducting body (the cytoplasm) surrounded by a thin dielectric sheath (the cell membrane) [5]. Thus, when an external electric field is applied to a cell, an induced transmembrane voltage (TMV) is formed across its membrane, which varies with position on the membrane and increases linearly with the strength of the applied electric field [6,7]. When the TMV exceeds a certain critical absolute value (typically reported on the order of several 100 mV), it causes structural changes in the cell membrane that increase its permeability and conductivity. The phenomenon is called electroporation (also electropermeabilization) and allows the influx and efflux of ions and molecules that otherwise cannot readily pass through the cell membrane.

Once the cell membrane is electroporated, the mechanisms contributing to the transmembrane transport are diffusion, electrophoresis, electroosmosis, and endocytosis [6,8–10]. Diffusive transport is due to a concentration gradient between the intracellular and extracellular sides of the membrane. Electrophoretic transport is due to the Coulomb force exerted on charged particles by the local electric field. Electroosmotic transport is the motion of intracellular and/or extracellular fluid (water and solutes) through pores in the membrane, which is induced by an electric field acting on charged ions at the membrane-water interface. Endocytosis is a process in which particles are internalized through an area of the cell membrane that forms a vesicle. During pulse application, transport is mainly electrophoretic and possibly electroosmotic [9,11–13]. After pulse application, when no external electric field is present, the transport is governed by a combination of diffusion, electrophoresis driven by the intrinsic (resting)

* Corresponding author.
E-mail address: lea.rems@fe.uni-lj.si (L. Rems).

https://doi.org/10.1016/j.bioelechem.2022.108216
Received 7 June 2022; Received in revised form 19 July 2022; Accepted 20 July 2022
Available online 25 July 2022

membrane voltage, and in some cases endocytosis [8,13,14]. The transport mechanisms that contribute most to the total amount of transported molecules depend on the pulse duration and/or amplitude, the charge and size of the molecule, and the time taken for the membrane to recover to its impermeable state (resealing time) [8,15]. A visual schematic of the process of electroporation and the associated molecular transport is presented in Fig. 1.

Electroporation is used for enhancing transmembrane transport in a broad range of applications, including medicine (e.g., electrochemotherapy, gene electrotransfer, transdermal drug delivery) [3], biotechnology [16], food technology [17], and environmental science [18,19]. The parameters of electric pulses used in these applications vary greatly, largely as a consequence of historical development and the availability of pulse generators, but also because certain pulse waveforms have been found better suited for specific applications [8,20–22]. Nowadays, the pulse durations span 9 orders of magnitude from hundreds of picoseconds to hundreds of milliseconds, and electric field amplitudes achieved during the applied pulses span 3 orders of magnitude from hundreds of V/cm to hundreds of kV/cm. The electric field can be delivered in the form of individual electric pulses or bursts of pulses. The pulses can be monopolar or bipolar. The pulse shape can be rectangular, triangular, sinusoidal, or exponentially decaying. The number of pulses can vary from a single pulse to hundreds of pulses [3,23]. For each electroporation application, which aims to achieve transport of a sufficient amount of molecules through the membrane under conditions of reversible electroporation (cells survive), the pulse parameters must be carefully optimized. This optimization process is time-consuming, costly, and labor-intensive as it is based only on trial-and-error experimentation. In this context, models of electroporation can become an excellent tool to study the response of cells to different pulse parameters in various experimental configurations.

Scientists have developed different multiphysics and multiscale models which allow spatially and temporally resolved numerical simulations of electroporation and molecular transport through the electroporated membrane at the single-cell level. Many of these models have been compared qualitatively and/or quantitatively with experimental measurements of small molecule uptake into cells, as well as other measurements, such as an increase in membrane conductivity or time courses of the induced TMV [24–27]. Curiously, despite their differences, models containing different theoretical descriptions of electroporation and transmembrane molecular transport have generally reported good agreement with experimental results. Obviously, all these different models cannot simultaneously be valid. Is the electroporative molecular transport so insensitive to the details in the physical description of the electroporation process, or is there a general problem in how the models are developed and validated? In this paper, we investigate whether any of the existing single-cell models can be considered validated. Furthermore, we critically examine whether any of these models is universal enough to describe electroporation and associated molecular transport in general for all the different pulse parameters used in electroporation applications. To this end, we provide an overview of existing mathematical models of electroporation-induced transmembrane transport of small molecules at the level of single animal cells. We divide the models into three groups based on how they theoretically describe the increase in membrane permeability: (i) pore states models; (ii) pore distribution models; (iii) other phenomenological models, and we select three representative models from the first two groups. We implement the selected models and compare them to a set of previously published experimental measurements of small molecule uptake obtained with a wide range of pulse parameters. In particular, we focus on comparing the models with experimental results to which the models were not compared in their original publications. Using various examples, we show that none of the tested models can be universally applied to the full range of experimental measurements. Importantly, we show that none of the models has been confronted with sufficient amount of experimental data to confirm the model validity. Finally, we provide guidelines/recommendations on how to design experiments to validate an electroporation model, as well as how to improve the development of mechanistic models.

2. Literature survey

To identify models that describe the phenomenon of electroporation and the transport of small molecules through the electroporated membrane we began our study with a literature survey. We used the research platform Web of Science using the keywords: electroporation OR electropermeabili*ation **AND** mathematical OR numerical **AND** model OR simulation **AND** transport and searched for papers that were published up to the end of 2021. The search returned 91 papers. By assessing the content of all 91 papers (based on title, abstract, and additional information in the manuscripts), we selected 6 relevant papers

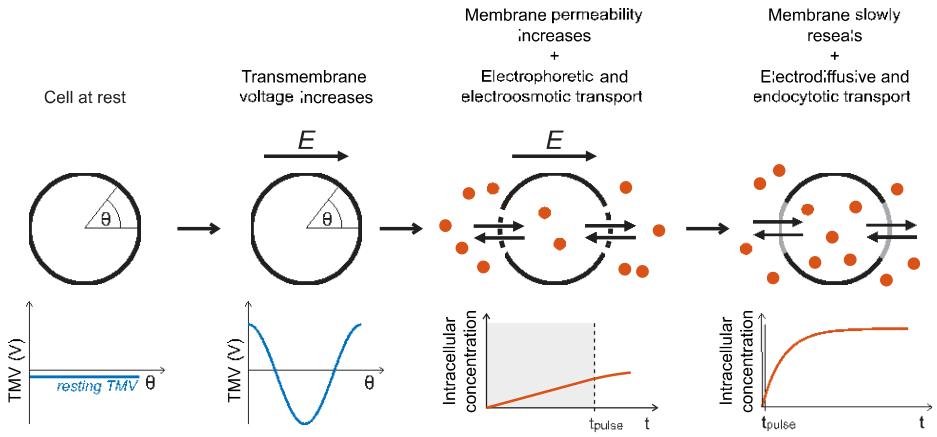

Fig. 1. The process of cell electroporation and the associated transmembrane molecular transport. Exposure to an electric field induces a TMV that varies with position on the membrane. In the regions, where the TMV exceeds a certain threshold (reported on the order of several 100 mV), enhanced transmembrane transport of ions and molecules is observed. Transmembrane transport is bidirectional; the red dots in the figure shows only the molecular uptake into the cell. During the pulse, the transport is primarily electrophoretic and possibly electroosmotic, whereas after the pulse the transport is electrodiffusive and in some cases endocytotic. After exposure to an electric field, the transmembrane molar flux decreases with time due to cell membrane resealing.

[12,29,36,38,41,48] that met our first criterium: 1) The model describes electroporation-mediated uptake of ions or small molecules in animal cells at the single-cell level. We limited our study to models describing the transport of small molecules, since, in the case of large molecules like DNA, the transport mechanisms are considerably more complex, less understood, and thus also less addressed by theoretical studies [8,28]. We also decided to exclude studies on plant and bacterial cells, not to include the cell wall as a confounding factor. In addition, most of the quantitative measurements of molecular uptake have been carried out in animal cells. We then searched for additional papers meeting criterium 1) by looking through the titles and abstracts of the cited and citing references of the selected 6 papers, which yielded 23 papers in total (Table 1). Based on the theoretical approach describing the increase in membrane permeability we divided the models into three groups: (i) pore states models; (ii) pore distribution models; (iii) other phenomenological models. The first two groups attribute the increase in membrane permeability specifically to the creation of pores in the lipid domains of the cell membrane under the influence of the induced TMV. The pore states models are based on a kinetic scheme that describes the transition between distinct states of pores created in the cell membrane. The pore distribution models describe pores created in the membrane by a distribution function defined in a pore radius space, whereby the pore size can change to minimize the membrane free energy. The third group corresponds to other phenomenological models, which generally do not make specific assumptions on the molecular mechanisms of the increase in membrane permeability but describe the latter using a strong phenomenological component. We then assessed the models using additional criteria: 2) The model enables numerical simulations of the spatially-resolved time course of electroporation-mediated molecular transport. 3) The model is mechanistic, i.e., it needs to include the proposed mechanisms of electroporation and transport at the single-cell level that can be traced back to the molecular nature of the structural changes in the cell membrane. We focused on mechanistic instead of phenomenological models, as mechanistic models have the potential to be universally applied to different experimental conditions, provided that they correctly capture the physical mechanisms of electroporation

Table 1
Papers describing models of electroporation and molecular transport and meeting criterium 1). Highlighted bold are papers that meet all criteria.

Model group	Authors	Year	Spatio-temporal	Mechanistic	Comparison with experiment	No. cit.**
Pore states models	Neumann et al. [25]	1998	no	yes	Quantitative comparison with the percentage of mouse B cells stained with Serva Blue G dye [25]	175
	Schmeer et al. [24]	2004	no	yes	Quantitative comparison with measurements of the changes in the conductivity of CHO cell pellets due to transport of monovalent ions [24]	82
	Miklavcic and Towhidi [29]	**2010**	yes	yes	Qualitative comparison with lucifer yellow uptake in DC3F hamster fibroblasts at a fixed time point induced by pulses of different shapes [32]	76
Pore distribution models	**Li and Lin** [12]	**2011**	yes	yes	Qualitative comparison with 2D profiles of calcium uptake measured in single CHO cells [33]	97
	Li et al. [30]	**2013**	yes	yes	Qualitative comparison with the percentage of electroporated Sp2 mouse myeloma cells stained with propidium iodide [34]	61
	Sadik et al. [35]	**2014**	yes	yes	Qualitative comparison with the total amount of fluorescein-dextran uptake in NIH-3T3 mouse fibroblasts induced by a double-pulse protocol [35]	36
	Mahboubi et al. [36]	2017	yes	yes	no	2
	Shil et al. [37]	2018	yes*	yes	no	3
	Goldberg et al. [38]	**2018**	yes	yes	Qualitative comparison with 2D profiles of calcium uptake measured in single CHO cells [33] Quantitative comparison with electrodeformation measured in erythrocytes [39] and GUVs [40]	32
	Goldberg et al. [41]	**2021**	yes	yes	Quantitative comparison with cisplatin uptake in B16F1 mouse melanoma cells at a fixed time point induced by different numbers of 100 us pulses [42]	3
	Yan et al. [43]	2021	yes	yes	no	2
	Guo et al. [44]	2021	yes	yes	no	2
	Smith [31]	**2011**	yes	yes	Quantitative comparison with lucifer yellow uptake in DC3F hamster fibroblasts and calcein uptake in DU 145 prostate cancer cells at a fixed time point induced by single pulses of different shape, duration and amplitude [10,45]	25
	Son et al. [46]	2014	yes	yes	no	91
	Son et al. [47]	2016	yes	yes	no	31
	Mi et al. [48]	2019	yes	yes	no	14
	Mi et al. [49]	**2021**	yes	yes	Qualitative and quantitative comparison with the time course of propidium iodide uptake in A375 human melanoma cells [49]	1
Other phenomenological models	Puc et al. [10]	2003	no	no	Quantitative comparison with lucifer yellow uptake in DC3F hamster fibroblasts at a fixed time point induced by 100 μs and 1 ms pulses of different amplitude [10].	153
	Pavlin et al. [50]	2007	no	no	Quantitative comparison with measurements of the changes in the	101
	Pavlin et al. [51]	2008	no	no	conductivity of dense suspensions of B16F1 mouse melanoma cells due to transport of monovalent ions [50]	120
	Leguebe et al. [52]	2014	yes	no	Qualitative comparison with 2D profiles of propidium iodide uptake in CHO cells and Jurkat T lymphocytes [53,54]. Qualitative interpretation of the effect of pulse repetition frequency on molecular uptake in potato tissue and mouse liver [55]	75
	Dermol et al. [42]	2018	no	no	Quantitative comparison with cisplatin uptake in B16F1 mouse melanoma cells at a fixed time point induced by different numbers of 100 μs pulses [42]	10
	Sweeney et al. [56]	2018	no	no	Quantitative comparison with the time course of propidium iodide uptake in CHO cells [57]	13

*The spatiotemporal resolution was limited since the cell was divided into 8 segments only.
**The number of citations for the given paper on July 18, 2022, according to Google Scholar. Note that some of the papers [10,24,25,35,42,49–51] report also original experimental measurements and are not necessarily cited for the developed model.

and transmembrane transport. 4) The model has been compared to quantitative, or at least qualitative experimental data.

All of our criteria were met by eight models (Table 1, highlighted bold), from which we selected three representatives for further testing: Miklavčič and Towhidi [29], Li et al. [12,30], and Smith [31] models. For brevity, we refer to these models as the MT2010 [29], LL2011 [12,30], and S2011 [31]. The MT2010 was chosen as the only model from the group of pore state models meeting all our criteria. The S2011 and LL2011 from the group of pore distribution models were selected because they formed the basis for all other published models. Moreover, S2011 and LL2011 models are hypothesized to be relatively universal, as they have already been used to simulate the uptake of different ions and molecules over a wide range of pulse parameters and experimental conditions (Table 2). Subsections 2.1–2.3 briefly describe the models from each of the groups, with emphasis on the MT2010, S2011, and LL2011 models. Table 2 shows, for each of the three selected models, the range of pulse parameters, for which the model was designed; the molecules, which were used to optimize/validate the model; the proposed dominant transport mechanism; and how the optimization/validation of the model was performed. As listing all equations behind each model is extremely lengthy, we focus in the main paper on the model aspects, which are important to understand the differences between individual models and their effect on the results presented in the paper. Full details of the models together with their numerical implementation are provided in Supplementary Information. All models used in this study are also available at https://github.com/learems/EPmodels-Electroporation-MolTransport.

2.1. Pore states models

A kinetic scheme describes the rate of chemical reactions or transitions between distinct states as a step-by-step sequence. Pore states models are based on the kinetic scheme which describes the transitions of the cell membrane: from the initial state when the cell membrane is intact, to the porous state when a sufficiently high electric field is applied, and back to the initial state when there is no electric field applied.

The first electroporation model based on a kinetic scheme was proposed by Neumann et al. in 1989 [58]. In 1998 the model was upgraded from one porous state [58] to three porous states to account for a second-order membrane resealing process observed experimentally [25]. Later on, Schmeer et al. [24] revised the model and proposed that there are two closed states (C and C_1) and two porous states (P_1 and P_2).

$$C \underset{k_{-1}}{\overset{k_1}{\rightleftarrows}} C_1 \underset{k_{-2}}{\overset{k_2}{\rightleftarrows}} P_1 \underset{k_{-3}}{\overset{k_3}{\rightleftarrows}} P_2 \tag{1}$$

where C is the intact membrane and C_1 is the stage in which membrane lipids reorganize tilting their headgroups. States P_1 and P_2 correspond to the formation of prepores and final pores, respectively, whereby only pores P_2 mediate the transmembrane transport of molecules. Molecular dynamics simulations of lipid bilayer electroporation corroborated the four-state model [59]. The forwards rates k_i ($i = 1, 2, 3$) in eq. (1) depend exponentially on the transmembrane voltage (TMV), whereas the backward rates k_{-i} are constant and independent of the TMV. Schmeer et al. [24] fitted the proposed model to the measurements of the change in the conductivity of Chinese hamster ovary (CHO) cell pellets. Unfortunately, their model cannot be reconstructed completely, as they did not report the values of all parameters, specifically the values of the backward rates.

The models described in [24,25,58] were based on analytical approaches for obtaining a solution to a system of equations, which require many simplifying assumptions and are only suitable for spherical cells. Furthermore, the distribution of pores in the electroporated regions at which the transport took place was assumed uniform, and the dynamic behavior of other parameters such as TMV and membrane conductivity and permeability was not considered. Miklavčič and Towhidi [29] solved these shortcomings by performing numerical simulations of electroporation and associated molecular transport in whole cells using a finite-element approach. They built upon the earlier models [24,25,58] and added a description for long-term diffusive and endocytic-like molecular uptake [29]. The model was in qualitative agreement with measurements of lucifer yellow uptake induced by pulses of different shapes [32]. The MT2010 model is the only one based on the kinetic scheme that enables simulations of the entire spatiotemporal dynamics of the electroporation and molecular transport process; therefore, it was chosen for testing in our study.

The MT2010 model describes the electroporation dynamics with eq. (1) following previous models. Similarly, as in previous models [24,25,58], the forward rates depend exponentially on TMV. The

Table 2
Models selected for further testing. For each model, the table reports the range of pulse parameters and the molecules, for which the model was designed (and which were used to optimize/validate the model); the proposed dominant transport mechanism, and how the modeling results were compared to experimental measurements.

		Pulse parameters	Molecules	Transport mechanism	Comparison with experiment
Pore states model	**MT2010 model** [29]	Electric field: 1 kV/cm No. pulses: 1 and 8 Pulse shape: unipolar/bipolar rectangular, triangular, sinusoidal, sinusoidal modulated rectangular pulses with 10 % and 90 % modulation Pulse duration: 1 ms Pulse rise time: 2 μs, 10 μs,100 μs Pulse repetition rate: 1 Hz	lucifer yellow	diffusion and endocytosis	Qualitative comparison with lucifer yellow uptake into DC3F spontaneously transformed Chinese hamster fibroblasts [32]. Cells were electroporated in suspension in the presence of lucifer yellow and incubated for 10 min. Afterward, the cells were washed by consecutive centrifugations, lysed by ultrasonication, and the fluorescence of the lysate was measured in arbitrary units on a spectrofluorometer.
Pore distribution models	**S2011 model** [31]	Electric field: 0–3.5 kV/cm [45]; 0–2 kV/cm [10] No. pulses: 1 Pulse shape: exponentially decaying [45]; rectangular pulses [10] Pulse duration: 50 μs to 21 ms [45]; 100 μs and 1 ms [10]	calcein [45] lucifer yellow [10]	electrophoresis and diffusion	Quantitative comparison with experimental measurements of calcein uptake into DU 145 prostate cancer cells exposed to exponentially decaying pulses [45] and lucifer yellow uptake into DC3F fibroblasts exposed to rectangular pulses [10].
	LL2011 model [12,30]	Electric field: 1 kV/cm [12]; 160 kV/cm [30] No. pulses: 1 Pulse shape: rectangular [12,30] Pulse duration: 6 ms [12]; 11–95 ns [30]	calcium [12] propidium [30]	electrophoresis and FASS (Field Amplified Sample Stacking)	Qualitative comparison with single-cell fluorescence microscopy of calcium uptake in CHO cells detected by Fluo3 dye [12,33] and with measurements of the percentage of Sp2 mouse myeloma cells stained with propidium [30,34].

backward rates are constants chosen based on data from different experimental reports. Addition of the MT2010 model is that the membrane can transition from P_2 further into memory state M, which represents a state of enhanced membrane perturbation and is associated with diffusive and endocytotic-like uptake. The flux of molecules $\mathbf{J_m}$ through the membrane is thus calculated as.

$$\mathbf{n}\cdot\mathbf{J_m} = \underbrace{[P_2]\ D_{X,m}\ \frac{[X]_e - [X]_i}{d_m}}_{\text{Diffusion}} + \underbrace{[M]\ D_{X,r}\ \frac{[X]_e - [X]_i}{d_m}}_{\text{Memory effect}} \tag{2}$$

where $\mathbf{n}$ is the inward vector normal to the membrane surface, $[X]_e$ and $[X]_i$ are the extra- and intracellular concentration, respectively, and d_m is the membrane thickness. P_2 state is characterized by relatively fast relaxation (characteristic time of ~1 s), whereas the M state is characterized by slow relaxation (characteristic time of several minutes). $D_{X,m}$ and $D_{X,r}$ are the diffusion coefficients for the diffusive and endocytotic-like transport, respectively. Note that MT2010 neglects electrophoretic and electroosmotic transmembrane transport.

2.2. Pore distribution models

Pore distribution models consider that pores can randomly fluctuate and change their size to minimize the membrane free energy. Pores are not described as distinct states but as a distribution function n, defined in the space of pore radius r_p such that ndr_p corresponds to the number of pores with a radius between r_p and $r_p + dr_p$. The pores can change their radius due to random thermal fluctuations and due to the act of a generalized force F_p, which corresponds to the negative gradient $F_p = -\partial W_p/\partial r_p$ of the pore energy W_p. The equation governing the dynamics of the pore distribution function is often called the Fokker-Planck equation or the Smoluchowski equation, and was first proposed for pores in planar lipid bilayers [60–62]:

$$\frac{\partial n}{\partial t} = -\frac{\partial J_p}{\partial r_p} \qquad J_p = -D_p\frac{\partial n}{\partial r_p} - \frac{D_p}{kT}n\frac{\partial W_p}{\partial r_p} \tag{3}$$

where J_p is the flux of pores in the pore radius space with D_p denoting the pore diffusion coefficient, k the Boltzmann constant, and T the temperature.

2.2.1. Models based on Krassowska and colleagues

The partial differential equation (3) is analytically unsolvable and computationally demanding when applied to describe the electroporation of whole cells. Neu and Krassowska [63] simplified equation (3) to an asymptotic ordinary differential form, which essentially describes the creation and annihilation of pores with minimum radius $r_{p,\,\min}$.

$$\frac{dN}{dt} = \underbrace{ae^{\left(\frac{U_m}{V_{ep}}\right)^2}}_{\text{Pore creation}} - \underbrace{ae^{\left(\frac{U_m}{V_{ep}}\right)^2}\frac{N}{N_0}e^{q\left(\frac{U_m}{V_{ep}}\right)^2}}_{\text{Pore annihilation}} \tag{4}$$

where N represents the pore density (number of pores per unit area), U_m denotes the TMV, N_0 is the pore density when $U_m = 0$ V, and V_{ep}, a, and q are model parameters.

However, pores do expand in size under an electric field, as shown in molecular dynamics simulations and experiments on lipid bilayers [64–66]. Therefore, Krassowska and Filev [67] upgraded the asymptotic model by developing a numerical algorithm that tracks the expansion of individual pores, whereby each pore changes its radius according to the differential equation.

$$\frac{dr_i}{dt} = \frac{D_p}{kT}\frac{\partial W_p}{\partial r_p} = \frac{D_p}{kT}F_p \quad j = 1, 2, \cdots, k \tag{5}$$

Note that eq. (5) is directly related to the second term in eq. (3). The algorithm of Krassowska and Filev is thus a slightly simplified version of the full equation (3). F_p denotes the force that acts to expand the pore radius and is described by eq. (6):

$$F_p = 4B\left(\frac{r_*}{r_p}\right)^4\frac{1}{r_p} - 2\pi\gamma + 2\pi\Gamma_{eff}r_p + \frac{F_{max}U_m^2}{1+\frac{r_h}{r_p}\frac{1}{r_t}} \tag{6}$$

The first term of eq. (6) accounts for the steric repulsion between the lipid heads; the second for the force due to edge tension acting on the pore perimeter; the third for the force due to surface tension of the cell membrane; and the fourth for the electric force acting on the pore edge due to Maxwell stress. Parameter B is the steric repulsion energy, r_* is the minimum radius of hydrophilic pores, γ is the pore edge tension, Γ_{eff} is the effective surface tension of the membrane, and F_{max}, r_t, and r_h are parameters obtained as fits to numerical calculations for a toroidal pore.

Li and Lin [12] (LL2011) were the first to couple the model of Krassowska and Filev with transmembrane molecular transport. In their first paper, they simulated the uptake of calcium into single cells and its binding to the intracellular calcium indicator Fluo-3 according to the kinetic scheme.

$$Ca^{2+} + \quad Fluo \quad \underset{k_{dis}}{\overset{k_{ass}}{\rightleftarrows}} \quad CaFluo \tag{7}$$

where k_{ass} and k_{dis} are the association and dissociation rate constants, respectively. They suggested electrophoresis and diffusion as the main mechanisms of transmembrane molecular transport, which they described with Nernst-Planck equations for each considered species:

$$\begin{aligned}\frac{\partial[Ca^{2+}]}{\partial t} &= \nabla\cdot\left(D_{Ca2+}\nabla[Ca^{2+}] - \frac{z_{Ca2+}F}{RT}D_{Ca2+}[Ca^{2+}]\nabla V\right)\\ &\quad - k_{ass}[Fluo][Ca^{2+}] + k_{dis}[CaFluo]\\ \frac{\partial[Fluo]}{\partial t} &= \nabla\cdot\left(D_{Fluo}\nabla[Fluo] - \frac{z_{Fluo}F}{RT}D_{Fluo}[Fluo]\nabla V\right)\\ &\quad - k_{ass}[Fluo][Ca^{2+}] - k_{dis}[CaFluo]\\ \frac{\partial[CaFluo]}{\partial t} &= \nabla\cdot\left(D_{CaFluo}\nabla[CaFluo] + \frac{z_{CaFluo}F}{RT}D_{CaFluo}[CaFluo]\nabla V\right)\\ &\quad + k_{ass}[Fluo][Ca^{2+}] - k_{dis}[CaFluo]\end{aligned} \tag{8}$$

Constants D_x and z_x are the diffusion coefficient and the valence of species X. The transmembrane flux of molecules through pores is derived from the one-dimensional Nernst-Planck equation [30].

$$\mathbf{n}\bullet\mathbf{J_m} = \rho D_{m,X}\frac{u_m + \ln(\chi)}{d_m}\frac{\chi - 1}{\ln(\chi)}\frac{[X]_e - [X]_i\exp(u_m)}{(1 - \chi\exp(u_m))} \tag{9}$$

where $D_{m,\,X}$ is the diffusion coefficient of species X within the pore, $\chi = \sigma_i/\sigma_e$ is the ratio between the intracellular and extracellular conductivity, and d_m is the membrane thickness. u_m is a nondimensionalized transmembrane voltage (also the Péclet number) $u_m = (z_X q_e/kT)U_m$, where q_e is the elementary charge. The scaling variable ρ is the pore area density, i.e. the local areal fraction of all pores.

LL2011 model prediction was in good agreement with qualitative measurements of calcium uptake by Gabriel and Teissie [33]. In their subsequent paper [30], they considered the intracellular uptake of fluorescent dye propidium and its binding to nucleic acids within the cytoplasm and found good agreement with the experimental measurements of Müller et al. [34]. In another subsequent paper, they combined modeling with qualitative measurements of fluorescein-dextran uptake and found good agreement as well [35].

Several other researchers have then used and/or adapted the theoretical framework layed down by Krassowska and Filev [67] and Li and Lin [12] to describe molecular transport in different systems. Mahboubi et al. [36] used the LL2011 model to study the electroporation of a cell within a microchannel. Shil et al. [37] studied the influence of cholesterol on doxorubicin uptake by modifying the term for the edge energy

in eq. (6). Goldberg et al. [38,41] included electrodeformation of the cell membrane at the whole-cell level by considering the Maxwell stress induced by the electric field. Yan et al. [43] added the effect of the Joule heating by computing the temperature increase with the heat-transfer equation and by considering the temperature dependence of the electrical properties of the aqueous solutions and the diffusion coefficients of the considered species. Guo et al. [44] included the dielectric dispersion of the membrane electrical properties. However, these subsequent models were made independently from each other, often without a thorough analysis of how the added changes affect the model prediction, and often without comparison to any experimental measurements (exceptions are the papers of Goldberg et al. [38,41]).

2.2.2. Model-based on Smith and colleagues

In parallel with Li and Lin [12], Smith et al. [31] (S2011) developed a somewhat different model of electroporation and associated molecular uptake. They also built upon the model of Krassowska and Filev [67] but modified the description of the pore creation and annihilation rate and the description of the pore energy landscape (see Suppl. Sections S4 and Table S4 for details). Furthermore, they developed a description of molecular transport through pores that consider the size, shape, and charge of the molecules and take into account the drag between the molecule and the pore wall (hindrance) and the energy cost of placing a charged solute from an aqueous environment into the membrane with low dielectric permittivity (partitioning). Hindrance and partitioning considerably reduce the electrophoretic and diffusive transport for molecules whose size is comparable to the pore size, even beyond an order of magnitude (Suppl. Fig. S4). The S2011 model was in good agreement with quantitative measurements of molecular uptake of calcein [45] and lucifer yellow [10] for a wide range of pulse durations (from 50 μs to 20 ms). The model was subsequently used by Son et al. [46,47] to study the uptake of propidium, calcein, and calcium following pulses of different duration and number. The S2011 model was later adapted by Mi et al. [48,49]. In their first paper [48], they derived a simplified expression for membrane surface tension from the Maxwell stress tensor to account for mechanical stress caused by electrodeformation. They also made slight modifications to the expression for the steric pore energy, the pore destruction rate, and the value of the maximum pore radius, which they have not discussed. In their second paper [49], they divided the pores into three classes based on their radius: unstable reversible pores with a radius < 5 nm, stable reversible pores with a radius between 5 nm and r_d, and irreversible pores with a radius larger than r_d, where $r_d \approx 20$ nm corresponds to the global maximum in the pore energy landscape. Although their pore classification is not fully consistent with the original theoretical description of the pore population [31,60,68], they showed that their modifications improve the agreement with their experimental measurements.

2.3. Other phenomenological models

The last group of models in Table 1 are models that have a strong phenomenological component, especially with respect to how the increase in membrane permeability due to electroporation is described. Puc et al. [10] developed a two-compartment pharmacokinetic model, representing the extracellular and intracellular space, and described the transmembrane transport of fluorescent dye lucifer yellow with a phenomenological function which parameters were fitted to their experimental measurements. Pavlin et al. [50 51] designed experiments that enabled them to estimate the fraction of pores formed in the membrane. Their theoretical analysis pointed to two distinct types of pores, short-lived pores that are numerous but exist mainly during the presence of an electric field, and long-lived pores that are smaller in number but persist for seconds to minutes after the pulse exposure and accumulate when applying multiple pulses. Their model uses a phenomenological description of how the fraction of pores depends on the amplitude and number of applied pulses, and the model was not developed to the extent that would enable spatiotemporal simulations of single-cell electroporation. Unlike most other groups, Leguebe et al. [52] developed a model which attributes the increase in membrane permeability not only to lipid pores but also to lipid peroxidation. The pores are considered short-lived whereas the increase in permeability due to lipid peroxidation is considered long-lived. The mathematical description for pores has a mechanistic background and is derived in a (strongly) simplified form from eq. (4). However, the increase in membrane permeability due to lipid peroxidation, and how it relates to lipid pores, is described in a phenomenological way with a simple mathematical function without any mechanistic background. The multiscale model of Dermol-Černe et al. [42] connects a mathematical description of molecular transport at the single-cell level and the tissue level; however, the increase in membrane permeability was determined experimentally and was not related to any mechanistic description of membrane electroporation. Finally, Sweeney et al. [56] developed a two-stage ordinary differential equation model to describe electroporation and molecular transport, which yielded good agreement with quantitative measurements of propidium iodide uptake. Nevertheless, the model is based on two-stage ordinary differential equations of phenomenological origin, whereby all model parameters need to be obtained based on fits to experimental measurements.

Since all phenomenological models largely depend on the subset of experimental measurements for which they were fitted, we have excluded them from further testing in our study.

3. Results and Discussion

The main aim of our study was to critically examine whether any of the existing single-cell electroporation models is universal enough to describe electroporation and the associated molecular transport generally for all different pulse parameters used in electroporation applications related to animal cells. We approached our question by first surveying the literature. We searched for mechanistic mathematical models designed to describe the phenomenon of electroporation and induced transmembrane transport of small molecules at the single-cell level with full spatiotemporal resolution. We selected three representative models, which met all our selection criteria: MT2010 [29], S2011 [31], and LL2011 [12] models. We then tested these models against experimental measurements of intracellular uptake of different small molecules made by Puc et al. [10]., Canatella et al. [45], Sozer et al. [69], and Gabriel and Teissie [33].

Showing how each selected model describes all selected experiments would be lengthy and unnecessary to reach the main conclusions of the study. Instead, we show different examples that illustrate the shortcomings of current electroporation models and provide guidelines for further development of these models. In this light, the Results and Discussion are divided into four sections, according to the four main takeaway messages we would like to convey:

1. Qualitative validation is not sufficient to establish the goodness/validity of a model;
2. Quantitative validation in a fixed time point does not necessarily indicate the correct description of the kinetics of the uptake;
3. Certain experiments are not selective enough for model validation;
4. Further development of mechanistic models requires a better understanding of the molecular mechanisms of electroporation.

3.1. Qualitative validation is not sufficient to establish the goodness/validity of a model

The MT2010 [29] model was originally compared with results from Kotnik et al. [32], who reported measurements of intracellular uptake of lucifer yellow induced by 1-ms-long pulses of different shapes. The model correctly predicted the greatest uptake for a rectangular pulse,

followed by pulses with sinusoidal and triangular shapes. The model further correctly predicted a decrease in transport when modulating rectangular pulses with a 50 kHz sinewave. Finally, the model correctly predicted no change in transport when applying a unipolar or bipolar rectangular pulse and when changing the rise time of a unipolar rectangular pulse from 2 μs to 100 μs. However, the comparison was only qualitative, as the reported lucifer yellow measurements were in arbitrary fluorescence units. Therefore, we tested if the MT2010 model can quantitively simulate the experimental study of Puc et al. [10] in which the intracellular concentration of lucifer yellow was quantified 10 min after exposing cells to a single 100 μs or 1 ms rectangular pulse of different amplitudes [10]. Fig. 2 shows that the uptake of lucifer yellow increases with increasing applied electric field both in the model and in the experiment. However, the MT2010 model overestimates the experimental values of intracellular concentration by almost an order of magnitude. For both pulse durations, the model fails to quantitatively reproduce the experimental data. This demonstrates how qualitative comparison between model and experiment is not sufficient for model validation.

3.2. *Quantitative validation in a fixed time point does not necessarily indicate the correct description of the kinetics of the uptake*

The S2011 model was originally compared with quantitative experimental measurements of lucifer yellow uptake from Puc et al. [10] and calcein uptake from Canatella et al. [45] showing excellent agreement (Fig. 3 shows our reproduction of the modeling results presented in [31]). This agreement is impressive, as there are many differences in the experiments of Canatella et al. and Puc et al. Namely, Canatella et al. measured the uptake of calcein in DU 145 prostate cancer cells exposed to exponentially decaying pulses, whereas Puc et al. measured the uptake of lucifer yellow in DC-3F spontaneously transformed fibroblasts exposed to rectangular pulses. Furthermore, the duration of the electric pulses used in these experiments collectively spans nearly 3 orders of magnitude (50 μs to 21 ms). However, we need to consider that the agreement between the model and experiments was obtained after fitting the values of five model parameters, including the pore diffusion coefficient D_p, symmetric pore creation rate β, asymmetric pore creation rate α, maximum pore radius $r_{p,\max}$, and characteristic time of pore closure τ_p. When fitting many parameters of a complex model to a given dataset, two main problems can occur. The first problem is that such a complex model can be too flexible and can be fitted to almost any data, which prevents one from critically assessing the validity of the model. The second problem is that multiple combinations of parameter values can yield an adequate fit to the given dataset. Therefore, it is crucial to measure or assess independently as many model parameters as possible. While the first four listed parameters (D_p, β, α, $r_{p,\max}$) cannot (yet) be directly measured experimentally, membrane resealing time can be.

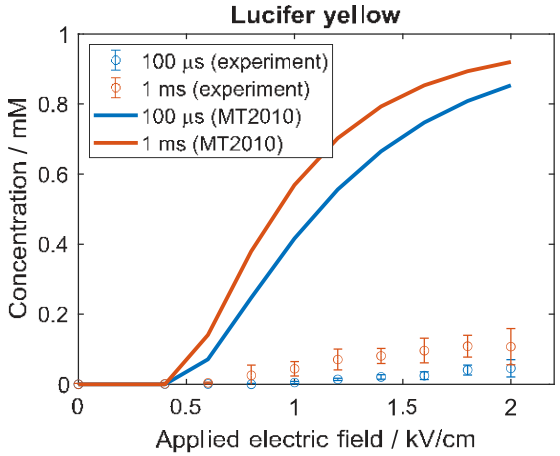

Fig. 2. Intracellular concentration of lucifer yellow as a function of the applied electric field strength upon exposure to a single 100 μs or 1 ms pulse. Circles and solid lines, respectively, show the experimental measurements of intracellular concentration from Puc et al. [10] and the results of the MT2010 model.

Recently, Sözer et al. [69] reported the first spatially resolved quantitative measurements of the kinetics of intracellular uptake of calcein, propidium, and yo-pro1 during and after exposure of U937 histiocytic lymphoma cells to either a single 220 μs, 2.5 kV/cm pulse or ten 6 ns, 200 kV/cm pulses. The results of Sözer et al. thus offer an excellent opportunity to further test the validity of the S2011 model. Calcein is fluorescent by itself, whereas the fluorescence of propidium and yo-pro1 increases dramatically upon binding to nucleic acids in the cytoplasm. Consequently, for propidium and yo-pro1 we need to take into account the binding reaction with nucleic acids, as the detected fluorescent signal is emitted practically exclusively from the bound molecules. Out of the three molecules considered, we chose to focus on calcein and propidium; calcein, because the model has already been used to model calcein uptake in the experiments of Canatella et al. [45], and propidium, because the binding reaction between propidium and nucleic acids in the cytoplasm has already been described and modeled in previous studies [30,70–72].

To compare the S2011 model with experiments of Sözer et al. we adapted the values for the cell radius and extracellular medium conductivity to correspond to U937 cells and RPMI growth medium, respectively, and we also considered the shape of the pulse waveforms used by Sözer et al. (Suppl. Fig. S15). Measurements of Sözer et al. upon exposing the cells to a 220 μs pulse, specifically the kinetics of calcein uptake, showed that membrane resealing took tens of seconds (Fig. 4a). Fitting the data to a first-order exponential function gave a resealing time constant of 25 s (Suppl. Fig. S14). Thus, we also changed the value of τ_p in the S2011 model from 4 s to 25 s. Other parameter values were kept the same as for Puc et al. and Canatella et al. experiments (see Suppl. Tables S4, S5, and S6 for details).

We first computed the molecular uptake induced by 220 μs, 2.5 kV/cm pulse. Interestingly, the total uptake of calcein predicted by the S2011 model was in good agreement with the experiment. However, the model failed to reproduce the uptake kinetics of both calcein and propidium. Fig. 4b shows that, for both molecules, the electrophoretic uptake during the pulse is dramatically overestimated, as can be seen from the rapid jump in the intracellular concentration around time $t = 5$ s when the pulse is applied. Such a jump is not observed in the experimental measurements (Fig. 4a). Furthermore, the measurements of the propidium uptake showed that the uptake is greater on the cathodic (- electrode) compared to the anodic (+ electrode) cell side, not *vice versa* as suggested by the model. Since propidium is positively charged (valence $z_{Pr} = +2$), greater uptake on the cathodic side can only be explained if diffusion is the dominant mechanism of molecular transport and if the cathodic side becomes more permeable compared to the anodic side. The latter is indeed assumed based on experimental observations in the original S2011 model. Therefore, we made additional calculations, where we neglected the electrophoretic transport: we considered that molecules can move only due to concentration gradient but not due to the electric field. The resulting concentration profiles were more reasonable but quantitatively more than an order of magnitude too low (Suppl. Fig. S17). Note that in the S2011 model all pores shrink to a minimum size after the pulse, whereby the smaller the minimum pore size, the more the molecular transport through pores is hindered. Therefore, we additionally increased the minimum pore radius from 1.0 nm to 1.35 nm to allow greater molecular flux, and the model came in reasonable agreement with the experimental measurement (Fig. 4c). The model could describe the symmetric uptake of calcein and the asymmetric uptake of propidium with the dominant transport occurring on the cathodic side. This exercise demonstrates

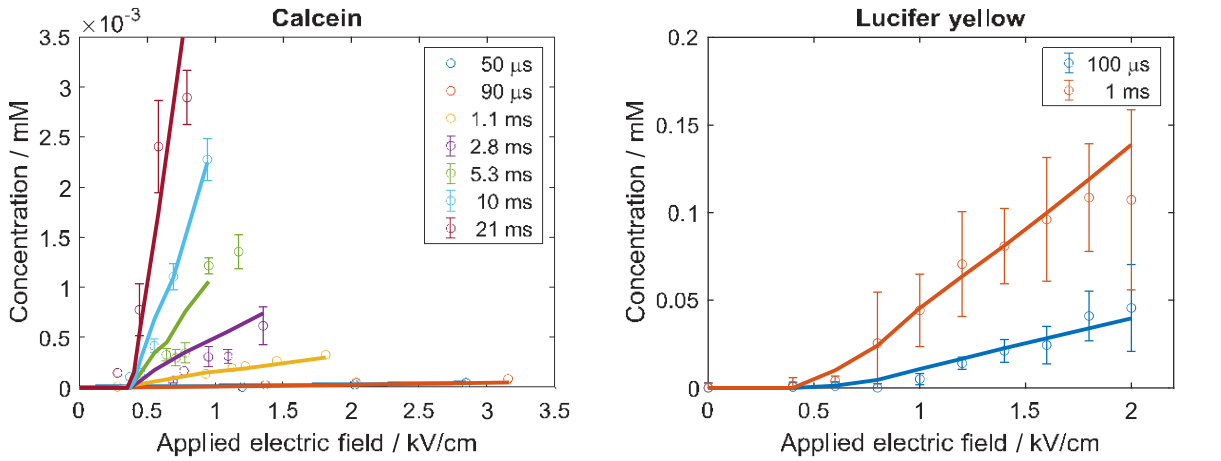

Fig. 3. Final intracellular concentration of calcein and lucifer yellow internalized after exposing cells to a single pulse of a given duration and a given amplitude. Circles denote experimental measurements carried out by Canatella et al. [45] and Puc et al. [10] for calcein and lucifer yellow, respectively. Solid lines show the prediction of the S2011 model.

how a complex model such as S2011 can rather quickly be adapted to a given experiment; by making a few well-thought, yet arbitrary changes to the model, we were able to bring the model in good agreement with the experimental measurements.

We next computed the uptake of calcein and propidium upon exposure to ten 6 ns, 200 kV/cm pulses, which was also measured by Sözer et al [69]. We again consider the original S2011 model with electrophoretic and diffusive transport and with a minimum pore radius of 1.0 nm. Pulses with a duration of 6 ns are extremely short, therefore electrophoretic uptake is practically negligible and most of the transport occurs after the pulses, as can be seen, both in the experiment and the model (Fig. 5). However, the model disagrees quantitatively with the experiment. The comparison between Fig. 5a and Fig. 5b shows that the computed change in the normalized concentration of calcein and propidium is, respectively, about 3x and 10x higher than the measured one. Furthermore, the measurements show asymmetric uptake of propidium, with greater uptake on the anodic side, whereas the model predicts symmetric uptake of propidium from the anodic and cathodic sides. Another discrepancy between the model and experiment is that the model predicts almost equal molecular uptake induced by a single 6 ns pulse as induced by ten 6 ns pulses (Fig. 5b). While Sözer et al. have not reported the uptake of calcein and propidium upon a single 6 ns pulse, they have shown that the uptake of yo-pro-1 induced by a single 6 ns pulse is about an order of magnitude lower than induced by ten 6 ns pulses [69]. The fact that the S2011 model predicts similar uptake for single and multiple pulses has also been shown by Son et al. [47].

Overall, the results presented in this section demonstrate that quantitative measurements of the kinetics of molecular uptake are crucial to assess whether the model correctly describes the dominant transport mechanisms (electrophoresis, diffusion, etc.). Quantitative measurements of the total molecular uptake at a fixed point in time are not sufficient for this purpose. Furthermore, the results show how the characterization of the asymmetry of molecular transport at the cathodic and anodic side of the cell provides important information about the mechanism of transmembrane molecular transport and should be included when validating an electroporation model. Finally, the results indicate that to develop and validate a mechanistic electroporation model, the model should be tested against experiments using single and multiple pulses, as well as a wide range of pulse durations, including nanosecond pulses.

3.3. *Certain experiments are not selective enough for model validation*

The LL2011 model [12] was originally compared to the experimental measurements of calcium uptake into Chinese hamster ovary (CHO) cells measured by Gabriel and Teissié [33] and showed good agreement. We performed similar calculations and compared the predictions of the LL2011 and S2011 models. Note that the S2011 model is related to the LL2011 model with respect to the description of pore dynamics, but differs in the values of the model parameters and the description of the transmembrane molar flux (see Section 2.2.2 and Suppl. Section S4). Despite their differences, both models predict practically identical concentration profiles, in good agreement with the experiment (Fig. 6). However, when we use the LL2011 model to calculate, e.g., the uptake of lucifer yellow measured by Puc et al. [10], the model overestimates the final intracellular concentration by an order of magnitude (Fig. 6d). This exercise shows how models, which appear valid for a specific experiment, can fail in a broader context when applied to a different experiment. It further shows that the experiment of Gabriel and Teissié is not in itself suitable for validating an electroporation model, as both S2011 and LL2011 models can describe the experimental results well despite their differences in describing poration dynamics and molecular transport. Thus, experiments intended for validating an electroporation model need to be carefully and critically designed.

3.4. *Further development of mechanistic models requires a better understanding of the molecular mechanisms of electroporation*

All models tested in our study reached limitations when quantitatively confronted with different experimental measurements covering a wide range of pulse parameters. Thus, the models need to be used with care when being applied outside the range of parameters, for which they have been developed, and necessarily combined with experimental validation. While no mathematical model can be truly universal in any field of study, the tested models (and variations thereof) have often been used as though they can be commonly applied for any electroporation experiment (see Table 2 reporting the range of pulse parameters, cell lines, and molecules considered with the tested models, as well as the studies listed in Table 1 and the references therein). Our study shows that there is a need for further development of mechanistic electroporation models to assess the associated molecular transport for the entire range of experimental conditions used in electroporation applications. One strategy would be to further optimize the values of the existing model's parameters and/or replace certain expressions/equations,

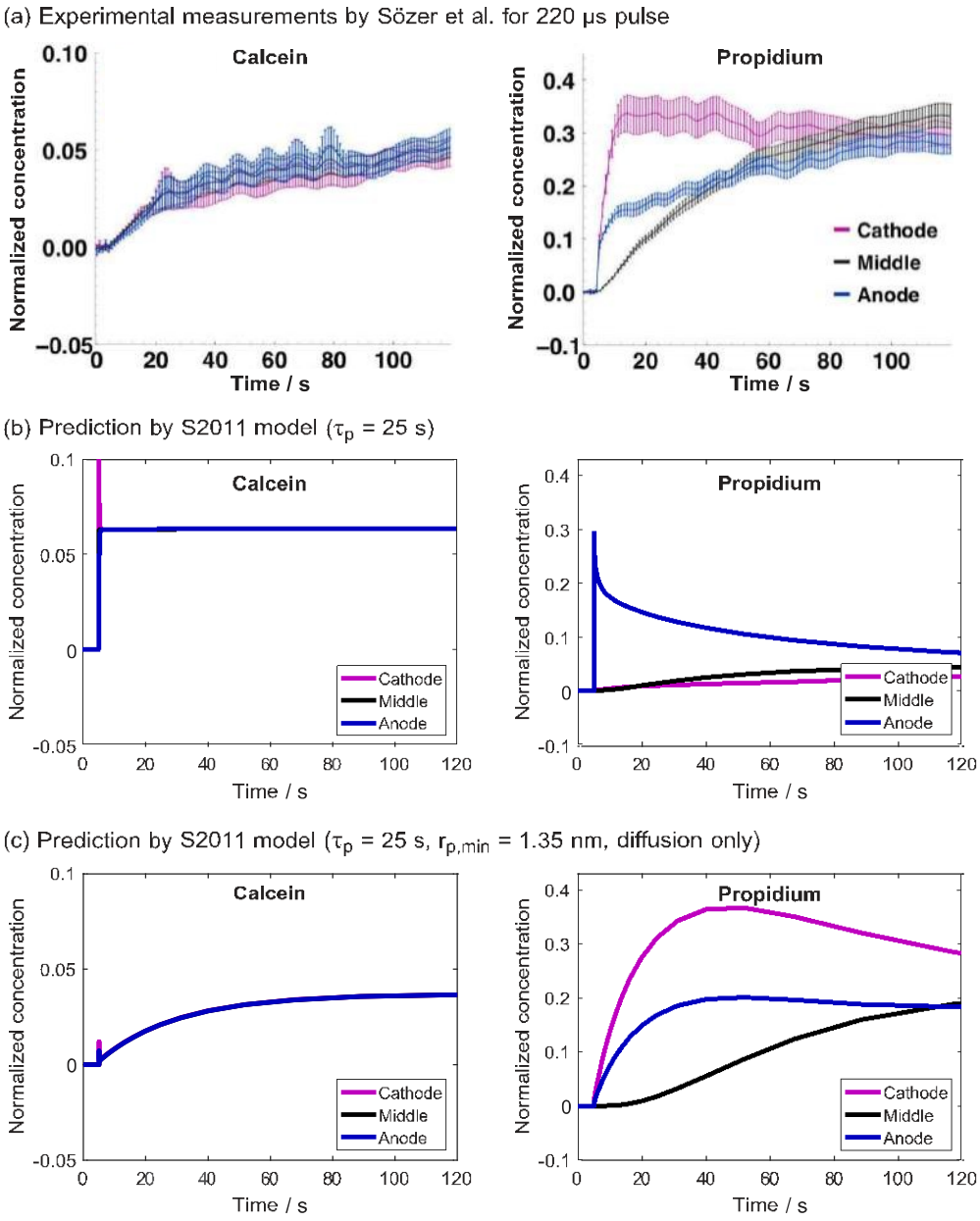

Fig. 4. Intracellular concentration of calcein and propidium upon exposure to a single 220 µs, 2.5 kV/cm pulse. The intracellular concentration is normalized to the initial extracellular concentration. For propidium, the concentration of bound molecules, normalized to the initial concentration of extracellular free propidium, is shown. (a) Experimental measurements, reproduced with permission from Sözer et al. [69]. (b) Modeling results using default model parameters (Suppl. Table S4). (c) Modeling results when neglecting electrophoretic transport and increasing the minimum pore radius to 1.35 nm.

which have been oversimplified in a model, with their unsimplified version. However, this strategy leads to a dead-end, if a model is in its essence based on incorrect assumptions.

Almost all current electroporation models assume that the increase in cell membrane permeability can be attributed to a single mechanism: the creation of pores in the lipid domains of the cell membrane, which passively close upon removal of the external electric field. In addition, most models assume that all pores exhibit similar kinetic behavior. However, accumulating evidence from experiments and simulations on model systems speaks against these assumptions. Firstly, if lipid pores formed by an electric field are the sole mechanism of increased membrane permeability, such pores need to stay open for minutes after exposure to the electric field to corroborate the experimentally measured slow uptake/leakage of ions and molecules. Such a long pore closure time requires one to assume that there exists a large energy barrier of several 10 kT for pore closure [31,73]. This assumption does not agree with free energy calculations for pores in pure lipid bilayers [74] as well as with experimental measurements on pure lipid systems [75,76]. Secondly, electroporation has been associated with oxidative damage of polyunsaturated lipids through experiments on pure lipids vesicles and cells *in vitro* [77,78]. Oxidative damage can lead to partial cleavage of the lipids tails (i.e., leads to secondary peroxidation

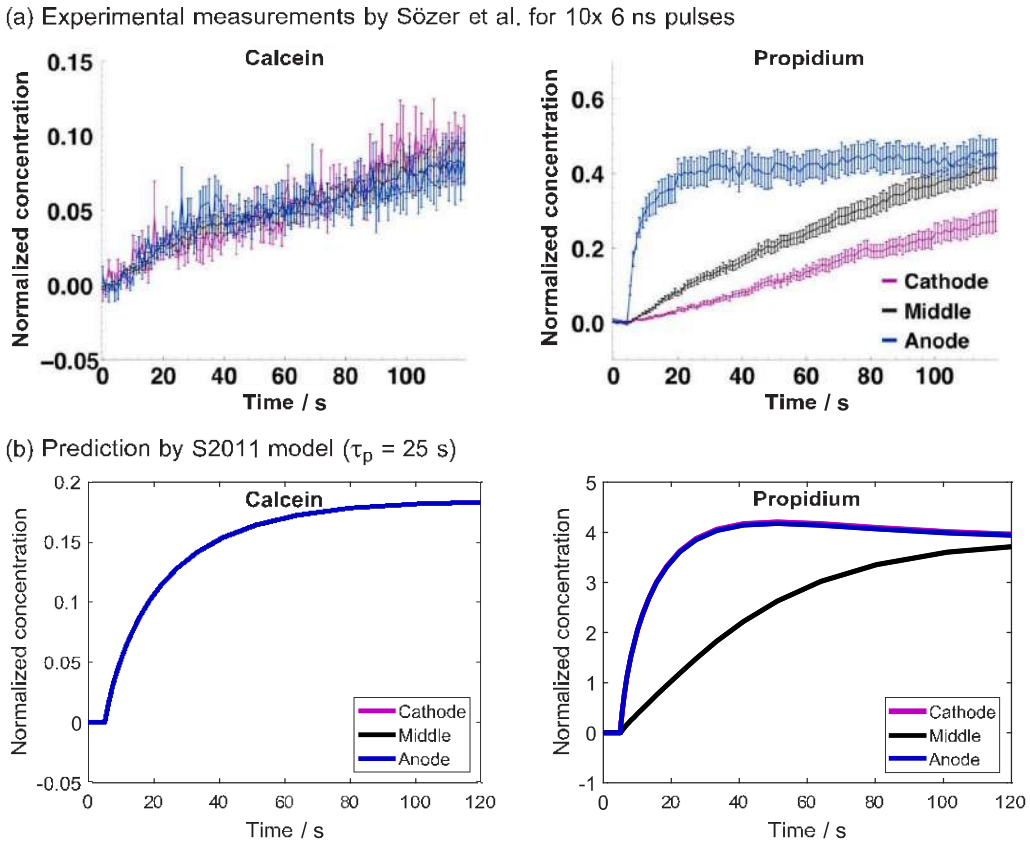

Fig. 5. Intracellular concentration of calcein and propidium upon exposure to 6 ns, 200 kV/cm pulses. The intracellular concentration is normalized to the initial extracellular concentration. (a) Experimental measurements were reproduced with permission from Sözer et al. [69]. (b) Modeling results using default S2011 model parameters. Note the different y-axes in (a) and (b). Note also that the normalized propidium concentration exceeds 1, which is possible because most propidium molecules bind to nucleic acids, allowing a continuous flow of free propidium into the cell (until all binding sites on nucleic acids are occupied).

products), whereby in such oxidatively damaged membrane lesions, pore-like defects can spontaneously form even in the absence of an electric field [79,80]. Such pore-like defects are different from the "conventional" lipid pores that form directly by an electric field: the kinetics of their formation is different, they do not need an electric field to stay open, and they can disappear only after lateral diffusion of oxidized lipids or by cell membrane repair mechanisms. Therefore, such pores are more likely to explain the persistent increase in cell membrane permeability following exposure to electric pulses. Thirdly, computational simulations supported by electrophysiological measurements suggest that pores can nucleate within some membrane proteins, specifically voltage-gated ion channels, causing protein denaturation [81,82]. Such complex pores, stabilized by both lipids and protein residues, can be more stable than pure lipid pores and, to disappear, the damaged proteins need to be replaced by the cell repair mechanisms. Therefore, protein denaturation is also a possible mechanism of persistent increase in cell membrane permeability due to electric pulses. Finally, experiments have shown that pore formation and/or expansion is affected by the actin cytoskeleton, either via actin's influence on lipid organization or the mechanical properties of the membrane [83,84]. At the same time, the actin cytoskeleton can become disrupted by electroporation [85]. This points to a complex role of the actin cytoskeleton in the increased membrane permeability.

Identification of the different possible mechanisms of increased membrane permeability prompts us to understand electroporation in the sense of multiple types of pores/defects that can form simultaneously in the cell membrane, but by different molecular mechanisms. This view is related to the distinction between short-lived and long-lived pores, proposed earlier by Pavlin et al. [50]. Interestingly, Schmeer et al. [24], who contributed to the development of pore states models, noted in the paper that their model would be in agreement with experiments even if they considered that P_1 and P_2 pore states form independently and in parallel, rather than in series. Phenomenological models are also suggesting distinct types of increased membrane permeability with different relaxation times, as discussed in Section 2.3. Overall, there is ample evidence in the literature, supporting the view of multiple distinct types of pores/defects occurring in electroporation. However, the main challenge of adding these different types of pores/defects to an electroporation model is the lack of knowledge required for developing mathematical expressions governing the formation kinetics and dynamic behavior of these pores. Filling the gaps in knowledge will require multiscale approaches including molecular modeling such as molecular dynamics simulations together with enhanced sampling methods to determine the free energy barriers for the formation of the different types of pores. In addition, experiments on model membrane systems of increasing complexity, including lipid bilayers with complex lipid mixtures, bilayers containing membrane proteins and/or cytoskeletal components, as well as cells genetically engineered to express selected cellular components (or knock out the expression) can be designed to provide the required information [82–84,86,87]. Further studies on the

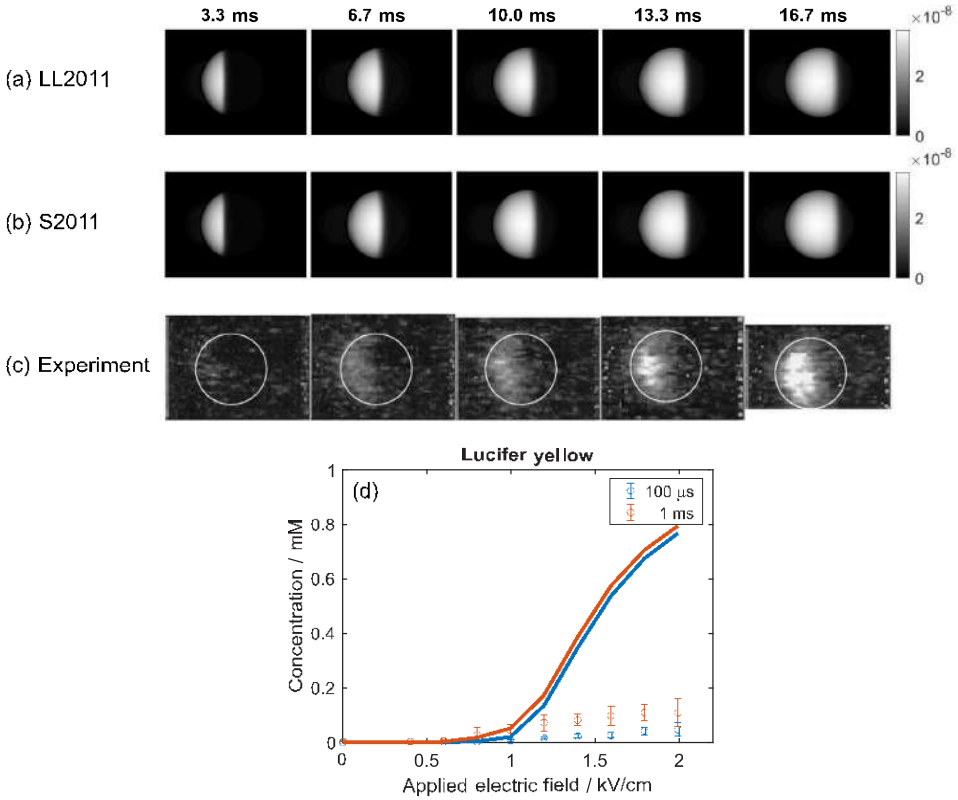

Fig. 6. Comparison between S2011 and LL2011 model. (a,b) Calculations of the intracellular concentration of calcium bound to Fluo-3 at different times after the onset of a 6 ms pulse. The intracellular concentration is presented as would appear on an epifluorescence microscope. (c) Corresponding experimental results, reproduced with permission from Gabriel and Teissié [33]. (d) Intracellular uptake of lucifer yellow, as measured by Puc et al. [10] (circles with error bars) and as predicted by the LL2011 model (solid lines). The model overestimates the intracellular uptake by roughly an order of magnitude.

biological mechanisms which could help cells repair the membrane after electroporation are also needed [88]. Much inspiration on how to develop the required mathematical expressions can actually be found in the historical development leading to the existing models of electroporation and molecular transport [24,25,31,68].

4. Conclusions and recommendations

Our study concludes that none of the existing single-cell models describing electroporation and the associated transmembrane molecular transport is universal enough to describe the entire range of experimental measurements of small molecule transport through the membrane. While upgrading and/or adapting the existing models might enable some progress, we anticipate that investments into a better understanding of the molecular mechanisms of the increased membrane permeability are more likely to result in successful development of a mechanistic electroporation model that can be applied for the entire range of pulse parameters used in electroporation applications (is such a model can exist). To this end, insights from molecular modeling and experiments on different model membrane systems with increasing complexity will undoubtedly play one of the crucial roles. Another crucial role will be played by well-designed and well-reported experimental measurements against which an electroporation model can be compared and validated [89]. Based on our findings we suggest that the experiments designed to validate electroporation models include:

- quantitative measurements of molecular uptake (or leakage);
- time courses of the intracellular concentration(s);
- 2D profiles of the intracellular concentration (to show asymmetric or symmetric uptake);
- measurements carried out over a wide range of pulse durations and amplitudes and also considering different number of pulses;
- measurements carried out for different molecules (at least one anionic and one cationic to determine the role of electrophoresis in the total uptake).

The experiments further need to report on cell size and shape, cell density, the conductivity of the extracellular electroporation medium, pulse shape, exact values of molecules characteristics (concentration and, if possible, the diffusion constant within the extracellular/intracellular medium), and temperature at which the experiments were performed, as these are all parameters which affect the modeling results but are in practice often not all reported. The experiments should also estimate the electric field strength experienced by the cells correcting for chemical oxidation or electrolytic reaction that might reduce the voltage established on the sample. For microscopic images, relevant details of the imaging configuration should be reported, for example, the focal depth in wide-field microscopy or the thickness of the focal plane in confocal microscopy.

Finally, we encourage authors to share their models through open access repositories, as we often find that the descriptions of the models in the publications do not provide sufficient detail and/or contain typographic errors that impede reproducibility and reuse of the reported models.

Declaration of Competing Interest

The authors declare that they have no known competing financial interests or personal relationships that could have appeared to influence the work reported in this paper.

Data availability

All models used in this study are available at https://github.com/learems/EPmodels-Electroporation-MolTransport.

Acknowledgements

The study was supported by the Slovenian Research Agency (ARRS) within project no. J2-2503. LR gratefully acknowledges funding from the Europen Comission via European Union`s Horizon 2020 research and innovation program under the Marie Skłodowska-Curie grant agreement No. 893077. PEB gratefully acknowledges funding from the ENW-M-2 project (project number OCENW.M20.308, ROCKET) which is financed by the Dutch Research Council (NWO). The authors thank Damijan Miklavčič for his useful comments to the manuscript, and Pim Reijniersc for assistance with some of the preliminary numerical calculations.

Appendix A. Supplementary material

Supplementary data to this article can be found online at https://doi.org/10.1016/j.bioelechem.2022.108216.

References

[1] J. Yang, Y. Huang, X.-B. Wang, F.F. Becker, P.R. Gascoyne, Cell separation on microfabricated electrodes using dielectrophoretic/gravitational field-flow fractionation, Anal. Chem. 71 (5) (1999) 911–918.
[2] D. Issadore, T. Franke, K.A. Brown, R.M. Westervelt, A microfluidic microprocessor: controlling biomimetic containers and cells using hybrid integrated circuit/microfluidic chips, Lab Chip 10 (21) (2010) 2937–2943.
[3] B. Geboers, et al., High-voltage electrical pulses in oncology: irreversible electroporation, electrochemotherapy, gene electrotransfer, electrofusion, and electroimmunotherapy, Radiology 295 (2) (2020) 254–272.
[4] L. Lambricht, A. Lopes, S. Kos, G. Sersa, V. Préat, G. Vandermeulen, Clinical potential of electroporation for gene therapy and DNA vaccine delivery, Expert opinion on drug delivery 13 (2) (2016) 295–310.
[5] K. R. Foster and H. P. Schwan, "Dielectric properties of tissues," *CRC handbook of biological effects of electromagnetic fields*, pp. 27–96, 1986.
[6] T. Kotnik, L. Rems, M. Tarek, D. Miklavčič, Membrane electroporation and electropermeabilization: mechanisms and models, Annu. Rev. Biophys. 48 (2019) 63–91.
[7] T. Kotnik, F. Bobanović, D. Miklavčič, Sensitivity of transmembrane voltage induced by applied electric fields—a theoretical analysis, Bioelectrochem. Bioenerg. 43 (2) (1997) 285–291.
[8] C. Rosazza, S. Haberl Meglic, A. Zumbusch, M.-P. Rols, D. Miklavcic, Gene electrotransfer: a mechanistic perspective, Curr. Gene Ther. 16 (2) (2016) 98–129.
[9] D.S. Dimitrov, A.E. Sowers, Membrane electroporaton—fast molecular exchange by electroosmosis, Biochimica et Biophysica Acta (BBA)-Biomembranes 1022 (3) (1990) 381–392.
[10] M. Puc, T. Kotnik, L.M. Mir, D. Miklavčič, Quantitative model of small molecules uptake after in vitro cell electropermeabilization, Bioelectrochemistry 60 (1–2) (2003) 1–10.
[11] M.M. Sadik, J. Li, J.W. Shan, D.I. Shreiber, H. Lin, Quantification of propidium iodide delivery using millisecond electric pulses: experiments, Biochimica et Biophysica Acta (BBA)-Biomembranes 1828 (4) (2013) 1322–1328.
[12] J. Li, H. Lin, Numerical simulation of molecular uptake via electroporation, Bioelectrochemistry 82 (1) (2011) 10–21.
[13] G. Pucihar, T. Kotnik, D. Miklavčič, J. Teissié, Kinetics of transmembrane transport of small molecules into electropermeabilized cells, Biophys. J . 95 (6) (2008) 2837–2848.
[14] E.B. Sözer, C.F. Poccetti, P.T. Vernier, Transport of charged small molecules after electropermeabilization—drift and diffusion, BMC biophysics 11 (1) (2018) 1–11.
[15] J.-M. Escoffre, T. Portet, L. Wasungu, J. Teissié, D. Dean, M.-P. Rols, What is (still not) known of the mechanism by which electroporation mediates gene transfer and expression in cells and tissues, Mol. Biotechnol. 41 (3) (2009) 286–295.
[16] T. Kotnik, W. Frey, M. Sack, S.H. Meglič, M. Peterka, D. Miklavčič, Electroporation-based applications in biotechnology, Trends Biotechnol. 33 (8) (2015) 480–488.
[17] S. Mahnič-Kalamiza, E. Vorobiev, D. Miklavčič, Electroporation in food processing and biorefinery, The Journal of membrane biology 247 (12) (2014) 1279–1304.
[18] D.Y. Lyon, J. Pivetal, L. Blanchard, T.M. Vogel, Bioremediation via in situ electrotransformation, Biorem. J. 14 (2) (2010) 109–119.
[19] Z. Chen, W.G. Lee, Electroporation for microalgal biofuels: a review, Sustainable Energy Fuels 3 (11) (2019) 2954–2967.
[20] C.B. Arena, et al., High-frequency irreversible electroporation (H-FIRE) for non-thermal ablation without muscle contraction, Biomed. Eng. Online 10 (1) (2011) 1–21.
[21] K. Čepurnienė, P. Ruzgys, R. Treinys, I. Šatkauskienė, S. Šatkauskas, Influence of plasmid concentration on DNA electrotransfer in vitro using high-voltage and low-voltage pulses, The Journal of Membrane Biology 236 (1) (2010) 81–85.
[22] M.-P. Rols, J. Teissié, Electropermeabilization of mammalian cells to macromolecules: control by pulse duration, Biophys. J . 75 (3) (1998) 1415–1423.
[23] J.C. Weaver, K.C. Smith, A.T. Esser, R.S. Son, T.R. Gowrishankar, A brief overview of electroporation pulse strength–duration space: A region where additional intracellular effects are expected, Bioelectrochemistry 87 (2012) 236–243.
[24] M. Schmeer, T. Seipp, U. Pliquett, S. Kakorin, E. Neumann, Mechanism for the conductivity changes caused by membrane electroporation of CHO cell-pellets, PCCP 6 (24) (2004) 5564–5574.
[25] E. Neumann, K. Tönsing, S. Kakorin, P. Budde, J. Frey, Mechanism of electroporative dye uptake by mouse B cells, Biophys. J . 74 (1) (1998) 98–108.
[26] K.A. DeBruin, W. Krassowska, Modeling electroporation in a single cell. I. Effects of field strength and rest potential, Biophys. J . 77 (3) (1999) 1213–1224.
[27] M. Hibino, H. Itoh, K. Kinosita Jr, Time courses of cell electroporation as revealed by submicrosecond imaging of transmembrane potential, Biophys. J . 64 (6) (1993) 1789–1800.
[28] S. Sachdev, T. Potočnik, L. Rems, D. Miklavčič, Revisiting the role of pulsed electric fields in overcoming the barriers to in vivo gene electrotransfer, Bioelectrochemistry (2021), 107994.
[29] D. Miklavcic, L. Towhidi, Numerical study of the electroporation pulse shape effect on molecular uptake of biological cells, Radiology and oncology 44 (1) (2010) 34–41.
[30] J. Li, W. Tan, M. Yu, H. Lin, The effect of extracellular conductivity on electroporation-mediated molecular delivery, Biochimica et Biophysica Acta (BBA)-Biomembranes 1828 (2) (2013) 461–470.
[31] K.C. Smith, A unified model of electroporation and molecular transport, PhD Thesis, Massachusetts Institute of Technology (2011).
[32] T. Kotnik, G. Pucihar, M. Rebersek, D. Miklavčič, L.M. Mir, Role of pulse shape in cell membrane electropermeabilization, Biochimica et Biophysica Acta (BBA)-Biomembranes 1614 (2) (2003) 193–200.
[33] B. Gabriel, J. Teissie, Time courses of mammalian cell electropermeabilization observed by millisecond imaging of membrane property changes during the pulse, Biophys. J . 76 (4) (1999) 2158–2165.
[34] K.J. Müller, V.L. Sukhorukov, U. Zimmermann, Reversible electropermeabilization of mammalian cells by high-intensity, ultra-short pulses of submicrosecond duration, The Journal of membrane biology 184 (2) (2001) 161–170.
[35] M.M. Sadik, et al., Scaling relationship and optimization of double-pulse electroporation, Biophys. J . 106 (4) (2014) 801–812.
[36] M. Mahboubi, S. Movahed, R. Abardeh, V. Hoshyargar, Theoretical Study of Molecular Transport Through a Permeabilized Cell Membrane in a Microchannel, J. Membr. Biol. 250 (3) (Jun. 2017) 285–299, https://doi.org/10.1007/s00232-017-9961-2.
[37] P. Shil, K. B. Achary, and K. Alagarasu, "Numerical analyses of electroporation-mediated doxorubicin uptake in eukaryotic cells: role of membrane cholesterol content," 2018.
[38] E. Goldberg, C. Suárez, M. Alfonso, J. Marchese, A. Soba, G. Marshall, Cell membrane electroporation modeling: A multiphysics approach, Bioelectrochemistry 124 (2018) 28–39.
[39] H. Engelhardt, E. Sackmann, On the measurement of shear elastic moduli and viscosities of erythrocyte plasma membranes by transient deformation in high frequency electric fields, Biophys. J . 54 (3) (1988) 495–508.
[40] C. Mauroy, I. Rico-Lattes, J. Teissié, M.-P. Rols, Electric destabilization of supramolecular lipid vesicles subjected to fast electric pulses, Langmuir 31 (44) (2015) 12215–12222.
[41] E. Goldberg, A. Soba, D. Gandía, M.L. Fernández, C. Suárez, Coupled mathematical modeling of cisplatin electroporation, Bioelectrochemistry 140 (2021), 107788.
[42] J. Dermol-Cerne, J. Vidmar, J. Ščančar, K. Uršič, G. Serša, D. Miklavčič, Connecting the in vitro and in vivo experiments in electrochemotherapy-a feasibility study modeling cisplatin transport in mouse melanoma using the dual-porosity model, J. Control. Release 286 (2018) 33–45.
[43] Z. Yan, C. Hao, L. Yin, K. Liu, J. Qiu, Simulation of the Influence of Temperature on the Dynamic Process of Electroporation Based on Finite Element Analysis, IEEE Trans. Plasma Sci. 49 (9) (2021) 2839–2850.
[44] F. Guo, K. Qian, L. Zhang, X. Liu, H. Peng, Multiphysics modelling of electroporation under uni-or bipolar nanosecond pulse sequences, Bioelectrochemistry 141 (2021), 107878.
[45] P.J. Canatella, J.F. Karr, J.A. Petros, M.R. Prausnitz, Quantitative study of electroporation-mediated molecular uptake and cell viability, Biophys. J . 80 (2) (2001) 755–764.
[46] R.S. Son, K.C. Smith, T.R. Gowrishankar, P. Thomas Vernier, P. Thomas Vernier, J. C. Weaver, Basic Features of a Cell Electroporation Model: Illustrative Behavior for Two Very Different Pulses, The Journal of Membrane Biology (2014), https://doi.org/10.1007/s00232-014-9699-z.
[47] R.S. Son, T.R. Gowrishankar, K.C. Smith, J.C. Weaver, Modeling a conventional electroporation pulse train: decreased pore number, cumulative calcium transport and an example of electrosensitization, IEEE Trans. Biomed. Eng. 63 (3) (2015) 571–580.

[48] Y. Mi, J. Xu, C. Yao, C. Li, H. Liu, Electroporation modeling of a single cell exposed to high-frequency nanosecond pulse bursts, IEEE Trans. Dielectr. Electr. Insul. 26 (2) (2019) 461–468.

[49] Y. Mi, J. Xu, Q. Liu, X. Wu, Q. Zhang, J. Tang, Single-cell electroporation with high-frequency nanosecond pulse bursts: Simulation considering the irreversible electroporation effect and experimental validation, Bioelectrochemistry 140 (2021), 107822.

[50] M. Pavlin, V. Leben, D. Miklavčič, Electroporation in dense cell suspension—Theoretical and experimental analysis of ion diffusion and cell permeabilization, Biochimica et Biophysica Acta (BBA)-General Subjects 1770 (1) (2007) 12–23.

[51] M. Pavlin, D. Miklavčič, Theoretical and experimental analysis of conductivity, ion diffusion and molecular transport during cell electroporation—relation between short-lived and long-lived pores, Bioelectrochemistry 74 (1) (2008) 38–46.

[52] M. Leguebe, A. Silve, L.M. Mir, C. Poignard, Conducting and permeable states of cell membrane submitted to high voltage pulses: mathematical and numerical studies validated by the experiments, J. Theor. Biol. 360 (2014) 83–94.

[53] J.-M. Escoffre, T. Portet, C. Favard, J. Teissié, D.S. Dean, M.-P. Rols, Electromediated formation of DNA complexes with cell membranes and its consequences for gene delivery, Biochimica et Biophysica Acta (BBA)-Biomembranes 1808 (6) (2011) 1538–1543.

[54] P.T. Vernier, Y. Sun, L. Marcu, S. Salemi, C.M. Craft, M.A. Gundersen, Calcium bursts induced by nanosecond electric pulses, Biochem. Biophys. Res. Commun. 310 (2) (2003) 286–295.

[55] A. Silve, A.G. Brunet, B. Al-Sakere, A. Ivorra, L.M. Mir, Comparison of the effects of the repetition rate between microsecond and nanosecond pulses: Electropermeabilization-induced electro-desensitization? Biochimica et Biophysica Acta (BBA)-General Subjects 1840 (7) (2014) 2139–2151.

[56] D. C. Sweeney, T. A. Douglas, and R. V. Davalos, "Characterization of cell membrane permeability in vitro part II: computational model of electroporation-mediated membrane transport," *Technology in cancer research & treatment*, vol. 17, p. 1533033818792490, 2018.

[57] D. C. Sweeney, J. C. Weaver, and R. V. Davalos, "Characterization of cell membrane permeability in vitro part I: transport behavior induced by single-pulse electric fields," *Technology in cancer research & treatment*, vol. 17, p. 1533033818792491, 2018.

[58] E. Neumann, E. Boldt, "Membrane electroporation: biophysical and biotechnical aspects", in *Charge and Field Effects in Biosystems—2*, Springer (1989) 373–382.

[59] R.A. Böckmann, B.L. De Groot, S. Kakorin, E. Neumann, H. Grubmüller, Kinetics, statistics, and energetics of lipid membrane electroporation studied by molecular dynamics simulations, Biophys. J . 95 (4) (2008) 1837–1850.

[60] V.F. Pastushenko, Y.A. Chizmadzhev, V.B. Arakelyan, Electric breakdown of bilayer lipid membranes: II. Calculation of the membrane lifetime in the steady-state diffusion approximation, J. Electroanal. Chem. Interfacial Electrochem. 104 (1979) 53–62.

[61] A. Barnett, J.C. Weaver, Electroporation: a unified, quantitative theory of reversible electrical breakdown and mechanical rupture in artificial planar bilayer membranes, Bioelectrochem. Bioenerg. 25 (2) (1991) 163–182.

[62] K.T. Powell, J.C. Weaver, Transient aqueous pores in bilayer membranes: a statistical theory, Bioelectrochem. Bioenerg. 15 (2) (1986) 211–227.

[63] J.C. Neu, W. Krassowska, Asymptotic model of electroporation, Phys. Rev. E 59 (3) (1999) 3471.

[64] J.T. Sengel, M.I. Wallace, Imaging the dynamics of individual electropores, Proc. Natl. Acad. Sci. 113 (19) (2016) 5281–5286.

[65] M.L. Fernández, M. Risk, R. Reigada, P.T. Vernier, Size-controlled nanopores in lipid membranes with stabilizing electric fields, Biochem. Biophys. Res. Commun. 423 (2) (2012) 325–330.

[66] M. Casciola, M.A. Kasimova, L. Rems, S. Zullino, F. Apollonio, M. Tarek, Properties of lipid electropores I: Molecular dynamics simulations of stabilized pores by constant charge imbalance, Bioelectrochemistry 109 (2016) 108–116.

[67] W. Krassowska, P.D. Filev, Modeling electroporation in a single cell, Biophys. J . 92 (2) (2007) 404–417.

[68] J.C. Weaver, Y.A. Chizmadzhev, Theory of electroporation: a review, Bioelectrochem. Bioenerg. 41 (2) (1996) 135–160.

[69] E.B. Sözer, C.F. Pocetti, P.T. Vernier, Asymmetric patterns of small molecule transport after nanosecond and microsecond Electropermeabilization, The Journal of membrane biology 251 (2) (2018) 197–210.

[70] C.S. Djuzenova, U. Zimmermann, H. Frank, V.L. Sukhorukov, E. Richter, G. Fuhr, Effect of medium conductivity and composition on the uptake of propidium iodide into electropermeabilized myeloma cells, Biochimica et Biophysica Acta (BBA)-Biomembranes 1284 (2) (1996) 143–152.

[71] V.L. Sukhorukov, C.S. Djuzenova, H. Frank, W.M. Arnold, U. Zimmermann, Electropermeabilization and fluorescent tracer exchange: The role of whole-cell capacitance, Cytometry: The Journal of the International Society for Analytical Cytology 21 (3) (1995) 230–240.

[72] W.D. Wilson, C.R. Krishnamoorthy, Y.-H. Wang, J.C. Smith, Mechanism of intercalation: ion effects on the equilibrium and kinetic constants for the interaction of propidium and ethidium with DNA, Biopolymers: Original Research on Biomolecules 24 (10) (1985) 1941–1961.

[73] Z. Vasilkoski, A.T. Esser, T.R. Gowrishankar, J.C. Weaver, Membrane electroporation: The absolute rate equation and nanosecond time scale pore creation, Phys. Rev. E 74 (2) (2006), 021904.

[74] C.L. Ting, N. Awasthi, M. Müller, J.S. Hub, Metastable prepores in tension-free lipid bilayers, Phys. Rev. Lett. 120 (12) (2018), 128103.

[75] E.B. Sözer, S. Haldar, P.S. Blank, F. Castellani, P.T. Vernier, J. Zimmerberg, Dye transport through bilayers agrees with lipid electropore molecular dynamics, Biophys. J . 119 (9) (2020) 1724–1734.

[76] J.T. Sengel, M.I. Wallace, Measuring the potential energy barrier to lipid bilayer electroporation, Philosophical Transactions of the Royal Society B: Biological Sciences 372 (1726) (2017) 20160227.

[77] M. Maccarrone, N. Rosato, A.F. Agrò, Electroporation enhances cell membrane peroxidation and luminescence, Biochem. Biophys. Res. Commun. 206 (1) (1995) 238–245.

[78] M. Breton, L.M. Mir, Investigation of the chemical mechanisms involved in the electropulsation of membranes at the molecular level, Bioelectrochemistry 119 (2018) 76–83.

[79] D. Wiczew, N. Szule, M. Tarek, Molecular dynamics simulations of the effects of lipid oxidation on the permeability of cell membranes, Bioelectrochemistry 141 (2021), 107869.

[80] P. Boonmoy, V. Jarerattanachat, M. Karttunen, J. Wong-Ekkabut, Bilayer deformation, pores, and micellation induced by oxidized lipids, The journal of physical chemistry letters 6 (24) (2015) 4884–4888.

[81] K. Hristov, U. Mangalanathan, M. Casciola, O.N. Pakhomova, A.G. Pakhomov, Expression of voltage-gated calcium channels augments cell susceptibility to membrane disruption by nanosecond pulsed electric field, Biochimica et Biophysica Acta (BBA)-Biomembranes 1860 (11) (2018) 2175–2183.

[82] L. Rems, M.A. Kasimova, I. Testa, L. Delemotte, Pulsed electric fields can create pores in the voltage sensors of voltage-gated ion channels, Biophys. J . 119 (1) (2020) 190–205.

[83] A. Muralidharan, L. Rems, M.T. Kreutzer, P.E. Boukany, Actin networks regulate the cell membrane permeability during electroporation, Biochimica et Biophysica Acta (BBA)-Biomembranes 1863 (1) (2021), 183468.

[84] D.L. Perrier, et al., Response of an actin network in vesicles under electric pulses, Sci. Rep. 9 (1) (2019) 1–11.

[85] P.M. Graybill, R.V. Davalos, Cytoskeletal disruption after electroporation and its significance to pulsed electric field therapies, Cancers 12 (5) (2020) 1132.

[86] L. Rems, X. Tang, F. Zhao, S. Pérez-Conesa, I. Testa, and L. Delemotte, "Identification of electroporation sites in the complex lipid organization of the plasma membrane," *eLife*, vol. 11, p. e74773, Feb. 2022, doi: 10.7554/eLife.74773.

[87] I. van Uitert, S. Le Gac, A. van den Berg, The influence of different membrane components on the electrical stability of bilayer lipid membranes, Biochimica et Biophysica Acta (BBA)-Biomembranes 1798 (1) (2010) 21–31.

[88] T.B. Napotnik, T. Polajžer, D. Miklavčič, Cell death due to electroporation–A review, Bioelectrochemistry 141 (2021), 107871.

[89] M. Cemazar, G. Sersa, W. Frey, D. Miklavcic, J. Teissié, Recommendations and requirements for reporting on applications of electric pulse delivery for electroporation of biological samples, Bioelectrochemistry 122 (2018) 69–76.

2.4. Paper 4

Title: **Characterization of experimentally observed complex interplay between pulse duration, electrical field strength, and cell orientation on electroporation outcome using a time-dependent nonlinear numerical model**

Authors: **Maria Scuderi,** Janja Dermol-Černe, Tina Batista Napotnik, Sebastien Chaigne, Olivier Bernus, David Benoist, Daniel C. Sigg, Lea Rems, and Damijan Miklavčič

Publication: Biomolecules vol. 13, no. 5, pp. 727, April 2023

Impact Factor on the date of publication: 6.1 (2021)

Quartile:

- Q2 (Biochemistry & Molecular Biology)

Rank:

- 75/297 (Biochemistry & Molecular Biology)

DOI: https://doi.org/10.3390/biom13050727

biomolecules

MDPI

Article

Characterization of Experimentally Observed Complex Interplay between Pulse Duration, Electrical Field Strength, and Cell Orientation on Electroporation Outcome Using a Time-Dependent Nonlinear Numerical Model

Maria Scuderi [1], Janja Dermol-Černe [1], Tina Batista Napotnik [1], Sebastien Chaigne [2], Olivier Bernus [2], David Benoist [2], Daniel C. Sigg [3], Lea Rems [1] and Damijan Miklavčič [1,*]

[1] Faculty of Electrical Engineering, University of Ljubljana, SI-1000 Ljubljana, Slovenia
[2] INSERM, CRCTB, U 1045, 1HU Liryc, University of Bordeaux, F-33000 Bordeaux, France
[3] Medtronic, Cardiac Ablation Solutions, Minneapolis, MN 55105, USA
* Correspondence: damijan.miklavcic@fe.uni-lj.si

Abstract: Electroporation is a biophysical phenomenon involving an increase in cell membrane permeability to molecules after a high-pulsed electric field is applied to the tissue. Currently, electroporation is being developed for non-thermal ablation of cardiac tissue to treat arrhythmias. Cardiomyocytes have been shown to be more affected by electroporation when oriented with their long axis parallel to the applied electric field. However, recent studies demonstrate that the preferentially affected orientation depends on the pulse parameters. To gain better insight into the influence of cell orientation on electroporation with different pulse parameters, we developed a time-dependent nonlinear numerical model where we calculated the induced transmembrane voltage and pores creation in the membrane due to electroporation. The numerical results show that the onset of electroporation is observed at lower electric field strengths for cells oriented parallel to the electric field for pulse durations >10 µs, and cells oriented perpendicular for pulse durations ~100 ns. For pulses of ~1 µs duration, electroporation is not very sensitive to cell orientation. Interestingly, as the electric field strength increases beyond the onset of electroporation, perpendicular cells become more affected irrespective of pulse duration. The results obtained using the developed time-dependent nonlinear model are corroborated by in vitro experimental measurements. Our study will contribute to the process of further development and optimization of pulsed-field ablation and gene therapy in cardiac treatments.

Keywords: finite element model; time domain; electroporation; pulsed-field ablation; cardiomyocyte; intracellular calcium; lethal electric field strength; cell orientation; anisotropy

Citation: Scuderi, M.; Dermol-Černe, J.; Batista Napotnik, T.; Chaigne, S.; Bernus, O.; Benoist, D.; Sigg, D.C.; Rems, L.; Miklavčič, D. Characterization of Experimentally Observed Complex Interplay between Pulse Duration, Electrical Field Strength, and Cell Orientation on Electroporation Outcome Using a Time-Dependent Nonlinear Numerical Model. *Biomolecules* **2023**, *13*, 727. https://doi.org/10.3390/biom13050727

Academic Editor: Chi Keung Lam

Received: 28 February 2023
Revised: 17 April 2023
Accepted: 18 April 2023
Published: 23 April 2023

1. Introduction

Electroporation is the underlying mechanism in a new promising cardiac ablation method—Pulsed Field Ablation (PFA)—currently being developed for the treatment of atrial fibrillation and other cardiac arrhythmias [1–3]. Electroporation has also been attributed to performing a role in cardiac defibrillation [4] and has shown promise for cardiac regeneration based on gene therapy [5,6].

Electroporation is a phenomenon where the application of high-voltage electric pulses to isolated cells or tissues transiently increases membrane permeability allowing the transport of ions and molecules otherwise deprived of or having hindered transmembrane transport mechanisms [7,8]. Following electroporation, cells may recover and survive (i.e., reversible electroporation), or lose homeostasis and undergo cell death (i.e., irreversible electroporation). The increase in cell membrane permeability is due to a supraphysiological transmembrane voltage (more than a few 100 mV) induced by an external electric

field [9,10] and can involve pore formation in the lipid bilayer of the cell membrane, oxidative lipid damage, and structural alteration of specific membrane proteins [11]. The induced transmembrane voltage varies with the position on the membrane and depends on cell size, shape, and orientation with respect to the applied electric field [11–13]. The time course of the induced transmembrane voltage for spherical and other regularly shaped cells can be determined analytically, and for cells with more complex and irregular shapes, such as isolated cardiomyocytes, it can be calculated numerically [12,13]. In general, electroporation follows a "size rule" in the sense that larger cells are electroporated at lower electric field strengths than smaller ones, as the induced transmembrane voltage is proportional to the electric field strength and cell radius.

Cardiac tissue is composed of different types of cells (e.g., cardiomyocytes, fibroblasts, smooth muscle cells, immune cells, neuronal cells, etc. [14]), whereby the target of the electroporation therapy are typically cardiomyocytes. Cardiomyocytes are cardiac muscle cells that are elongated and rod-shaped with a non-smooth membrane surface and a complex array of tubules. Cardiac transverse tubules (t-tubules) are invaginations of cardiomyocyte sarcolemma and are involved in the maintenance of resting membrane voltage, action potential initiation, regulation and propagation, signaling transduction, and the coupling for the excitation-contraction cycle [15]. Cardiac myocytes are organized in fibers and their orientation within the heart is variable. For example, in ventricular tissue, fibers turn from a circumferential orientation on the epicardium to an apicobasal orientation in the endocardium [16–18]. Fiber orientation in the atria is more irregular than that of the ventricles [19–21]. In the context of cardiac arrhythmia treatment, a wide range of pulse shapes and durations have been investigated and used in vitro and in vivo, from exponentially decaying pulses to monophasic pulses with duration ranging from milliseconds to nanoseconds, and most recently, short µs-long biphasic pulses referred to as high-frequency irreversible electroporation (HFIRE) [22–29]. The orientation of elongated cardiac cells and the different pulse parameters (e.g., amplitude, duration, number, and repetition frequency), which are used for the treatment, might affect the efficiency of PFA treatment. An efficient way to determine the effect of an external electric field on a cell is by numerical modeling combined with in vitro experimental results.

Milan et al. [30] studied the induced transmembrane voltage due to the applied external electric field on a single cardiomyocyte from the modeling point of view and showed that the shape of cardiomyocytes can be approximated by a prolate spheroid. Under steady-state conditions, the cardiomyocytes (and other elongated cells) are predicted to be more affected when oriented parallel to an external electric field compared to perpendicular orientation. However, it was observed experimentally that cardiomyocytes are electroporated by nanosecond pulses at lower electric field strengths when oriented perpendicularly to the electric field compared to the parallel orientation [27,31]. Surprisingly, to some extent, effects associated with electroporation do not always follow the "size rule" [32] as intuitively expected based on simple steady-state calculations. A study published by Dermol-Černe et al. [31] showed that parallel orientation is more affected than perpendicular orientation when a single monophasic pulse of >1 µs duration is applied to different electric fields. Chaigne et al. [33] recently published a study in which authors investigated the lethal electric field strengths of a single-oriented cardiomyocyte when applying a single monophasic pulse of 10 ms or 100 µs pulse duration. The authors showed that the cells oriented perpendicular to the electric field had a lower lethal threshold at 100 µs than parallel cells, but cells oriented parallel to the electric field had a lower lethal threshold at 10 ms than perpendicular cells [33]. Interestingly, they showed that perpendicular orientation is more affected than the parallel one when using 100 µs pulse duration which seems to be in contrast to the findings from Dermol-Černe et al. [31]. To gain a better mechanistic understanding of the in vitro experimental data published by Dermol-Černe et al. [31] and Chaigne et al. [33], we developed a time-dependent nonlinear numerical model which included membrane electroporation. We built upon a previously published steady-state model of a single cardiomyocyte with realistic shape and simplified prolate spheroid shape,

which was exposed to electric field [30]. In contrast to the steady-state model, our model also captures the nonlinear behavior of the induced transmembrane voltage as the membrane is being electroporated [34,35]. We used our developed model to investigate the effect of cardiomyocyte orientation on electroporation induced by a single monophasic pulse of durations from 10 ms to 100 ns pulses. These pulse parameters were chosen specifically to be able to compare the modeling findings with in vitro experimental data previously reported by Dermol-Černe et al. [31] and Chaigne et al. [33]. Since the cardiomyocyte model did not include t-tubules, we have numerically modeled these by varying the membrane capacitance to determine how these would affect the induced transmembrane voltage and electroporation. The modeling results suggest that the orientation at which cardiomyocytes become preferentially affected by electroporation pulses depends in a complex way both on pulse duration and the electric field strength. The model findings corroborate and bring better mechanistic understanding on the apparently conflicting experimental results published previously [31,33]. In addition, the modeling results may become relevant for interpreting results at the tissue level in clinical applications of PFA.

2. Materials and Methods

2.1. The Time-Dependent Numerical Model with Electroporation

A time-dependent nonlinear numerical model was developed, including the phenomenon of electroporation, to study the effect of the external applied electric field on a cardiomyocyte. The model was developed using COMSOL Multiphysics 5.6 software (Comsol, Inc., Burlington, MA, USA). Two different geometries, prolate spheroid (Figure 1A) and the real-shaped geometry of a cardiomyocyte (Figure 1B) were used to represent a single cardiomyocyte. The real-shaped geometry of a cardiomyocyte was kindly provided by Milan et al. [30]. Both geometries were modeled in the center of the simulation cube with dimensions 400 μm × 400 μm × 400 μm (Figure 1C).

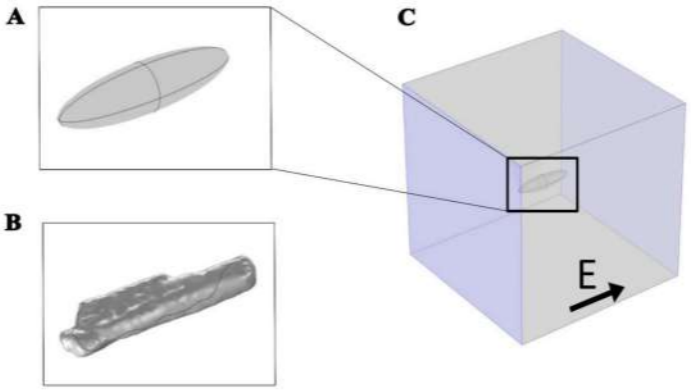

Figure 1. Geometries used to represent a cardiomyocyte with an electric field applied parallel to the long axis of the cell. (**A**) Prolate spheroid geometry, 120 μm long, 30 μm wide, and 30 μm high. (**B**) Real-shaped geometry 142 μm long, 36 μm wide, and 21 μm high. Both the real-shaped geometry and its prolate spheroid approximation were the same as in Milan et al. [30]. (**C**) The cell was at the center of the box when the electric field was applied parallel to the long axis of the cell. The violet-colored sides of the box represent the electrodes to which the voltage was applied.

The electric potential distribution, V, in the intracellular and extracellular subdomains was calculated in the *AC/DC module*, *Electric Currents* physics by solving the Laplace equation:

$$\nabla \cdot \left[\left(\sigma_{i,e} + \varepsilon_{i,e} \frac{\partial}{\partial t} \right) \nabla V_{i,e} \right] = 0 \quad (1)$$

where $\sigma_{i,e}$ and $\varepsilon_{i,e}$ denote, respectively, the conductivity and the dielectric permittivity of either intracellular (subscript *i*) or extracellular (subscript *e*) medium. The cell membrane was modeled using the *Contact Impedance Boundary Condition:*

$$\boldsymbol{n}\cdot\boldsymbol{J} = \frac{1}{d_m}\left(\sigma_m + \varepsilon_0\varepsilon_m\frac{\partial}{\partial t}\right)(V_i - V_e) \tag{2}$$

where $\boldsymbol{n}$ is the normal vector, $\boldsymbol{J}$ is the current density, d_m is the cell membrane thickness, σ_m is the cell membrane conductivity, ε_m is the cell membrane permittivity, ε_0 is the permittivity of the vacuum, and V_e and V_i are the electric potentials at the outer and inner surfaces of the membrane, respectively. The induced transmembrane voltage (TMV) is calculated as the difference between the extracellular, V_e, and intracellular, V_i, electric potential, TMV = $V_i - V_e$.

A monophasic electric pulse with different pulse durations of 10 ms, 1 ms, 100 µs, 10 µs, 1 µs, and 100 ns was applied on the two opposite boundaries of the simulation cube, either parallel or perpendicular to the main axis of the cardiomyocyte. The remaining four faces of the cube were modeled as insulating surfaces. The electric pulse was obtained by subtracting two Heaviside functions using the COMSOL's built-in function *flc1hs* [36]. The pulse rise time was set to 1/100 of the pulse duration. The values of the electric field applied in the numerical model were from 10 V/cm to 10^5 V/cm.

Pore formation was calculated as a function of time and thus can only be added in the time-dependent simulations. The pore formation was described by the following differential Equation (3) implemented in COMSOL Multiphysics as a *Weak Form Boundary partial differential equation:*

$$\frac{dN}{dt} = \alpha e^{\left(\frac{U_m}{V_{ep}}\right)^2} - \alpha\frac{N}{N_0}e^{(-q)\left(\frac{U_m}{V_{ep}}\right)^2} \tag{3}$$

where N represents the pore density (number of pores per unit area), U_m denotes the TMV, N_0 is the pore density when U_m = 0 V, and V_{ep}, a, and q are model parameters, respectively. The first term of Equation (3) represents pore creation and the second one the pore annihilation [37,38].

The increase in cell membrane conductivity during electroporation, σ_{ep}, was calculated as:

$$\sigma_{ep} = \sigma_m + N\frac{2\pi r_p{}^2\sigma_p d_m}{\pi r_p + 2d_m} \tag{4}$$

where r_p and σ_p are the radius and conductivity of a single pore, respectively. The first term of Equation (4) represents the passive membrane conductivity and the second one is the increase in conductivity due to electroporation [37,38]. The parameters used in the numerical model are shown in Table 1.

Table 1. Model parameters.

Parameter	Symbol	Value	Ref.
Intracellular permittivity	ε_i	80	[39]
Extracellular permittivity	ε_e	80	[39]
Intracellular conductivity	σ_i	0.8 S/m	[30]
Extracellular conductivity	σ_e	1.4 S/m	[30]
Membrane conductivity	σ_m	1.4925×10^{-8} S/m	[30]
Membrane thickness	d_m	5 nm	[37]
Membrane capacitance	C_m	0 µF/cm^2 5–10 µF/cm^2 *	[37] [40]
Block length	L	400 µm	Arbitrary

Table 1. *Cont.*

Parameter	Symbol	Value	Ref.
Electroporation constant	q	1.46	[31]
Electroporation parameter	A	10^9 1/(m^{2}s)	[37]
Characteristic voltage of electroporation	V_{ep}	0.258 V,	[37]
Equilibrium pore density	N_0	$1.5{\cdot}10^9$ 1/m^2	[37]
Pore radius	r_p	0.76 nm	[37]
Pore Conductivity (cell membrane)	σ_p	$(\sigma_e - \sigma_i)/\ln(\sigma_e - \sigma_i)$	[36]

* Used in calculations presented in Figure 4.

2.2. *In Vitro Experiments: Calcium Transients in Cardiomyocyte-Derived Cell Lines*

We compared our numerical model with experimental results previously published by Dermol-Černe et al. [31]. The electroporation extent was evaluated by calcium uptake to cells from the external medium [41]. In brief, H9c2 rat cardiac myoblast cell line (European Collection of Authenticated Cell Cultures ECACC 88092904) and AC16 human cardiomyocyte cell line (Merck Millipore, SCC109) were stained with a fluorescent calcium indicator Fura-2 AM and exposed to a single monophasic electric pulse of different durations, ranging from 10 ms to 100 ns. In each experiment, cultured cells were exposed to a single monophasic pulse of the same duration, but increasing voltage was applied 8 to 12 min apart that allow the cells to reseal and restore low internal calcium concentration. Cells were monitored under a fluorescence microscope (Zeiss Axiovert 200, Oberkochen, Germany) in ratiometric measurements using two excitation wavelengths (340 and 380 nm). When internal calcium concentration increased due to calcium uptake, the Fura-2 340/380 ratio increased. With the use of an image-processing program ImageJ (National Institutes of Health, Bethesda, MD, USA), the orientations of cells in an electric field were determined and a mean ratio of Fura-2 340/380 was calculated for each cell. The Fura-2 signal was expressed as a Fura-2 ratio 340/380 peak change, which occurred 8 s after the pulse application (see Supplementary Figure S1). The in vitro data of the aforementioned experimental work are presented in a way that it is possible to evaluate two different outcomes. The first outcome is the quantification of the difference in fluorescent calcium indicator Fura-2 signal in parallel and perpendicular cells already published in Dermol-Černe et al. [31]. The second outcome is the determination of the Fura-2 ratio 340/380 peak change observed when the cells are oriented parallel or perpendicular to the applied electric field (unpublished data and presented in this study). Statistical analysis for the aforementioned cell experiments was performed using Excel and SigmaPlot 11.0 (Systat Software, Chicago, IL, USA). The results in Figure 6 (unpublished data) are expressed as means ± SD. The normality of the data distribution was tested with the Kolmogorov–Smirnov test. Significant differences ($p < 0.05$) in Fura-2 responses were determined by paired t-test. In very rare occasions (2 out of 60 groups), the distribution was not normal, and instead, the Wilcoxon signed-rank test was used; however, in these two cases, the differences were not significant.

2.3. *In Vitro Experiments: Electric Field Effect on Diastolic Calcium Level in Primary Cardiomyocytes*

A detailed methodology was provided before [33]. Briefly, adult rat cardiomyocytes were enzymatically isolated from the left ventricle and loaded with 4 μM Fura-2 AM (Invitrogen) to monitor intracellular calcium. Myocytes were placed between parallel electrodes with 4 mm gap distance and exposed to monophasic 100 μs pulses of increasing voltage: 80 V, 140 V, and lethal high voltage pulses. For the latter, the voltage applied was different for cells oriented parallel and perpendicular relative to the electric field as a consequence of their different sensitivity to pulsed electric fields. The diastolic calcium level, corresponding to the 340/380 ratio at rest, was measured prior to and at the maximum level following the application of the electroporating pulse. Statistical analysis for this

experiment was performed with a two-way repeated-measure ANOVA, followed by a Bonferroni multiple comparison test using SigmaPlot 14.0.

3. Results and Discussion

3.1. The Time-Dependent Numerical Model with Included Electroporation

A time-dependent nonlinear numerical model was developed to investigate the phenomenon of electroporation when exposing a cardiomyocyte to a single monophasic electric pulse of different pulse durations, i.e., 10 ms, 1 ms, 100 µs, 10 µs, 1 µs, and 100 ns. Numerical simulations were performed for a prolate spheroid, which was previously used as a simplified model of cardiomyocyte geometry [24,30,42,43], and for a real-shaped cardiomyocyte geometry [30]. Figure 2A first shows the spatial distribution of the induced transmembrane voltage (TMV) at the end of exposure to a non-electroporating 10 ms, 1 V/cm pulse, when the cell is oriented with its long axis either parallel or perpendicular to the applied electric field. The induced TMV is, by absolute value, always the highest at the membrane regions facing the electrodes, both for prolate spheroid and real-shaped geometry, and both for parallel and perpendicular orientation of the cell. When applying a non-electroporating pulse, the induced TMV reaches higher values when the cell is oriented parallel with respect to the electric field, compared with perpendicular orientation. Figure 2B again shows the spatial distribution of the induced TMV, but now at the end of an electroporating 10 ms, 500 V/cm pulse. When the absolute value of the TMV becomes sufficiently high (several 100 mV), pores start forming in the membrane, and consequently, membrane conductivity increases and the induced transmembrane voltage settles to a value of approximately 1 V [37,44]. In this case, the maximum induced TMV is ~1 V both in the parallel and perpendicular orientation of the cell. However, the maximum pore density (number of pores formed per unit membrane area) is different in parallel and perpendicular orientations, as shown in Figure 2C. These results show that the induced transmembrane voltage and the number of pores formed in the membrane depend on the cell orientation and the strength of the applied electric field.

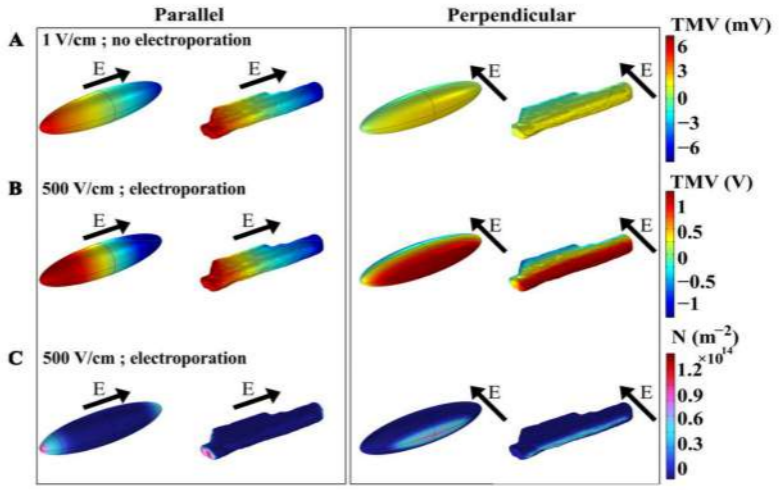

Figure 2. The spatial distribution of transmembrane voltage (TMV) induced by a 10 ms pulse of (**A**) 1 V/cm (without electroporation) or (**B**) 500 V/cm (with electroporation). (**C**) The spatial distribution of the pore density (m^{-2}) induced by the end of a 10 ms, 500 V/cm pulse (with electroporation). In each panel, the results are shown for prolate spheroid and real-shaped geometry when the electric field is applied either parallel or perpendicular to the long axis of the cell. The direction of the applied electric field is indicated by the arrows. Note different scales of TMV for panels (**A**,**B**).

The total number of pores formed in the cell membrane was evaluated as a function of the applied electric field strength from 10 V/cm to 10^5 V/cm when exposing the cell

to a single monophasic pulse of different durations (10 ms, 1 ms, 100 µs, 10 µs, 1 µs, and 100 ns). Simulations were again performed for both prolate spheroid and real-shaped geometry and in both parallel and perpendicular orientations. The results are presented on the left side of Figure 3. Overall, the relationship between the pore number and the electric field strength for a real-shaped geometry is very similar to that of a prolate spheroid. This was additionally confirmed by comparing the local pore density in prolate spheroid and real-shaped geometry in a specified membrane region around the poles of the cell (Supplementary Figures S2 and S3). In general, the number of pores in the cell membrane always increases with increasing the applied electric field. However, the relationship between the number of pores and the applied electric field strongly depends on both the cell orientation and pulse duration. This can be observed in the graphs on the right side of Figure 3, which show the ratio of the number of pores formed in the cell membrane when the cell is oriented either parallel or perpendicular (parallel/perpendicular). For pulses with a pulse duration of ≥10 µs, cells oriented parallel to the electric field become electroporated at lower electric field strengths. In contrast, for a 1 µs pulse, the electric fields at which electroporation onsets are comparable for both perpendicular and parallel orientation. For a 100 ns pulse, cells oriented perpendicular (not parallel!) to the electric field become electroporated at lower electric field strength. Thus, there is a "crossover" at a pulse duration at the order of ~1 µs, Figure 3K, at which the orientation with the lower onset of electroporation shifts from parallel to perpendicular as observed in experiments and reported before [31].

In addition, the model suggests that the orientation, at which cells form more pores due to electroporation, depends not only on the pulse duration but also on the electric field strength. Interestingly, for pulses with a duration of ≥10 µs, parallel orientation is the one in which pores start forming preferentially (at lower electric field strengths); however, as the electric field is increased beyond a certain value, cells in perpendicular (not parallel!) orientation achieves a greater pore number and thus become more electroporated. This can be observed both for the real-shaped geometry and the prolate spheroid, suggesting that such behavior would be observed for any cell of elongated shape. Thus, the model suggests there is another "crossover" at which the orientation of cells that are more electroporated shifts from parallel to perpendicular. This crossover appears as the electric field is increased and can be observed only for pulses with a duration of ≥10 µs, Figure 3A–D. For a 1 µs pulse, the onset of electroporation occurs at similar electric field strengths for both orientations; however, the perpendicular orientation becomes more electroporated at higher electric field strengths. For a 100 ns pulse, perpendicular orientation is always more electroporated compared to parallel orientation, regardless of the applied electric field strength.

3.2. The Effect of T-Tubules

Cardiomyocytes have a complex membrane shape with many t-tubules, which results in a higher effective membrane capacitance [17,40]. T-tubules density and organization are variable depending on the type of myocyte considered. While ventricular myocytes have a dense and well-organized t-tubular network, t-tubules density is much lower in atrial cardiac myocytes or Purkinje fibers [45]. In our model, the effect of t-tubules on the formation of the pores in the membrane was considered by increasing the membrane capacitance from 1 µF/cm^2 to 5 µF/cm^2 and 10 µF/cm^2. The number of pores in the cell membrane was again evaluated as a function of the applied electric field from 10 V/cm to 10^5 V/cm at different pulse durations (10 ms, 1 ms, 100 µs, 10 µs, 1 µs, and 100 ns), Figure 4.

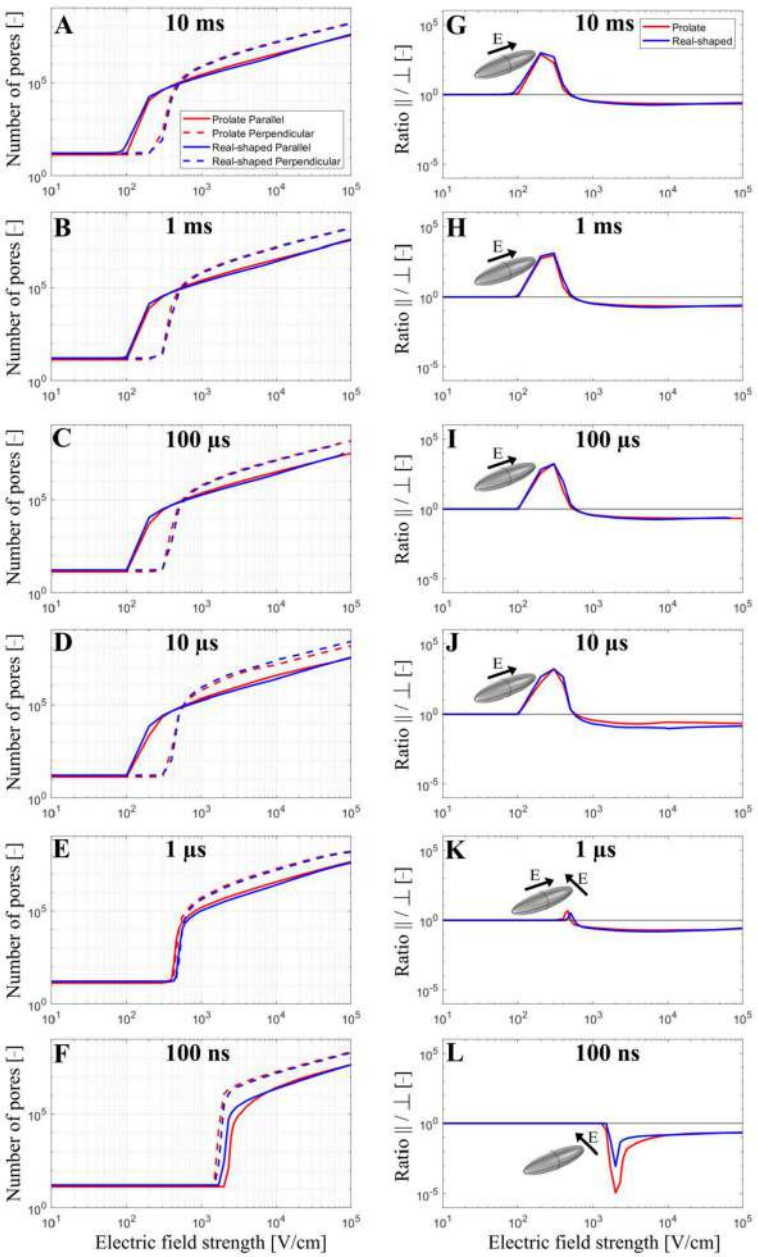

Figure 3. The number of pores (**A**–**F**) and the ratio of the number of pores parallel/perpendicular (**G**–**L**) as a function of the electric field when a single monophasic pulse of 10 ms, 1 ms, 100 µs, 10 µs, 1 µs, and 100 ns long is applied. In (**A**–**F**), the red and blue curves present the number of pores obtained using prolate spheroid or real-shaped geometry, respectively, when the electric field is applied parallel (solid curves) or perpendicular (dotted curves) to the long axis of the cell. In (**G**–**L**), red or blue curves represent the ratio of the number of pores parallel/perpendicular formed in the cell membrane using prolate spheroid and real-shaped geometry, respectively. The black solid line in (**G**–**L**) indicates when the ratio of the number of pores parallel/perpendicular is 1. In (**G**–**L**), the representation of the cell with the orientation of the applied electric field highlights which cell orientation is more sensitive to pore formation when the electric field is applied. The symbol [-] in the Y axis indicates that the unit of the number of pores (**A**–**F**) and the ratio parallel/perpendicular (**G**–**L**) is adimensional.

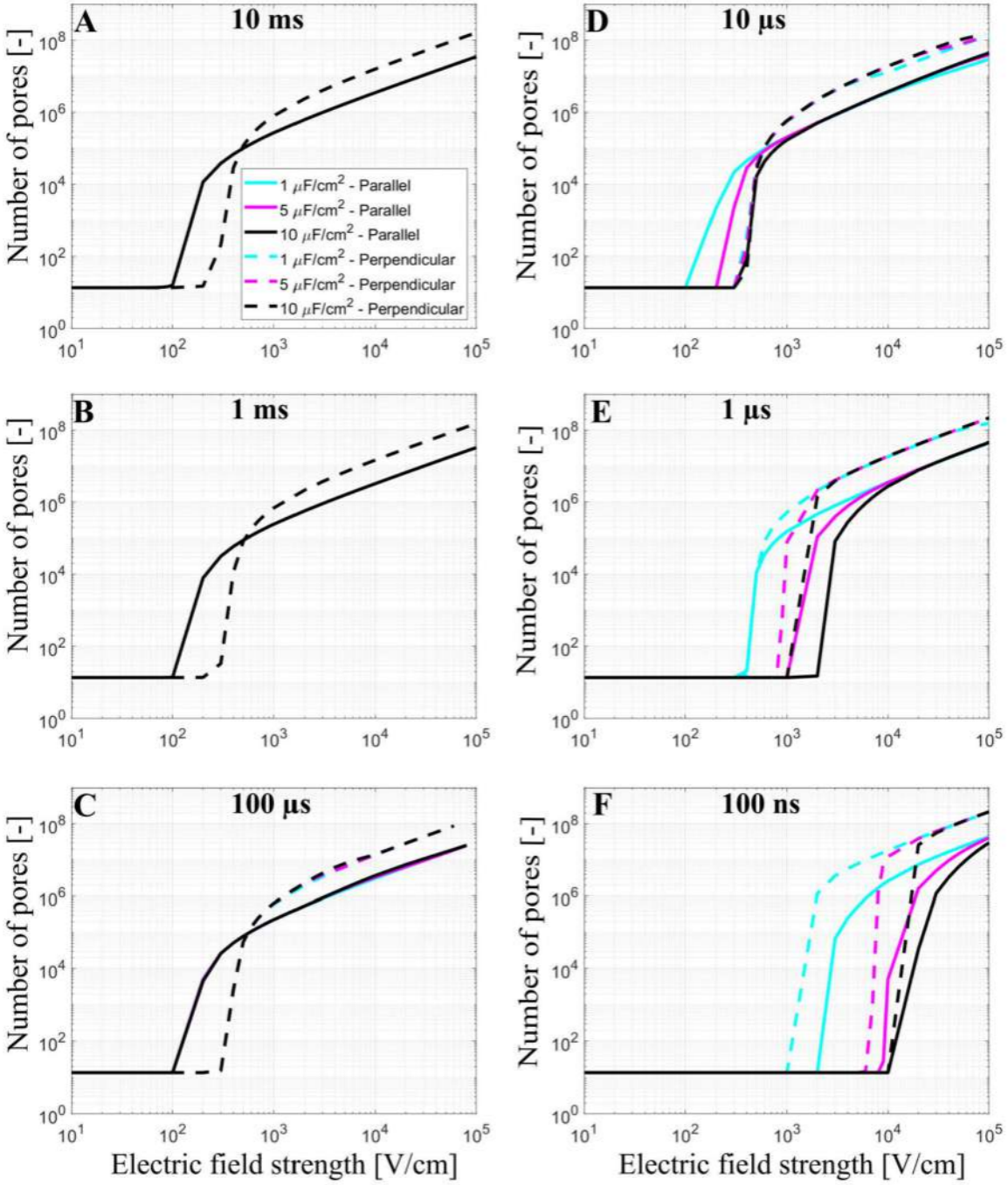

Figure 4. The number of pores as a function of the electric field using prolate spheroid geometry when a single monophasic pulse of (**A**) 10 ms, (**B**) 1 ms, (**C**) 100 µs, (**D**) 10 µs, (**E**) 1 µs, and (**F**) 100 ns long is applied. The electric field is applied parallel (solid line) or perpendicular (dashed line) to the long axis of the cell. The cyan, magenta, and black curves represent the number of pores obtained using a membrane capacitance of 1 µF/cm^2, 5 µF/cm^2, and 10 µF/m^2, respectively. The symbol [-] in the Y axis of (**A**–**F**) indicates that the unit of the number of pores is adimensional. Please note that in (**A**–**C**) the cyan, magenta, and black lines are overlapping.

The cyan, magenta, and black curves in Figure 4 represent the number of pores obtained using prolate spheroid geometry with 1 $\mu F/cm^2$, 5 $\mu F/cm^2$, and 10 $\mu F/cm^2$ as membrane capacitance, respectively, when the electric field is applied parallel (solid line) or perpendicular (dashed line) to the long axis of the cell. When the membrane has a greater capacitance (representative of t-tubules), a higher electric field is needed to observe the onset of electroporation when using pulses of 100 ns, 1 µs, (for both orientations), and 10 µs (only for the parallel orientation), which is directly related to the longer membrane charging time. When 100 µs, 1 ms, and 10 ms pulses are used, the different values of capacitance do not affect the number of pores in the cell membrane, as their pulse durations are all considerably longer than the membrane charging time, even for the highest value of the capacitance. The charging time of the cardiomyocyte using the prolate spheroid geometry is ~2 µs (parallel orientation) and ~0.8 µs (perpendicular orientation). Another interesting observation is that the pulse duration, at which electroporation is not very sensitive to cell orientation (both parallel and perpendicular orientation were similarly affected), shifts from 1 µs to 10 µs, as the membrane capacitance increases from 1 $\mu F/cm^2$ to 10 $\mu F/cm^2$. This means that the above-mentioned "crossover" with respect to pulse duration would be observed at roughly 10× longer pulse duration in cardiomyocytes compared to other cell types with similar aspect ratios but are devoid of t-tubules.

3.3. Experimental Results and Model Predictions: Calcium Transients in Cardiomyocyte-Derived Cell Lines

The numerical results that have been presented so far have shown that the total number of pores predicted by the model depends on cell orientation, pulse duration, and electric field strength, whereby the results are very similar in both prolate spheroid and real-shaped cardiomyocyte geometries. In continuation, our modeling results are compared to experimental results from cardiomyocyte-derived cell lines and primary cardiomyocytes (later in Section 3.4). Dermol-Černe et al. [31] reported experimental measurements of calcium transients using Fura-2 dye in two cardiomyocyte-derived cell lines, H9c2 and AC16, induced by monophasic pulses of different duration (from 10 ms down to 100 ns) and electric field strengths. Calcium transients were observed as a consequence of the uptake of Ca^{2+} ions to cells from the extracellular medium due to electroporation [46]. Most of the cells of both cell lines were elongated, with their long axis at least twice the size of their short one. They quantified the difference in fluorescent calcium indicator Fura-2 signal in parallel and perpendicular cells (Figure 5A,B, published data). Their study also included numerical simulations, similar to ours, for prolate spheroid cells with different aspect ratios. Consistent with their model, they observed parallel cells being electroporated at lower electric field strengths compared to perpendicular cells for long pulses (1 ms and 10 ms). For pulses of intermediate duration (1 to 100 µs), the difference in Fura-2 signal in cells parallel and perpendicular to the electric field was close to zero, meaning that cells of both orientations, parallel and perpendicular, were electroporated to a similar extent. For the shortest 100 ns pulses, cells oriented perpendicularly were the ones preferentially electroporated at lower electric field strengths. This can be observed by looking at the left-most data points of each curve in Figure 5A,B.

Our model considering the prolate spheroid geometry was used to plot the ratio of the number of pores formed in the cell membrane when the cell is oriented either parallel or perpendicular (parallel/perpendicular) for pulse durations and the electric field strengths used in the experiments (Figure 5C). Assuming pores act as pathways for cellular calcium influx induced by electroporation, the total number of pores is expected to be roughly proportional to the maximum achievable intracellular calcium concentration. The modeling results represent well the trends observed in the aforementioned in vitro cell electroporation experiments. As was discussed extensively in the previous study [31], both experimental and modeling data show a crossover of more affected cells from parallel to perpendicular when reducing the pulse duration from milliseconds to nanoseconds. In other words, parallel cells are more sensitive for longer pulse durations (>1 µs), whereas perpendicular cells are more sensitive for shorter pulse durations (<1 µs). While the

model suggests this crossover occurs around a pulse duration of ~1 µs, experimentally this crossover was observed in the range of pulse durations between 1 µs and 100 µs, whereby the shift towards shorter pulse duration in the model could be related to an underestimated membrane capacitance (representative of t-tubule presence), as shown in Section 3.2. Furthermore, our modeling results also suggest that there is another crossover from parallel to perpendicular orientation, which occurs for a given pulse duration as the electric field is increased, provided that the pulse duration is more than ~1 µs long. While this crossover has not been explicitly discussed in the previous study [31], it is evident in the experimental data, especially for AC16 cells shown in Figure 5B (see the crossing of the brown and grey lines with the horizontal line as the electric field increases).

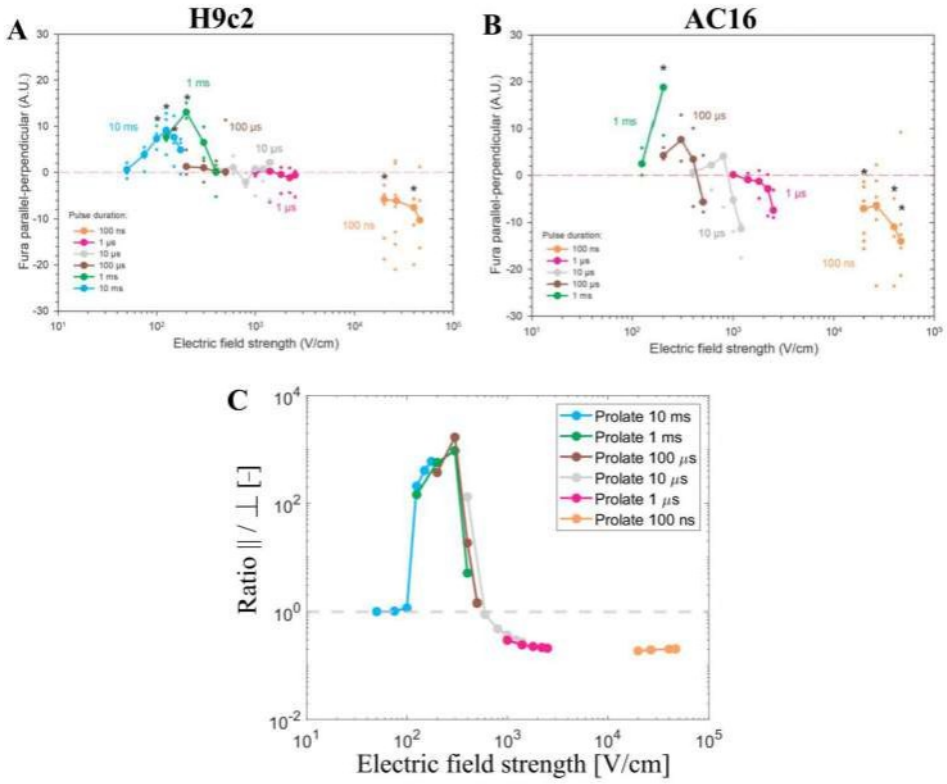

Figure 5. Experimental measurements of calcium transients using Fura-2 ratio 340/380 peak change using H9c2 and AC16 cell lines when different pulse durations were applied (from 10 ms down to 100 ns) published by Dermol-Černe et al. (**A**,**B**). *—statistically significant differences from control ($p < 0.05$), the Kruskal–Wallis One Way Analysis of Variance on Ranks, followed by Multiple Comparisons versus Control Group (the Dunn's Method), see Dermol-Černe et al. [31]. Figure 5 (A,B) are reprinted with permission from [31]. (**C**) represents the ratio of the number of pores parallel/perpendicular obtained with the model using pulse durations and the electric field strengths of the one used in the experiments (**A**,**B**). The symbol [-] in the Y axis of (**C**) indicates that the unit of the ratio parallel/perpendicular is adimensional.

In addition, to further support the modeling prediction of a crossover as the electric field strength is increased, we decided to show the Fura-2 ratio 340/380 peak change observed when the cells are oriented parallel or perpendicular to the applied electric field (unpublished data, see Section 2.2). Indeed, careful inspection of the results obtained with ≥1-us-long pulses shows that as the electric field increases, the Fura-2 signal becomes similar for both parallel and perpendicular cells, or even the perpendicular cells, start to exhibit a greater Fura-2 signal indicating greater calcium uptake. This was statistically significant in data for 10 µs and visible

in data for 100 μs pulse in AC16 cells (Figure 6I,J). For 1 ms pulse in AC16 cells, the electric field was not increased high enough to approach this crossover; however, the crossover is indicated in the results from H9c2 where higher electric fields were used (Figure 6B). It should be noted that the Fura-2 fluorescence signal is linearly proportional to the intracellular calcium until the Fura-2 binding sites for Ca^{2+} are saturated. Unavoidably the use of high electric field strengths will induce cellular Ca^{2+} influx approaching the saturation level of the Fura-2 dye, whereby such saturation can mask the above-discussed crossover with respect to electric field strength. Thus Fura-2 calcium measurements in Figure 6 cannot unequivocally confirm the modeling predictions; nevertheless, they are not contradicting them.

3.4. Experimental Results and Model Predictions: Lethal Electric Field Strengths in Primary Cardiomyocytes

Monitoring intracellular calcium levels with Fura-2 can be a very sensitive indicator of electroporation at low electric field strengths [41]. However, at high electric field strengths approaching irreversible electroporation, Fura-2 binding sites can become saturated and the difference between calcium uptake in parallel and perpendicular cells becomes difficult to assess. Thus, we further compared our modeling results to the results from the study of Chaigne et al. [33] who studied electroporation in isolated primary rat cardiomyocytes. The authors showed that the lethal electric field strength depends on cardiomyocyte orientation and pulse duration. When applying a single 10 ms pulse, the lethal electric field strength for 80% probability of lethality is 240 V/cm and 328 V/cm for parallel and perpendicular orientation, respectively, meaning that cardiomyocytes oriented parallel are more sensitive to the electric field (as expected). However, when applying a single 100 μs pulse, the effect of cardiomyocyte orientation on the lethal electric field strength unexpectedly changed, and cardiomyocytes became more sensitive in perpendicular orientation; the lethal electric field strength for cardiomyocytes oriented parallel or perpendicular was found to be 1072 V/cm and 595 V/cm, respectively. We used our model considering the real-shaped cardiomyocyte geometry to help interpret the experimental results described. Our calculations (Figure 4) suggest that 10 ms, and 100 μs, pulse is too long for its effects to be influenced by increased effective membrane capacitance due to t-tubules. Thus, we plotted the relationship between the total number of pores and the electric field strength for cardiomyocytes with default membrane capacitance (1 $\mu F/cm^2$) oriented parallel and perpendicular when exposed to a 10 ms or 100 μs pulse. Then, we indicated the lethal electric field strengths obtained in experiments, as shown in Figure 7A,B. For electric field strengths, which were lethal at a 10 ms pulse, there were considerably more pores formed in parallel orientation (Figure 7A), supporting the experimental observation that parallel cells are more sensitive than perpendicular. However, for higher electric field strengths, which are lethal at 100 μs pulse, there are more pores formed in perpendicular orientation compared to parallel orientation (and a greater fraction of the membrane area electroporated, Supplementary Figure S4), supporting the experimental observation that perpendicular cells are more prone to irreversible electroporation when exposed to 100 μs pulse. These experiments thus additionally support the modeling prediction that there is a crossover with respect to the electric field strength, at which perpendicular cells become more affected compared to parallel cells. To further confirm that there is indeed a crossover that occurs at high electric field strengths, Figure 7D presents experimental measurements of Ca^{2+} uptake using Fura-2 dye in rat primary cardiomyocytes exposed to 100 μs pulse but of lower (sublethal) electric field strengths. Otherwise, the electroporation protocol was the same as in Chaigne et al. [33]. The results in Figure 7D present the level of diastolic intracellular Ca^{2+} measured after exposure to an electric pulse. We consider that the level of diastolic Ca^{2+} can be best compared to our model, which predicts the number of pores in the membrane formed by the electric pulse. Indeed, the experiments show that the level of diastolic Ca^{2+} becomes more increased in parallel cells compared to perpendicular cells for these lower electric field strengths, consistent with the model (vertical dashed lines in Figure 7B indicate these lower electric field strengths and show that the model predicts a greater number of pores formed in parallel cells).

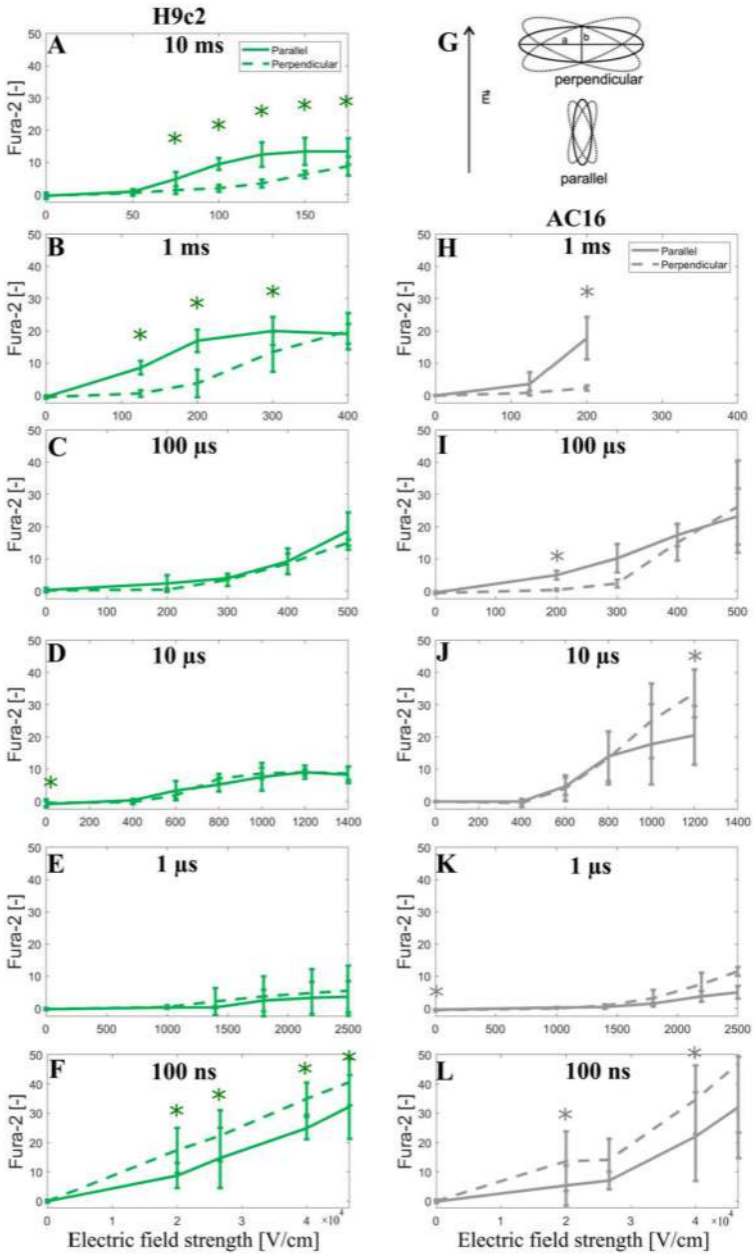

Figure 6. Fura-2 ratio 340/380 peak change as a function of the applied electric field using H9c2 cell line (**A**–**F**) and AC16 cell line (**H**–**L**) when a single pulse of either 10 ms, 1 ms, 100 µs, 10 µs, 1 µs, and 100 ns long is applied. (**G**) represents the elongated cells (a > 2b) with their longer axes (a) oriented parallel or perpendicular to the applied electric field E, with 20° tolerance in angle. The symbol [-] in the Y axis of (**A**–**F**,**H**–**L**) indicates that the unit of Fura-2 signal is adimensional. Experimental results of H9c2 cells (**A**–**F**) were obtained from 5–30 cells per experiment, an average of three independent experiments, except for 1 ms (N = 4), 10 ms (N = 5), 100 ns, 40 and 46.6 kV/cm (N = 5), 100 ns, 20 kV/cm (N = 6), and 100 ns, 26.6 kV/cm (N = 9). Experimental results of AC16 cells (**H**–**L**) were obtained from 4–23 cells per experiment, an average of three independent experiments, except for 100 ns, 40 kV/cm (N = 5), 100 ns, 46.6 kV/cm (N = 6), 100 ns, 20 kV/cm (N = 7) and 100 ns, 26.6 kV/cm (N = 7). N is the number of repetitions. Results are expressed as a mean ± standard deviation. *—statistically significant differences from control ($p < 0.5$), paired *t*-test.

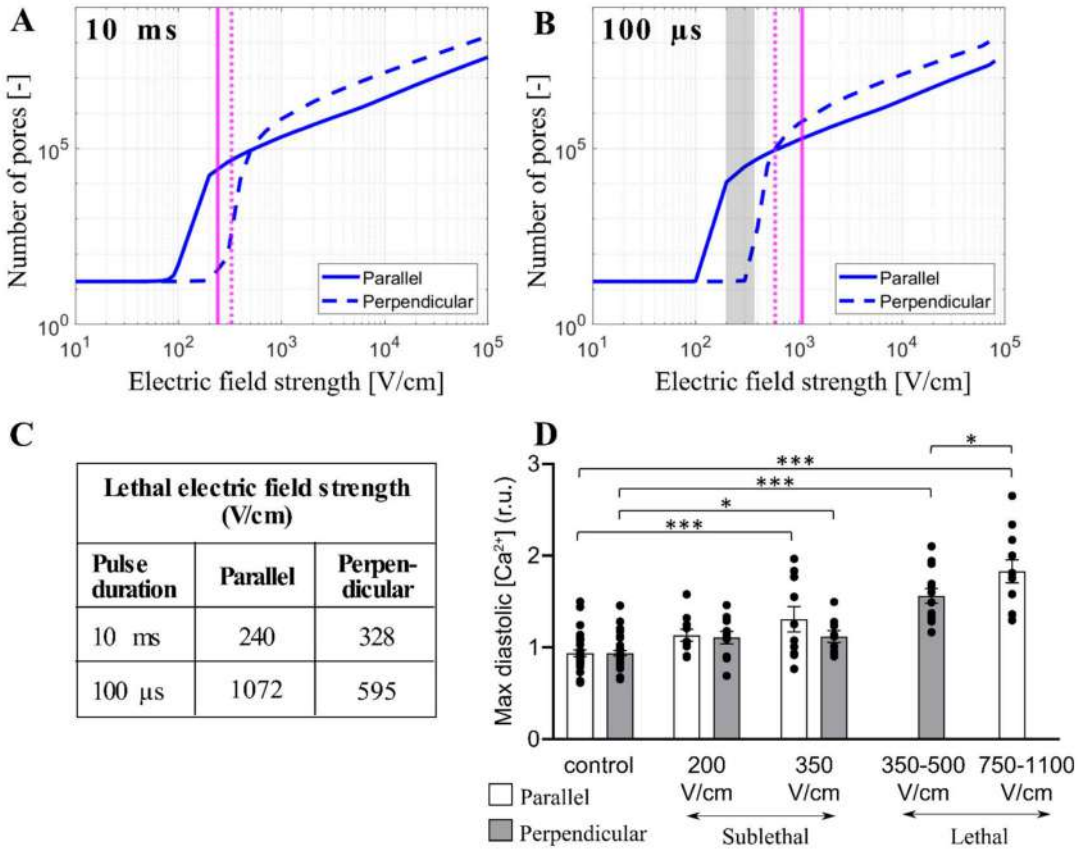

Lethal electric field strength (V/cm)		
Pulse duration	**Parallel**	**Perpendicular**
10 ms	240	328
100 µs	1072	595

Figure 7. Comparison between the model and experimental results in primary cardiomyocytes. (**A**,**B**) The predicted number of pores as a function of the electric field when a single pulse of 10 ms (**A**) or 100 µs (**B**) is delivered. The electric field is applied parallel (solid blue line) or perpendicular (dashed blue line) to the long axis of the cell. The vertical solid and dashed magenta lines indicate the value of the lethal electric field for the parallel and perpendicular orientation, respectively that are reported in [33]. The symbol [-] in the Y axis of (**A**,**B**) indicates that the unit of the number of pores is adimensional. (**C**) Tabulated lethal electric field strengths were determined experimentally in [33] for parallel and perpendicular orientation when a single 10 ms or 100 µs pulse was applied. Lethal electric field strengths are estimated as the lethal voltage, reported in [33] divided by the electrode distance (4 mm). (**D**) Comparison of maximum diastolic $[Ca^{2+}]$ for parallel and perpendicular orientation after exposure to 100 µs pulse of increasing electric field strengths [33]. These sublethal electric fields (experimental results) are indicated with the grey region in (**B**). In (**D**), the results are expressed as a mean ± standard error of the mean with individual values for each cell. The asterisks represent: *: $p < 0.05$, ***: $p < 0.001$.

3.5. *Limitations of the Model*

Our modeling results suggest that the orientation at which cardiomyocytes (and other elongated cells) become preferentially affected by electroporation pulses depends both on pulse duration and the electric field strength. According to the model, there are two crossovers were preferentially affected orientation shifts from parallel to perpendicular. One crossover can be observed for relatively low electric fields (likely corresponding to reversible electroporation, i.e., sublethal) when reducing the pulse duration from milliseconds to nanoseconds. The other crossover can be observed for pulses with a duration of >1 µs when increasing the electric field strength. The first crossover has been confirmed previously by measurements of calcium uptake into cardiomyocyte-derived cell lines [31]. The second

crossover identified in this study is supported by measurements of the lethal electric field strengths and calcium uptake in primary rat cardiomyocytes ([33] and Figure 7C,D), and by the revisited measurements in cardiomyocyte-derived cell lines (Figure 6). Thus, the prediction of the two crossovers seems to be robustly confirmed by experimental data.

Nevertheless, the existing electroporation models, including the one used in this study, have several limitations [47]. Electroporation models consider that the increase in membrane permeability can mainly be attributed to pores formed in the lipid bilayer of the cell membrane. While this mechanism is probably dominant during the on-time of the pulse, other mechanisms are considered to contribute and may even dominate in the increased membrane permeability after the pulse, including membrane defects due to oxidative lipid damage [48–50] and electric-field mediated perturbation of membrane proteins such as voltage-gated ion channels [51]. This post-pulse increase in permeability lasts up to several minutes (at room and physiological temperature) and mediates most of the transmembrane transport of small ions, such as calcium, and small molecules, such as ATP [52–54]. Furthermore, the resealing process of the cell membrane that takes place after the pulse is not merely a passive pore closure as assumed in the models, but involves membrane repair mechanisms, such as exocytosis and endocytosis [55,56].

Our electroporation model in principle considers only lipid pores that form in the cell membrane during the pulse. Nevertheless, it is reasonable to assume that other effects, including the post-pulse increased membrane permeability, intracellular calcium uptake, and effects leading to cell death, are at least roughly correlated with the number of pores that we simulate with our model. Indeed, the model predictions are found to be qualitatively in agreement with experimental measurements of calcium uptake and lethal electric field strength when assessing the orientation in which the cell is preferentially affected for a given pulse duration and electric field strength. However, the total number of pores returned by the model has limited utility for predicting lethal electric field strength (irrespective of orientation) for different pulse durations. Specifically, the model predicts a considerably greater number of pores at electric field strengths that are lethal when applying a 100 µs pulse (>10^5 pores) compared to a 10 ms pulse (>2×10^3 pores), cf. Figure 7A,B. Thus, the pore number predicted by the model cannot be used as a proxy for cell death when comparing pulses of different duration. Indeed there are additional effects associated with electroporation that could contribute to cell death, apart from pore formation and increased membrane permeability, including electrodeformation of the cell shape [57] and disassembly of the cytoskeletal network [58], both of which are expected to be more profound with longer pulses. Overall, the mechanisms of cell death following electroporation at present remain elusive and require further research [59].

In our model, we investigated the effects of an external electric field on a single cardiomyocyte when a single monophasic pulse of different pulse durations and electric field strengths was applied. Our modeling is largely motivated by in vitro experimental data published by Dermol-Černe et al. [31] and Chaigne et al. [33] and is aimed at gaining a better understanding thereof. However, clinical applications of PFA use a wide range of pulse waveforms, including monophasic and biphasic pulses with durations ranging from nanoseconds to milliseconds, and more importantly, most of these waveforms are composed of large numbers of pulses—trains of pulses [2,28,29]. Therefore, it is important to admit that existing electroporation models (including the one used in our study) have strong limitations when it comes to representing the experimentally observed cumulative effect of the number of pulses, as shown in ours and others' previous numerical studies [47,60]. Thus, further development of electroporation models is required to model more complex pulse waveforms that are being used in or are being developed for clinical applications.

While our model considered a single cardiomyocyte, our modeling findings regarding the influence of cell orientation for given pulse duration and electric field strength are nevertheless informative for interpreting the results at the tissue level. Even though in tissue, the electric field distribution is always inhomogeneous due to many factors, among them electrode/catheter geometry, tissue conductivity heterogeneity, and anisotropy, it

should be noted that an individual cell within the tissue will be locally exposed to roughly homogeneous field of a specific magnitude over the length scale of one cell (similarly as modeled in our study).

Finally, in our model, we consider the effects of t-tubules only by changing the values of membrane capacitance since the explicit representation of t-tubules is computationally much more demanding due to their small and elongated size, which requires a potentially large number of discretization elements (finite elements in our case) and more importantly difficult validation of the results. However, in the future, it would be interesting to model the realistic structure of t-tubules in the cardiomyocyte studying how they affect electroporation.

3.6. Clinical Relevance

Understanding the effect of orientation with regard to sensitivity to electrical fields in anisotropic tissues, such as the cardiac tissue, is important, and this particular study further informs translational research aimed at developing novel and improved PFA device therapies. One issue that has become apparent in the PFA literature is the relatively high variability in lesion size using PFA devices, a finding that merits further investigation [61–64]. Tissue anisotropy and the specific orientation of the cardiac myocytes to the electric fields on ablation electrodes are possible hypotheses for this observation.

While the present investigation has focused on modeling ventricular cells, the primary anatomical targets for PFA are currently the pulmonary veins (PVs) to isolate PVs from the rest of the atrium. Rapid electrical activity in PVs has been suggested as a key mechanism for focal atrial fibrillation [65]. The myocardial anatomy, histology, and architecture of PVs, while similar to atrial myocardium [66], is different from ventricular cells. PV myocytes are oriented circumferentially in the veins and the PV sleeves containing the myocytes extend into the veins for 4–20 mm [66]. Atrial myocytes are generally thinner than ventricular myocytes with reported widths of 6 to 15 μm [67,68], while the length is within the range of ventricular myocytes (120 μm) [68]. Thus, the reported calculations in the present paper are relevant for not only ventricular but also atrial cells, including the atrial cells of the PVs.

Interestingly, the orientation of the atrial myocytes in the PVs will likely be perpendicular to applied fields due to their circumferential orientation in the PV sleeves, assuming circular or balloon-shaped PFA ablation electrodes. Based on the present data, it could then be argued that a pulse duration of 100 ns might be advantageous as cells oriented perpendicular (not parallel) to the electric field become electroporated at lower electric field strengths. Thus, a relatively lower electric field strength would be needed to achieve electroporation in perpendicularly oriented PV cardiomyocytes when a 100 ns pulse was used, which could, at least in theory, further improve the safety profile of the therapy.

Conversely, in tissues where the orientation of tissue relative to the ablation electrodes is difficult to control, a 1–10 μs pulse may be advantageous as the electric fields at which electroporation onsets are comparable for both perpendicular and parallel orientation (per Figures 3 and 4), so in a sense is "orientation agnostic", i.e., independent of orientation. For example, ventricular tissue is known to be multi-layered, and heavily trabeculated, and the orientation of the ablation electrodes (with various shapes and resulting electrical fields) relative to those tissues are less controlled and conceivably less predictable than in a simpler PV anatomy. The example does not consider the effects of t-tubules (which results in increases in membrane capacitance and a shift of those cross-over values).

It needs to be understood that the aforementioned is a little bit of an oversimplification as at higher field strengths perpendicular cardiomyocytes become more electroporated. In this respect, it should also be stressed that the electric field around the catheter will always be high and decrease with distance from the catheter, so the simultaneous presence of high and low electric fields is unavoidable. Therefore, the complex interplay between pulse durations, electric field strengths, and cell orientation should in general always be taken into account. These examples in principle demonstrate how findings from numerical models describing electroporation at the single-cell level can inform translational PFA research efforts.

4. Conclusions

To study the effect of electroporation on a single cardiomyocyte we developed a time-dependent nonlinear numerical model of electroporation building upon Milan et al. model [30]. In particular, we investigated how the induced transmembrane voltage and the number of pores in the cell membrane are affected when applying a monophasic pulse of different pulse durations and electric field strength, considering different cell shapes, the presence of t-tubules by increasing the membrane capacitance, and the cell orientation with respect to the applied electric field. To gain a better understanding of seemingly conflicting in vitro experimental data published by Dermol Černe et al. [31] and Chaigne et al. [33], we compared the experimental results with the modeling findings.

The modeling results show that prolate spheroid geometry is a reasonable approximation of a real-shaped cardiomyocyte geometry when modeling electroporation. In addition, prolate spheroid geometry (simple geometry) is computationally less demanding than using real-shaped geometry (complex geometry). The main difference between both geometries is at intermediate electric field strengths, where the onset of electroporation slightly differs for a prolate spheroid and real-shaped cardiomyocyte. The presence of t-tubules effectively increases the membrane capacitance and thus affects electroporation when 100 ns, 1 μs, and 10 μs pulses are used. Thus, t-tubules should be taken into account when modeling electroporation of cardiomyocytes exposed to pulses with a duration less or equal to ~10 μs. This becomes relevant for cardiac cell types which have many t-tubules, such as ventricular cardiomyocytes being targeted in ventricular ablations, which may thus require longer pulses.

The orientation at which the cells are preferentially affected by electroporation depends on both pulse duration and electric field strength. For sub-microsecond pulses, cells are more affected in the perpendicular orientation at all electric field strengths. For pulses with duration on the order of 1 μs, the onset of electroporation is observed at comparable electric field strengths regardless of the orientation; however, as the electric field is increased considerably beyond the onset, perpendicularly oriented cells become more affected. For pulses on the order 10 μs and longer, the onset of electroporation is observed at lower electric field strengths for parallel orientation; however, perpendicularly oriented cells become more affected as the electric field is increased. The presence of t-tubules shifts these crossovers to the right towards longer pulse durations. Thus, our modeling findings show that for low electric fields with 100 μs pulse duration, the parallel orientation is more affected than the perpendicular one according to Dermol-Černe et al. [31]. However, interestingly, for higher electric fields, there is a shift and the perpendicular orientation is more sensitive than the parallel one according to Chaigne et al. [33] with 100 μs pulse duration. Thus, in vitro experimental results from the two studies can be explained by our model.

Our results are important for developing electroporation for cardiac treatments, including irreversible electroporation for cardiac ablation, i.e., Pulsed Field Ablation [28], and reversible electroporation for cardiac gene therapy [69]. The presented model can aid in interpreting experimental results on the influence of cell orientation on electroporation propensity.

Supplementary Materials: The following supporting information can be downloaded at: https://www.mdpi.com/article/10.3390/biom13050727/s1, Figure S1: The in vitro experimental setup for calcium transients in cardiomyocyte-derived cell lines; Figure S2: Areas in which the average induced transmembrane voltage and the average pore density are evaluated; Figure S3: The pore density and the relative error of the logarithmic values of the pore density as a function of the electric field when a single pulse of 10 ms, 1 ms, 100 μs, 10 μs, 1 μs, and 100 ns is applied; Figure S4: The predicted number of pores and the area with pore density $>10^{13}$ as a function of the electric field when a single pulse of 10 ms or 100 μs long is applied.

Author Contributions: Conceptualization, D.M.; methodology, M.S., L.R., J.D.-Č., T.B.N., S.C., O.B. and D.B.; formal analysis, M.S., T.B.N. and D.B.; investigation, M.S., T.B.N., S.C. and D.B.; writing—original draft preparation, D.M., M.S., L.R. and J.D.-Č.; writing—review and editing, D.C.S., T.B.N., S.C., O.B. and D.B.; visualization, M.S., L.R., J.D.-Č. and D.M.; supervision, D.M.; funding acquisition, D.M. All authors have read and agreed to the published version of the manuscript.

Funding: The study was supported by the Slovenian Research Agency (ARRS) within research program no. P2-0249 and research project no. J2-2503, the French Agence Nationale de la Recherche (ANR-10-IAHU04-LIRYC), and by Medtronic, Inc.

Institutional Review Board Statement: All experiments on primary rat cardiomyocytes were performed in the scope of a previous published study [33] in accordance with the European Union council directive 2010/63/EU for the protection of animals used for scientific purposes following local ethical committee approval.

Informed Consent Statement: Not applicable.

Data Availability Statement: The data presented in this study are available on request from the corresponding author.

Conflicts of Interest: D.C.S. is an employee of Medtronic. D.M. is a Medtronic consultant. M.S., T.B.N., L.R. and D.M. received a Medtronic grant. S.C., O.B. and D.B. received funding from Medtronic through a service agreement. Other authors declare no conflict of interest.

References

1. McBride, S.; Avazzadeh, S.; Wheatley, A.M.; O'Brien, B.; Coffey, K.; Elahi, A.; O'Halloran, M.; Quinlan, L.R. Ablation Modalities for Therapeutic Intervention in Arrhythmia-Related Cardiovascular Disease: Focus on Electroporation. *J. Clin. Med.* **2021**, *10*, 2657. [CrossRef] [PubMed]
2. Bradley, C.J.; Haines, D.E. Pulsed Field Ablation for Pulmonary Vein Isolation in the Treatment of Atrial Fibrillation. *J. Cardiovasc. Electrophysiol.* **2020**, *31*, 2136–2147. [CrossRef] [PubMed]
3. Verma, A.; Haines, D.E.; Boersma, L.V.; Sood, N.; Natale, A.; Marchlinski, F.E.; Calkins, H.; Sanders, P.; Packer, D.L.; Kuck, K.-H. Pulsed Field Ablation for the Treatment of Atrial Fibrillation: PULSED AF Pivotal Trial. *Circulation* **2023**. [CrossRef] [PubMed]
4. Nikolski, V.P.; Efimov, I.R. Electroporation of the Heart. *EP Eur.* **2005**, *7*, S146–S154. [CrossRef]
5. Ayuni, E.L.; Gazdhar, A.; Giraud, M.N.; Kadner, A.; Gugger, M.; Cecchini, M.; Caus, T.; Carrel, T.P.; Schmid, R.A.; Tevaearai, H.T. In Vivo Electroporation Mediated Gene Delivery to the Beating Heart. *PLoS ONE* **2010**, *5*, e14467. [CrossRef]
6. Bulysheva, A.A.; Hargrave, B.; Burcus, N.; Lundberg, C.G.; Murray, L.; Heller, R. Vascular Endothelial Growth Factor-A Gene Electrotransfer Promotes Angiogenesis in a Porcine Model of Cardiac Ischemia. *Gene Ther.* **2016**, *23*, 649–656. [CrossRef]
7. Vižintin, A.; Miklavčič, D. The Electropermeome: Cellular Response to Electroporation. *Slov. Med. J.* **2022**, *91*, 483–495.
8. Tsong, T.Y. Electroporation of Cell Membranes. In *Electroporation and Electrofusion in Cell Biology*; Springer: Berlin/Heidelberg, Germany, 1989; pp. 149–163.
9. Kotnik, T.; Pucihar, G.; Miklavčič, D. Induced Transmembrane Voltage and Its Correlation with Electroporation-Mediated Molecular Transport. *J. Membr. Biol.* **2010**, *236*, 3–13. [CrossRef]
10. Kinosita, K.; Tsong, T.T. Hemolysis of Human Erythrocytes by Transient Electric Field. *Proc. Natl. Acad. Sci. USA* **1977**, *74*, 1923–1927. [CrossRef]
11. Kotnik, T.; Rems, L.; Tarek, M.; Miklavčič, D. Membrane Electroporation and Electropermeabilization: Mechanisms and Models. *Annu. Rev. Biophys.* **2019**, *48*, 63–91. [CrossRef]
12. Kotnik, T.; Miklavčič, D. Analytical Description of Transmembrane Voltage Induced by Electric Fields on Spheroidal Cells. *Biophys. J.* **2000**, *79*, 670–679. [CrossRef]
13. Pucihar, G.; Kotnik, T.; Valič, B.; Miklavčič, D. Numerical Determination of Transmembrane Voltage Induced on Irregularly Shaped Cells. *Ann. Biomed. Eng.* **2006**, *34*, 642. [CrossRef] [PubMed]
14. Litviňuková, M.; Talavera-López, C.; Maatz, H.; Reichart, D.; Worth, C.L.; Lindberg, E.L.; Kanda, M.; Polanski, K.; Heinig, M.; Lee, M. Cells of the Adult Human Heart. *Nature* **2020**, *588*, 466–472. [CrossRef] [PubMed]
15. Hong, T.; Shaw, R.M. Cardiac T-Tubule Microanatomy and Function. *Physiol. Rev.* **2017**, *97*, 227–252. [CrossRef] [PubMed]
16. Sengupta, P.P.; Krishnamoorthy, V.K.; Korinek, J.; Narula, J.; Vannan, M.A.; Lester, S.J.; Tajik, J.A.; Seward, J.B.; Khandheria, B.K.; Belohlavek, M. Left Ventricular Form and Function Revisited: Applied Translational Science to Cardiovascular Ultrasound Imaging. *J. Am. Soc. Echocardiogr.* **2007**, *20*, 539–551. [CrossRef]
17. Clayton, R.H.; Bernus, O.; Cherry, E.M.; Dierckx, H.; Fenton, F.H.; Mirabella, L.; Panfilov, A.V.; Sachse, F.B.; Seemann, G.; Zhang, H. Models of Cardiac Tissue Electrophysiology: Progress, Challenges and Open Questions. *Prog. Biophys. Mol. Biol.* **2011**, *104*, 22–48. [CrossRef] [PubMed]
18. Trifunović-Zamaklar, D.; Jovanović, I.; Vratonjić, J.; Petrović, O.; Paunović, I.; Tešić, M.; Boričić-Kostić, M.; Ivanović, B. The Basic Heart Anatomy and Physiology from the Cardiologist's Perspective: Toward a Better Understanding of Left Ventricular Mechanics, Systolic, and Diastolic Function. *J. Clin. Ultrasound* **2022**, *50*, 1026–1040. [CrossRef] [PubMed]
19. Deng, D.; Jiao, P.; Ye, X.; Xia, L. An Image-Based Model of the Whole Human Heart with Detailed Anatomical Structure and Fiber Orientation. *Comput. Math. Methods Med.* **2012**, *2012*, 891070. [CrossRef]
20. Pashakhanloo, F.; Herzka, D.A.; Ashikaga, H.; Mori, S.; Gai, N.; Bluemke, D.A.; Trayanova, N.A.; McVeigh, E.R. Myofiber Architecture of the Human Atria as Revealed by Submillimeter Diffusion Tensor Imaging. *Circ. Arrhythm. Electrophysiol.* **2016**, *9*, e004133. [CrossRef]

21. Roney, C.H.; Bendikas, R.; Pashakhanloo, F.; Corrado, C.; Vigmond, E.J.; McVeigh, E.R.; Trayanova, N.A.; Niederer, S.A. Constructing a Human Atrial Fibre Atlas. *Ann. Biomed. Eng.* **2021**, *49*, 233–250. [CrossRef]
22. Ye, X.; Liu, S.; Yin, H.; He, Q.; Xue, Z.; Lu, C.; Su, S. Study on Optimal Parameter and Target for Pulsed-Field Ablation of Atrial Fibrillation. *Front. Cardiovasc. Med.* **2021**, *8*, 690092. [CrossRef] [PubMed]
23. Prado, L.N.; Goulart, J.T.; Zoccoler, M.; Oliveira, P.X. Ventricular Myocyte Injury by High-Intensity Electric Field: Effect of Pulse Duration. *Gen. Physiol. Biophys.* **2016**, *35*, 121–130. [CrossRef]
24. de Oliveira, P.X.; Bassani, R.A.; Bassani, J.W.M. Lethal Effect of Electric Fields on Isolated Ventricular Myocytes. *IEEE Trans. Biomed. Eng.* **2008**, *55*, 2635–2642. [CrossRef] [PubMed]
25. Wittkampf, F.H.; Van Driel, V.J.; Van Wessel, H.; Vink, A.; Hof, I.E.; Gründeman, P.F.; Hauer, R.N.; Loh, P. Feasibility of Electroporation for the Creation of Pulmonary Vein Ostial Lesions. *J. Cardiovasc. Electrophysiol.* **2011**, *22*, 302–309. [CrossRef] [PubMed]
26. Neuber, J.U.; Varghese, F.; Pakhomov, A.G.; Zemlin, C.W. Using Nanosecond Shocks for Cardiac Defibrillation. *Bioelectricity* **2019**, *1*, 240–246. [CrossRef]
27. Semenov, I.; Grigoryev, S.; Neuber, J.U.; Zemlin, C.W.; Pakhomova, O.N.; Casciola, M.; Pakhomov, A.G. Excitation and Injury of Adult Ventricular Cardiomyocytes by Nano-to Millisecond Electric Shocks. *Sci. Rep.* **2018**, *8*, 8233. [CrossRef]
28. Hartl, S.; Reinsch, N.; Füting, A.; Neven, K. Pearls and Pitfalls of Pulsed Field Ablation. *Korean Circ. J.* **2022**, *53*, e26. [CrossRef]
29. Maan, A.; Koruth, J. Pulsed Field Ablation: A New Paradigm for Catheter Ablation of Arrhythmias. *Curr. Cardiol. Rep.* **2022**, *24*, 103–108. [CrossRef]
30. Milan, H.F.; Bassani, R.A.; Santos, L.E.; Almeida, A.C.; Bassani, J.W. Accuracy of Electromagnetic Models to Estimate Cardiomyocyte Membrane Polarization. *Med. Biol. Eng. Comput.* **2019**, *57*, 2617–2627. [CrossRef]
31. Dermol-Černe, J.; Batista Napotnik, T.; Reberšek, M.; Miklavčič, D. Short Microsecond Pulses Achieve Homogeneous Electroporation of Elongated Biological Cells Irrespective of Their Orientation in Electric Field. *Sci. Rep.* **2020**, *10*, 9149. [CrossRef]
32. Henslee, B.E.; Morss, A.; Hu, X.; Lafyatis, G.P.; Lee, L.J. Electroporation Dependence on Cell Size: Optical Tweezers Study. *Anal. Chem.* **2011**, *83*, 3998–4003. [CrossRef] [PubMed]
33. Chaigne, S.; Sigg, D.C.; Stewart, M.T.; Hocini, M.; Batista Napotnik, T.; Miklavčič, D.; Bernus, O.; Benoist, D. Reversible and Irreversible Effects of Electroporation on Contractility and Calcium Homeostasis in Isolated Cardiac Ventricular Myocytes. *Circ. Arrhythm. Electrophysiol.* **2022**, *15*, e011131. [CrossRef] [PubMed]
34. Mercadal, B.; Vernier, P.; Ivorra, A. Dependence of Electroporation Detection Threshold on Cell Radius: An Explanation to Observations Non Compatible with Schwan's Equation Model. *J. Membr. Biol.* **2016**, *249*, 663–676. [CrossRef] [PubMed]
35. Smith, K.C.; Weaver, J.C. Active Mechanisms Are Needed to Describe Cell Responses to Submicrosecond, Megavolt-per-Meter Pulses: Cell Models for Ultrashort Pulses. *Biophys. J.* **2008**, *95*, 1547–1563. [CrossRef] [PubMed]
36. Rems, L.; Ušaj, M.; Kandušer, M.; Reberšek, M.; Miklavčič, D.; Pucihar, G. Cell Electrofusion Using Nanosecond Electric Pulses. *Sci. Rep.* **2013**, *3*, 3382. [CrossRef] [PubMed]
37. DeBruin, K.A.; Krassowska, W. Modeling Electroporation in a Single Cell. I. Effects of Field Strength and Rest Potential. *Biophys. J.* **1999**, *77*, 1213–1224. [CrossRef] [PubMed]
38. Krassowska, W.; Filev, P.D. Modeling Electroporation in a Single Cell. *Biophys. J.* **2007**, *92*, 404–417. [CrossRef]
39. Kotnik, T.; Miklavčič, D.; Slivnik, T. Time Course of Transmembrane Voltage Induced by Time-Varying Electric Fields—A Method for Theoretical Analysis and Its Application. *Bioelectrochem. Bioenerg.* **1998**, *45*, 3–16. [CrossRef]
40. Fozzard, H.A. Membrane Capacity of the Cardiac Purkinje Fibre. *J. Physiol.* **1966**, *182*, 255. [CrossRef]
41. Napotnik, T.B.; Miklavčič, D. In Vitro Electroporation Detection Methods–An Overview. *Bioelectrochemistry* **2018**, *120*, 166–182. [CrossRef]
42. Fishler, M.G.; Sobie, E.A.; Tung, L.; Thakor, N.V. Cardiac Responses to Premature Monophasic and Biphasic Field Stimuli: Results from Cell and Tissue Modeling Studies. *J. Electrocardiol.* **1995**, *28*, 174–179. [CrossRef] [PubMed]
43. Gomes, P.A.P.; Bassani, R.A.; Bassani, J.W.M. Electric Field Stimulation of Cardiac Myocytes during Postnatal Development. *IEEE Trans. Biomed. Eng.* **2001**, *48*, 630–636. [CrossRef] [PubMed]
44. Hibino, M.; Itoh, H.; Kinosita, K., Jr. Time Courses of Cell Electroporation as Revealed by Submicrosecond Imaging of Transmembrane Potential. *Biophys. J.* **1993**, *64*, 1789–1800. [CrossRef] [PubMed]
45. Boyden, P.A.; Hirose, M.; Dun, W. Cardiac Purkinje Cells. *Heart Rhythm* **2010**, *7*, 127–135. [CrossRef] [PubMed]
46. Pucihar, G.; Krmelj, J.; Reberšek, M.; Napotnik, T.B.; Miklavčič, D. Equivalent Pulse Parameters for Electroporation. *IEEE Trans. Biomed. Eng.* **2011**, *58*, 3279–3288. [CrossRef]
47. Scuderi, M.; Dermol-Černe, J.; da Silva, C.A.; Muralidharan, A.; Boukany, P.E.; Rems, L. Models of Electroporation and the Associated Transmembrane Molecular Transport Should Be Revisited. *Bioelectrochemistry* **2022**, *147*, 108216. [CrossRef]
48. Rems, L.; Viano, M.; Kasimova, M.A.; Miklavčič, D.; Tarek, M. The Contribution of Lipid Peroxidation to Membrane Permeability in Electropermeabilization: A Molecular Dynamics Study. *Bioelectrochemistry* **2019**, *125*, 46–57. [CrossRef]
49. Wiczew, D.; Szulc, N.; Tarek, M. Molecular Dynamics Simulations of the Effects of Lipid Oxidation on the Permeability of Cell Membranes. *Bioelectrochemistry* **2021**, *141*, 107869. [CrossRef]
50. Breton, M.; Mir, L.M. Investigation of the Chemical Mechanisms Involved in the Electropulsation of Membranes at the Molecular Level. *Bioelectrochemistry* **2018**, *119*, 76–83. [CrossRef]

51. Rems, L.; Kasimova, M.A.; Testa, I.; Delemotte, L. Pulsed Electric Fields Can Create Pores in the Voltage Sensors of Voltage-Gated Ion Channels. *Biophys. J.* **2020**, *119*, 190–205. [CrossRef]
52. Rols, M.-P.; Teissie, J. Electropermeabilization of Mammalian Cells. Quantitative Analysis of the Phenomenon. *Biophys. J.* **1990**, *58*, 1089–1098. [CrossRef] [PubMed]
53. Sözer, E.B.; Pocetti, C.F.; Vernier, P.T. Asymmetric Patterns of Small Molecule Transport after Nanosecond and Microsecond Electropermeabilization. *J. Membr. Biol.* **2018**, *251*, 197–210. [CrossRef] [PubMed]
54. Polajzer, T.; Jarm, T.; Miklavcic, D. Analysis of Damage-Associated Molecular Pattern Molecules Due to Electroporation of Cells in Vitro. *Radiol. Oncol.* **2020**, *54*, 317–328. [CrossRef] [PubMed]
55. Ciobanu, F.; Golzio, M.; Kovacs, E.; Teissié, J. Control by Low Levels of Calcium of Mammalian Cell Membrane Electropermeabilization. *J. Membr. Biol.* **2018**, *251*, 221–228. [CrossRef] [PubMed]
56. Huynh, C.; Roth, D.; Ward, D.M.; Kaplan, J.; Andrews, N.W. Defective Lysosomal Exocytosis and Plasma Membrane Repair in Chediak–Higashi/Beige Cells. *Proc. Natl. Acad. Sci. USA* **2004**, *101*, 16795–16800. [CrossRef]
57. Shamoon, D.; Dermol-Černe, J.; Rems, L.; Reberšek, M.; Kotnik, T.; Lasquellec, S.; Brosseau, C.; Miklavčič, D. Assessing the Electro-Deformation and Electro-Poration of Biological Cells Using a Three-Dimensional Finite Element Model. *Appl. Phys. Lett.* **2019**, *114*, 063701. [CrossRef]
58. Graybill, P.M.; Davalos, R.V. Cytoskeletal Disruption after Electroporation and Its Significance to Pulsed Electric Field Therapies. *Cancers* **2020**, *12*, 1132. [CrossRef]
59. Napotnik, T.B.; Polajžer, T.; Miklavčič, D. Cell Death Due to Electroporation–A Review. *Bioelectrochemistry* **2021**, *141*, 107871. [CrossRef]
60. Son, R.S.; Gowrishankar, T.R.; Smith, K.C.; Weaver, J.C. Modeling a Conventional Electroporation Pulse Train: Decreased Pore Number, Cumulative Calcium Transport and an Example of Electrosensitization. *IEEE Trans. Biomed. Eng.* **2015**, *63*, 571–580. [CrossRef]
61. Im, S.I.; Higuchi, S.; Lee, A.; Stillson, C.; Buck, E.; Morrow, B.; Schenider, K.; Speltz, M.; Gerstenfeld, E.P. Pulsed Field Ablation of Left Ventricular Myocardium in a Swine Infarct Model. *Clin. Electrophysiol.* **2022**, *8*, 722–731. [CrossRef]
62. Koruth, J.S.; Kuroki, K.; Iwasawa, J.; Viswanathan, R.; Brose, R.; Buck, E.D.; Donskoy, E.; Dukkipati, S.R.; Reddy, V.Y. Endocardial Ventricular Pulsed Field Ablation: A Proof-of-Concept Preclinical Evaluation. *EP Eur.* **2020**, *22*, 434–439. [CrossRef] [PubMed]
63. Nakagawa, H.; Castellvi, Q.; Neal, R.; Girouard, S.; Ikeda, A.; Kuroda, S.; Hussein, A.A.; Saliba, W.I.; Wazni, O.M. B-PO03-131 Effects of Contact Force on Lesion Size during Pulsed Field Ablation. *Heart Rhythm* **2021**, *18*, S242–S243. [CrossRef]
64. Yavin, H.D.; Higuchi, K.; Sroubek, J.; Younis, A.; Zilberman, I.; Anter, E. Pulsed-Field Ablation in Ventricular Myocardium Using a Focal Catheter: The Impact of Application Repetition on Lesion Dimensions. *Circ. Arrhythm. Electrophysiol.* **2021**, *14*, e010375. [CrossRef]
65. Haissaguerre, M.; Jaïs, P.; Shah, D.C.; Takahashi, A.; Hocini, M.; Quiniou, G.; Garrigue, S.; Le Mouroux, A.; Le Métayer, P.; Clémenty, J. Spontaneous Initiation of Atrial Fibrillation by Ectopic Beats Originating in the Pulmonary Veins. *N. Engl. J. Med.* **1998**, *339*, 659–666. [CrossRef]
66. Verheule, S.; Wilson, E.E.; Arora, R.; Engle, S.K.; Scott, L.R.; Olgin, J.E. Tissue Structure and Connexin Expression of Canine Pulmonary Veins. *Cardiovasc. Res.* **2002**, *55*, 727–738. [CrossRef]
67. Mary-Rabine, L.; Albert, A.; Pham, T.D.; Hordof, A.; Fenoglio, J.J., Jr.; Malm, J.R.; Rosen, M.R. The Relationship of Human Atrial Cellular Electrophysiology to Clinical Function and Ultrastructure. *Circ. Res.* **1983**, *52*, 188–199. [CrossRef]
68. Nygren, A.; Fiset, C.; Firek, L.; Clark, J.W.; Lindblad, D.S.; Clark, R.B.; Giles, W.R. Mathematical Model of an Adult Human Atrial Cell: The Role of K+ Currents in Repolarization. *Circ. Res.* **1998**, *82*, 63–81. [CrossRef] [PubMed]
69. Hargrave, B.; Downey, H.; Strange, R.; Murray, L.; Cinnamond, C.; Lundberg, C.; Israel, A.; Chen, Y.-J.; Marshall, W.; Heller, R. Electroporation-Mediated Gene Transfer Directly to the Swine Heart. *Gene Ther.* **2013**, *20*, 151–157. [CrossRef]

3. Conclusions and future work

The presented thesis shows that different types of pulses are equivalent for potentiating cisplatin cytotoxicity and can thus potentially be used in ECT with equal effectiveness of the treatment. In addition, the thesis demonstrates that none of the existing theoretical models of electroporation can reliably predict molecular transmembrane transport for the entire range of pulse parameters and experimental conditions used in *in vitro* cell electroporation; nevertheless, the models can still help interpret certain experimental outcomes. The results of the studies are already thoroughly discussed in the papers, thus in this chapter, I will give the final concluding remarks and discuss future work.

In Paper 1 and Paper 2, we compared the effect of different types of electric pulses including classical ECT pulses, bursts of high-frequency short bipolar pulses, and millisecond pulses on cisplatin uptake and cisplatin cytotoxicity using *in vitro* ECT experiments. We observed that all tested types of pulses potentiate cisplatin uptake and cisplatin cytotoxicity in an equivalent manner, provided that the electric field is properly adjusted for each pulse type. Specifically, we achieved similar levels of cisplatin uptake and cisplatin cytotoxicity with all tested types of pulses. Thus, we conclude that ECT could be performed with various types of pulses alternative to classical ECT pulses. Replacement of classical ECT pulses with bursts of high-frequency short bipolar pulses would be beneficial to reduce muscle contractions and pain, potentially avoiding the need for anesthetics and muscle relaxants. Replacement with millisecond pulses could be beneficial when combining ECT with GET for immunotherapy. In studies that combine ECT with GET, first, the classical ECT pulses are applied to enhance the uptake of the chemotherapeutic drug, followed by millisecond pulses which promote the transport of protein-encoding DNA. The millisecond pulses are commonly used in GET to electrophoretically drive the DNA molecules toward the cell membrane and allow the uptake. However, it would be beneficial to use the same type of pulse when ECT is combined with GET, as this would allow the use of less complex pulse generators. Nevertheless, our studies only demonstrated that different types of pulses are equivalent to enhancing the uptake of chemotherapeutic drugs and its cytotoxicity in individual cells. The future goal is to evaluate the efficacy of different types of pulses *in vivo* by comparing their effect on the immune response and vasoconstriction, which are mechanisms that contribute to ECT but cannot be evaluated *in vitro*.

The number of bleomycin molecules needed to kill the cells has been already determined by Tounekti et al. [114] and is in the range of a few thousand molecules per cell. In Paper 2 we experimentally quantified the number of cisplatin molecules needed to achieve a cytotoxic effect, which is in the range of $2{-}7{\times}10^7$ when classical ECT pulses, bursts of high-frequency short bipolar pulses, and millisecond pulses are used. Such range is in agreement with a previous study published by Vižintin et al. [105], which used the same experimental protocols as in our study, but compared classical ECT pulses and nanosecond pulses. However, it is important to consider that *in vitro* conditions are to some extent different than *in vivo*. In our *in vitro* experiments the extracellular concentration of 50 μM of cisplatin was sufficient to guarantee the uptake of sufficient number of cisplatin molecules to cause cell death but *in vivo,* the needed extracellular concentration of cisplatin might be different. In *in vitro* experiments with cells in suspension, the solute homogeneously surrounds the cells and freely passes through the electroporated membrane. The extracellular space is large compared to the volume fraction of the cells, therefore, the transport of the solute stops only when the cell membrane reseals. In tissue, the cells are densely packed and the extracellular reservoir containing the drug is comparatively small and can limit the amount of drug that can enter into electroporated cells due to its depletion. Furthermore, *in vivo,* the transport of drugs can be hindered by the increased interstitial pressure in the tumor, heterogeneous distribution, lymphatic circulation, binding of the drug to non-target molecules, and metabolism [115]–[117].

ECT of deep-seated tumors typically requires treatment planning. Currently, this treatment planning considers a fixed electric field threshold to deem the tumor permeabilized or not, without considering the uptake of chemotherapeutic drugs. The permeabilization of the cells within the tissue does not guarantee the uptake of a sufficient amount of the chemotherapeutic drug and thus the success of the ECT treatment. Therefore, the future goal to improve the treatment planning is to include a model that describes the transport and the uptake of chemotherapeutics drugs in the tumor tissue/cells. In Paper 3, we took the first step towards this goal by critically assessing the existing mechanistic models that describe the phenomenon of electroporation and transmembrane molecular transport at the single-cell level. We observed that i) qualitative validation is not sufficient to establish the validity of a model, ii) quantitative validation in a fixed time point does not necessarily indicate the

correct description of the kinetics of the uptake, and iii) experiments need to be carefully designed to be specific enough for model validation. None of the existing mechanistic models is good enough to describe the phenomenon of electroporation and molecular transport for the entire range of pulse parameters and types of delivered molecules used in electroporation research and applications. Further work is needed to improve these models, for example, by including mechanisms, that have been identified to participate in increased membrane permeability due to electroporation in addition to pores formed in the lipid bilayer, such as oxidative lipid damage and protein denaturation. However, this requires further research to better understand how and why lipid oxidation and protein denaturation take place and what is the kinetics of these processes. Nevertheless, the existing mechanistic models can still help interpret specific experimental results, such as the influence of cardiomyocyte orientation on electroporation using pulses of different durations, as we demonstrated in Paper 4. Furthermore, we tested a phenomenological model which was fitted with cisplatin uptake data obtained in Paper 2. The model quantitatively predicted cisplatin uptake when different types of pulses parameters were applied.

4. Original scientific contributions

Testing the equivalence of different types of pulse parameters for electrochemotherapy with cisplatin

We performed *in vitro* ECT experiments to compare the effect of classical ECT pulses, bursts of high-frequency short bipolar pulses, and millisecond pulses on the uptake of cisplatin, and cisplatin cytotoxicity. The use of bursts of high-frequency short bipolar pulses has been suggested as a valuable option to mitigate pain and muscle contraction during electroporation-based treatments. We, thus, performed the first study comparing the effect of bursts of high-frequency short bipolar pulses with conventional ECT pulses in *in vitro* ECT experiments (Paper 1). Preclinical and clinical studies have also shown that the use of ECT in combination with gene electrotransfer (i.e., use of millisecond pulses with protein-encoding DNA) stimulates the immune response, for this reason, we also tested millisecond pulses. We found that a similar cisplatin uptake and cytotoxic effect is achieved when using the three tested types of pulses if the electric field is properly adjusted (Paper 2). **Thus, different types of pulses can be used in ECT.**

Determination of the number of cisplatin molecules needed to achieve a cytotoxic effect

Treatment planning is helping scientists and clinicians identify the optimal parameters to treat specific tumors by using numerical models. However, having a sufficiently high electric field to permeabilize tumor cells does not guarantee the success of ECT treatment. It is also important to have a sufficient amount of chemotherapeutic drugs in the cell. We have experimentally quantified the number of cisplatin molecules needed in the cell to achieve a cytotoxic effect (Paper 2). We performed an *in vitro* ECT experiment to determine cisplatin uptake and cisplatin cytotoxicity when different extracellular cisplatin concentrations were used in combination with different types of pulse parameters. Combining the results of cisplatin uptake and cisplatin cytotoxicity **we determined the number of cisplatin molecules needed in an individual cell to achieve a cytotoxic effect which is in the range of 2-7×10^7 cisplatin molecules per cell**. Our results further show, that, different types of pulses can be used in an equivalent way: classical ECT pulses, high-

frequency bipolar pulses, millisecond pulses, and nanosecond pulses all allow the uptake of 2-7×10^7 cisplatin molecules per cell when the electric field is adequately adjusted.

Evaluation of the existing electroporation models for predicting molecular transport and/or other associated phenomena at the individual cell level

We compared existing mathematical models that describe the phenomenon of electroporation and the transmembrane transport of molecules in individual biological cells. First, we made a literature survey of all the existing models. We then critically assessed three selected mechanistic models, which formed the basis for all other published models, by comparing their predictions to various quantitative measurements of molecular transport following electroporation. Two of the tested models describe electroporation in terms of the formation of lipid pores described with pore distribution function and consider the transport of molecules through pores due to both electrophoretic and diffusional transport. The third tested model describes cell membrane permeability using a chemical kinetic scheme and considers the transport of molecules through pores due to diffusion and endocytosis. Even though these models were validated against specific experimental data set **we found that none of the tested mechanistic models is sufficiently good to describe the phenomenon of electroporation and molecular transport** over the entire range of pulse parameters and experimental conditions used in electroporation research (Paper 3). Nevertheless, existing mechanistic models can still be useful for interpreting certain experimental outcomes, such as the influence of cardiomyocyte orientation on electroporation using pulses of different duration (Paper 4).

5. References

[1] T. Kotnik, L. Rems, M. Tarek, and D. Miklavčič, "Membrane electroporation and electropermeabilization: mechanisms and models," *Annual review of biophysics*, vol. 48, pp. 63–91, 2019.

[2] T. Y. Tsong, "Electroporation of cell membranes," *Biophysical journal*, vol. 60, no. 2, pp. 297–306, 1991.

[3] M. L. Yarmush, A. Golberg, G. Serša, T. Kotnik, and D. Miklavčič, "Electroporation-based technologies for medicine: principles, applications, and challenges," *Annual review of biomedical engineering*, vol. 16, pp. 295–320, 2014.

[4] B. Geboers *et al.*, "High-voltage electrical pulses in oncology: irreversible electroporation, electrochemotherapy, gene electrotransfer, electrofusion, and electroimmunotherapy," *Radiology*, vol. 295, no. 2, pp. 254–272, 2020.

[5] S. McBride *et al.*, "Ablation modalities for therapeutic intervention in arrhythmia-related cardiovascular disease: focus on electroporation," *Journal of clinical medicine*, vol. 10, no. 12, p. 2657, 2021.

[6] C. J. Bradley and D. E. Haines, "Pulsed field ablation for pulmonary vein isolation in the treatment of atrial fibrillation," *Journal of cardiovascular electrophysiology*, vol. 31, no. 8, pp. 2136–2147, 2020.

[7] A. Verma *et al.*, "Pulsed Field Ablation for the Treatment of Atrial Fibrillation: PULSED AF Pivotal Trial," *Circulation*, 2023.

[8] T. Kotnik, W. Frey, M. Sack, S. H. Meglič, M. Peterka, and D. Miklavčič, "Electroporation-based applications in biotechnology," *Trends in biotechnology*, vol. 33, no. 8, pp. 480–488, 2015.

[9] S. Mahnič-Kalamiza, E. Vorobiev, and D. Miklavčič, "Electroporation in food processing and biorefinery," *The Journal of membrane biology*, vol. 247, no. 12, pp. 1279–1304, 2014.

[10] A. J. P. Clover *et al.*, "Electrochemotherapy in the treatment of cutaneous malignancy: Outcomes and subgroup analysis from the cumulative results from the pan-European International Network for Sharing Practice in Electrochemotherapy database for 2482 lesions in 987 patients (2008–2019)," *European Journal of Cancer*, vol. 138, pp. 30–40, 2020.

[11] B. Mali, T. Jarm, M. Snoj, G. Sersa, and D. Miklavcic, "Antitumor effectiveness of electrochemotherapy: a systematic review and meta-analysis," *european Journal of surgical Oncology (eJsO)*, vol. 39, no. 1, pp. 4–16, 2013.

[12] M. Marty *et al.*, "Electrochemotherapy–An easy, highly effective and safe treatment of cutaneous and subcutaneous metastases: Results of ESOPE (European Standard Operating Procedures of Electrochemotherapy) study," *European Journal of Cancer Supplements*, vol. 4, no. 11, pp. 3–13, 2006.

[13] L. M. Mir *et al.*, "Standard operating procedures of the electrochemotherapy: Instructions for the use of bleomycin or cisplatin administered either systemically or locally and electric pulses delivered by the CliniporatorTM by means of invasive or non-invasive electrodes," *European Journal of Cancer Supplements*, vol. 4, no. 11, pp. 14–25, 2006.

[14] J. Gehl *et al.*, "Updated standard operating procedures for electrochemotherapy of cutaneous tumours and skin metastases," *Acta oncologica*, vol. 57, no. 7, pp. 874–882, 2018.

[15] "Overview | Electrochemotherapy for metastases in the skin from tumours of non-skin origin and melanoma | Guidance | NICE." Accessed: Aug. 02, 2023. [Online]. Available: https://www.nice.org.uk/guidance/ipg446

[16] "Overview | Electrochemotherapy for primary basal cell carcinoma and primary squamous cell carcinoma | Guidance | NICE." Accessed: Aug. 02, 2023. [Online]. Available: https://www.nice.org.uk/guidance/ipg478

[17] A. J. Stratigos *et al.*, "European interdisciplinary guideline on invasive squamous cell carcinoma of the skin: Part 1. epidemiology, diagnostics and prevention," *European journal of cancer*, vol. 128, pp. 60–82, 2020.

[18] A. J. Stratigos *et al.*, "European interdisciplinary guideline on invasive squamous cell carcinoma of the skin: Part 2. Treatment," *European Journal of Cancer*, vol. 128, pp. 83–102, 2020.

[19] K. Peris *et al.*, "Diagnosis and treatment of basal cell carcinoma: European consensus–based interdisciplinary guidelines," *European Journal of cancer*, vol. 118, pp. 10–34, 2019.

[20] C. Garbe *et al.*, "European consensus-based interdisciplinary guideline for melanoma. Part 1: Diagnostics: Update 2022," *European Journal of Cancer*, vol. 170, pp. 236–255, 2022.

[21] C. Garbe *et al.*, "European consensus-based interdisciplinary guideline for melanoma. Part 2: Treatment-Update 2022," *European Journal of Cancer*, vol. 170, pp. 256–284, 2022.

[22] C. Lebbe *et al.*, "Diagnosis and treatment of Kaposi's sarcoma: European consensus-based interdisciplinary guideline (EDF/EADO/EORTC)," *European Journal of Cancer*, vol. 114, pp. 117–127, 2019.

[23] D. Miklavčič, B. Mali, B. Kos, R. Heller, and G. Serša, "Electrochemotherapy: from the drawing board into medical practice," *Biomedical engineering online*, vol. 13, pp. 1–20, 2014.

[24] I. Edhemovic *et al.*, "Intraoperative electrochemotherapy of colorectal liver metastases," *Journal of surgical oncology*, vol. 110, no. 3, pp. 320–327, 2014.

[25] D. Miklavčič *et al.*, "Electrochemotherapy: technological advancements for efficient electroporation-based treatment of internal tumors," *Med Biol Eng Comput*, vol. 50, no. 12, pp. 1213–1225, Dec. 2012, doi: 10.1007/s11517-012-0991-8.

[26] V. Granata *et al.*, "Electrochemotherapy in locally advanced pancreatic cancer: Preliminary results," *International Journal of Surgery*, vol. 18, pp. 230–236, 2015.

[27] L. Tarantino *et al.*, "Electrochemotherapy of cholangiocellular carcinoma at hepatic hilum: a feasibility study," *European Journal of Surgical Oncology*, vol. 44, no. 10, pp. 1603–1609, 2018.

[28] C. H. Martin and R. C. Martin, "Optimal Dosing and Patient Selection for Electrochemotherapy in Solid Abdominal Organ and Bone Tumors," *Bioengineering*, vol. 10, no. 8, p. 975, 2023.

[29] G. Sersa, D. Miklavcic, M. Cemazar, Z. Rudolf, G. Pucihar, and M. Snoj, "Electrochemotherapy in treatment of tumours," *European Journal of Surgical Oncology (EJSO)*, vol. 34, no. 2, pp. 232–240, 2008.

[30] G. Serša, M. Čemažar, and D. Miklavčič, "Antitumor effectiveness of electrochemotherapy with cis-diamminedichloroplatinum (II) in mice," *Cancer research*, vol. 55, no. 15, pp. 3450–3455, 1995.

[31] S. Orlowski, J. Belehradek Jr, C. Paoletti, and L. M. Mir, “Transient electropermeabilization of cells in culture: increase of the cytotoxicity of anticancer drugs,” *Biochemical pharmacology*, vol. 37, no. 24, pp. 4727–4733, 1988.
[32] L. M. Mir, “Bases and rationale of the electrochemotherapy,” *Ejc Supplements*, 2006, doi: 10.1016/j.ejcsup.2006.08.005.
[33] A. Deodhar *et al.*, “Irreversible electroporation near the heart: ventricular arrhythmias can be prevented with ECG synchronization,” *American journal of roentgenology*, vol. 196, no. 3, pp. W330–W335, 2011.
[34] B. Mali *et al.*, “The effect of electroporation pulses on functioning of the heart,” *Medical & biological engineering & computing*, vol. 46, no. 8, p. 745, 2008.
[35] A. Županič, S. Ribarič, and D. Miklavčič, “Increasing the repetition frequency of electric pulse delivery reduces unpleasant sensations that occur in electrochemotherapy,” *Neoplasma*, vol. 54, no. 3, pp. 246–250, 2007.
[36] D. Miklavčič *et al.*, “The effect of high frequency electric pulses on muscle contractions and antitumor efficiency in vivo for a potential use in clinical electrochemotherapy,” *Bioelectrochemistry*, vol. 65, no. 2, pp. 121–128, 2005.
[37] R. Fusco, E. Di Bernardo, V. D’Alessio, S. Salati, and M. Cadossi, “Reduction of muscle contraction and pain in electroporation-based treatments: An overview,” *World Journal of Clinical Oncology*, vol. 12, no. 5, p. 367, 2021.
[38] A. Golberg and B. Rubinsky, “Towards Electroporation Based Treatment Planning considering Electric Field Induced Muscle Contractions,” *Technol Cancer Res Treat*, vol. 11, no. 2, pp. 189–201, Apr. 2012, doi: 10.7785/tcrt.2012.500249.
[39] A. Cvetkoska, A. Maček-Lebar, P. Trdina, D. Miklavčič, and M. Reberšek, “Muscle contractions and pain sensation accompanying high-frequency electroporation pulses,” *Scientific reports*, vol. 12, no. 1, pp. 1–15, 2022.
[40] M. B. Sano *et al.*, “Reduction of muscle contractions during irreversible electroporation therapy using high-frequency bursts of alternating polarity pulses: a laboratory investigation in an ex vivo swine model,” *Journal of Vascular and Interventional Radiology*, vol. 29, no. 6, pp. 893–898, 2018.
[41] E. L. Latouche *et al.*, “High-frequency irreversible electroporation for intracranial meningioma: A feasibility study in a spontaneous canine tumor model,” *Technology in cancer research & treatment*, vol. 17, p. 1533033818785285, 2018.
[42] C. B. Arena *et al.*, “High-frequency irreversible electroporation (H-FIRE) for non-thermal ablation without muscle contraction,” *Biomedical engineering online*, vol. 10, no. 1, pp. 1–21, 2011.
[43] S. Dong, H. Wang, Y. Zhao, Y. Sun, and C. Yao, “First human trial of high-frequency irreversible electroporation therapy for prostate cancer,” *Technology in cancer research & treatment*, vol. 17, p. 1533033818789692, 2018.
[44] M. Scuderi, M. Rebersek, D. Miklavcic, and J. Dermol-Cerne, “The use of high-frequency short bipolar pulses in cisplatin electrochemotherapy in vitro,” *Radiology and oncology*, vol. 53, no. 2, pp. 194–205, 2019.
[45] E. Pirc, D. Miklavčič, K. Uršič, G. Serša, and M. Reberšek, “High-frequency and high-voltage asymmetric bipolar pulse generator for electroporation based technologies and therapies,” *Electronics*, vol. 10, no. 10, p. 1203, 2021.
[46] P. Lyons, D. Polini, K. Russell-Ryan, and A. J. P. Clover, “High-Frequency Electroporation and Chemotherapy for the Treatment of Cutaneous Malignancies: Evaluation of Early Clinical Response,” *Cancers*, vol. 15, no. 12, p. 3212, 2023.

[47] G. Sersa *et al.*, "Vascular disrupting action of electroporation and electrochemotherapy with bleomycin in murine sarcoma," *British journal of cancer*, vol. 98, no. 2, pp. 388–398, 2008.
[48] B. Markelc, G. Sersa, and M. Cemazar, "Differential mechanisms associated with vascular disrupting action of electrochemotherapy: intravital microscopy on the level of single normal and tumor blood vessels," *PloS one*, vol. 8, no. 3, p. e59557, 2013.
[49] T. Jarm, M. Cemazar, D. Miklavcic, and G. Sersa, "Antivascular effects of electrochemotherapy: implications in treatment of bleeding metastases," *Expert review of anticancer therapy*, vol. 10, no. 5, pp. 729–746, 2010.
[50] A. I. Daud *et al.*, "Phase I trial of interleukin-12 plasmid electroporation in patients with metastatic melanoma," *Journal of clinical oncology*, vol. 26, no. 36, p. 5896, 2008.
[51] M. Cemazar *et al.*, "Efficacy and safety of electrochemotherapy combined with peritumoral IL-12 gene electrotransfer of canine mast cell tumours," *Veterinary and comparative oncology*, vol. 15, no. 2, pp. 641–654, 2017.
[52] A. Vižintin and D. Miklavčič, "The electropermeome: cellular response to electroporation," *Slov. Med. J.*, vol. 91, pp. 483–495, 2022.
[53] D. Purves and S. M. Williams, Eds., *Neuroscience*, 3. ed. Sunderland, Mass: Sinauer Associates, 2004.
[54] J. Teissie, M. Golzio, and M. P. Rols, "Mechanisms of cell membrane electropermeabilization: a minireview of our present (lack of?) knowledge," *Biochimica et Biophysica Acta (BBA)-General Subjects*, vol. 1724, no. 3, pp. 270–280, 2005.
[55] J. Teissié, N. Eynard, B. Gabriel, and M.-P. Rols, "Electropermeabilization of cell membranes," *Advanced drug delivery reviews*, vol. 35, no. 1, pp. 3–19, 1999.
[56] T. Y. Tsong, "Electroporation of cell membranes," in *Electroporation and Electrofusion in Cell Biology*, Springer, 1989, pp. 149–163.
[57] M. Tarek, "Membrane electroporation: a molecular dynamics simulation," *Biophysical journal*, vol. 88, no. 6, pp. 4045–4053, 2005.
[58] K. A. DeBruin and W. Krassowska, "Modeling electroporation in a single cell. I. Effects of field strength and rest potential," *Biophysical journal*, vol. 77, no. 3, pp. 1213–1224, 1999.
[59] K. C. Melikov, V. A. Frolov, A. Shcherbakov, A. V. Samsonov, Y. A. Chizmadzhev, and L. V. Chernomordik, "Voltage-induced nonconductive pre-pores and metastable single pores in unmodified planar lipid bilayer," *Biophysical journal*, vol. 80, no. 4, pp. 1829–1836, 2001.
[60] I. G. Abidor, V. B. Arakelyan, L. V. Chernomordik, Y. A. Chizmadzhev, V. F. Pastushenko, and M. P. Tarasevich, "Electric breakdown of bilayer lipid membranes: I. The main experimental facts and their qualitative discussion," *Journal of electroanalytical chemistry and interfacial electrochemistry*, vol. 104, pp. 37–52, 1979.
[61] J. C. Weaver and Y. A. Chizmadzhev, "Theory of electroporation: a review," *Bioelectrochemistry and bioenergetics*, vol. 41, no. 2, pp. 135–160, 1996.
[62] R. W. Glaser, S. L. Leikin, L. V. Chernomordik, V. F. Pastushenko, and A. I. Sokirko, "Reversible electrical breakdown of lipid bilayers: formation and evolution of pores," *Biochimica et Biophysica Acta (BBA)-Biomembranes*, vol. 940, no. 2, pp. 275–287, 1988.

[63] L. Rems, M. Viano, M. A. Kasimova, D. Miklavčič, and M. Tarek, “The contribution of lipid peroxidation to membrane permeability in electropermeabilization: A molecular dynamics study,” *Bioelectrochemistry*, vol. 125, pp. 46–57, 2019.

[64] B. Gabriel and J. Teissie, “Generation of reactive-oxygen species induced by electropermeabilization of Chinese hamster ovary cells and their consequence on cell viability,” *European Journal of Biochemistry*, vol. 223, no. 1, pp. 25–33, 1994.

[65] V. Nesin, A. M. Bowman, S. Xiao, and A. G. Pakhomov, “Cell permeabilization and inhibition of voltage-gated Ca2+ and Na+ channel currents by nanosecond pulsed electric field,” *Bioelectromagnetics*, vol. 33, no. 5, pp. 394–404, 2012.

[66] W. Chen, Z. Zhongsheng, and R. C. Lee, “Supramembrane potential-induced electroconformational changes in sodium channel proteins: A potential mechanism involved in electric injury,” *Burns*, vol. 32, no. 1, pp. 52–59, 2006.

[67] L. Rems, M. A. Kasimova, I. Testa, and L. Delemotte, “Pulsed electric fields can create pores in the voltage sensors of voltage-gated ion channels,” *Biophysical journal*, vol. 119, no. 1, pp. 190–205, 2020.

[68] T. Kotnik, F. Bobanović, and D. Miklavc̆ic̆, “Sensitivity of transmembrane voltage induced by applied electric fields—a theoretical analysis,” *Bioelectrochemistry and bioenergetics*, vol. 43, no. 2, pp. 285–291, 1997.

[69] T. Kotnik, D. Miklavčič, and T. Slivnik, “Time course of transmembrane voltage induced by time-varying electric fields—a method for theoretical analysis and its application,” *Bioelectrochemistry and bioenergetics*, vol. 45, no. 1, pp. 3–16, 1998.

[70] G. Pucihar, T. Kotnik, B. Valič, and D. Miklavčič, “Numerical determination of transmembrane voltage induced on irregularly shaped cells,” *Annals of biomedical engineering*, vol. 34, no. 4, p. 642, 2006.

[71] D. Gross, L. M. Loew, and W. W. Webb, “Optical imaging of cell membrane potential changes induced by applied electric fields,” *Biophysical journal*, vol. 50, no. 2, pp. 339–348, 1986.

[72] M. Hibino, M. Shigemori, H. Itoh, K. Nagayama, and K. Kinosita Jr, “Membrane conductance of an electroporated cell analyzed by submicrosecond imaging of transmembrane potential,” *Biophysical journal*, vol. 59, no. 1, pp. 209–220, 1991.

[73] M. Hibino, H. Itoh, and K. Kinosita, “Time courses of cell electroporation as revealed by submicrosecond imaging of transmembrane potential,” *Biophysical journal*, vol. 64, no. 6, pp. 1789–1800, 1993.

[74] B. Gabriel and J. Teissié, “Direct observation in the millisecond time range of fluorescent molecule asymmetrical interaction with the electropermeabilized cell membrane,” *Biophysical journal*, vol. 73, no. 5, pp. 2630–2637, 1997.

[75] B. Gabriel and J. Teissié, “Mammalian cell electropermeabilization as revealed by millisecond imaging of fluorescence changes of ethidium bromide in interaction with the membrane,” *Bioelectrochemistry and bioenergetics*, vol. 47, no. 1, pp. 113–118, 1998.

[76] W. Chen and R. C. Lee, “An improved double vaseline gap voltage clamp to study electroporated skeletal muscle fibers,” *Biophysical journal*, vol. 66, no. 3, pp. 700–709, 1994.

[77] L. H. Wegner, “Patch Clamp in Use of Electroporation Mechanisms Studies,” in *Handbook of Electroporation*, D. Miklavcic, Ed., Cham: Springer International Publishing, 2017, pp. 1–23. doi: 10.1007/978-3-319-26779-1_147-1.

[78] U. Pliquett, “Biophysics and Metrology of Electroporation in Tissues,” in *Handbook of Electroporation*, D. Miklavcic, Ed., Cham: Springer International Publishing, 2016, pp. 1–33. doi: 10.1007/978-3-319-26779-1_71-1.

[79] Q. Castellví, B. Mercadal, and A. Ivorra, “Assessment of Electroporation by Electrical Impedance Methods,” in *Handbook of Electroporation*, D. Miklavcic, Ed., Cham: Springer International Publishing, 2016, pp. 1–20. doi: 10.1007/978-3-319-26779-1_164-1.

[80] S. Romeo, Y.-H. Wu, Z. A. Levine, M. A. Gundersen, and P. T. Vernier, “Water influx and cell swelling after nanosecond electropermeabilization,” *Biochimica et Biophysica Acta (BBA)-Biomembranes*, vol. 1828, no. 8, pp. 1715–1722, 2013.

[81] M. Golzio, M.-P. Mora, C. Raynaud, C. Delteil, J. Teissié, and M.-P. Rols, “Control by osmotic pressure of voltage-induced permeabilization and gene transfer in mammalian cells,” *Biophysical journal*, vol. 74, no. 6, pp. 3015–3022, 1998.

[82] T. B. Napotnik and D. Miklavčič, “In vitro electroporation detection methods–An overview,” *Bioelectrochemistry*, vol. 120, pp. 166–182, 2018.

[83] C. Rosazza, S. Haberl Meglic, A. Zumbusch, M.-P. Rols, and D. Miklavcic, “Gene electrotransfer: a mechanistic perspective,” *Current gene therapy*, vol. 16, no. 2, pp. 98–129, 2016.

[84] D. S. Dimitrov and A. E. Sowers, “Membrane electroporaton—fast molecular exchange by electroosmosis,” *Biochimica et Biophysica Acta (BBA)-Biomembranes*, vol. 1022, no. 3, pp. 381–392, 1990.

[85] M. Puc, T. Kotnik, L. M. Mir, and D. Miklavčič, “Quantitative model of small molecules uptake after in vitro cell electropermeabilization,” *Bioelectrochemistry*, vol. 60, no. 1–2, pp. 1–10, 2003.

[86] E. B. Sözer, C. F. Pocetti, and P. T. Vernier, “Transport of charged small molecules after electropermeabilization—drift and diffusion,” *BMC biophysics*, vol. 11, no. 1, pp. 1–11, 2018.

[87] T. Potočnik, S. Sachdev, T. Polajžer, A. Maček Lebar, and D. Miklavčič, “Efficient gene transfection by electroporation—in vitro and in silico study of pulse parameters,” *Applied Sciences*, vol. 12, no. 16, p. 8237, 2022.

[88] J.-M. Escoffre, T. Portet, L. Wasungu, J. Teissié, D. Dean, and M.-P. Rols, “What is (still not) known of the mechanism by which electroporation mediates gene transfer and expression in cells and tissues,” *Molecular biotechnology*, vol. 41, no. 3, pp. 286–295, 2009.

[89] E. Neumann, S. Kakorin, and K. Tøensing, “Fundamentals of electroporative delivery of drugs and genes,” *Bioelectrochemistry and bioenergetics*, vol. 48, no. 1, pp. 3–16, 1999.

[90] M.-P. Rols and J. Teissié, “Electropermeabilization of mammalian cells to macromolecules: control by pulse duration,” *Biophysical journal*, vol. 75, no. 3, pp. 1415–1423, 1998.

[91] S. Satkauskas *et al.*, “Mechanisms of in vivo DNA electrotransfer: respective contributions of cell electropermeabilization and DNA electrophoresis,” *Molecular therapy*, vol. 5, no. 2, pp. 133–140, 2002.

[92] M. F. Bureau, J. Gehl, V. Deleuze, L. M. Mir, and D. Scherman, “Importance of association between permeabilization and electrophoretic forces for intramuscular DNA electrotransfer,” *Biochimica et Biophysica Acta (BBA)-General Subjects*, vol. 1474, no. 3, pp. 353–359, 2000.

[93] M. Scuderi, J. Dermol-Černe, C. A. da Silva, A. Muralidharan, P. E. Boukany, and L. Rems, "Models of electroporation and the associated transmembrane molecular transport should be revisited," *Bioelectrochemistry*, vol. 147, p. 108216, 2022.
[94] E. Neumann, K. Tönsing, S. Kakorin, P. Budde, and J. Frey, "Mechanism of electroporative dye uptake by mouse B cells," *Biophysical journal*, vol. 74, no. 1, pp. 98–108, 1998.
[95] D. Miklavcic and L. Towhidi, "Numerical study of the electroporation pulse shape effect on molecular uptake of biological cells," *Radiology and oncology*, vol. 44, no. 1, pp. 34–41, 2010.
[96] K. C. Smith, "A unified model of electroporation and molecular transport," PhD Thesis, Massachusetts Institute of Technology, 2011.
[97] W. Krassowska and P. D. Filev, "Modeling electroporation in a single cell," *Biophysical journal*, vol. 92, no. 2, pp. 404–417, 2007.
[98] J. Li, W. Tan, M. Yu, and H. Lin, "The effect of extracellular conductivity on electroporation-mediated molecular delivery," *Biochimica et Biophysica Acta (BBA)-Biomembranes*, vol. 1828, no. 2, pp. 461–470, 2013.
[99] J. Li and H. Lin, "Numerical simulation of molecular uptake via electroporation," *Bioelectrochemistry*, vol. 82, no. 1, pp. 10–21, 2011.
[100] D. C. Sweeney, T. A. Douglas, and R. V. Davalos, "Characterization of cell membrane permeability in vitro part II: computational model of electroporation-mediated membrane transport," *Technology in cancer research & treatment*, vol. 17, p. 1533033818792490, 2018.
[101] M. Leguebe, A. Silve, L. M. Mir, and C. Poignard, "Conducting and permeable states of cell membrane submitted to high voltage pulses: mathematical and numerical studies validated by the experiments," *Journal of theoretical biology*, vol. 360, pp. 83–94, 2014.
[102] J. Dermol-Černe, J. Vidmar, J. Ščančar, K. Uršič, G. Serša, and D. Miklavčič, "Connecting the in vitro and in vivo experiments in electrochemotherapy-a feasibility study modeling cisplatin transport in mouse melanoma using the dual-porosity model," *Journal of controlled release*, vol. 286, pp. 33–45, 2018.
[103] M. Pavlin and D. Miklavcic, "Theoretical and experimental analysis of conductivity, ion diffusion and molecular transport during cell electroporation--relation between short-lived and long-lived pores," *Bioelectrochemistry*, vol. 74, no. 1, pp. 38–46, Nov. 2008, doi: 10.1016/j.bioelechem.2008.04.016.
[104] M. Pavlin, V. Leben, and D. Miklavčič, "Electroporation in dense cell suspension–theoretical and experimental analysis of ion diffusion and cell permeabilization.," *Biochimica et Biophysica Acta*, 2007, doi: 10.1016/j.bbagen.2006.06.014.
[105] A. Vizintin, S. Markovic, J. Scancar, J. Kladnik, I. Turel, and D. Miklavcic, "Nanosecond electric pulses are equally effective in electrochemotherapy with cisplatin as microsecond pulses," *Radiology and Oncology*, vol. 56, no. 3, pp. 326–335, 2022.
[106] M. Scuderi, J. Dermol-Černe, J. Ščančar, S. Marković, L. Rems, and D. Miklavčič, "The equivalence of different types of electric pulses for electrochemotherapy with cisplatin - an in vitro study," *submitted*.
[107] T. Kotnik, G. Pucihar, M. Reberšek, D. Miklavčič, and L. M. Mir, "Role of pulse shape in cell membrane electropermeabilization," *Biochimica et Biophysica Acta (BBA)-Biomembranes*, vol. 1614, no. 2, pp. 193–200, 2003.

[108] P. J. Canatella, J. F. Karr, J. A. Petros, and M. R. Prausnitz, "Quantitative study of electroporation-mediated molecular uptake and cell viability," *Biophysical journal*, vol. 80, no. 2, pp. 755–764, 2001.
[109] E. B. Sözer, C. F. Pocetti, and P. T. Vernier, "Asymmetric patterns of small molecule transport after nanosecond and microsecond electropermeabilization," *The Journal of membrane biology*, vol. 251, pp. 197–210, 2018.
[110] B. Gabriel and J. Teissie, "Time courses of mammalian cell electropermeabilization observed by millisecond imaging of membrane property changes during the pulse," *Biophysical journal*, vol. 76, no. 4, pp. 2158–2165, 1999.
[111] M. Scuderi *et al.*, "Characterization of Experimentally Observed Complex Interplay between Pulse Duration, Electrical Field Strength, and Cell Orientation on Electroporation Outcome Using a Time-Dependent Nonlinear Numerical Model," *Biomolecules*, vol. 13, no. 5, p. 727, 2023.
[112] J. Dermol-Černe, T. Batista Napotnik, M. Reberšek, and D. Miklavčič, "Short microsecond pulses achieve homogeneous electroporation of elongated biological cells irrespective of their orientation in electric field," *Scientific reports*, vol. 10, no. 1, pp. 1–17, 2020.
[113] S. Chaigne *et al.*, "Reversible and Irreversible Effects of Electroporation on Contractility and Calcium Homeostasis in Isolated Cardiac Ventricular Myocytes," *Circulation: Arrhythmia and Electrophysiology*, vol. 15, no. 11, p. e011131, 2022.
[114] O. Tounekti, G. Pron, J. Belehradek, and L. M. Mir, "Bleomycin, an apoptosis-mimetic drug that induces two types of cell death depending on the number of molecules internalized," *Cancer research*, vol. 53, no. 22, pp. 5462–5469, 1993.
[115] L. T. Baxter and R. K. Jain, "Transport of fluid and macromolecules in tumors. I. Role of interstitial pressure and convection," *Microvascular research*, vol. 37, no. 1, pp. 77–104, 1989.
[116] L. T. Baxter and R. K. Jain, "Transport of fluid and macromolecules in tumors. II. Role of heterogeneous perfusion and lymphatics," *Microvascular research*, vol. 40, no. 2, pp. 246–263, 1990.
[117] L. T. Baxter and R. K. Jain, "Transport of fluid and macromolecules in tumors: III. Role of binding and metabolism," *Microvascular research*, vol. 41, no. 1, pp. 5–23, 1991.
[118] H. Cindrič, D. Miklavčič, F. H. Cornelis, and B. Kos, "Optimization of Transpedicular Electrode Insertion for Electroporation-Based Treatments of Vertebral Tumors," *Cancers*, vol. 14, no. 21, p. 5412, 2022.
[119] H. Cindrič *et al.*, "Retrospective study for validation and improvement of numerical treatment planning of irreversible electroporation ablation for treatment of liver tumors," *IEEE Transactions on Biomedical Engineering*, vol. 68, no. 12, pp. 3513–3524, 2021.
[120] D. Miklavcic, S. Corovic, G. Pucihar, and N. Pavselj, "Importance of tumour coverage by sufficiently high local electric field for effective electrochemotherapy," *European Journal of Cancer Supplements*, vol. 4, no. 11, pp. 45–51, 2006.
[121] R. C. Martin, E. Schwartz, J. Adams, I. Farah, and B. M. Derhake, "Intra-operative anesthesia management in patients undergoing surgical irreversible electroporation of the pancreas, liver, kidney, and retroperitoneal tumors," *Anesthesiology and pain medicine*, vol. 5, no. 3, 2015, Accessed: Oct. 10, 2023. [Online]. Available: https://www.ncbi.nlm.nih.gov/pmc/articles/PMC4493723/

[122] W. Stillwell, “Membrane transport,” *An introduction to biological membranes*, p. 305, 2013.
[123] C. S. Djuzenova, U. Zimmermann, H. Frank, V. L. Sukhorukov, E. Richter, and G. Fuhr, “Effect of medium conductivity and composition on the uptake of propidium iodide into electropermeabilized myeloma cells,” *Biochimica et Biophysica Acta (BBA)-Biomembranes*, vol. 1284, no. 2, pp. 143–152, 1996.
[124] K. J. Müller, V. L. Sukhorukov, and U. Zimmermann, “Reversible Electropermeabilization of Mammalian Cells by High-Intensity, Ultra-Short Pulses of Submicrosecond Duration,” *Journal of Membrane Biology*, vol. 184, no. 2, pp. 161–170, Nov. 2001, doi: 10.1007/s00232-001-0084-3.
[125] D. C. Sweeney, M. Reberšek, J. Dermol, L. Rems, D. Miklavčič, and R. V. Davalos, “Quantification of cell membrane permeability induced by monopolar and high-frequency bipolar bursts of electrical pulses,” *Biochimica et Biophysica Acta (BBA)-Biomembranes*, vol. 1858, no. 11, pp. 2689–2698, 2016.